Use of *in vitro* Primary Culture Models to investigate the activity of Standard and Novel Therapies in Haematological Malignancies

Lenushka Maharaj

Barts Cancer Institute

Queen Mary's School of Medicine and Dentistry

Submitted in partial fulfilment of the requirements of the Degree of Doctor of Philosophy

Abstract

Despite improved treatments for Non-Hodgkin's Lymphoma (NHL) and Multiple Myeloma (MM), most patients eventually relapse and these diseases remain largely incurable. This has precipitated recent research into more clinically relevant *in vitro* models to enable development of more effective therapies. We have validated and standardised two *in vitro* primary culture models using tumour samples derived from patients with NHL, Chronic Lymphocytic Leukaemia (CLL) and MM. Several novel findings have been demonstrated. *In vitro* sensitivity of primary NHL cells cocultured in a CD40L model predicted clinical response to bortezomib in patients receiving the drug in a phase II trial. *In vitro* sensitivity correlated with CD40 expression, identifying a potential surrogate biomarker for response to bortezomib.

The novel HDAC inhibitor, UCL67022 was 10-fold more potent than vorinostat in NHL and produced synergy when combined with bortezomib. UCL67022 maintained its potency in primary MM samples grown in an HS-5 stromal model. It modulated cytokine secretion resulting in downregulation of cytokine-induced signalling pathways (JAK/STAT3). A novel Hsp90 inhibitor, KW-2478 maintained activity in the HS-5 model and enhanced the activity of bortezomib and melphalan. Hsp70 was identified as a potential surrogate biomarker to monitor the combinatorial effect in future clinical trials.

A highly synergistic and schedule-dependent cytotoxic effect occurred when primary MM cells were pre-treated with melphalan followed by bortezomib, with important implications for future clinical trial design. IL-6, IL-8 and VEGF levels correlated with resistance to bortezomib and melphalan and were associated with activation of JAK/STAT, MAPK and PI3K/Akt signalling pathways. Antibody neutralization of IL-6, IL-8 and VEGF resulted in restoration of drug sensitivity. We have therefore demonstrated the ability of primary culture models to predict response to chemotherapy, to identify therapeutically beneficial novel agents and to enable study of tumour microenvironmental interactions responsible for drug resistance in patients with haematological malignancies.

Table of Contents

List of Figures

List of Tables

List of Abbreviations

NHL	(Non-Hodgkin Lymphomas)
DLBCL	(Diffuse Large B-Cell Lymphoma)
FL	(Follicular lymphoma)
MCL	(Mantle cell lymphoma)
MM	(Multiple Myeloma)
CLL	(Chronic lymphocytic leukaemia)
CML	(Chronic Myeloid Leukaemia)
MMCLs	(Multiple Myeloma Cell Line)
LLCLs	(Leukaemia-Lymphoma Cell Lines)
ATCC	(American Type Culture Collection)
DXMZ	(German Collection of Microorganisms and Cell Culture)
FDCs	(Follicular Dendritic Cells)
IFN-γ	(Interferon gamma)
TNF-α and β	(Tumour Necrosis Factor-α and β)
TRAFs	(TNF-R associated factor)
NFκβ	(Nuclear Factor Kappa-beta)
P13-K	(phosphatidylinositol 3-kinase)
sCD40L	(soluble CD40L)
BMM	(Bone Marrow Microenvironment)
IL-4	(interleukin-4)
CHO	(Chinese Hamster Ovary)
PHA	(Phytohaemagglutinin)
TGF-β	(Transforming Growth Factor-beta)
BMSCs	(Bone Marrow Stromal Cells)
LTBMC	(Long-Term Bone Marrow Stromal Cells)
HUVEC-C	(Human Umbilical Vein Endothelial cell line)
BMEC-1	(Bone Marrow Endothelial cell line)
HS-27	(an epithelioid cell line)
MHC	(Major Histocompatibility Complex)
VCAM-1	(Vascular Cellular Adhesion Molecule)

CAM-DR	(Cell Adhesion Mediated-Drug Resistance)
AML	(Acute Myeloid Leukaemia)
EM-DR	(Environment Mediated-Drug Resistance)
BAFF	(B-cell Activating Factor)
LTb	(Lymphotoxin-β)
IL-6	(interleukin-6)
MRD	(Minimal Residual Disease)
B-ALL	(B-acute lymphoblastic leukaemia)
Mcl-1	(Myeloid cell leukemia-1)
IL-8/CXCL8	(interleukin-8)
siRNA	(small interfering RNA)
VEGF	(Vascular Endothelial Growth Factor)
M1P-α	(Macrophage Inflammatory Protein-1α)
SDF-1	(Stromal Derived Factor-1)
IGF-1	(Insulin-like Growth Factor)
HGF	(Hepatocyte Growth Factor)
bFGF	(basic Fibroblast Growth Factor)
PC	(Plasma Cell)
MTT	(Microtetrazolium)
DiSC assay	(Differential Staining Cytotoxicity assay)
NCI	(National Cancer Institute)
SRB	(Sulforhodamine B)
GI50	(Growth inhibition of 50%)
TGI	(total growth inhibition)
LC50	(50% of the lethal concentration)
ATP	(adenosine triphosphate)
PI	(propidium iodide)
ATP	(adenosine triphosphate)
UPP	(Ubiquitin-Proteasome Pathway)
HIF-1α	(hypoxia inducible factor 1 alpha)
PBMCs	(Peripheral Blood Mononuclear Cells)
AML	(Acute Myelogenous Leukaemia)

MAPK	(Mitogen-Activated Protein Kinase)
MDM2	(Mouse Double Minute 2 homolog)
DNA-PKCs	(DNA-dependent protein kinase catalytic subunit)
ER	(endoplasmic reticulum)
PARP	(Poly ADP-Ribose Polymerase)
MZL	(Marginal Zone Lymphoma)
WM	(Waldenstrom's Macroglobulinemia)
HDACs	(histone deacetylases)
HAT	(Histone acetyltransferase)
NAD	(Nicotinamide Adenine Dinucleotide)
HDACIs	(HDAC Inhibitors)
CTCL	(Cutaneous T cell Lymphoma)
TSA	(Trichostatin)
ROS	(Reactive Oxygen Species)
UCL67022	(C1 l-Phenylcarbamoyl-octanedioic acid 8-hydroxyamide 1-phenylamide)
Hsp90	(Heat shock protein 90)
ATP	(Adenosine Triphosphate)
CHIP	(C-Terminus of Heat shock Cognate 70 Interacting Protein)
STAT3	(Signal Transducer and Activator of Transcription 3)
IMiDs	(Immunomodulatory Drugs)
4-HC	(4-hydroperoxycyclophosphamide)
F-ara-ATP	(fuoroadenine arabinoside triphosphate)
PBS	(Phosphate Buffered Saline)
MSD	(Meso Scale Discovery)
ANOVA	(Analysis of Variance)
Ig	(Immunoglobulin)
huCD40LT	(CD40L trimer)
PIs	(Proteasome Inhibitors)
PE	(Phycoerythrin)
PR	(partial response)
CT	(Computerized Tomography)

CI	(combination index)
HMCLs	(human multiple myeloma cell lines)
ICLs	(inter-strand cross-links)
UPR	(unfolded protein response)
CM	(conditioned medium)
ECM	(extracellular matrix)
JAK	(jun-activated kinase)
FSC	(Forward Scatter)
SSC	(Side Scatter)
hBMSCs	(patient bone marrow-derived stromal cells)
CHOP	(cyclophosphamide-doxorubicin-vincristine, and prednisone)
MTD	(maximum tolerated dose)
MSCs	(mesenchymal stem cells)
CSCs	(cancer stem cells)
ADME	(absorption, distribution, metabolism and elimination)

Acknowledgements

I would like to thank my supervisors Dr. Simon Joel and Prof. John Gribben for their ongoing guidance, support and inspiration. I would also like to thank members of Barts Cancer Institute for their camaraderie and especially the group from the Barry Reed Oncology Laboratory for their technical help and friendship over the last several years. I would also like to thank Dr. Rakesh Popat for his collaboration with publications and Dr. Jude Fitzgibbon for his support and guidance. This work would not have been possible without the patients who donated their tumour samples for which I am most grateful. Finally, I would like to thank my family who has been a constant source of support and inspiration, and my fiancé Aaron for his unfaltering patience and encouragement.

This work was partly funded by: Millenium Pharmaceuticals Inc., Astra Zeneca and Kyowa Hakko Kirin. I would like to thanks Barts Cancer Institute for funding attendances at international meetings.

CHAPTER 1: Introduction

1.1 Haematological malignancies

Haematological malignancies are broadly divided into myeloid neoplasms, lymphoid neoplasms (leukaemias and lymphomas), lymphoproliferative disorders, and histiocytic/dendritic cell neoplasms. They are widely recognized as arising out of specific stages of myeloid or lymphoid development or specific subsets of these types of cells. Immunophenotyping and gene expression profiling studies have been useful tools in confirming how these entities mimic normal cell types and how they are distinct from each other.

By definition a leukaemia is any myeloid or lymphoid malignancy that largely involves the peripheral blood and bone marrow (Swerdlow 2008). They may be classified as acute or chronic, depending maturity of the cell of origin (acute = blasts and chronic = more mature cells), which also tends to correlate with the clinical acuity (acute = weeks and chronic = years). A lymphoma is a lymphoid malignancy that involves lymph nodes and/or other extramedullary sites. They are broadly classified as being Hodgkin or non-Hodgkin and are treated with very different therapies. Non-Hodgkin lymphomas may be immature (lymphoblastic), although the vast majority have a mature B, T, or NK cell phenotype. Extramedullary myeloid proliferations are unusual and most commonly seen in the setting of acute myeloid leukaemia, in which case it represents a myeloid sarcoma (extramedullary accumulation of myeloid blasts). Histiocytic and dendritic cell neoplasms are generally rare except for Langerhans cell histiocytosis (an entity whose neoplastic nature is controversial), which is seen relatively more commonly, especially in children.

Although morphology and clinical history are very helpful in the initial differential diagnosis, detailed immunophenotyping by either flow cytometry or immunohistochemistry is usually needed to classify a leukaemia or lymphoma according the cell lineage (myeloid, B, T, NK) and stage of maturation. This is done by

taking advantage of the antigens expressed on the cell surface and/or in the cytoplasm of the cells. Cytogenetic and/or molecular genetic studies are often useful as many of these neoplasms harbour characteristic abnormalities that are very distinct and helpful for classification and often prognosis (Swerdlow 2008). In the next sections, the haematological malignancies studied in this project are addressed in more detail.

1.1.1 Non-Hodgkin's Lymphoma

Of the approximately 14,000 new cases of lymphoma diagnosed in the UK each year around 12,000 are Non-Hodgkin lymphomas (NHL), representing the 5th most common cancer in the UK (CRUK 2010). They are divided into B- and T-cell lymphomas (of which over 85% are of B-cell origin) and are a heterogeneous group of malignant disorders with differing clinical, histopathological, immunophenotypic and molecular characteristics. The incidence in western countries has been increasing over the last 20 years, for reasons that remain unclear. Diffuse large B cell lymphoma (DLBCL) is the most common subtype of NHL accounting for up to 40% of cases and follicular lymphoma (FL) the second most common, accounting for 20% of cases (NHL 1997). Mantle cell lymphoma (MCL) comprises 6% of all cases. Although treatments for these malignancies have improved over recent years there is a need for better therapies. Less than 50% of patients with DLBCL are cured with conventional therapeutic approaches and although FL is associated with a median survival of 8-10 years, treatment is characterised by recurrent relapses and the majority of patients will either die as a result of the disease or as a complication of therapy (Gribben 2007). Mantle cell lymphoma is a rarer more aggressive subtype with a very poor prognosis as it is notoriously refractory to chemotherapy and survival is short. Chemotherapy agents used to treat these disorders are toxic and because these malignancies affect mainly older patients, are often not well tolerated. Thus relapses and subsequent resistance to therapy is common to all subtypes of this disease, stressing the urgent need for novel strategies (Sawas, Diefenbach et al. 2011).

1.1.2 Multiple Myeloma

Myeloma is a B-cell malignancy characterised by excessive monoclonal plasma cells in the bone marrow. There are nearly 5000 new cases of Multiple Myeloma (MM) in the UK each year, and 2,600 deaths (CRUK 2010). The incidence of MM in Europe has increased by around 30% (Gribben 2007) over the last 30 years, in both sexes. Despite considerable advances in the understanding of the biology of MM over the last few years the outcome remains poor, and with a median survival of only 4 years it remains a largely incurable disease. While patients usually respond to initial therapy, and often to subsequent novel therapies, they typically relapse and eventually become refractory to treatment (Borrello 2012). The bone marrow microenvironment has been shown to play an important role in patient response to therapy as it up-regulates the expression of various factors that induce growth, survival and drug resistance (Podar, Chauhan et al. 2009). New treatment options are clearly required, including those that target key cellular proteins involved in myeloma and the interaction with the bone marrow microenvironment.

1.1.3 Chronic Lymphocytic Leukaemia

There are around 2,500 new cases of chronic lymphocytic leukaemia (CLL) in the UK each year (CRUK 2010). CLL does not fall under the category of NHL but is a B-cell disorder that is the commonest form of leukaemia in western countries. Disease characteristics and clinical course vary considerably between patients such that there are a number of different therapeutic strategies employed (Parker and Strout 2011). Patients with early stage disease who are asymptomatic typically do not receive treatment and randomised trials have shown that this does not adversely affect survival (Auer, Gribben et al. 2007). Early stage patients with poor prognostic factors, such as mutated p53, receive therapy with established chemotherapy agents and a targeted antibody, as single agents or in combination. In patients with advanced disease the mainstay of treatment remains chlorambucil as a single agent, which performs as well as combination chemotherapy. However, despite the success of first line therapy in advanced disease the vast majority of patients relapse and require additional lines of established therapies, transplantation or novel agents. These

approaches are less effective than first line treatments and over 1000 CLL patients in the UK go on to die of their disease each year (CRUK 2010).

1.1.4 Novel agents for the treatment of haematological malignancies

Over the last decade a large number of novel therapies that target changes that take place in malignant cells have been introduced into the clinic. Many of these are small molecules that target proteins involved in cell signalling pathways, proliferation or apoptosis. These proteins are often kinases that control important cellular processes by the phosphorylation of substrate proteins. Still the best example of this approach is Gleevec (imatinib maleate) that targets the BCR-ABL protein altered in 95% of patients with chronic myeloid leukaemia (CML) (Deininger, Buchdunger et al. 2005). Used continuously as an orally administered single agent this drug can control the disease in patients (Gschwind, Fischer et al. 2004). Receptor tyrosine kinase inhibitors have also had an impact in specific diseases, such as Iressa (gefitinib) in non-small cell lung cancer and Sutent (sunitinib) in renal cancers. Non-kinase proteins that have been shown to be valid therapeutic targets in haematological malignancies include the proteasome, targeted by Velcade (bortezomib) in MM (Mitsiades, Mitsiades et al. 2006)and the PML-RARA protein in acute promyelocytic leukaemia targeted by all trans-retinoic acid (Wang and Chen 2008).

Other approaches likely to be of value in the future involve targeting angiogenesis and invasion by inhibiting proteins involved in those processes and the relief of transcriptional silencing by targeting histone deacetylases or DNA methylating enzymes. Other agents that have made an impact in haematological cancers include Mabthera (rituximab) (Maloney 2005), a monoclonal antibody that targets CD20 antigen on the surface of NHL and CLL cells, and Myelotarg (gemtuzumab) that binds to the CD33 antigen on the surface of leukaemia cells and delivers the powerful cytotoxic agent calicheamycin (Stasi, Evangelista et al. 2008). Many other approaches are under preclinical or clinical development, particularly in haematological malignancies where more is known about the genetic and protein changes that drive these diseases.

1.2 The need for better *in vitro* models to study haematological malignancies

1.2.1 The need for better drug therapies

New anticancer agents for the treatment of haematological malignancies are generated by either large-scale drug screening programs or are designed for tumor specific targets based on a biological rationale and improved understanding of tumour-host interactions (Decker, Hollingshead et al. 2004). As a result, there has been a rapid emergence of new agents in the past decade that have higher specificity and efficacy combined with a lower toxicity than classical cytotoxic agents (Zips, Thames et al. 2005). Although this has also resulted in improved outcomes for patients, most patients eventually relapse and haematological malignancies remain largely incurable. This indicates a clear need for more effective drug therapies, and represents a huge challenge for pre-clinical and clinical research to evaluate and eventually integrate the most promising new agents into the clinic.

The question of whether a new drug improves cancer therapy in patients can ultimately only be answered in a clinical trial. However, due to ethical, medical and economic limitations, most of the research has to be done in experimental systems (Zips, Thames et al. 2005). The pre-clinical evaluation of novel agents is a vital part in the process of drug development. It is critical that prior to entry into clinical studies the drug has demonstrated *in vitro* and *in vivo* evidence of efficacy and acceptable toxicity. Pre-clinical models range from cell lines to primates with each stage giving different levels of information. Over the past decades, researchers have developed many *in vitro* cell line assays to evaluate treatment response. However, use of these assays can be time-consuming and costly; therefore research institutions tend to focus on just a few of the most promising drugs (Baumann, Bentzen et al. 2001). Thus an important part of cancer research is to develop and improve on current *in vitro* models to expedite evaluation of new drugs and to identify the best drug candidates for future clinical use.

1.2.2 Advantages of using cell lines as disease models

A cell line is a permanently established cell culture that will proliferate indefinitely given appropriate fresh medium and space. Most stable human cell lines are established from cancer tissues. Over the last 5 decades since the first tumor cell line, HeLa was established from a cervical adenocarcinoma (Hsu, Schacter et al. 1976) they have made an enormous contribution to the development of cancer biology and are a widely used and valuable resource. Currently, numerous myeloma cell lines (MMCLs) and leukemia-lymphoma cell lines (LLCLs) are available. These continuous cell lines have proven to be particularly informative in haematological, immunological, molecular biological, cytogenetic, pharmacological, toxicological, and virological studies, but also in several other areas of biomedicine and biotechnology. Their major advantage is the unlimited supply of cellular material. Furthermore, cell lines can be stored in liquid nitrogen and recovered without any detrimental loss of cellular features or cell viability.

In general, under optimal culture conditions, cell lines stably retain the major features of their original cells (including classical and molecular cytogenetic aberrations). In fact this is one of the areas in which cell lines have made a striking contribution. Cell lines provide the material to further examine the occurrence, mechanisms and biological effects of cytogenetic alterations in tumorigenesis. For example, the discovery of the Philadelphia chromosome [t(9;22)(q34;q11)] rearrangement revealed that specific structural rearrangements might be associated with different tumours, and that such recurrent chromosome rearrangements effect specific gene rearrangements such as fusion oncogene formation (BCR-ABL). The presence of recurrent translocations provides proof that the cell lines carrying them share clonal descent with the malignant clone present in the patient and, if consistent with immunological and functional characteristics, that such cell lines are likely to be appropriate models for the disease in question.

Furthermore, because fusion gene translocations are stable *in vitro*, cell lines carrying them are widely used as sources of RNA/DNA for positive controls in PCR assays routinely used in clinical diagnosis. Without the ready availability of well-characterized

and stable rearrangements in continuous cell lines, diagnosis would rely on a supply of patient material, which is often scarce, especially for disease subtypes with low incidences. Therefore, haematopoietic cell lines have become indispensable tools in cancer research. However, cell line models have many limitations:

1.2.3 Limitations of cell lines as disease models

1. Most primary human cells including cancer cells have a very short lifespan *in vitro* and it is thus difficult to establish permanent cell lines from human primary tumors. Advances in DNA recombinant technology and gene transfer have enabled the establishment of a variety of cell lines via infection or transfection of two main types of viral and cellular immortalizing genes, the anti-tumour suppressor immortalizing genes (SV40, human papilloma virus E6 and E7, adenovirus E1A and E1B, polyoma virus large T, mutant p53) and the oncogene-relating immortalizing genes (c-Myc, Bmi-1, ras and raf, telomerase, Epstein-Barr Virus-EBV) (Pantel, Dickmanns et al. 1995; Li, Schlag et al. 1997). Most B-cell malignancies are transformed into permanent cell lines via EBV infection. Many of these cell lines such as those of B-CLL origin, cannot be cultured long-term without EBV transformation and there are therefore relatively few authentic B-CLL tumour cell lines reported (Nilsson 1992).

2. The obvious problem with using transformed cell lines is that very few human tumours possess immortalizing genes such as EBV. Furthermore, continuously cultured cell lines have often evolved and acquired mutations that are not present within a patient. For example, myeloma cells in patients do not usually divide rapidly, but all the existing MMCLs do so (Drexler and Matsuo 2000). Therefore, therapeutics that target cell division and thus require rapid cell turnover, may work well in the myeloma cell line culture model, but this may not translate into activity in myeloma patients. This is true for vincristine, which shows efficacy against nearly all MMCLs but has not translated well in the clinical setting (Drexler and Matsuo 2000). Thus cell line phenotypes can differ markedly from those found in native cells *in vivo*, and do not accurately represent or model the human pathology.

3. Furthermore, the vast majority of the over 100 MMCLs reported in the literature were derived from samples obtained at relapse or in the leukemic/terminal phase of the disease. There is a shortage of cell lines derived from early-stage patients as they are much more difficult to grow *in vitro* (Matsuoka, Moore et al. 1967; Nilsson 1970). Therefore, cell lines are unable to fully reflect the heterogeneity observed in patients at different stages of disease.

4. There are also additional practical problems inherent in using continuous cell lines such as their frequent infection with a type of bacteria called mycoplasma which are highly resistant to antibiotics and difficult to detect due to their very small size (less than 1 micron). Mycoplasma can produce extensive changes in the cultures they infect including chromosome aberrations and changes in metabolism and cell growth. Due to various sources of contamination and sharing of cell lines between different laboratories, mycoplasma contamination still persists in many labs, presumably resulting in misleading and erroneous findings.

5. Sharing of cell lines between labs, as well as cross-contamination can also cause cell line misclassification, leading to uncertainty about what tumour type researchers are working with (Capes-Davis, Theodosopoulos et al.). Studies suggest that anywhere from 18–31% of the time, cells used in experiments have been misidentified or contaminated with another cell line (Capes-Davis, Theodosopoulos et al. ; Drexler, MacLeod et al. 2001; Cabrera, Cobo et al. 2006; Lacroix 2008; MacLeod, Dirks et al. 2008). Cross contamination has even been detected in cell lines from the National Cancer Institute (NCI)-60 panels, which are used routinely for drug-screening studies, and major cell line repositories including the American Type Culture Collection (ATCC) and the German Collection of Microorganisms and Cell Cultures (DSMZ) (MacLeod, Dirks et al. 1999; Chatterjee 2007; Liscovitch and Ravid 2007). Such contamination poses a problem for the quality of research produced using cell lines.

6. The most commonly used cell lines today were chosen based on their ease of use with prevailing screening technologies, such as the NCI-60 panel used for drug discovery studies since 1990 (Shoemaker 2006). These lines are highly selected and

may have little resemblance to their original tumour (Drexler and Matsuo 2000). These issues have now raised concerns amongst many researchers regarding the dependence on the use of immortalized cells in terms of the clinical relevance of the data generated. Consequently, some drug discovery programmes are now employing primary cells in cell-based screening, as well as adopting sophisticated cell-based assays in order to identify new more effective treatment agents (Zanella, Lorens et al.).

1.2.4 Primary culture models

Physicians have become increasingly aware that individuals with the same tumour and stage can respond quite differently to treatment, especially in relapsed patients, making it difficult for them to know what chemotherapy is best for the patient. Coupled with this is the increasing evidence supporting the role of the tumour microenvironment in conferring protection to tumour cells from the toxic effects of chemotherapy, contributing to the development of drug-resistance, failure of chemotherapy and patient relapse. This stimulated the search for more relevant *in vitro* models than commonly used cell line models that better reflect the true value of a drug in a particular tumour type.

Primary cultures by definition are started from cells/tissue taken from the organism/patient and before the first passage (2010). In primary cells the drug target is assumed to be expressed in an environment that more closely resembles that found in the human disease, and at levels that resemble those found *in vivo*. Therefore primary culture models are thought to more closely resemble the original tumour compared to established cell lines (Lerescu, Tucureanu et al. 2008). It may be that a drug or combination of drugs that are effective in a cell line model alone could lose its efficacy in a primary culture model and so further development into animal models may be halted, saving valuable resources and allowing focus elsewhere. Another clear advantage to such systems is that they can permit studying the effects of a novel drug in the lab from a sample taken from a patient receiving the drug in a clinical trial thus providing invaluable correlative data. Using such systems in the lab would enable therapies to be tailored to the individual in the lab and translated to its use in the

clinic, thus avoiding the administration of toxic and ineffective therapies, whilst identifying treatment to which the patient is more likely to respond (Bosanquet 1991).

1.2.5 Primary culture models: challenges

The culture of primary cells presents many challenges. In a standard monolayer of primary cultured cells, those cells that survive the disaggregation technique will form the basis of the culture. As time progresses, cells capable of proliferating will increase and cells sensitive to density limitation will stop dividing (Freshney 2006), therefore in theory, malignant cells will overgrow and normal cells, will die off. In theory this concept is simple, but in practice, it is not always achievable.

One of the reasons for this is that tumour cells have poor plating efficiencies (<0.1%) (Runge, Neumann et al. 1986; Bellamy 1992) and require a large starting cell number, which is not always possible when there is limited access to patient material. One solution would be to culture and expand the initial, small number of primary cells to sufficient numbers to be of analytical value. However, by the time a clone has grown to sufficient numbers, it may have changed significantly due to genetic instability and phenotypic drift. Furthermore, factors like genetic aberrations, terminal differentiation, spontaneous apoptosis or terminal senescence may limit the lifespan of the tumour cells so that only a few cells will survive in culture media (Freshney 2006). Primary tumour cells also require stimulation by growth factors specific to each tumour type, in order to proliferate *ex vivo* (Rousset, Garcia et al. 1992; van Kooten and Banchereau 2000; Woltman, de Haij et al. 2000). Successful propagation of primary cultures depends on knowledge and provision of these correct stimuli and culture conditions. A number of approaches have been evaluated for *in vitro* expansion of primary cells. However, no consensus has been reached on the optimal culturing conditions or the most appropriate drug sensitivity assays to use as endpoints for evaluation of standard and novel therapeutics (Blumenthal 2005).

Access to samples from the licensed Haemato-Oncology tissue bank has in recent years allowed us the unique opportunity to use primary tumour cells from patients with

leukaemia, lymphoma and myeloma to evaluate drug activity, under a series of separate ethics approvals for each drug studied. The next sections discuss the requirements that we have taken into consideration when establishing 2 different *in vitro* primary culture models to study cell growth and drug activity in (a) NHL lymphoma and CLL, and (b) multiple myeloma. These employed normal fibroblasts or stromal cells that provide better conditions for cell growth.

1.3 A primary B-cell (NHL or CLL) coculture model

All B-cells undergo proliferation in response to immunogenic stimulation of the CD40 signaling pathway which is the main signaling pathway of T- and B-cell interaction. We thus exploited this interaction in the NHL coculture model investigates in this study. Use of CD40 to expand B-cell populations was first described by Ghia et al. (Ghia, Boussiotis et al. 1998).

1.3.1 CD40 expression

CD40 is a transmembrane glycoprotein cell surface receptor, belonging to the tumour necrosis factor (TNF) receptor superfamily and is expressed throughout B-cell development, and on haematopoietic progenitor cells, monocytes, basophils, eosinophils, dendritic cells, endothelial and epithelial cells, and malignant B-cells (van Kooten and Banchereau 1997; van Kooten and Banchereau 1997; Younes and Carbone 1999; Fiumara and Younes 2001). The ligand for CD40 (CD40L, CD154, or gp39) is predominately expressed by activated CD4+ T-cells but also on activated B-cells, and other cells including natural killer cells, and those mentioned above (Fiumara and Younes 2001). B-cell survival and proliferation in response to immune stimulation is dependent on CD40 activation. CD40 cross-linking or ligation with cells expressing CD40L, triggers a cascade of events including activation, upregulation of surface immunoglobulin (Ig), antigen presentation, Ig isotype switching, germinal centre formation, and differentiation into either antibody-secreting plasma cells or memory B-cells (Figure 1.1) (DiSanto, Bonnefoy et al. 1993; Korthauer, Graf et al. 1993). During these events, B-cells interact with surface molecules and cytokines, presented by

antigens, T cells, follicular dendritic cells (FDCs) and macrophages. Some of these cytokines, in particular IL-2, IL-3, IL-4, IL-10, interferon gamma (IFN-γ) and tumour necrosis factor-α and β (TNF-α and β) have been shown to contribute to B-cell proliferation via activation of several signaling pathways, including the TNF-R associated factor (TRAFs) nuclear factor kappa-β (NF-κB) and phosphatidylinositol 3-kinase (P13-K) (Friedman and Glaubiger 1982; Defrance, Aubry et al. 1986; Defrance, Vanbervliet et al. 1987; Defrance, Vanbervliet et al. 1992; Rousset, Garcia et al. 1992; Tai, Podar et al. 2003; Davies, Mason et al. 2004).

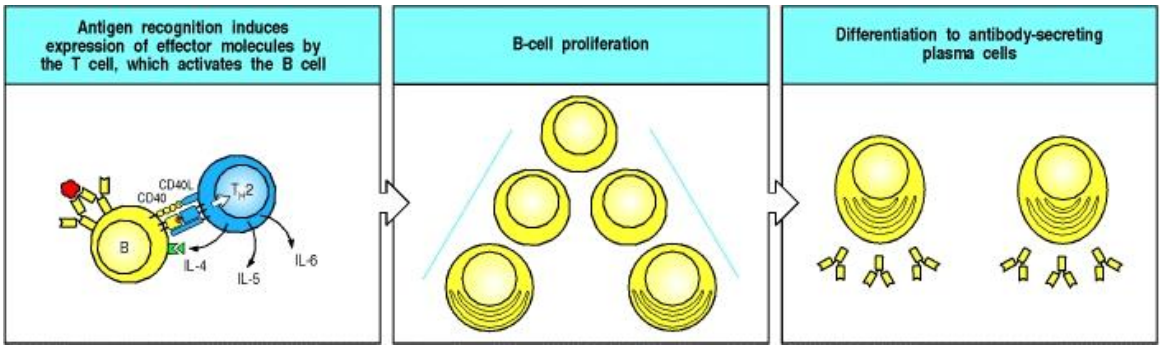

Figure 1.1 Binding of B cells with helper T cells (CD4+) leads to expression of B-cell stimulatory molecule CD40L and cytokines IL-4, IL-5 and IL-6, which drive the proliferation and differentiation of B cells into either memory B cells or antibody-secreting plasma cells (Janeway 2001).

1.3.2 CD40L promotes B cell growth

Several studies have demonstrated B-cell growth promotion in response to CD40 activation, some of which used soluble monomeric CD40L, which causes B-cells to enter limited DNA synthesis. Others used CD40L-transfected fibroblasts (the CD40 system), or a variation of this using fibroblasts transfected with an anti-CD40 antibody (FcγRII/CDw32) which acts as an agonist for the CD40 receptor. The CD40 system has resulted in B-cells being rescued from apoptosis (Banchereau, de Paoli et al. 1991; Banchereau and Rousset 1991; Armitage, Macduff et al. 1993; Johnson, Watt et al. 1993) which was observed in both germinal centre B-cells and peripheral blood B-cells (Holder, Wang et al. 1993; Lomo, Blomhoff et al. 1997).

Malignant B-cells also receive a strong survival signal by CD40 activation. Primary FL cells treated with soluble CD40L (sCD40L) showed increased survival compared to cells cultured in media alone or in the presence of various cytokines, and prolonged growth of isolated primary FL cells cultured on a mouse fibroblast monolayer transfected with the CDw32 Fc receptor to present CD40 mAb in the presence of interleukin-4 (IL-4) (the CD40 system), also achieved similar results (Johnson, Watt et al. 1993). A soluble CD40L trimer (huCD40LT) has also been used to induce selective cell cycle progression and DNA synthesis in MCL primary cultures, and an anti-CD40mAb, or a Jurkat cell line constitutively expressing CD40L, induced S phase entry and cell proliferation of MCL cells, which was enhanced by addition of IL-4 (Castillo, Mascarenhas et al. 2000).

CLL cells also receive growth signals from CD40 activation, and studies have shown it to rescue B-CLL cells from spontaneous, fludarabine- and Fas-induced apoptosis (Kitada, Zapata et al. 1999). In MM, CD40L was shown to exert effects on the bone marrow microenvironment (BMM), where it enhanced myeloma cell adhesion to fibronectin or BMSCs, and consequently upregulated secretion of IL-6 and VEGF. Similar results were found using NIH3T3 CD40L-transfected cells (Urashima, Chauhan et al. 1995; Tai, Podar et al. 2003; Tai, Li et al. 2005).

Some studies using DLBCL cell lines and EBV-induced human lymphoblastoid cell lines have shown CD40 activation to result in growth arrest and/or apoptosis, as opposed to cell proliferation, but it is noteworthy that the latter cell lines are not commonly classified as malignant cell lines as they can be established from normal or diseased individuals (Drexler, Matsuo et al. 2000; Drexler and Matsuo 2000). Growth inhibition was also found in the Burkitt's cell lines, Ramos and Daudi, and in MM cell lines cultured in the CD40 system (Funakoshi, Longo et al. 1994; Pellat-Deceunynck, Amiot et al. 1996; Bergamo, Bataille et al. 1997; Teoh, Tai et al. 2000; Guikema, Vellenga et al. 2002; Szocinski, Khaled et al. 2002). Possible reasons for this are described in the upcoming myeloma sections, however it is important to note that the proapoptotic effects of CD40 activation has only ever been observed in cell lines and not in primary cultures, which again questions the validity of extrapolating results from cell line data alone. Based on the ample evidence described above, there is a clear role for CD40L in

promoting the growth of B-lymphoid and leukemic cells however, studies also suggests that an additional stimulant may be required to achieve optimal B cell proliferation.

1.3.3 Co-stimulation via interleukin-4 (IL-4)

Activation of B-cells is the process by which they undergo several successive rounds of cell division and differentiation into either memory or plasma cells. Memory cells are B-cells in their 'resting' state that survive *in vivo* for many years, during which they are in readiness for further activation and division, given the correct stimuli. Plasma cells are the short-lived, antibody-producing effecter B cells that bind to target antigen and initiate their removal via receptor-mediated endocytosis. For the purposes of establishing long term B-cell cultures, the selection of memory B-cells is preferable.

IL-4 is a cytokine produced by CD4+ helper T cells (activated T cells – figure 1.1) that acts to specifically stimulate the differentiation of B-cells into memory B-cells. This effect is different to that elicited by the other cytokines released by CD40 ligation. For example IL-10 steers B-cells into plasma cells and IL-2 synergises with lymphokines to augment cellular expansion of memory and plasma cells (Zhang, Li et al. 2001). Studies have shown that addition of IL-4 to B-cells cultured in the CD40 system, results in increased B-cell expression of CD19, CD20, CD40, CD23, isotype switching: IgG1 to IgE and MHC class II antigens, and their sustained proliferation (Banchereau and Rousset 1991; Rousset, Garcia et al. 1991; Banchereau, Briere et al. 1994). Furthermore, IL-4 displays these effects only when acting in concert with other activatory signals, that is, it acts as a co-stimulator of CD40-dependent B-cell proliferation (Pound and Gordon 1997).

In summary, CD40 activation via stromal presentation, combined with co-stimulation in the form of IL-4, can provide the necessary stimulation to induce B-cell proliferation *in vitro*. This stromal-cell/cytokine combination formed the basis of the lymphoma primary co-culture system presented in this report. Ideally T cells present in isolated PBMC cell fractions would provide the IL-4 and CD40L required, however T cells die rapidly *in vitro* without stimulation by appropriate antigens for example PHA, pokeweed mitogen or concanavalin A and thus Chinese Hamster Ovary (CHO)

fibroblasts transfected with CD40L acted as the surrogate T cell population also providing structural support (Johnson, Watt et al. 1993).

1.4 A primary multiple myeloma coculture model

1.4.1 CD40 activation in multiple myeloma

Triggering of multiple myeloma (MM) cells by cell surface CD40 has been shown to induce the proliferation of tumour cells in some studies (Tong, Zhang et al. 1994; Westendorf, Ahmann et al. 1994; Urashima, Chauhan et al. 1995; Planken, Dijkstra et al. 1996; Tong and Stone 1996; Urashima, Ogata et al. 1996) and, as mentioned above, to trigger growth arrest (Pellat-Deceunynck, Amiot et al. 1996) and apoptosis (Bergamo, Bataille et al. 1997) in others.

Ligation of CD40 on MM cells also induces the secretion of transforming growth factor-β1 (TGF-β1) (Urashima, Ogata et al. 1996) and increases the expression of adhesion molecules (Urashima, Chauhan et al. 1995) and the Ku86 autoantigen (Teoh, Urashima et al. 1998) on the MM cell surface, thereby augmenting homotypic tumour cell adhesion and heterotypic binding of tumour cells to bone marrow stromal cells (BMSCs) and fibronectin. Up-regulation of MM cell adhesion to BMSCs in turn triggers the transcription and secretion of interleukin-6 (IL-6) mRNA expression and protein secretion in BMSCs (Uchiyama, Barut et al. 1993; Lokhorst, Lamme et al. 1994; Barille, Collette et al. 1995; Urashima, Chauhan et al. 1995; Chauhan, Uchiyama et al. 1996; Teoh and Anderson 1997; Teoh, Urashima et al. 1998).

Some early studies demonstrated that apoptosis of MM cells, induced by wild-type p53 (wtp53) (Yonish-Rouach, Resnitzky et al. 1991; Yonish-Rouach, Grunwald et al. 1993) and p21 (Urashima, Teoh et al. 1997) can be abrogated by treatment with exogenous IL-6. These studies established IL-6 as a major autocrine and paracrine growth factor, especially in CD40-activated MM cells. Cell cycle regulatory proteins, including wtp53, directly regulate IL-6 secretion; wtp53 represses the IL-6 promoter, whereas IL-6 promoter activity is not downregulated by mutated p53 (Margulies and

Sehgal 1993; Wang, Rayanade et al. 1995; Teoh, Urashima et al. 1997; Rayanade, Ndubuisi et al. 1998). These findings were verified by Teoh et al (Teoh, Tai et al. 2000) who showed that the CD40 activation of MM cells may induce growth and survival rather than growth arrest and apoptosis, depending on their p53 status: in the absence of wtp53-like activity cells proliferate however, in the presence of functional wt-like p53 activity, cells undergo growth arrest. This may correlate with the tumour cell growth and resistance to apoptosis observed in late-stage MM, in which p53 abnormalities exist at high frequency (Portier, Moles et al. 1992). Thus CD40 activation-induced stimulation of MM cells may also be exploited in a primary myeloma culture model, and this avenue was investigated in this project.

1.4.2 Stromal-based primary cocultures

Communication between cells is essential for normal and tumour cell growth. Cancer cells are influenced by and are largely dependent on the extrinsic factors provided by their surrounding microenvironment such as antigens, cytokines, and cell to cell interactions. In fact, tumour cells will undergo spontaneous apoptosis within hours of removal from these external stimuli, despite supplementation with culture media and sera (Dierks, Grbic et al. 2007). A heterogeneous population of adherent cells called the 'stroma' is a key component of the normal cellular microenvironment and interactions between stroma and B cells is crucial in promoting haematopoeisis.

This was first demonstrated in short term bone marrow cultures grown in agar similar to a colony formation assay (Pike and Robinson 1970) and in long-term bone marrow (BM) cultures using stromal feeder layers, and was subsequently used to develop a culture system to study the early stages of B-cell maturation (Dexter, Allen et al. 1977; Whitlock and Witte 1982). It has since been discovered that tumour cells exploit the supportive properties of the stroma to promote their own growth and proliferation (Mitsiades, Mitsiades et al. 2006).

The rationale for using stromal cell-based coculture assays is that, by providing the correct external stimuli, tumour cells can be grown in a microenvironment which more closely models *in vivo* conditions, making findings from these studies more relevant to

the clinical setting. Stromal coculture assays can also enable investigation of crucial tumour-stromal cell interactions, and address whether a drug is acting directly on the tumour cells or whether the effect seen is influenced by drug effects on the stromal cells that support tumour growth.These interactions are not targeted by current conventional chemotherapeutics which could explain why some B-cell malignancies still remain incurable. It is therefore important to assess drug activity in the context of a supportive microenvironment, and this type of assay has become increasingly important in drug activity studies.

1.4.3 Clinical relevance of the stromal microenvironment

The clinical relevance of the stromal microenvironment was elegantly demonstrated in two different studies using gene expression signatures which predicted length of survival of FL and in DLBCL patients. This correlated with aspects of the biology of nonmalignant immune cells (such as tumour-infiltrating T-cells, dendritic cells, monocytes and macrophages) present in the tumour at diagnosis, rather than by random accrual of genetic abnormalities after diagnosis (Dave, Wright et al. 2004). This suggests that signals provided by immune cells in the germinal-centre environment could account for the clinical heterogeneity observed in FL. Similarly, two gene expression signatures in patients with DLCBL demonstrated that differences in immune cells, fibrosis and angiogenesis in the tumour microenvironment influence patient survival after treatment of this disease (Lenz, Wright et al. 2008).

Hence, a complimentary two-pronged approach to future management of these diseases may be envisaged: firstly at the pre-clinical stage using a stromal coculture model to delineate the nature of the microenvironment interactions and drug sensitivity in individual patient-derived tumour cells; followed by quantitative approaches such as gene expression profiling in the same patients enrolled on clinical trials. This approach could provide new targets for therapy and enable tumour responses to be related to defined tumour phenotypes.

1.4.4 Bone marrow stromal cells

Bone marrow stromal cells (BMSCs) are fibroblastic cells that together with endothelial cells, adipocytes, smooth muscle cells, reticular cells and osteoblasts, form the bone marrow stroma (Banfi, Bianchi et al. 2002). The bone marrow stroma exists alongside malignant cells, pericytes, endothelial progenitor cells, dendritic cells, and the extracellular matrix to form the greater bone marrow microenvironment or BMM. BMSCs are able to support haematopoeisis and harbour the potential to differentiate towards osteogenic, chondrogenic and adipogenic lineage and are therefore believed to provide the elements necessary for the perpetuation and expansion of haematopoietic cells (Banfi, Bianchi et al. 2002).

The ability of BMSCs to support haematopoietic cell growth was initially shown using murine BMSCs which inhibited spontaneous apoptosis of the UT-7 cell line, and of primary lymphoma cells (Weekes, Pirruccello et al. 1998). Long-term bone marrow stromal cells (LTBMC) from patient samples were shown to regulate myeloma cell growth *in vitro* via production of IL-6, possibly via induction of a functional IL-6 receptor on the tumour cells (Bloem, Lamme et al. 1998). These results supported the concept that BMSC/myeloma tumour cell interaction may be essential in the pathogenesis of myeloma. Subsequently, the importance of BMSCs in regulating drug response and apoptosis in MM, has been clearly demonstrated (Bertrand, Eckfeldt et al. 2000).

1.4.5 Bone marrow stromal cell lines – HS-5

BMSCs can be isolated from iliac crest bone marrow aspirates based on their rapid adherence to culture flasks and their fibroblastic-like cell growth (Digirolamo, Stokes et al. 1999), however, extensive *in vitro* expansion is required to obtain enough cells to use in drug activity assays given the low frequency of BMSCs in a marrow sample. Thus, several different BMSC lines have been generated from different components of the bone marrow stroma, such as HS-27 (an epithelioid cell line), HUVEC-C (human umbilical vein endothelial cell line) BMEC-1 (bone marrow endothelial cell line) and the murine MS-5 stromal cell line, but the most commonly used is the human fibroblastoid

cell line, HS-5 (Jaffe, Nachman et al. 1973; Roecklein and Torok-Storb 1995) which we have employed in our myeloma co-culture assay.

HS-5 is an immortalised, human BMSC line, generated using the E6 and E7 human papillomavirus genes. It quickly and reproducibly forms feeder monolayers, secretes significant levels of cytokines including IL-6, IL-8 and GM-CSF, and is capable of sustaining the *ex vivo* proliferation of haematopoietic cells, without requiring additional growth factors (Roecklein and Torok-Storb 1995). HS-5 does not express major histocompatibility complex (MHC) class II antigens, CD34, endothelial markers or the haematopoietic marker CD45 (Garrido, Appelbaum et al. 2001).

HS-5 cells express fibronectin; collagen types I, III and IV; and vascular cellular adhesion molecule (VCAM-1), which may contribute to its proliferative effects (Torok-Storb, Iwata et al. 1999) and may confer resistance to a variety of cytotoxics (known as cell adhesion mediated-drug resistance or CAM-DR), as well as to FAS-mediated cell death in MM, CML and AML cells (Dalton 2002; Shain, Landowski et al. 2002). In support of this, HS-5 cells were shown to reduce spontaneous apoptosis in a panel of nine NHL cell lines and also protected them against mitoxantrone-induced apoptosis (Bendall, Daniel et al. 1994; Panayiotidis, Jones et al. 1996; Lwin, Hazlehurst et al. 2007). These studies concluded that protective signals from BMSCs from within the stromal microenvironment maintained residual lymphoid or myeloma cell longevity, leading to recurrence of the disease.

Lwin et al also showed that conditioned medium from HS-5 cultures protected lymphoma cells from drug-induced apoptosis, an effect which was greatly enhanced when cells were in direct contact with stroma. This suggested a role for soluble factors (environment mediated-drug resistance or EM-DR) as well as CAM-DR, in the survival and resistance of lymphoma cells (Lwin, Hazlehurst et al. 2007). The additive antiapoptotic effects of soluble factors and stroma were further observed in studies using HS-5 cells separated from AML cells with transwell inserts (Garrido, Appelbaum et al. 2001; Konopleva, Konoplev et al. 2002).

The mechanisms by which stromal cells support tumour cell survival and drug resistance have not yet been fully elucidated, however studies suggest that NFκB may be involved through both the canonical and noncanonical pathways. The noncanonical pathway may be activated via stromal secretion of cytokines like B-cell activating factor (BAFF), lymphotoxin-β (LTb) and CD40L (figure 1.2), which sustain B-cell survival and via the NFκB–regulated antiapoptotic proteins c-IAP and x-IAP, which have been shown to be upregulated upon stromal adhesion (Garrido, Appelbaum et al. 2001; Lwin, Hazlehurst et al. 2007). This latter effect is suppressed by the proteasome inhibitor, bortezomib, and the specific IKK inhibitor SN50, which likely contributed to their effect in overcoming CAM-DR (Garrido, Appelbaum et al. 2001; Lwin, Hazlehurst et al. 2007).

In addition to that already described, the studies referred to above also demonstrated the use of HS-5 cells in studying the activity of drug therapies in the presence of a stromal microenvironment. This model could therefore be used to study the effects of bortezomib in the bone marrow microenvironment (BMM) as recent studies have demonstrated (Baumann, Mandl-Weber et al. 2009; Baumann, Mandl-Weber et al. 2009; Emmons, Gebhard et al. 2011). As part of the current study, we aimed to replicate previous findings with bortezomib in order to validate the use of our MM coculture model, and in order to suggest more effective combination therapies.

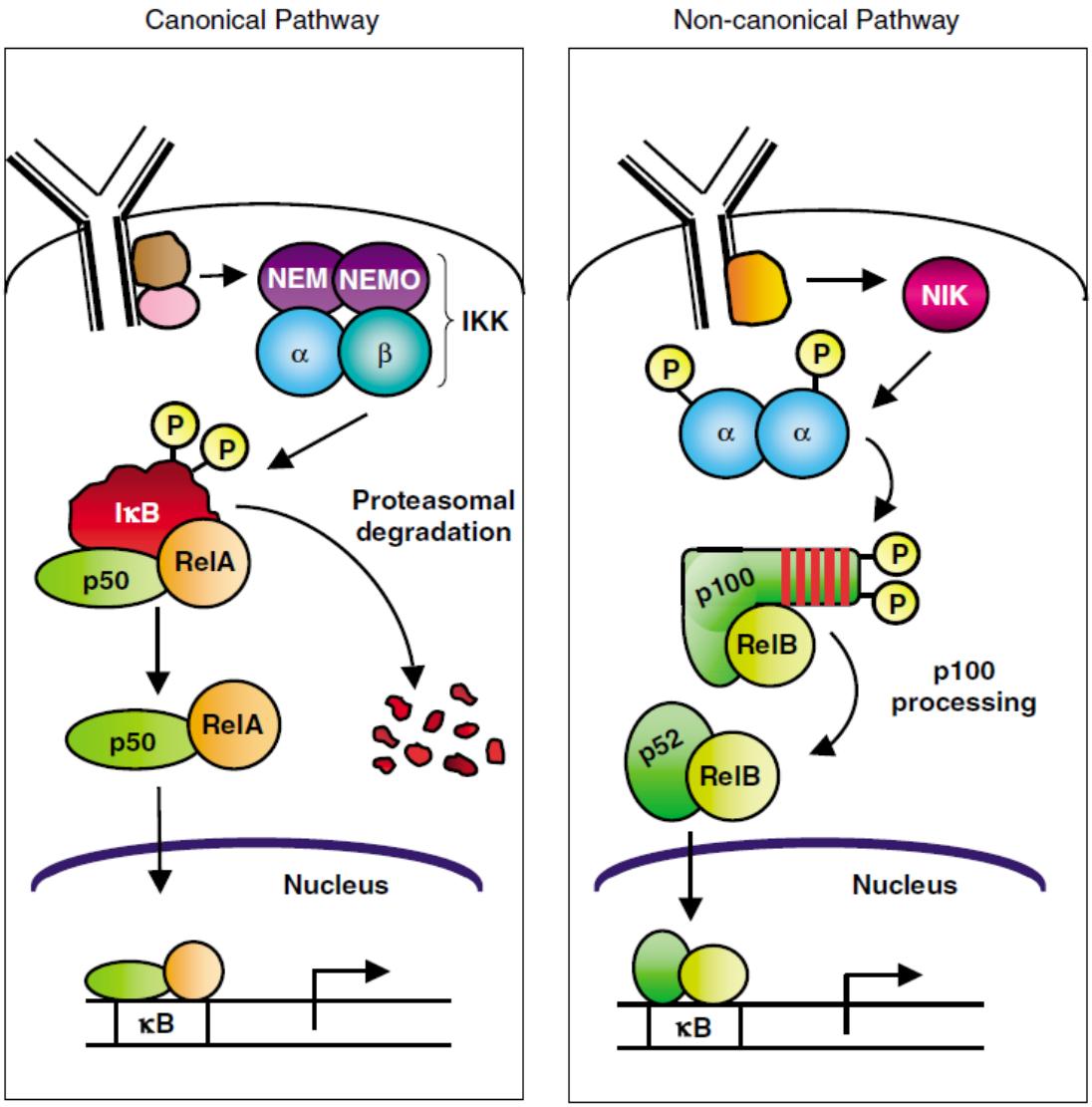

Figure 1.2 NF-κB signal transduction pathways. In the canonical NF-κB pathway, NF-κB dimers such as p50/RelA are maintained in the cytoplasm by interaction with an IκB molecule. Binding of a ligand to a cell surface receptor (e.g., tumour necrosis factor-receptor (TNF-R) or a Toll-like receptor) recruits adaptors (e.g., TRAFs and RIP) to the cytoplasmic domain of the receptor. These adaptors recruit an IKK complex (containing the α and β catalytic subunits and 2 molecules of the regulatory scaffold NEMO) thereby activating it. IKK then phosphorylates IκB at 2 serine residues, which leads to its ubiquitination and degradation by the proteasome. NF-κB then enters the nucleus to turn on target genes. The non-canonical pathway differs from the canonical pathway in that only certain receptor signals (e.g. LTb, BAFF & CD40L) activate this pathway and because it proceeds through an IKK complex that contains 2 IKKα subunits (but not NEMO). Here, receptor binding leads to activation of the NF-κB-inducing kinase NIK, which phosphorylates and activates an IKKα complex, which in turn phosphorylates 2 serine residues of p100, leading to its partial proteolysis and liberation of the p52/RelB complex (Gilmore 2006).

1.5 Significance of the bone marrow microenvironment in MM

1.5.1 Development of drug resistance

As described above, the BMM is a heterogeneous mix of many different cell types and some of these cell types, specifically bone marrow endothelial cells (BMECs) and BMSCs, are able to promote growth and resistance of myeloma cells to anti-MM treatment through cell-adhesion (direct) and cytokine-mediated (indirect) mechanisms (Asosingh, Gunthert et al. 2001; Mitsiades, Mitsiades et al. 2004).

Direct adherence of MM cells to cells of the BMM causes activation of pro-inflammatory cytokines in stromal cells, growth factors and angiogenic factors such as IL-6 and VEGF (figure 1.3) and activates a cascade of proliferative/antiapoptotic signaling pathways, including PI3K/Akt/mTOR, IKKα/NF-κB, Ras/Raf/MEK/MAPK and JAK/STAT3, Wnt as well as downstream effectors like caspase inhibitors, Bcl-2 and HIF1α (Hideshima, Nakamura et al. 2001; Lwin, Hazlehurst et al. 2007). The net effect of this adhesion-mediated signaling cascade is the emergence of CAM-DR in myeloma cells, which was demonstrated by the observed correlation between integrin-mediated fibronectin adhesion and a decreased response to doxorubicin (Damiano, Cress et al. 1999).

Indirect drug resistance occurs as a result of soluble factors, such as IL-6 (EM-DR), produced by the interaction of MM cells and BMSCs, and this can be additive to the protective effects of CAM-DR, thereby preventing drug-induced apoptosis (Garrido, Appelbaum et al. 2001; Konopleva, Konoplev et al. 2002; Nefedova, Landowski et al. 2003; Lwin, Hazlehurst et al. 2007). This may be responsible for the presence of minimal residual disease (MRD), which eventually leads to disease recurrence and the lack of curative outcomes with conventional therapies. These ‘de novo’ resistance mechanisms have also been observed in B-acute lymphoblastic leukemia (B-ALL), CLL, AML and NHL (Mudry, Fortney et al. 2000; Garrido, Appelbaum et al. 2001; Konopleva, Konoplev et al. 2002; Nefedova, Landowski et al. 2003). Furthermore, inter-patient

variability in the intrinsic biological behaviour of the BMM might influence the development of drug-related resistance in haematopoietic malignancies.

1.5.2 The role of interleukin-6

The most important of the soluble factors in myeloma is IL-6, which prolongs plasma cell survival in a paracrine and autocrine manner via stimulation by pro-inflammatory cytokines TNF-α, IL-1β and by IL-6 itself (Hitzler, Martinez-Valdez et al. 1991; Barton 2005) mostly triggered by adhesion of MM cells to BMSCs as already mentioned. CD40 stimulation also results in IL-6 production (Urashima, Chauhan et al. 1995). IL-6 production from BMSCs is predominantly mediated by NF-κB (Hideshima, Chauhan et al. 2002) and also by p38/MAPK, TGF-β and X-box binding protein (XBP-1) (Hayashi, Hideshima et al. 2004).

Expression of the receptor for IL-6 (IL-6R/gp80) can be detected on plasma cells from the majority of myeloma patients with active disease and functionality of IL-6R is required to activate the PI3-K/Akt and JAK/STAT3 intracellular signaling cascades that induce MM cell growth (Kishimoto, Akira et al. 1995; Klein, Zhang et al. 1995). This leads to expression of the antiapoptotic molecules, Bcl-XL and myeloid cell leukemia-1 (Mcl-1), resulting in suppression of dexamethasone-mediated apoptosis via activation of caspase-9 (Hideshima, Nakamura et al. 2001).

The IL-6R exists in both membrane-bound and soluble forms. An alternative route for growth stimulation is the association of gp130 (signal transducing unit) with a complex of IL-6 and soluble gp80 (sIL-R). This form of IL-6 signalling, known as trans-signalling, can thereby bypass the requirement for membrane-bound gp80/IL-6R thus allowing IL-6 signalling in cells that express either low or non-detectable surface IL-6R (Yasukawa, Futatsugi et al. 1992; Treon and Anderson 1998). Kaplan-Meyer analysis demonstrated that elevated levels of sIL-6R were associated with shorter survival as opposed to the longer survival found among patients with low levels of sIL-6R at the time of diagnosis (Kyrtsonis, Dedoussis et al. 1996; Stasi, Brunetti et al. 1998). Both IL-6 and sIL-R are found in high concentrations in the serum of MM patients and both serve as prognostic markers (Bataille, Jourdan et al. 1989; Gaillard, Bataille et al. 1993).

Thus inhibition of IL-6 release or disruption of its signaling pathways is a promising therapeutic strategy in MM. For example, the humanized anti-IL-6 monoclonal antibody 1339 showed antimyeloma activity in a preclinical model and inhibition of bone marrow turnover *in vitro* and *in vivo*(Fulciniti, Hideshima et al. 2009). Siltuximab (CNTO328) is a chimeric mAb with high affinity for IL-6 which has shown little efficacy as monotherapy in a phase II study in patients with relapsed/refractory MM; however more encouraging results were observed with the addition of dexamethasone (Voorhees, Chen et al. 2007) and its clinical evaluation is currently ongoing.

1.5.3 Interleukin-8

Interleukin-8 (IL-8/CXCL8) is a CXC chemokine associated with neutrophil migration and chemotaxis via activation of multiple intracellular signaling pathways including PI3K/Akt and MAPK/ERK signaling downstream of its G protein-coupled cell surface receptors CXCR1 and CXCR2 (Knall, Young et al. 1996; Knall, Worthen et al. 1997). Increased expression of IL-8 and/or its receptors has been characterised in cancer cells including myeloma cells, endothelial cells and neutrophils/tumour-associated macrophages suggesting that IL-8 may function as a regulatory factor within the tumour microenvironment (Pellegrino, Ria et al. 2005). Indeed IL-8 signaling promotes angiogenesis in endothelial cells, increases proliferation and survival of cancer cells and endothelial cells and infiltrating neutrophils at the tumour site. Its expression correlates with angiogenesis, tumourigenicity and metastasis of tumours in numerous xenograft and orthotopic *in vivo* models (Dong, Han et al. 2007) and has been implicated in regulating transcription of the androgen receptor in prostate cancer cells (MacManus, Pettigrew et al. 2007). In addition, stress and drug-induced IL-8 signaling has been shown to confer chemotherapeutic resistance in cancer cells (Viani, Peralta et al. 2006; Maxwell, Gallagher et al. 2007; Wilson, Wilson et al. 2008).

Therefore, inhibiting IL-8 signaling may be significant therapeutically in targeting the tumour microenvironment. Humanized monoclonal antibodies against IL-8 such as ABX-IL-8 has been shown to attenuate the growth of bladder cancer xenograft models (Mian, Dinney et al. 2003), to decrease the tumorigenenic and metastatic potential of A375SM and TXM-13 melanoma xenograft models, and to enhance the cytotoxicity of

chemotherapy in melanoma (Huang, Mills et al. 2002). In ovarian tumour xenografts use of liposome-encapsulated small interfering RNA (siRNA) suppressed IL-8 expression in causing growth inhibition, reduced microvessel density and importantly increased response to docetaxel (Merritt, Lin et al. 2008). Therefore, targeting IL-8 through using antibodies or siRNA has proven effective in solid tumours; however these strategies have not yet been evaluated in MM.

1.5.4 Vascular endothelial growth factor

Vascular endothelial growth factor (VEGF) is regarded as the most important pro-angiogenic factor in cancer (Dong, Han et al. 2007). Serum and plasma levels of IL-6, IL-8 and VEGF are increased in patients with MM and reflect disease severity (Klein, Wijdenes et al. 1991; Nachbaur, Herold et al. 1991; Emile, Fermand et al. 1994; Alexandrakis, Passam et al. 2003; Kuku, Bayraktar et al. 2005). In other haematological malignancies it has been found that pre-treatment plasma levels of IL-6, IL-8 and VEGF were the highest out of eight angiogenesis-related parameters (Negaard, Iversen et al. 2009).

Elevated levels of VEGF however do not necessarily imply that anti-VEGF drugs are effective, as pre-treatment plasma levels of VEGF did not correlate with response to the anti-VEGF monoclonal antibody bevacizumab (Avastin) in metastatic colorectal cancer or advanced pancreatic cancer (Jubb, Oates et al. 2006). On the other hand, the immunomodulatory drugs thalidomide and lenalidomide have been shown to reduce secretion of VEGF and IL-6 in MM/stromal cocultures resulting in reduced MM growth and angiogenesis (Gupta, Treon et al. 2001; Hideshima, Chauhan et al. 2001; Ribatti and Vacca 2005) and ongoing studies are evaluating the efficacy of bevacizumab in patients with relapsed or refractory MM, with or without thalidomide (Podar, Chauhan et al. 2009). Furthermore, bortezomib has also been found to display antiangiogenic effects including inhibition of caveolin-1 activation which is required for VEGF-mediated MM cell migration (Podar and Anderson 2006), thus studies exploring the combination of bortezomib with bevacizumab or with sorafenib (which targets VEGF1, and VEGF2 amongst other kinases) are also ongoing.

1.5.5 Macrophage inflammatory protein-1 alpha

Macrophage inflammatory protein-1 alpha (M1P-1α) is a chemokine that has also been characterised as a potent osteoclast stimulatory factor in MM (Choi, Cruz et al. 2000). Its levels are elevated in bone marrow plasma of patients with active MM. This correlates with the presence of lytic lesions (Choi, Cruz et al. 2000; Abe, Hiura et al. 2002) and has been associated with survival (Terpos, Politou et al. 2003). It also stimulates proliferation, migration and survival of plasma cells (Lentzsch, Gries et al. 2003) and blocking its activity by either neutralising antibodies or antisense oligonucleotides resulted in a reduction in bone disease as well as tumour burden in MM animal models (Choi, Oba et al. 2001).

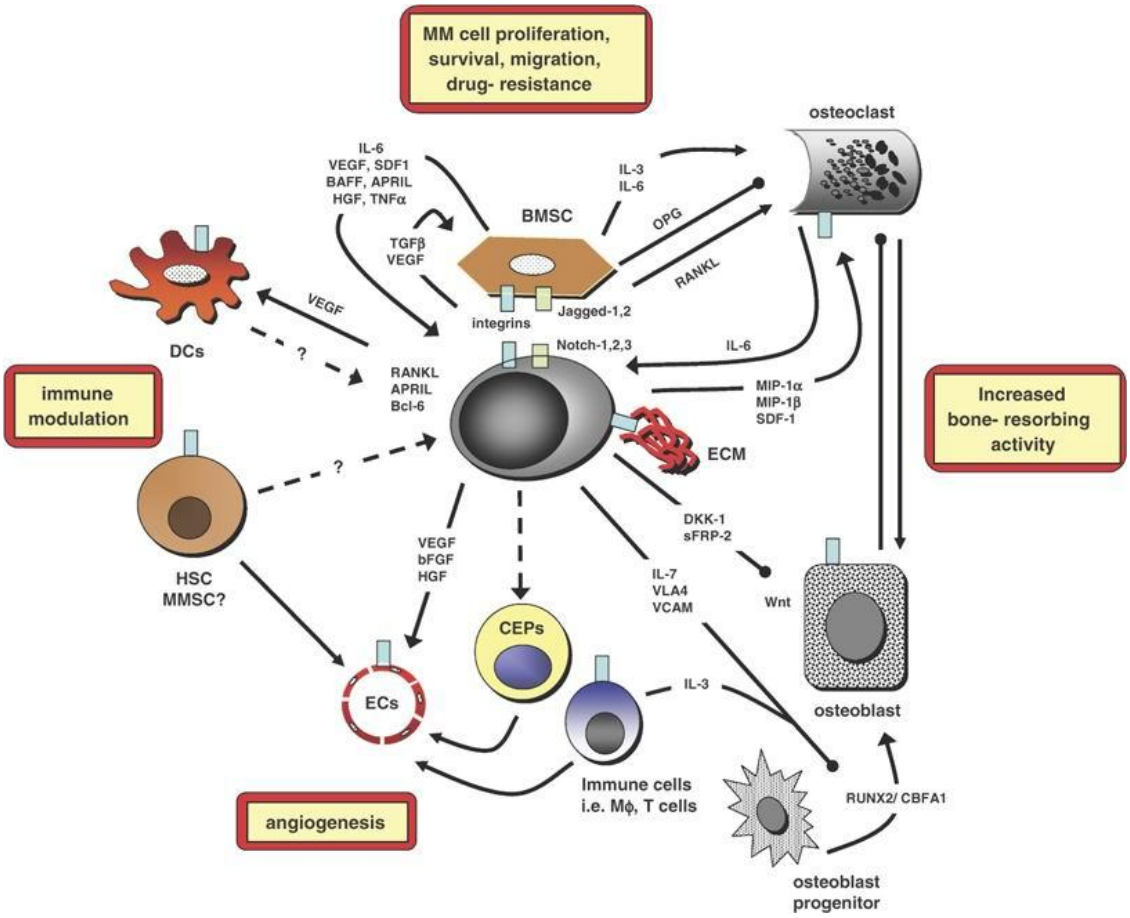

Figure 1.3 The MM cell and its interactions with the cellular and non-cellular and non-cellular bone marrow compartments (Podar, Chauhan et al. 2009). In addition to those mentioned above, other chemokine receptor ligands stromal derived factor-1α (SDF-1α) also show a stimulatory effect on osteoclast precursors and RANKL expression (Okamatsu, Kim et al. 2004; Lisignoli, Piacentini et al. 2007; Meads, Hazlehurst et al. 2008). The cytokines and growth/angiogenic factors IL-3, IL-6, IL-8, insulin-like growth factor (IGF-1), tumour necrosis factor-α (TNF-α), vascular endothelial growth factor (VEGF), hepatocyte growth factor (HGF) and basic fibroblast growth factor (bFGF) may also contribute to osteoclastogenesis and growth in the BMM (Chauhan, Uchiyama et al. 1996; Podar, Tai et al. 2001; Nefedova, Landowski et al. 2003; Hideshima, Podar et al. 2004; Mitsiades, Mitsiades et al. 2004; Mitsiades, Mitsiades et al. 2004; Podar and Anderson 2005; Mitsiades, Mitsiades et al. 2006) by stimulating endothelial cell growth, migration, mobilisation of endothelial precursors, vascular development and proliferation of stromal cells in MM (Bellamy, Richter et al. 1999; Hicklin and Ellis 2005). VEGF is directly produced by PCs, moreover, in a paracrine loop, where PC-derived VEGF stimulates IL-6 and VEGF secretion in stromal cells, and stromal cell-derived IL-6 promotes proliferation, survival and VEGF production in PCs (Schweigerer, Neufeld et al. 1987; Dankbar, Padro et al. 2000; Bisping, Leo et al. 2003). Thus, a bi-directional relationship exists between MM cells and their local BMM.

1.6 Cell cytotoxicity assays used to determine *in vitro* drug sensitivity

In vitro assays to determine tumour cell kill commonly employ dye-exclusion to differentiate between live and dead cells and inhibition of cellular metabolism to measure cell viability. These assays allow measurement of cell viability or cell death in proliferating and also in non-proliferating or slowly proliferating cells. The sections below contrast and compare the most commonly used cell cytotoxicity assays. The last 2 sections describe the trypan blue, guava and ATP assays, all of which we have used at different points during the course of this project.

1.6.1 The MTT assay

In 1983 Mossman described the microtetrazolium (MTT) assay which relies on the ability of mitochondria in live cells to reduce a soluble yellow tetrazolium salt (3-4, 5-dimethylthiazol-2, 5-diphenyl tetrazolium bromide) into insoluble blue-purple formazan crystals (Mosmann 1983). The absorbance intensity of the formazan precipitate can be read on a 96-well plate reader and is linearly correlated to the number of viable cells in the suspension. The MTT assay is much more efficient than its predecessors as result quantification is possible in 15mins vs. 12-16hrs in the DiSC assay. However, its application in the National Cancer Institute (NCI) drug screening program revealed disadvantages including requiring several wash steps which limits its practicability in a broad testing program (Friedman and Glaubiger 1982). Furthermore, the results may vary under a number of conditions such as MTT concentration and incubation time, thus leading to some large intra- and inter-assay variability (Price and McMillan 1990). An improvement on the MTT assay, the MTS assay is now available which does not require any wash steps. However, both assays are based on metabolic/mitochondrial function which means that their results can be influenced by glucose, pH, NADH and NADPH (Jabbar, Twentyman et al. 1989; Vistica, Skehan et al. 1991).

1.6.2 The SRB assay

To optimize laboratory efficiency, an alternative endpoint based on the use of a protein-binding dye, sulforhodamine B (SRB) was introduced into the NCI system

(Skehan, Storeng et al. 1990). The SRB assay was simpler, faster, more stable and more sensitive than the MTT assay, provided better linearity with cell number and higher reproducibility. It was also less sensitive to environmental fluctuations and was independent of intermediary metabolism (Skehan, Storeng et al. 1990). A major drawback of the SRB assay is that it only allows determination of total protein content such that differentiation of live and dead cells is not possible. Furthermore, the staining protocol involves time consuming and time sensitive steps like plate washing and cell fixation (Skehan, Storeng et al. 1990; Griffon, Merlin et al. 1995).

Despite these drawbacks, and due to its practical advantages for large-scale screening, the SRB assay has been adopted for routine use in the NCI *in vitro* antitumour drug screening program (Monks, Scudiero et al. 1991; Grever, Schepartz et al. 1992). Using the SRB assay, for each drug-cell line combination, a dose-response curve is generated and three levels of effect are calculated. Growth inhibition of 50% (GI_{50}) which is the drug concentration resulting in a 50% reduction in the net protein increase in control cells during the drug incubation, is calculated from $100 \times [(T-T_0)/(C-T_0)] = 50$, where C = control optical density; T = test optical density and T_0 = optical density at time zero. The drug concentration resulting in total growth inhibition (TGI) is calculated from $T = T_0$, where the amount of protein at the end of drug incubation is equal to the amount at the beginning. The LC_{50} is the concentration of drug causing a 50% reduction in the measured protein at the end of the drug treatment as compared to that at the beginning, indicating a net loss of cells following treatment. The LC_{50} is calculated from $100 \times [(T-T_0)/T_0] = -50$.

Values are calculated for each of these three parameters if the level of activity is reached; however, if the effect is not reached or is exceeded, the value for that parameter is expressed as greater or less than the maximum or minimum concentration tested (Monks, Scudiero et al. 1991). These three different mean response parameters allow the results to be summarised in a more informative manner.

1.6.3 The ATP Assay

The nucleotide adenosine triphosphate (ATP) is the principal energy donor present in all metabolically active cells (Crouch, Kozlowski et al. 1993). Cell injury or oxygen / substrate depletion results in a rapid decrease in cytoplasmic ATP. Thus measurement of cellular ATP can accurately indicate the functional integrity of living cells. The most successful ATP assay technique uses a bioluminescent method which yields a high sensitivity and wide dynamic range (Kurbacher, Mallmann et al. 1994; Andreotti, Cree et al. 1995). The reaction is catalyzed by the enzyme luciferase obtained from the firefly (Photinuspyralis). The Mg2+ converts the luciferin into a form which is capable of being catalytically oxidized by the luciferase in a high quantum yield chemiluminescent reaction, according to the following equation:

$$\text{ATP} + \text{luciferin} + O_2 \xrightarrow[Mg^{2+}]{\textbf{Luciferase}} \text{Oxyluciferin} + \text{AMP} \_ PP_i + CO_2 + \text{Light}$$

Under optimum conditions, light intensity is linearly related to ATP concentration where one molecule of ATP produces one photon. Cellular ATP can be measured by direct lysis of the cells with suitable detergent; the released ATP is then free to react with the luciferin-luciferase leading to light emission at 562 nm.

Advantages of this assay include its simple application which provides quick measurement readouts, not requiring any wash steps. Furthermore, it is highly sensitive; ATP can be measured in picomolar concentrations and is highly reproducible (Andreotti, Cree et al. 1995). Any form of cell injury results in a rapid decrease in cytoplasmic ATP levels, therefore the ATP assay reflects cell viability, as well as cell number as each individual cell contains ATP. This makes it a convenient alternative to tritiated thymidine uptake and the SRB or MTT assay in cell proliferation and cell cytotoxicity assays (Crouch, Kozlowski et al. 1993). Finally the assay can also be used to detect the effects of cytokines on cell proliferation (Crouch, Kozlowski et al. 1993). The ATP assay was found to accurately predict both clinical response and patient survival in primary ovarian cancer. In two prospective clinical trials in patients with heavily

pretreated ovarian cancer, chemotherapy selected for each patient by the ATP assay was found to nearly triple the response rates and double the survival compared to empirically chosen treatments (Andreotti, Cree et al. 1995; Kurbacher, Cree et al. 1998; Kurbacher and Cree 2005). It is thus deemed the best standard test for chemosensitivity testing of non-haematological tumours (Kurbacher and Cree 2005).

1.6.4 The Trypan Blue and Guava ViaCount Assays

Membrane integrity assays detect the loss of membrane integrity during the later stage of cell death. The trypan blue and Guava ViaCount fall under this category; both assays consist of dyes such as propidium iodide (PI) that are impermeable to healthy cells but can permeate through compromised membranes of dying cells. These dyes are either visible or fluorescent and can be counted manually using a heamacytometer or with an automated flow cytometer, respectively. The trypan blue assay involves manual cell counting using a Neubauer-type cell counting chamber. Cell samples are stained with an equal volume of 0.4% trypan blue solution, transferred to the counting chamber and scored under a light microscope for the live (colourless) and dead (blue) cell count. Total cell concentration and % viability can be derived from this assay. Limitations of the trypan blue assay include interpreting and classifying particles based on their size and their 'blueness', which results in subjectivity and imprecision. In addition, trypan blue has been reported in the literature to consistently overestimate cell viability (Altman, Randers et al. 1993; Mascotti, McCullough et al. 2000).

In comparison, the Guava ViaCount assay provides a more accurate and complete evaluation of cells. The Guava instrument is based on a capillary flow technology which enables rapid analysis of individual cells and the laser-based detection system allows for high sensitivity (Terashita 2003). The ViaCount Flex reagent contains a combination of two nucleic acid dyes which allows measurement of the size of each particle passing through the flow cell, along with its fluorescence in two spectrally distinct channels. The first of these dyes is membrane permeant, thus stains all nucleated cells, while excluding cellular debris. The second dye is a viability dye which penetrates and stains dead and dying cells with compromised membrane integrity, and is excluded by cells with intact membranes (Terashita 2003). The assay thus provides cell number as well

as cell viability information which allows differentiation between cytotoxic or cytostatic drug effects.

1.7. Novel therapies investigated in this study

1.7.1 Proteasome inhibitors

1.7.1.1 Function of the proteasome

The proteasome is a 2,000kDa adenosine triphosphate (ATP)-dependent multicatalytic enzyme complex forming the ubiquitin-proteasome pathway (UPP) that mediates the degradation of damaged, oxidised or misfolded intracellular proteins which are targeted for degradation by the conjugation of polyubiquitin chains to lysine residues of the protein (Nencioni, Grunebach et al. 2007). It represents the main protein degradation pathway in eukaryotic cells (Goldberg, Akopian et al. 1997; Voges, Zwickl et al. 1999; Kisselev and Goldberg 2001) and is expressed in the nucleus and cytoplasm. Polyubiquitinated proteins are recognized by the 19S regulatory subunits of the 26S proteasome, which cleaves the polyubiquitinated chain from the protein substrate and the denatured protein is degraded in the proteolytic 20S core, in an ATP-dependent fashion (figure 1.4) (Nussbaum, Dick et al. 1998).

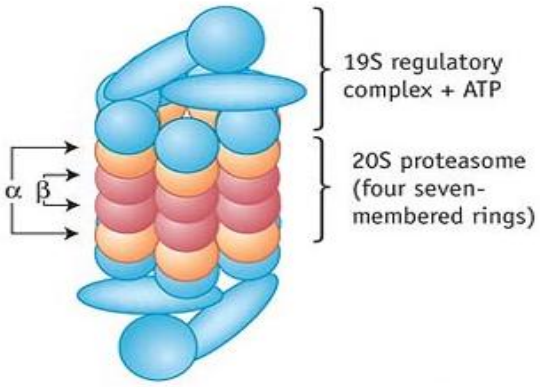

Figure 1.4 The 26S proteasome complex (Adams 2003).

The proteasome plays a key role in cellular metabolism and in controlling malignancy by its action on many proteins involved in tumourigenesis. These include transcription factors such as NF-κB and its inhibitory protein IκB, N-myc, SNAIL and hypoxia inducible factor 1 alpha (HIF1-α); cell cycle proteins such as the cyclins, cyclin-dependent kinases and their inhibitors p21 and p27; signaling molecules such as c-fos and c-jun; tumour suppressor genes such as p53; cell adhesion molecules such as β-catenin and apoptosis related proteins such as Bax and Bcl-2 (Myung, Kim et al. 2001; Adams 2003). In addition, many oncogenes and tumour suppressor genes are themselves involved in ubiquitination or are deubiquitinating enzymes, for example E3 ligases including Mouse Double Minute 2 homolog (MDM2), which regulates p53 and is over expressed in many cancers. Inhibition of the 26S proteasome results in the accumulation of these substrates and therefore causes cell cycle disruption and promotes cell death via multiple pathways.

1.7.1.2 Effects of proteasome inhibition

Malignant cells seem to be much more sensitive to the proapoptotic effects of proteasome inhibition than normal cells. For example, plasma cells from MM patients were 20–40 times more sensitive to bortezomib-mediated apoptosis than Peripheral Blood Mononuclear Cells (PBMCs). Fibroblasts and lymphoblasts transformed with *ras* and *c-myc* were up to 40-fold more susceptible to proteasome inhibitor-induced apoptosis than primary fibroblasts or non-transformed human lymphoblasts (Orlowski, Eswara et al. 1998; Hideshima, Richardson et al. 2001). This effect is consistent among other proteasome inhibitors for example the natural inhibitor lactacystin, induced apoptosis of CLL cells and oral squamous-cell carcinoma cells at concentrations that do not affect normal lymphocytes or gingival fibroblasts; and actively proliferating endothelial cells were 340-fold more sensitive to lactacystin-induced apoptosis than contact inhibited quiescent cells (Masdehors, Omura et al. 1999). Similarly, MG132 induces apoptosis of acute myelogenous leukemia (AML) stem cells, but has little effect on normal CD34+ stem cells (Guzman, Swiderski et al. 2002).

A mechanism for this has yet to be fully elucidated but it may be due to aberrantly cycling malignant cells with higher cellular replication rates leading to accumulation of

defective proteins, which are likely to rely on the proteasome for their degradation. In support of this, compared to normal lymphocytes, B-CLL cells have a three-fold higher level of chymotryptic-like proteasome activity and higher levels of nuclear ubiquitin-conjugated proteins (Masdehors, Omura et al. 1999). Abnormal or constitutive activation of the NF-κB pathway in malignant cells may also explain differential sensitivity as this has been shown to drive cell survival pathways in a variety of malignancies including multiple myeloma, Hodgkin's disease, subtypes of lymphoma, ALL, and a variety of solid tumours (Kordes, Krappmann et al. 2000; Munshi 2004).

1.7.1.3 Bortezomib (Velcade™, Milennium Pharmaceuticals Inc.)

A number of drugs inhibit the proteolytic activity of the 20s core of the proteasome, which contains the catalytic protease activity. There are five classes of proteasome inhibitors: peptide aldehydes, peptide vinyl sulphones, peptic boronates, peptide epoxyketones and β-lactones. The peptic boronates are the most progressed and were developed by Adams *et al* by substituting the aldehyde with boronic acid, creating compounds that form covalent and reversible complexes with improving potency and selectivity compared with their corresponding aldehydes (Adams 2003). Amongst a series of these compounds developed and screened *in vitro* using the standard NCI panel of 60 human tumour cell lines, bortezomib demonstrated promising *in vitro* cytotoxic activity. Formerly PS-341, (Velcade®), bortezomib is a dipeptide boronic acid analog that specifically inhibits chymotryptic-like activity of the proteasome by interacting with a threonine residue located on the β subunit. It is highly potent with a Ki of 0.6nM, binds to the proteasome with very high affinity, and dissociates slowly conferring stable but reversible proteasome inhibition (Figure 1.5).

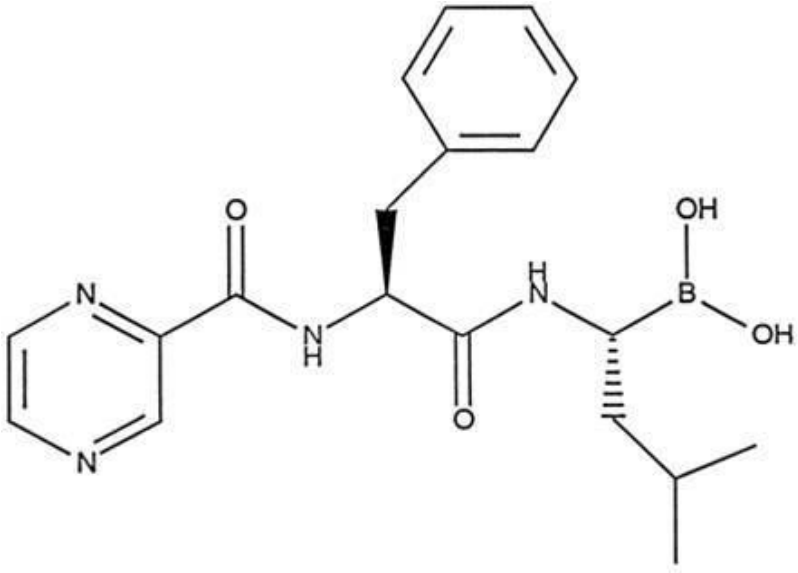

Figure 1.5 The chemical structure of bortezomib.

1.7.1.4 Bortezomib – Antitumour Effects

Bortezomib has demonstrated potent cytotoxic and growth inhibitory activity in a number of malignant cell lines, tumour xenograft models and nude mouse models. Its effects include causing rapid dose-dependent apoptosis, suppressing transcription factors and cell growth, and preventing the development of tumours (Schenkein 2002; Adams 2003; Adams and Kauffman 2004). In addition, in myeloma cells, bortezomib also inhibits angiogenesis leading to inhibition of tumour growth *in vivo*, and prolonged overall survival (LeBlanc, Catley et al. 2002). These effects have also been demonstrated in squamous cell carcinoma, human prostate cancer and lung mouse xenograft models (Grisham, Palombella et al. 1999; Teicher, Ara et al. 1999; Sunwoo, Chen et al. 2001).

1.7.1.5 Bortezomib - Mechanism of Action

The precise mechanism by which bortezomib induces cell death has yet to be fully established but much evidence has implicated the transcription factor NFκB, which was first observed as being important in the survival of MM cells and BMSCs (Chauhan, Uchiyama et al. 1996).

In quiescent cells NFκB is bound and inhibited in the cytoplasm by IκB, and is induced in response to stress from a wide variety of external signals, such as chemotherapy. IκB is then phosphorylated, ubiquinated and degraded by the proteasome, allowing NFκB to translate to the nucleus where it activates antiapoptotic and cell growth genes, causing increased synthesis of growth factors, cell adhesion molecules, and angiogenesis factors. The stabilization of IκB through proteasome inhibition therefore prevents NFκB activation, making cells more susceptible to stressors and apoptosis (Figure 1.2 & 1.6) (Adams 2003; Adams and Kauffman 2004).

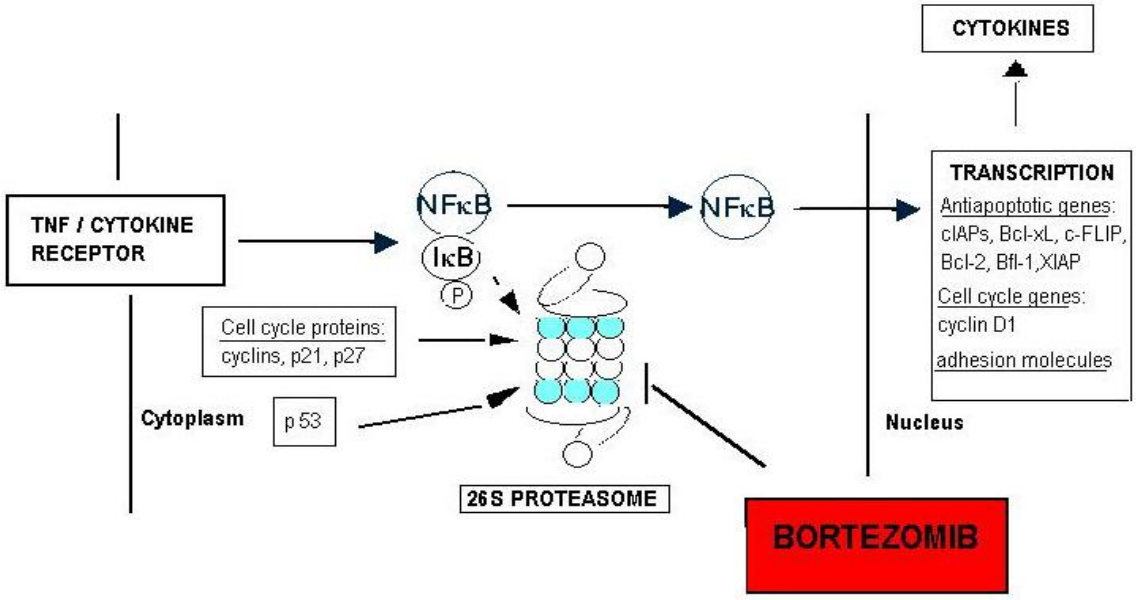

Figure 1.6 The possible mechanisms of action by which inhibition of the proteasome by bortezomib may lead to cell death.

In addition, certain lymphoid malignancies such as MM, MCL and FL demonstrate constitutive activation of NFκB and are therefore addicted to NFκB-induced survival signals. Furthermore, constitutive NFκB activation in plasma cells and BMSCs from MM patients has been shown to regulate cell adhesion molecule expression and induce cytokine expression and secretion, resulting in a positive feedback loop for further NFκB activation (Chauhan, Uchiyama et al. 1996). A functional proteasome is thus vital for the survival of these cells. Furthermore, studies have shown that NFκB activity correlates with chemo-resistance by protecting against apoptosis for example in MM cells treatment with SN50, a specific NFκB inhibitor, led to downregulation of

antiapoptotic proteins Bcl-2, A1, XIAP, cIAP-1, cIAP-2, and survivin, up-regulation of Bax, mitochondrial cytochrome c release, and activation of caspase-9 and caspase-3 (Hideshima, Richardson et al. 2001; Mitsiades, Mitsiades et al. 2002).

In MCL, bortezomib has been shown to downregulate the expression of the NFκB-activated gene, cyclin D1 (which is constitutively over expressed) leading to cell cycle arrest, further contributing to the apoptotic effect of bortezomib in MCL (Chiarle, Budel et al. 2000). In myeloma, bortezomib blocks constitutive, and cell adhesion induced activation of NFκB-dependent cytokine secretion in BMSCs thereby inhibiting binding of MM cells in the bone marrow microenvironment (BMM) (Hideshima, Richardson et al. 2001). However, NFκB inhibition only partially abrogated MM cell proliferation (20 – 50%) using the specific NFκB inhibitor, PS1145. Similarly in renal cell carcinoma cell lines, selective inhibition of NFκB was not sufficient to induce apoptosis (Hideshima, Chauhan et al. 2002). Therefore, NFκB-independent effects must also play a role in the induction of apoptosis by bortezomib.

1.7.1.6 Additional molecular targets of bortezomib

About 70 percent of all proteins are degraded by the proteasome therefore there is potentially a wide range of effects resulting from proteasome inhibition by bortezomib. For example, in myeloma, bortezomib was shown to activate p53 by phosphorylation of MDM2 and to induce apoptosis in chemotherapy-resistant MM cells despite activation of $p21^{waf1}$ and $p27^{cip1}$. In addition, bortezomib directly inhibited mitogen-activated protein kinase (MAPK) growth signaling and subsequently, DNA repair, via cleavage of the DNA-dependent protein kinase catalytic subunit (DNA-PKCs) (Hideshima, Richardson et al. 2001; Hideshima, Mitsiades et al. 2003). Furthermore, microarray gene expression profiling showed that bortezomib downregulates the transcription of genes that encode growth factors, with an associated induction of apoptotic, ubiquitin/proteasome and stress response gene transcription such as Hsp-27 and Hsp-70, in MM and NHL cells (Mitsiades, Mitsiades et al. 2002; Mitsiades, Mitsiades et al. 2002).

Microarray gene profiling also revealed that bortezomib rapidly induced a large number of genes associated with endoplasmic reticulum (ER) stress in pancreatic cancer and neuronal cells, head and neck squamous cell carcinoma cells and non-small cell lung cancer. This was associated with induction of G2/M cell cycle arrest, phosphorylation of Bcl-2, induction of apoptosis via caspase-9 and caspase-12, an increase in mitochondrial permeability associated with reactive oxygen species (ROS) generation, cytochrome c release and induction of poly(ADP-ribose) polymerase (PARP) cleavage (Ling, Liebes et al. 2003; Fribley, Zeng et al. 2004; Nawrocki, Carew et al. 2005; Nawrocki, Carew et al. 2005; Nawrocki, Carew et al. 2006). These effects were independent of p53, and the G2/M cell cycle arrest was associated with induction of $p21^{cip/waf-1}$, cyclin A, cyclin B, and their respective kinases (Ling, Liebes et al. 2003). This work demonstrates the numerous targets of bortezomib, which appear to contribute to cell death in these cell lines.

Proteasome inhibition with bortezomib has become an attractive treatment option especially in light of the potent *in vitro* and *in vivo* activity profile of bortezomib, and proven efficacy clinically in MM. Bortezomib has become the first proteasome inhibitor to be used clinically (Schenkein 2002; Adams and Kauffman 2004) and is approved for first treatment of MM in the U.S. and second-line treatment in Europe including the UK. The U.S. FDA granted bortezomib fast-track designation for relapsed and refractory MCL on the basis of data from 4 phase II trials of the agent in this treatment setting (Leonard, Furman et al. 2006). Furthermore, results and preliminary data from 9 phase II trials have shown bortezomib to have activity in a number of NHL subtypes including FL, Marginal Zone Lymphoma (MZL), MCL, and Waldenström's Macroglobulinemia (WM), suggesting its potential use in lymphoma, where it is currently being investigated.

1.7.2 Histone deacetylase (HDAC) inhibitors

1.7.2.1 Histones and cancer

In all eukaryotic cells, DNA exists in a condensed form, wrapped around histone proteins; a complex referred to as the nucleosome. This condensed chromatin

structure is less accessible to transcription factors and thus leads to a transcriptionally silent state. This state is facilitated by histone deacetylase (HDACs) enzymes, which remove acetyl groups from histones. Histone acetyltransferase (HAT) enzymes oppose the action of HDACs by acetylating histones which results in a loosened nucleosome structure allowing access of the transcriptional machinery to the DNA template and activating gene transcription (figure 1.7). In this manner, the action of HDACs and HATs controls gene expression (Bi and Jiang 2006).

Importantly, these proteins are responsible for the regulation of a large number of non-histone proteins, including enzyme cofactors, molecular chaperones and proteins involved in DNA repair, cell cycle arrest and apoptosis (Glozak and Seto 2007). There are 18 different known human HDAC enzymes, which can be divided into two families (the Classical and the Sirtuin families) and four classes (Noureen, Rashid et al. 1997; Khochbin, Verdel et al. 2001): class I (HDAC1, 2, 3 and 8) class IIa (HDAC4, 5, 7 and 9), class IIb (HDAC 6 and 10), class III (SIRT1 to 7) and class IV (HDAC11) (Walkinshaw and Yang 2008). Class I, II and IV HDACs have zinc as a cofactor whereas class III HDACs (sirtuins) use nicotinamide adenine dinucleotide (NAD)+ as the cofactor (Noureen, Rashid et al. 1997). Class I HDACs are localized mainly in the nucleus and are variably expressed whereas Class II HDACs are localized mainly in the cytoplasm and have tissue-specific expression. In regulating cell proliferation, class I HDACs are more significant than the class II enzymes (Park, Jung et al. 2004).

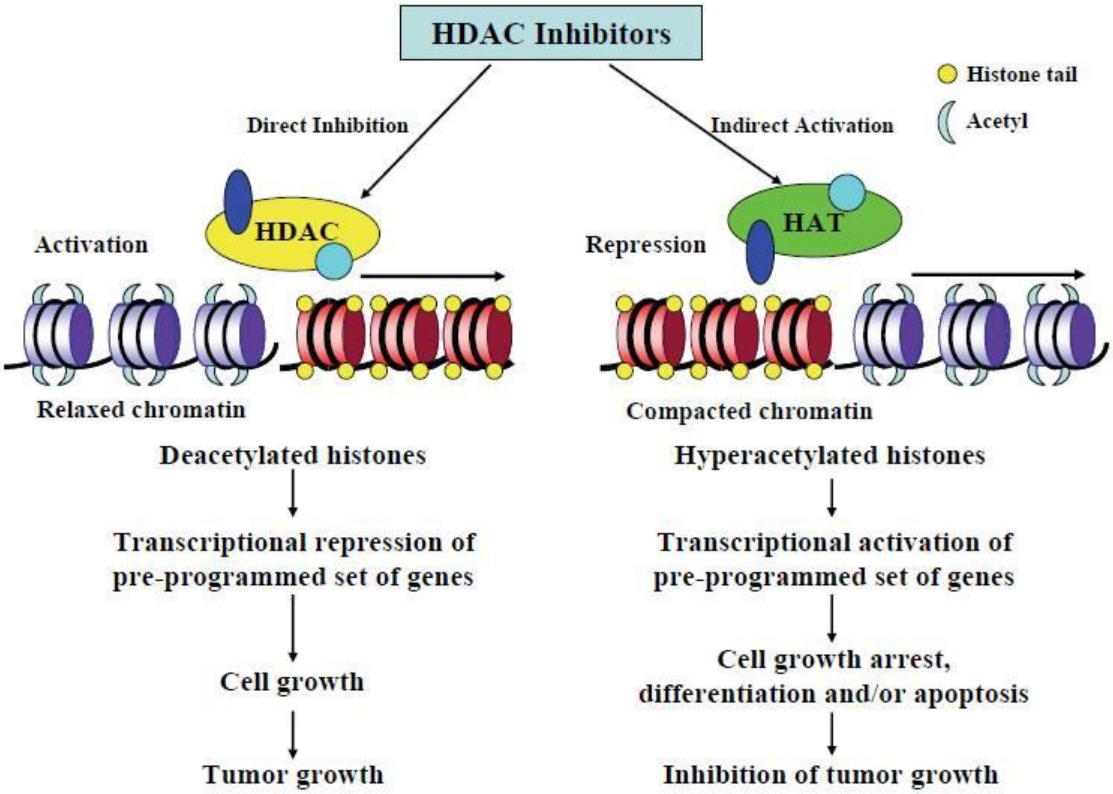

Figure 1.7 Proposed molecular mechanism of HDAC inhibitors in anticancer effects (Bi and Jiang 2006).

It is now clear that deacetylation of histones is associated with transcriptional repression and epigenetic silencing which is frequently observed in cancer. Research suggests that over expression of HDACs lead to aberrant gene repression, including a decrease in the expression of tumour suppressor genes (Bolden, Peart et al. 2006).HDACs are typically over-expressed in tumour cells from colon, breast, prostate and other cancers (Zhang, Freitas et al. 2004; Zhu, Huber et al. 2004; Wilson, Byun et al. 2006), thus inhibiting them can be a selective means of over expressing genes that promote growth arrest, differentiation and apoptosis of tumour cells, making HDACs inhibition a promising approach for the treatment of various cancers.

1.7.2.2 HDAC Inhibitors

HDAC inhibitors (HDACis) have thus emerged as an important class of antitumour agents (Elaut, Rogiers et al. 2007). However, the molecular basis of anticancer activity of these agents is not completely clear. Evidence suggests that HDACis can induce

differentiation, cell growth arrest and apoptosis of tumour cells through regulation of gene expression, specifically by promoting cell cycle arrest at the G1/S checkpoint (Fang 2005). This is thought to contribute to their anticancer activity, as it leads to upregulation of a variety of pro-apoptotic proteins such as Bax, and death receptor proteins such as DR4 and CD95, reduced expression of the apoptosis repressors XIP, survivin, Bcl-2 and Mcl-1 and the angiogenesis factors, VEGF and HIF-1α (Bolden, Peart et al. 2006). However, HDACIs have pleiotropic effects. HDACs also target many non-histone proteins (~1,750) which are affected by acetylation such as p53, tubulin, NFκB, heat shock protein 90 (Hsp90), β-catenin, retinoblastoma (Rb) and retinoblastoma-associated protein 1 (E2F1) (Marzio, Wagener et al. 2000; Chan, Krstic-Demonacos et al. 2001; Kawaguchi, Kovacs et al. 2003; Kovacs, Murphy et al. 2005; Peart, Smyth et al. 2005). Other reported effects of HDACis have been to stimulate ROS generation and to induce autophagy (Shao, Gao et al. 2004; Carew, Giles et al. 2008). As such, HDACis have a broad spectrum of activity and have demonstrated anticancer activity in many preclinical models (Glaser 2007).

Recent years have seen the development of various HDAC inhibitors and several of these are in various stages of clinical development, including butyrate, AN-9, LBH589, PXD101 and tubacin. Vorinostat™ (Suberoylanilide Hydroxamic Acid (saha)) is the most advanced clinically and is approved by the Food and Drug Administration (FDA) in the United States for the treatment of patients with cutaneous T cell lymphoma (CTCL) (Duvic and Vu 2007; Glaser 2007; Mann, Johnson et al. 2007). HDACIs can be divided into four main structural classes: the short-chain fatty acids (valproic acid, butyrate and sodium phenylbutyrate) the benzamides (MS-275), the cyclic tetrapeptides (depsipeptide, Romidepsin) and the hydroxamic acids (vorinostat and MGCD0103) (Bolden, Peart et al. 2006). The largest class of HDAC inhibitors with the greatest therapeutic potential is the hydroxamic acids. The first discovered natural product belonging to this group is trichostatin (TSA); however, due to its limited stability it has very little activity *in vivo* (Yoshida, Hoshikawa et al. 1990; Qiu, Kelso et al. 1999).

1.7.2.3 Vorinostat™

Vorinostat (Zolinza®) shown in figure 1.8 is a hydroxamic acid that inhibits HDAC 1, 2, 3 and 6. Since its proven efficacy in patients with CTCL, it has been studied in other lymphomas, for example, a recent phase II study in patients with relapsed or refractory FL, marginal zone lymphoma (MZL) or MCL (Piekarz, Frye et al. 2009) has shown vorinostat to be well tolerated with an overall response rate of 29%, all of which occurred in the FL and MZL patients with no responses in 8 MCL cases. However, this compound is also rapidly metabolised *in vivo* and requires large concentrations for the observed activity. Many analogs of vorinostat have since been developed, but a major drawback with their use in clinical trials has been their toxicity and side effects including decrease in renal function and even severe cardiotoxicity, as reported with depsipeptide. This is because HDACis target specific classes of HDACs rather than individual isoforms, for example saha inhibit class I and II, panabinostat (LBH589) inhibits class I, II and VI whereas MS-275 preferentially inhibits HDAC1 & 9 and HDAC2 & 3 (Bolden, Peart et al. 2006). Thus more effective HDACis are required that target specific HDAC isoforms, thereby reducing toxicity and increasing efficacy. The hydroxamic acid tubacin was the first ever domain-selective HDACI targeting one of the two catalytic domains of HDAC6 however; tubacin has limited activity in preclinical studies (Haggarty, Koeller et al. 2003; Hideshima, Bradner et al. 2005).

1.7.2.4 UCL67022

Through collaboration between Barts Cancer Institute and University College London, a panel of novel HDAC inhibitors have been synthesized and investigated. The lead compound, C1 l-Phenylcarbamoyl-octanedioic acid 8-hydroxyamide 1-phenylamide (UCL67022) (figure 1.8), represents a new class of HDACI comprising a bifuricated cap moiety, a linker and a zinc binding group (a hydroxamic acid group). The zinc binding group binds to zinc in the HDAC receptor pocket, while the cap moiety binds at the rim of the pocket. The addition of the second side chain in the cap moiety increases the polarity of the molecule which increases binding avidity of the HDACi in the receptor pocket (figure 1.8). This is believed to confer it greater potency than vorinostat and it also changes interactions with amino acids outside the pocket which may allow differential interaction between classes of HDACs.

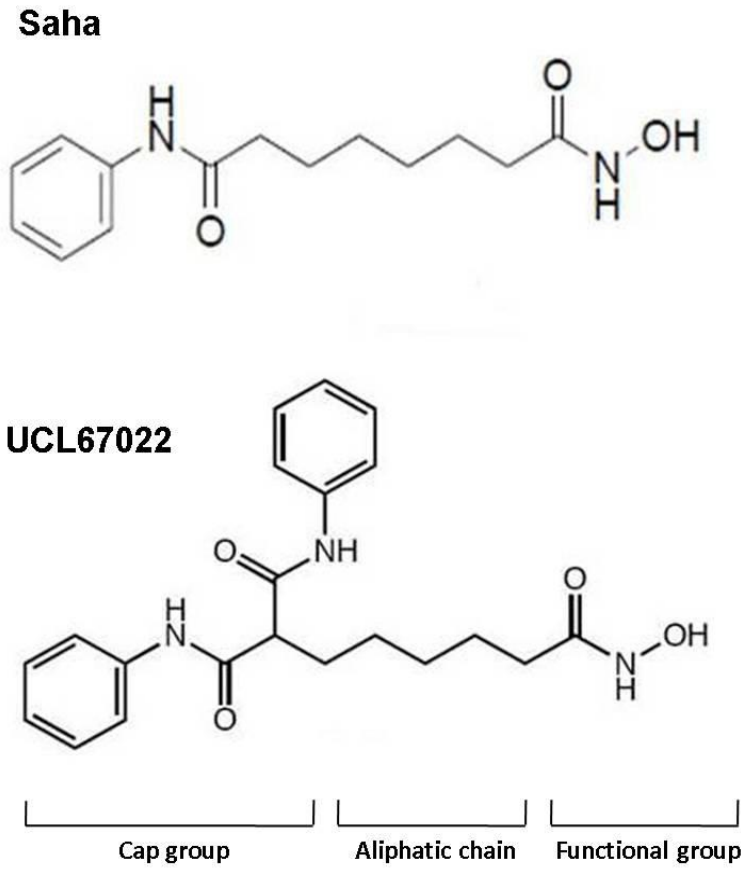

Figure 1.8 Chemical structures of saha (vorinostat) and of UCL67022

1.7.3 Heat shock protein 90 Inhibitors

1.7.3.1 Heat Shock Protein 90 (Hsp90)

Hsp90 is a ubiquitous, evolutionarily conserved molecular chaperone, that interacts with a variety of intracellular 'client proteins' to facilitate their proper folding, prevent misfolding or aggregation and preserve their 3-dimensional conformation to a functionally competent state (Isaacs, Xu et al. 2003; Allegra, Sant'antonio et al. 2011). It exists as multiple isoforms that includes Hsp90α and Hsp90β in the cytoplasm and GRP94 and Trap1 localized to the endoplasmic reticulum and mitochondria respectively (Sreedhar, Kalmar et al. 2004). The Hsp90 domain structure has 3 regions: an NH_2-terminal ATP-binding region, a middle client-binding region and a carboxy-terminal dimerization region. In the inactive state, an ATP molecule is bound to the N-terminal of Hsp90, and it adopts a closed conformation. When this ATP molecule is hydrolysed, conformational changes mediate a series of association-disassociation cycles between Hsp90 and the substrate client proteins, mediating its stabilising effects. This involves a series of co-chaperones such as Hsp70, Hsp40, HOP, AHA1 and p23 (Pearl, Prodromou et al. 2008). When client proteins are not being chaperoned by Hsp90, an E3 ubiquitin ligase such as the C-Terminus of Heat Shock Cognate 70 Interacting Protein (CHIP) is recruited and client proteins are degraded by the ubiquitin proteasome pathway (Connell, Ballinger et al. 2001).

1.7.3.2 Hsp90 in Cancer Therapy

Association with a plethora of signal transduction pathways marks Hsp90 as an attractive target for pharmacological modulation in cancer therapy. Hsp90 client proteins lack specific Hsp90 binding motifs and vary in terms of intracellular location, structure and function. Their common denominator is their involvement in intracellular cell proliferation pathways, and in the stabilization of anti-apoptotic proteins and tumour angiogenesis, the hallmarks of cancer (Whitesell and Lindquist 2005). Some of these proteins include Breakpoint Cluster Region-Abelson (BCR-ABL), erythroblastic leukemia viral oncogene homolog 2 (ERB-B2), epidermal growth factor receptor (EGFR), AKT, MET, murine leukemia viral oncogene homolog 1 (RAF-1), vascular endothelial growth factor receptor (VEGFR), fms-related tyrosine kinase 3

(FLT3), androgen and estrogen receptors, hypoxia inducible factor-1 alpha (HIF-1α), mutated p53 and telomerase (Beere 2004; Whitesell and Lindquist 2005; Cullinan and Whitesell 2006; Sanderson, Valenti et al. 2006), shown in figure 1.9.

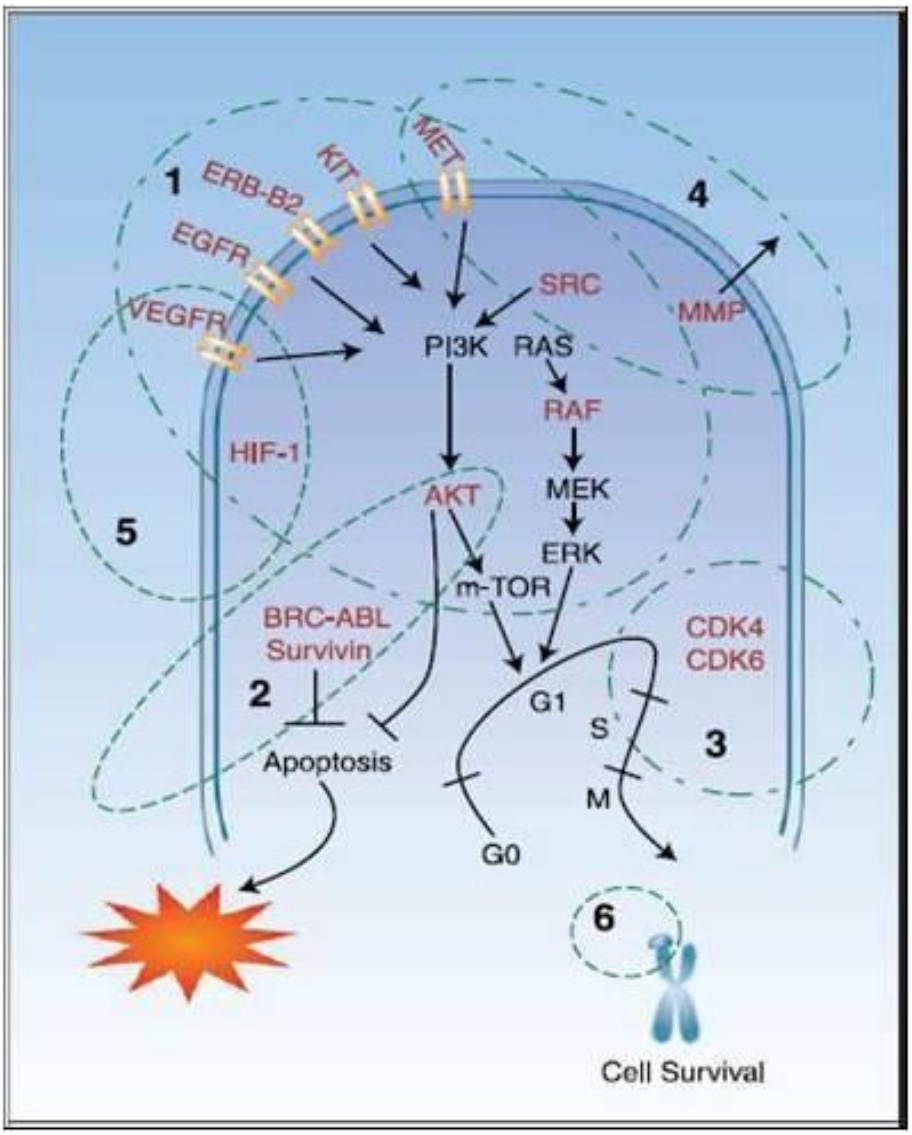

Figure 1.9 Contribution of Hsp-90 client proteins (red) on cancer cell survival and apoptosis (Banerji 2009).

1.7.3.3 Effects of Hsp90 Inhibition

A prominent feature of Hsp90 blockade in MM cell lines is down-regulation of cytokine triggered signaling pathways, such as those leading to activation of signal transducer and activator of transcription 3 (STAT3), mitogen activated protein kinase (MAPK) and

Ras/Raf, PI3K/Akt/p70S6K, nuclear factor-κ B (NF-κB). A synthetic analog of geldanomycin, 17-AAG, was shown to abrogate NFκB transcriptional activity, phosphorylation of MEK1 and 2, constitutive IGF-induced activity of telomerase, IGF-induced upregulation of chymotryptic 20S proteasome activity and inhibition of IGF-1R and IL-6R (Mitsiades, Mitsiades et al. 2006). Downstream activation of antiapoptotic molecules were also suppressed, such as caspase-8, FLIP, cIAP-2, XIAP, RANKL and the transcription factor XBP-1, a known downstream target of IL-6 signaling in myeloma and regulator of the ER stress response. Thus, inhibiting Hsp90 leads to combinatorial inhibition of multiple proliferative signal transduction pathways (Mitsiades, Mitsiades et al. 2006).

Selectivity of Hsp90 inhibitors for tumour cells may be explained by the fact that cancer cells are addicted to oncogenes that drive malignant processes, thus depletion of oncoproteins affects cancer cells to a greater extent than normal cells (Weinstein and Joe 2008).Furthermore, the oncoproteins are often expressed in their mutant forms which require greater stabilisation by Hsp90 than their wild-type counterparts. Cancer cells are also subjected to intratumoural acidosis, hypoxia and deprivation of nutrients, creating an environment of cellular stress that requires the chaperone machinery to a greater extent than normal cells. MM cells in particular may be more sensitive to Hsp90 inhibition as Hsp90 plays a crucial role in chaperoning immunoglobulins, including M protein. Interruption of this chaperoning activity leads to greater accumulation of mis/un-folded proteins, resulting in cell death caused by proteo-toxicity (Davenport, Moore et al. 2007). There is also evidence that some Hsp90 inhibitors bind preferentially to Hsp90 complexes in cancer cells compared with normal cells (Kamal, Thao et al. 2003).

1.7.3.4 Hsp90 Inhibitors

Successful pharmacological inhibition of Hsp90 has been achieved with the ansamycin antibiotic geldanomycin, but the compound proved too toxic for medical use (Supko, Hickman et al. 1995). Since then, there has been a host of Hsp90 inhibitors (Hsp90i) that have been evaluated in the clinic. These have been derivatives of geldanomycin and radicicol such as 17-AAG, 17-DMAG, KF58333 and IPI-504 (Kurebayashi, Otsuki et

al. 2001; Sydor, Normant et al. 2006).Some of these have shown considerably toxicity in preclinical data in animals (Glaze, Lambert et al. 2005) however, the compound, NVP-AUY922 was well-tolerated, suggesting a therapeutic window for Hsp90 inhibition may be achieved with these compounds, and subsequently a number of clinical trials have successfully been conducted in MM patients (Neckers 2003; Mitsiades, Mitsiades et al. 2006; Sydor, Normant et al. 2006).

The most recently developed Hsp90is are synthetic small molecule inhibitors such as AUY922A, BIIBO21 and SNX2112 which are being investigated in clinical trials (Eccles, Massey et al. 2008; Caldas-Lopes, Cerchietti et al. 2009; Fadden, Huang et al. 2010). Development of novel inhibitors is geared towards improving their hepatotoxicity properties and more convenient clinical formulations are desired. There is limited data about the consequences of Hsp90 blockade in patient cells, but in MM primary samples, Hsp90 inhibition has been shown to exert beneficial antitumour effects, not just through direct targeting of myeloma cells but also via direct effects on BMSCs. Specifically, through the temporary withdrawal of support from cells in the BMM (Mitsiades, Mitsiades et al. 2006).

1.7.3.5 KW-2478

KW-2478 is a novel inhibitor of the Hsp90 non-ansamycin non-purine analogue class, which was derived from microbial screening and designed by utilizing chemical synthesis and X-ray crystallography technologies. It directly inhibits proliferation of tumor cells and induces apoptosis while also inhibiting angiogenesis and metastasis. This has prompted entrance of KW-2478 into phase I clinical trials in patients with B-NHL and CLL, and it is now also indicated for use in solid tumors including non-small-cell lung cancer, breast, prostate and renal cell cancer (Kyowa Hakko Kirin Pharma Inc.http://www.kyowa-kirin-pharma.com/pipeline-clinical-trials/). Recently, we reported on the anti-tumor activity of KW-2478 as a single agent in MM cells cocultured in an *in vitro* primary MM coculture model, and these results are presented in chapter 6 (Nakashima, Ishii et al. 2010).

1.8 Combination therapy investigated in this study

1.8.1 Effects of bortezomib in combination

In addition to the promising single agent pre-clinical activity of bortezomib, it has demonstrated a valuable role in increasing sensitivity of malignant cells to chemotherapy, via inhibiting NFκB activation. For example, using specific repressors of NF-κB activation, or bortezomib, studies have shown that chemoresistance to the active metabolite of CPT-11, SN-38, could be overcome both in colorectal cell lines and in a xenograft model. Moreover, significantly greater growth inhibition was observed when bortezomib was combined with SN-38 (Cusack, Liu et al. 2001).

These effects have also been observed in MM where sub-toxic doses of bortezomib were able to sensitise myeloma cells from patients with doxorubicin-resistant disease, to doxorubicin and melphalan, and synergistic effects upon combination of bortezomib with these agents was also observed (Mitsiades, Mitsiades et al. 2003). Similarly, bortezomib in combination with dexamethasone or immunomodulatory derivatives of thalidomide (IMiDs) have demonstrated enhanced antitumour activity in MM cells. In pancreatic cancer, bortezomib in combination with irinotecan has been shown to block NFκB activation, inhibit cell proliferation and induce apoptosis in a xenograft model, and these effects were not observed with either agent alone (Shah, Potter et al. 2001).

Bortezomib sensitizes NHL cells to other therapeutic agents and, given the lack of significant additive toxicity, may therefore be appropriate as part of combination therapy in NHL treatment. Current phase II studies are exploring the integration of bortezomib into regimens including VRCD (velcade/rituximab/cyclophosphamide/dexamethasone) in low-grade NHL (Nabhan, Villines et al. 2012) and RiPAD+C: rituximab, bortezomib, doxorubicin, dexamethasone and chlorambucil in patients with relapsed/refractory MCL (Houot, Le Gouill et al. 2012). The order of treatment seems to be important when using bortezomib in combination, and interactions were additive or even antagonistic with simultaneous combination therapy. For example, combination treatment of MCL cell lines with

bortezomib plus doxorubicin or vincristine or 4-hydroperoxycyclophosphamide (4-HC), produced an enhanced synergistic effect only when cells were first sensitised with either doxorubicin or vincristine or 4-HC and then treated with bortezomib (Goy and Gilles 2004).

Bortezomib, thalidomide and lenalidomide are three novel agents recently approved by the US FDA for treatment of MM. Besides their direct activity against MM cells, their therapeutic success is also based on their activity against the BMM. However, due to their various degrees of clinical toxicity there is a need for development of new rational drug combinations that will allow less drug to be given for a longer period in order to improve patient outcome. Furthermore, given the heterogeneity of haematological disease and the emerging importance of the microenvironment in patient response and drug resistance, more preclinical research is required to decipher the role of the microenvironment in the context of novel drug combinations in order to make findings more relevant to understanding *in vivo* processes.

1.8.2 HDACIs in combination with bortezomib

Studies have shown that the inhibition of NFκB activity does not account for all the anticancer activity of bortezomib. Combination treatment of HDAC inhibitors with bortezomib has been reported to increase ROS, which has been associated with enhanced apoptosis (Pei, Dai et al. 2004) such that free radical scavengers such as N-acetyl-L-cysteine block ROS generation and significantly reduce apoptosis. This data suggests that the induction of oxidative stress contributes to the anticancer activity of the bortezomib-HDAC inhibitor combination. Bortezomib also causes a build-up of ubiquitin-conjugated misfolded proteins thereby triggering ER stress and aggresome formation in multiple myeloma cells (Hideshima, Chauhan et al. 2002; Landowski, Olashaw et al. 2003; Lee and Waldman 2003; Fribley, Zeng et al. 2004). Aggresome formation appears to form part of a cytoprotective response to handle overwhelming protein accrual that occurs when the proteasome is inhibited in malignant but not in normal cells. This therapeutic window exists because cancer cells are highly dependent on protein degradation due to continuous cell cycling and higher translation rates (Plemper and Wolf 1999; Garcia-Mata, Gao et al. 2002). Aggresome formation involves

HDAC6 binding to and deacetylating α-tubulin. This enables the formation of perinuclear aggresomes containing polyubiquitinated proteins which are fused with autophagosomal vacuoles (mediated by HDAC6) where they are lysosomally degraded (Kawaguchi, Kovacs et al. 2003).

In vitro and *in vivo* studies have revealed that HDAC6 inhibition by HDACIs such as tubacin and saha increases α-tubulin acetylation, accumulation of polyubiquitinated proteins and disrupts aggresome formation in malignant cells, which subsequently undergo caspase-8-mediated apoptosis (Haggarty, Koeller et al. 2003; Hitomi, Katayama et al. 2004; Hideshima, Bradner et al. 2005; Nawrocki, Carew et al. 2005; Nawrocki, Carew et al. 2005). Therefore, by targeting both proteasome-dependent pathways with bortezomib and the aggresome pathway with HDAC6 inhibitors, accumulation of polyubiquitinated proteins can be induced, resulting in ER stress and p53-independent apoptosis (figure 1.10). Importantly, the combination of bortezomib with tubacin or SAHA does not trigger cytotoxicity in normal PBMCs, in normal human pancreatic epithelial cells *in vitro* or in murine cells *in vivo* (Nawrocki, Carew et al. 2005; Nawrocki, Carew et al. 2005), thus showing tumour selectivity.

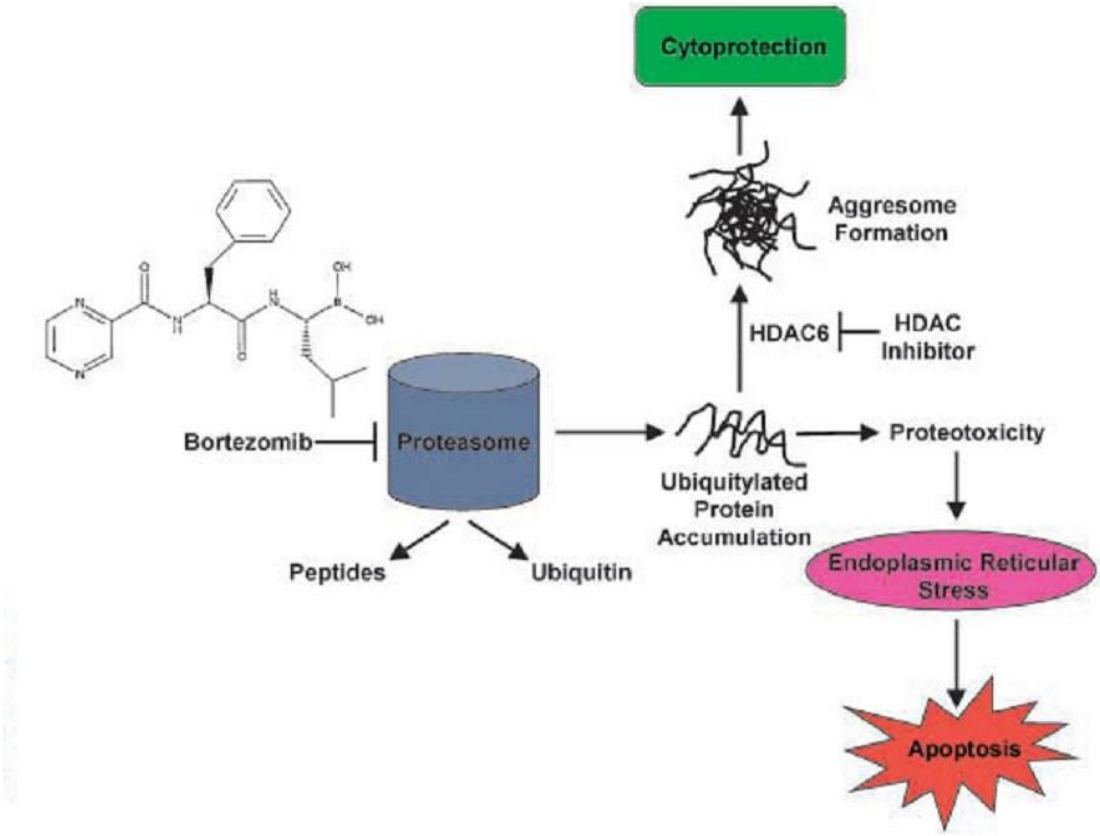

Figure 1.10 Rationale for combining bortezomib and HDAC inhibitors in multiple myeloma (Nawrocki, Carew et al. 2006).

1.8.3 Hsp-90 inhibitors and bortezomib

Hsp90 blockade is a multi-target approach as the effects are transmitted to such a large group of client proteins. As a result of this, using it in combination with other drugs that work through different mechanisms would likely result in more effective therapy in haematological malignancies. The strength of this concept has been shown with bortezomib, where inhibition of the proteasome also leads to deregulation of multiple pathways. Furthermore, bortezomib treatment typically induces upregulation of Hsp90 (which supports the function of client proteins IL-6R and IGF-R1) in MM (Mimnaugh, Xu et al. 2004; Mitsiades, Mitsiades et al. 2006).

This counterproductive effect warrants the use of Hsp90 inhibition, and KOS-953, was the first shown to enhance bortezomib activity in MM cells (Anderson 2007). The synergistic suppression of chymotryptic activity of the 20S proteasome was observed by combination of 17-AAG with bortezomib. In addition, because the anti-MM effect of

bortezomib has been associated with stimulation of ER stress, as described above, it is logical that combined proteasome and Hsp90 inhibition would result in synergy. In fact, this combination was found to trigger pronounced cleavage of caspase-12, which constitutes a critical event in ER stress-induced apoptosis (Mitsiades, Mitsiades et al. 2006).

This suggests that Hsp90 inhibitors can counteract the resistance of tumour cells to bortezomib by further impairing their ability to withstand the ER stress generated by proteasome inhibition. This model is further supported by the fact that 17-AAG plus bortezomib also causes XBP-1 splicing. Therefore, Hsp90 inhibitors and bortezomib may have complementing effects in simultaneously triggering intracellular accumulation of misfolded proteins, and subsequently generating ER stress. As part of this project, we investigated the efficacy of the combination of KW-2478 with bortezomib and with melphalan in patient-derived MM samples, cultured in the myeloma coculture model presented in chapter 6. Based on this promising preliminary data, a phase I study of KW-2478 in combination with bortezomib in patients with relapsed and/or refractory multiple myeloma, is currently ongoing in which Barts is participating (http://clinicaltrials.gov/show/NCT01063907).

1.9 Aims

1.9.1 Overall aim of this study:

To investigate *in vitro* primary coculture models as a means of testing the activity of current and novel therapies in patients with haematological malignancies. Use of these models may suggest new therapeutic approaches involving novel agents or rational drug combinations using standard therapies. Furthermore, by developing and validating reproducible and standardised models, they may be more easily adopted across research centres. The hope is that incorporation of these models as part of routine pre-clinical practice will enable patient response stratification in order to guide and individualise their treatment; thereby improving treatment response and overall survival.

1.9.2 Specific aims:

- To validate an *in vitro* CHO-CD40L/B-NHL coculture system in normal PBMCs and patient-derived NHL samples and to extend its scope to study novel therapies in chronic lymphocytic leukemia (CLL)

- To validate an *in vitro* multiple myeloma coculture model in myeloma cell lines and patient-derived myeloma samples

- To investigate the value of both coculture models to study and maximize the use of current therapies and novel therapies and to identify more effective drug combinations in NHL, CLL and MM. Therapies studied will include bortezomib, doxorubicin, UCL67022, dexamethasone, melphalan and KW-2478

- To study drug resistance conferred by the stromal microenvironment in multiple myeloma, and to investigate cytokine modulation by current therapies and by novel agents in the multiple myeloma coculture model

- To relate *in vitro* drug activity with patient characteristics and clinical response in samples where clinical data is available.

CHAPTER 2: Materials and Methods

2.1. Cell lines

2.1.1 Human lymphoma and leukemia cell lines

The following cell lines were used in experiments. A panel of B-NHL cell lines included SUD-4 (or SU-DHL4); DHL-4, DHL-5, DHL-6 and DHL-7 cell lines were obtained from the Dana Farber Cancer Institute (kind gift from Dr. Margaret Shipp). The CRL (or RL) and DoHH2 cell lines were obtained from Cancer Research UK cell services. A CLL cell line, MEC-1, was obtained from the German Collection of Microorganisms and cell cultures (DSMZ, Germany). Two MCL cell lines JEKO-1 and GRANTA-519 were obtained from the American Type Culture Collection (ATCC) and DSMZ, respectively. These suspension cell lines were all maintained in Roswell Park Memorial Institute-1640 (RPMI-1640) culture medium (Sigma-Aldrich, Poole, UK) with the exception of MEC-1 which was maintained in Iscove's Modified Dulbecco's Medium (IMDM) ((Sigma-Aldrich). All culture medium was supplemented with 10% fetal calf serum (Sigma-Aldrich) and 1% penicillin (100 units/ml) and streptomycin (100µg/ml) (both from Invitrogen™, California, USA) at 37°C in a humidified atmosphere with 5% CO_2. Cells were passaged twice weekly and reset at a density of $2x10^5$/ml.

2.1.2 Human myeloma cell lines

The following panel of human myeloma cell lines was used: U266 (Cancer Research UK cell services), RPMI 8226 and MM1.S (both ATCC). All myeloma cell lines grow in suspension except the MM1.S which grows semi-adherently. All cells were cultured in RPMI-1640 with the addition of the supplements detailed above. Cells were passaged twice weekly and reset at a density of $2x10^5$/ml. The weakly-adherent MM1.S cells required firm shaking of the culture flask and repeat washing to remove the lightly attached monolayer when resetting. All 3 cell lines were slowly growing with doubling times of approximately 72hrs.

2.1.3 Fibroblastic cell lines

Two different fibroblastic cell lines were used. Chinese hamster ovary (CHO) cells transfected with the CD40 ligand, (CHO-CD40L) were kindly provided by Professor Peter Johnson, Southampton Hospital. They were cultured in RPMI 1640 medium containing 5% FCS, 1% glutamine (200mM), 1% sodium pyruvate, 0.1% fungizone, and geneticin (G-418, 50mg/ml) for selection of transfected cells (Sigma, Poole, UK). The HS-5 cell line (ATCC) was maintained in Dulbecco's Modified Eagle Medium (DMEM) (ATCC) containing 10% FCS, 1% penicillin/streptomycin (GIBCO-Invitrogen, UK). Both stromal cell lines were adherent and were passaged using 5% trypsin, twice weekly at confluence and were reset at a density of 2 x 10^5/ml. For experiments, all cells were used in their exponential growth phase which involved resetting cells in fresh culture medium the day before exposure to various treatments. All cultures were routinely tested for mycoplasma contamination, and the cytogenetics of the cell lines donated by other labs was confirmed by short tandem repeat (STR) typing (service performed by LGC Standards (Teddington, UK).

2.1.4 Cell line characteristics

The CRL cell line is established from the ascites of a patient with DLBCL (Beckwith, Urba et al. 1991). The SUD-4 cell line, is derived from the pleural effusion of a patient with DLBCL (Epstein, Levy et al. 1978). The DoHH2 cell line is established from the pleural effusion of a patient with FL, which had transformed to DLBCL (Kluin-Nelemans, Limpens et al. 1991). The DHL4, DHL5, DHL6 and DHL7 cell lines are drug-resistant/drug sensitive variants of the SUD4 cell line, established in the lab of Dr. Margaret Shipp (Dana Farber Cancer Institute). The JeKo-1 cell line was established from the peripheral blood of a patient with a large cell variant of MCL showing leukemic transformation (Jeon, Kim et al. 1998). The GRANTA-519 cell line was established from the peripheral blood of a patient at relapse with a leukemic transformation of MCL (Jadayel, Lukas et al. 1997). Both MCL cell lines overexpress cyclin D1 and Bcl-2 proteins. The MEC-1 cell line was established from the peripheral blood of a patient with a B-CLL in prolymphocytoid transformation to B-PLL (Stacchini, Aragno et al. 1999). The CRL, SUD4, DoHH2, JeKo-1 and GRANTA-519 cell lines carry the t(14;18) chromosomal translocation and all of the B-NHL cell lines and the JeKo-1

cell line have mutated *p53*. All the *p53* mutations are homozygous except for the DoHH2 cell line which has a heterozygous mutation (Strauss, Higginbottom et al. 2007). In this thesis, the CRL, SUD4, DoHH2, DHL4, DHL-5, DHL6 and DHL7 cell lines are collectively termed DLBCL cell lines.

MM1.S is a glucocorticoid (dexamethasone)-sensitive cell line established from the peripheral blood of a patient with IgA myeloma. MM1.S cells harbor a reciprocal translocation involving 12q24.3 and 14q32.3 (Goldman-Leikin, Salwen et al. 1989). Both U266 and RPMI8226 are plasmacytomas of B cell origin. The U266 cells produce IL-6 and are resistant to glucocorticoids, while RPMI 8226 cells produces IgL chains but not H chain or IL-6. All three myeloma cell lines have mutated *p53* (Matsuoka, Moore et al. 1967; Nilsson, Bennich et al. 1970; Kawano, Hirano et al. 1988).

The CHO cell line was initiated from a biopsy of an ovary of an adult Chinese hamster (Puck 1957). CHO cells are commonly used as a transfection host. The human stromal cell line HS-5 was established from the bone marrow of a healthy volunteer (Roecklein and Torok-Storb 1995). It secretes significant levels of granulocyte colony-stimulating factor (G-CSF), granulocyte-macrophage-CSF (GM-CSF), macrophage-CSF (M-CSF), Kit ligand (KL), macrophage-inhibitory protein-1 alpha, interleukin-1 alpha (IL-1alpha), IL-1beta, IL-1RA, IL-6, IL-8 and IL-11.

2.2. Collection and handling of cells from patient samples

In all cases, disease diagnosis was confirmed by morphologic and immunophenotypic analysis of fresh-frozen samples. All patients provided written informed consent and ethical permission from the Institutional Review Board (IRB) was obtained prior to investigation. All patient samples were anonomised and coded with a unique identifier, prior to use in the lab.

2.2.1 Lymphoma and leukemic cells

Biopsy samples were obtained from lymph nodes from patients with NHL and in patients with leukemic infiltration, peripheral blood was obtained by venesection. All samples were procured as part of the routine management of patients' disease. Single cell suspensions were prepared from biopsies via mechanical disaggregation using a scalpel and forceps. Density gradient centrifugation was used to isolate mononuclear cell fractions: cell suspensions were combined with an equal volume of RPMI 1640, layered over half the volume of Ficoll-Hypaque (Nycomed, Oslo, Norway) and centrifuged at 1200rpm at room temperature for 20mins. The white-mononuclear cell layer was aspirated, washed and resuspended in RPMI 1640, for use in experiments or stored for later use (see below).

2.2.2 Myeloma cells

Bone marrow aspirates were obtained from MM patients at relapse, and the plasma cell fractions were enriched by negative selection using RosetteSep MM-enrichment cocktail (StemCell Technologies, London, UK). This cocktail of antibodies contains: anti-CD2, CD14, CD33, CD41, CD45RA, CD66b and glycophorin A. Once added to a diluted bone marrow sample, the antibody mixture was able to form immunorosettes that form a pellet upon density gradient centrifugation. 50µl/ml of neat antibody cocktail was added to undiluted bone marrow sample and the mixture was incubated on a roller at room temperature for 20mins. The mononuclear cell fraction was then isolated via density gradient centrifugation as outlined above. The main advantage of this technique compared to using a positive selection technique, was that the resultant cells were not antibody-labeled thus not inadvertently activated. Furthermore, the MM cells were enriched to >90% purity. Optimisation of this procedure was performed in the lab prior to the work detailed in this thesis.

2.2.3 Separation and culture of bone marrow stromal cells (BMSCs)

The method used was adapted from that used at the Jerome Lipper Myeloma Centre, Dana Farber Cancer Institute, Boston, USA. A minimum of 4ml bone marrow was required to generate sufficient BMSCs for culture. DMEM supplemented with 20% FCS,

10% penicillin and streptomycin (all Sigma-Aldrich) and 1µg/ml amphotericin B (fungizone, Sigma- Aldrich) was used throughout the BMSCs separation and culture. The original bone marrow sample was divided into two parts, for plasma cell enrichment and for BMSC culture (where sample volume permitted). The sample was centrifuged at 1200rpm for 30mins at room temperature and the cells above the interface carefully removed. These cells were washed in 2x volume of culture medium at 1200rpm for 6mins, and the supernatant discarded. The cells were then counted using trypan blue staining. The cells were resuspended in 5mls culture medium, transferred to a 25cm^2 culture flask and incubated at 37°C in a humidified atmosphere with 5% CO_2. The cell suspension therefore contained a mixture of mononuclear cells, including plasma cells.

The cells were cultured undisturbed for 5 days, after which the supernatant was aspirated and centrifuged at 1200rpm for 5mins, and the pellet resuspended in 5ml fresh medium. This suspension was added to a new flask and 5ml medium added to the original flask. The culture medium was renewed weekly by aspiration and the strongly adherent nature of BMSCs meant that they were not lost. After 4-6 weeks using this culture method, adherent fibroblastic-like BMSCs formed and the confluent flasks were passaged using trypsinsinisation. The cells were then used in experiments, or passaged into larger flasks for further propagation.

2.2.4 Cell Storage

Cells were either used immediately in experiments or frozen in liquid nitrogen for later use. Cells to be stored were diluted in 'freeze mix' consisting of 40% FCS, 50% RPMI, and 10% dimethyl sulfoxide (DMSO), to a concentration of 3-10 x 10^6 cells/ml for NHL and CLL primary cells (depending on the number of cells available), and 1 x 10^6 cells/ml for myeloma plasma cells. Cells (1ml/vial) were immediately transferred to polystyrene racks and frozen at -80^{o}C for 24hrs after which they were transferred to liquid nitrogen for long-term storage. This gradual freezing process maximized cell viability upon thawing (Farrant, Knight et al. 1974).

2.3 Drug preparation and Use

2.3.1 Bortezomib

Bortezomib was provided by Millenium Pharmaceuticals (Cambridge, MA, USA). 10mM stock solutions were prepared in less than 1% sterile dimethyl sulfoxide (DMSO, Sigma Aldrich Co. UK) and aliquoted and stored at -40˚C until use. Serial dilutions using sterile Hanks' Balanced Salt Solution (HBSS, Sigma Aldrich Co. UK) were used to obtain final treatment concentrations ranging from 2-2000nM.

2.3.2 Doxorubicin

Doxorubicin hydrochloride solution (Sigma-Aldrich), 3.45mmol/L, was made up to the desired concentration in cell culture medium prior to use.

2.3.3 4-hydroperoxycyclophosphamide (4-HC)

4-HC is the active metabolite of cyclophosphamide. It is formed in vivo in the liver by the action of p450 oxidases. Thus, for in vitro experiments, 4-HC (Squarix Biotechnology, Marl, Germany) was used. It forms aldophosphamide, which is in turn converted to phosphoramide mustard, the cytotoxic molecule. A 5mg/ml stock solution was prepared in deionised water and stored at -80°C. These stocks were further diluted prior to use in cell culture medium to obtain a range of working concentrations.

2.3.4 Fludarabine phosphate

Fludarabine Phosphate (Fludara, Stratech Scientific Ltd. Suffolk, UK) is formulated as the monophosphate form of F-ara-AMP to enhance solubility. Fludarabine phosphate is re-phosphorylated inside the cell which leads to fuoroadenine arabinoside triphosphate (F-ara-ATP), the major cytotoxic metabolite of F-ara-A. A 5mg/ml stock solution was prepared in deionised water and stored at -80°C. These stocks were further diluted prior to use in cell culture medium to obtain a range of working concentrations.

2.3.5 Suberoylanilide hydroxamic acid (SAHA) and UCL67022

These drugs were provided by the Department of Chemistry, UCL, London, in collaboration with the Barry Reed Oncology Lab, Queen Mary's School of Medicine and Dentistry. Stock solutions of 10mM for both compounds was prepared in sterile DMSO (<1%), aliquoted and frozen at -40^{o}C until use. Stocks were serially diluted and used in treatments at final concentrations ranging from 0.1-10uM.

2.3.6 KW-2478

KW-2478 was provided by Kyowa Hakko Kirin Co. Ltd., Tokyo, Japan. A stock solution of 10mM was made up in sterile dH_2O, aliquoted and frozen at -40^{o}C until use. Stocks were serially diluted and used in treatments at final concentrations ranging from 0.1-20uM.

2.3.7 Melphalan and Dexamethasone

These were purchased from Sigma, UK. Stock solutions of 10mM were made up in ethanol. The solutions were sterile filtered, aliquoted and frozen at -40^{o}C until use. Stocks were serially diluted and used in treatments at final concentrations ranging from 1-100uM.

2.4. Immunophenotyping of primary B-cells

2.4.1 Experimental and flow cytometry conditions

Immunophenotyping was performed on day 0, and repeated after 3 days in culture where sufficient cell numbers were available. Cells were washed with phosphate buffered saline (PBS, Sigma-Aldrich, UK) and exposed to antibodies for 30 minutes before re-washing & fixing in 1% paraformaldehyde (PFA) for another 30 minutes. The samples were then analysed by flow cytometry (FACScan, Becton Dickinson) using a 15W 488-nm argon ion laser. FITC staining was detected using a 515-545nm band-pass filter and PE staining with a 564-606nm band-pass filter. Relative antigen expression was determined by setting markers for the antigen-labeled cell population and

comparing them to markers set for the mouse IGg1 negative isotype control cells, thereby staging the cell population.

2.4.2 Cell surface markers

The following antibodies, all from Dako Products, Denmark, were used; B cell expression was assessed using CD19 (clone HD37) conjugated to mouse IgG1 phycoerythrin (PE). T cell expression was assessed using CD3 conjugated mouse IgG1 fluorescein isothiocyanate (FITC). Other markers included the immature germinal centre marker, CD10 (Clone SS2/36), conjugated to mouse IgG1 FITC, the mature germinal centre (lymphoplasmacytoid) marker CD38 (Clone AT13/5), and the monocyte/macrophage marker, CD14 (Clone TUK4), both conjugated to mouse IgG1 RPE. Clonality was confirmed using Kappa (κ) and Lambda (λ) (both Clone HD37) antibody staining conjugated to rabbit IgG1 FITC and RPE respectively.

2.5. Primary B-cell coculture using the CD40 system

2.5.1 Preparation of CHO-CD40L-coated plates

Chinese hamster ovary (CHO) cells transfected with the CD40 ligand, were grown to 80% confluence in 'CHO-cell medium': RPMI 1640 medium containing the antibiotic geneticin (50mg/ml, G418 Sigma-Aldrich) for the selection of transfectants; 5% FCS; 200mM glutamine; 1mM sodium pyruvate and 0.2% fungizone, all Sigma-Aldrich) in 50ml culture flasks. Cells were trypsinised, washed and resuspended in fresh medium and irradiated at a dose of 96Gy using an IBL 637 Cs137 Gamma Irradiator, according to the shielding required to generate the desired dosage (table 2.1). 96Gy was delivered by γ-irradiation at 3.6 Gy/min for 1600 sec. Following irradiation, cells were plated into 96-well plates at a density of $2x10^5$cells/ml and allowed to adhere overnight.

Table 2.1 Dose rate in Gy/min for the IBL 637 Cs137 Gamma Irradiator

Shelf Position	No Shielding	Light Shielding (2-fold attenuation)	Heavy Shielding (5-fold attenuation)
Top	0.8	0.4	0.1
2nd from top	1.2	0.6	0.2
3rd from top	1.7	0.9	0.3
Bottom shelf	3.6	1.8	0.6

2.5.2 Addition of B-cells

After overnight incubation of the CHO-CD40L cells, isolated B-cells were thawed by immediately transferring them from liquid nitrogen storage to a beaker of distilled water at 37^{o}C. Cells were washed in B-cell culture mix which comprised IMDM (Invitrogen, UK), 50 μg/ml human transferrin, 10% human serum, 5 μg/ml bovine insulin, 5ng/ml selenium, 1MM sodium pyruvate and 17 μg/ml gentamicin, all from Sigma-Aldrich. The cell pellet was resuspended at a concentration of 5x10^{5}cells/ml in fresh B-cell culture mix supplemented with 5ηg/ml recombinant human IL-4 (Sigma-Aldrich). Media from the pre-coated CHO-CD40L plates was removed and discarded and the wells were washed 3x in PBS. 100μl/well of the B-cell suspension was then added to the wells and the plates were incubated at 37^{o}C for 2hrs to allow the cells to settle and for CHO-CD40L/B-cell interactions to occur. Drugs were serially diluted from frozen stock solutions and 50ul drug or media was added (singly or in combination) to appropriate wells, in triplicate. Plates were incubated with drug for 48hrs or 72hrs after which cell viability and proliferation was measured using either haemocytometer-assisted cell counting via trypan blue dye exclusion or the ATP bioluminescence assay or the Guava ViaCount assay (described in section 2.8 below).

2.6 Primary B-cell culture using the sCD40L system

We investigate activity of drugs when primary samples were cultured in a simplified version of the CHO-CD40L system, which abrogates the need for stromal support by instead using exogenously added cytokines. Isolated B-cells were washed in B-cell culture mix and resuspended at a concentration of $5x10^5$cells/ml in fresh B-cell mix supplemented with 5ηg/ml recombinant human IL-4 (Sigma, UK). 100μl/well was then plated into 96-well plates and soluble recombinant human CD40L at a concentration of 100ng/ml (sCD40L, Enzo Life Sciences, UK) was added. Before addition of the sCD40L, it was ligated to a cross-linking enhancer (1μg/ml), which enables CD40 activation to occur at levels achieved with membrane-bound CD40L (Holler, Tardivel et al. 2003). Figure 2.1 shows a schematic of the CD40L and that its activity is increased in the presence of the enhancer ligand. IL-4 was added at 5ng/ml. Plated cells were incubated at 37^oC for 24hrs prior to drug treatment for a further 48hrs or 72hrs. Cell viability was measured using the ATP bioluminescence assay (see section 2.8.2 below). As part of the validation of this technique, we investigated cell viability with standard media, added IL-4, added sCD40L and both IL-4 and sCD40L.

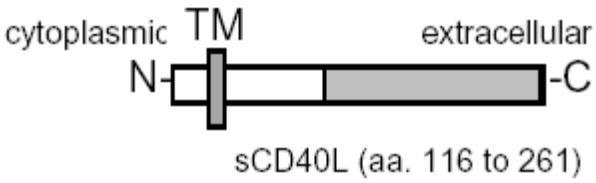

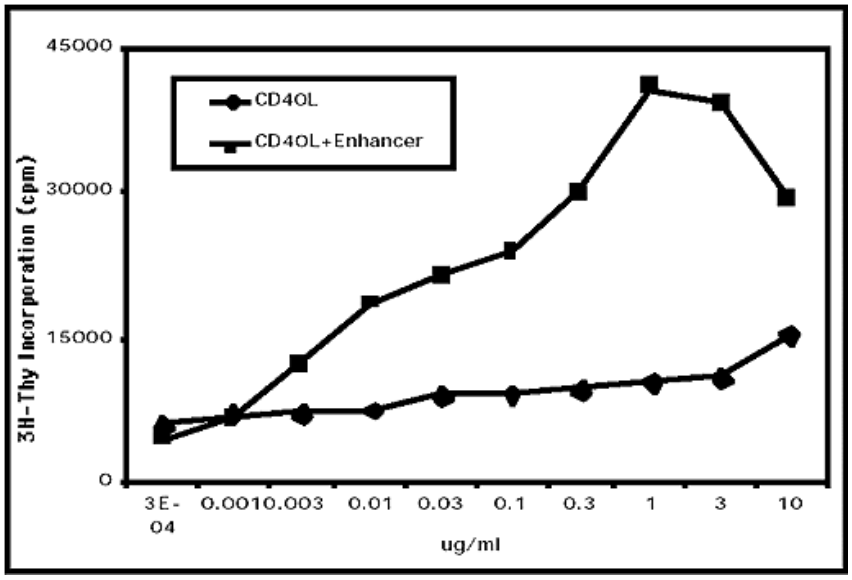

Figure 2.1 Schematic structure of human CD40L (peptide, aa. 116 to261) and a graph showing the activity of recombinant soluble CD40L increases 1000-fold (stimulation in the ηg/ml range) in the presence of cross-linking enhancer. CD19+ cells were incubated in 96-well plates (105 cells/well in 100µl RPMI supplemented with 10% FCS) for 72hrs in the presence of 10ηg/ml IL-4, 2µg/ml of goat anti-human µ chain antibody and the indicated concentration of CD40L in the presence or absence of 1µg/ml enhancer (Product number ALX-804-034). Cells were pulsed for an additional 6hrs with [3H] thymidine (1µCi/well) and harvested. [3H] thymidine incorporation was monitored by liquid scintillation counting. This figure was taken from the product data sheet April 2012 (Enzo Life Sciences Exeter, UK).

2.7 Primary MM cell coculture using the HS-5 system

2.7.1 Adhesion model

HS-5 stromal cells in serum-free DMEM (ATCC) were adhered at a concentration of $2x10^4$cells/ml at 37 ºC overnight into 24-well plates. The following day, stromal cells were washed 3x with serum-free RPMI 1640 medium (Sigma-Aldrich), and multiple myeloma cell lines (MMCLs) or primary MM plasma cells were layered over the adherent stromal cells at a concentration of $1x10^5$ cells/ml in serum-free RPMI 1640 medium (Sigma-Aldrich). Plates were incubated for a further 2h to allow for stromal/MM cell interaction, before the addition of serially diluted drugs. As a control, MMCLs or primary MM plasma cells were cultured in suspension. After 48h the Guava ViaCount assay (Guava®Technologies, Inc., Hayward, CA) was performed to measure cell viability and proliferation. Briefly, 100µl/well Guava ViaCount Flex reagent (Millipore, MA, USA) was added to the plate and cells were acquired using the ViaCount assay program (see section 2.8.3 below, Guava®Technologies, Inc., Hayward, CA). Propidium iodide cell staining was also used as a measure of cell viability, assessed using flow cytometry (see section 2.8.4 below).

2.7.2 Transwell and conditioned media (CM) models

24-well microplates were used in this set of experiment. Firstly, 1ml of either serum-free DMEM (ATCC) (Transwell - HS-5) or HS-5 stromal cells adhered overnight ($2x10^4$cells/ml) in serum-free DMEM (Transwell + HS-5) was added to wells of a 24-well plate. Transwell (TW) inserts were then added to the wells and 100µl of MMCLs or primary MM plasma cells ($1x10^6$cells/ml) were added to the upper chamber of the transwell insert. The smaller pore density ($1x10^8$pores/cm^2) and pore size (0.4µm) of the polycarbonate transwell insert (Costar, Corning, NY, USA) makes it impermeable to cells and permeable only to smaller soluble factors contained in the cell culture medium. Plates were incubated for 2hrs before the addition of serially diluted drugs. As an additional control, MM cells were cultured in conditioned media from 7 day-old HS-5 cultures. The medium was harvested on the day of its use by pipetting it from the adherent HS-5 monolayer and it was then centrifuged at 1300rpm for 5mins at room

temperature to pellet any HS-5 cells. The supernatant was collected and either MMCLs or primary MM was added at $1x10^5$ cells/ml in serum-free RPMI 1640 medium (Sigma-Aldrich). Figure 2.2 below illustrates the experimental set-up.

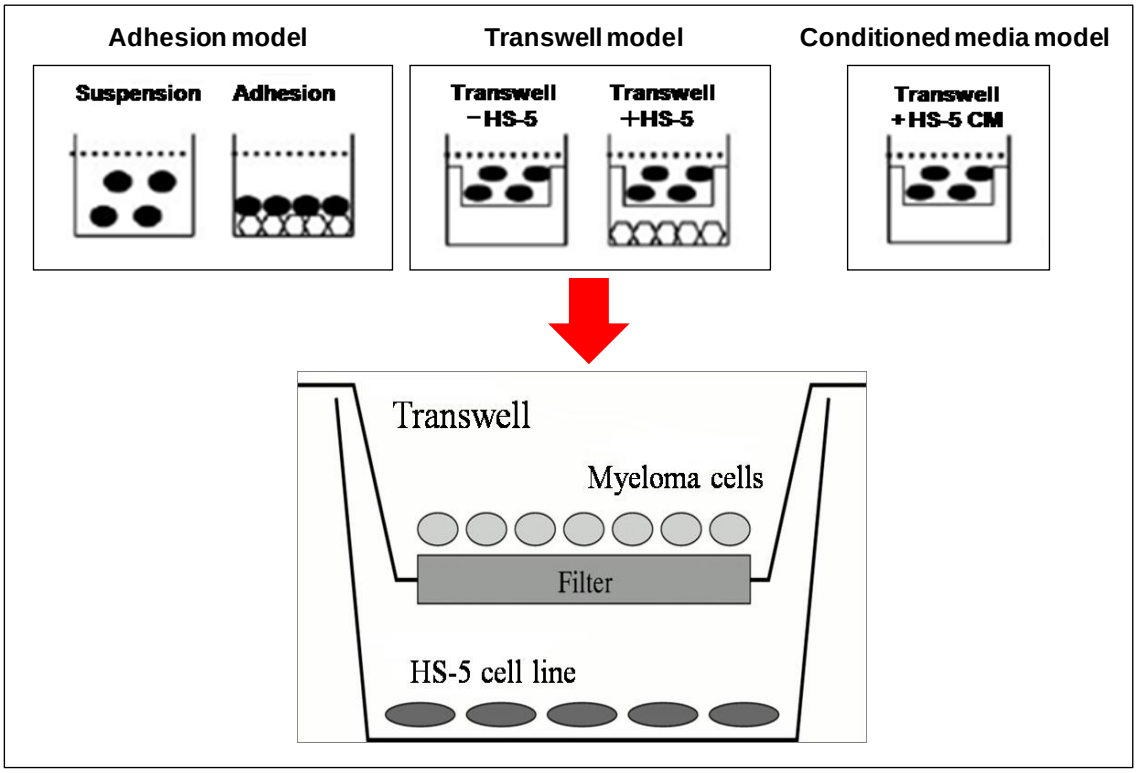

Figure 2.2 The transwell assay. Multiple myeloma cell lines and primary CD138+ MM cells were cultured using 3 different models: 1. the adhesion model where MM cells were in direct contact with HS-5 stroma, or cultured in suspension in media; 2. the transwell model where MM cells were cultured in the upper well of a 24-well microplate containing a transwell insert. MM cells were thus separated from the lower well containing either cell culture medium, (Transwell - HS-5) or HS-5 stromal cells (Transwell + HS-5); and 3. HS-5 conditioned medium (7 days) was also used. Cell viability was determined by flow cytometry (FACSCalibur, BD Biosciences) as described in section 2.8.4 below.

2.8 Cell Cytotoxicity assays

2.8.1 The Trypan Blue dye exclusion assay

The trypan blue dye exclusion assay measures cell viability based on the cell's ability to take up the dye. Apoptotic and necrotic cells with permeabilised cell membranes take up trypan blue whereas viable cells with intact cell membranes exclude it. 10µl of cells was mixed with 10µl 0.4% trypan blue (Sigma-Aldrich) and placed under light microscope using a heamocytometer (Neubauer). The number of viable (clear) and non-viable (blue) cells was scored and percentage viability calculated by dividing the number of live cells by the total cell number and multiplying by 100%.

2.8.2 The ViaLight® HS assay (ATP Assay)

Drug activity in a number of different cells lines and primary samples was determined using the ViaLight HS bioluminescence kit (Lonza, Basel, Switzerland). The ViaLight assay is based on the bioluminescent measurement of ATP and utilises the enzyme luciferase which catalyses the formation of light from ATP and luciferin according to the following reaction:

$$\text{ATP} + \text{luciferin} + O_2 \xrightarrow[Mg^{2+}]{\text{Luciferase}} \text{Oxyluciferin} + \text{AMP} + PP_i + CO_2 + \text{Light}$$

Thus the ATP assay is a functional cell-based cytotoxicity assay where the luminescence measured linearly correlates with cell viability and cell proliferation. Following the drug treatment period, 100ul nucleotide releasing reagent (NRR) was added to all used wells of the 96-well plate which was then incubated for 5mins at room temperature. For primary co-cultures, the medium containing lymphocytes in suspension was removed and transferred to a fresh 96-well plate before addition of NRR. After 5mins, 180ul medium from each well was transferred to a white-walled 96-well microtitre plate, and its luminescence measured immediately (POLARstar OPTIMA plate reader, BMG Labtech, Offenburg, Germany), following the addition of 20ul ATP

monitoring reagent (AMR) via automatic injection into each well. Following subtraction of background luminescence levels the results were expressed relative to the control value and were analysed using Graphpad PRISM® software to produce an EC_{50} value (effective drug concentration causing a 50% reduction in cell viability).

2.8.3 The Guava Viacount assay

The Guava Viacount assay uses a reagent which is a mixture of two DNA-binding dyes to obtain absolute cell counts and assess cell viability. The first dye is membrane permeable and stains all nucleated cells; the second is membrane impermeable and only enters cells with compromised cell membranes, thus identifying the apoptotic/dead cells. Cells stained with this reagent were analysed on the Guava® PCA-96 system (Guava®Technologies, Inc., Hayward, CA) which has a green laser for excitation, two fluorescence detectors and a detector of forward scatter that assess relative size. Cells were added to a 96-well plate at a concentration of $1x10^5$/ml or $2x10^5$/ml for coculture assays. Following the appropriate incubation time with or without drug (added after 24hrs), 100µl of the 1:200 diluted Flex reagent (Millipore) was added to all experimental wells. A worklist template was set up and the plate was analysed, with triplicate observations per treatment.

2.8.4 Propidium iodide (PI) and CD38+ staining via flow cytometry

After 48hrs of drug incubation, MMCLs or primary MM cells were harvested from 24-well plates and TW inserts and transferred to 5ml FACS tubes (BD Biosciences). Both the HS-5 stromal cells and MM cells were harvested in wells where they were in direct adherence. This was done by vigorous pipetting of the culture mixture containing MM cells and adhered HS-5 cells. This technique allowed efficient removal of both cell types and preservation of cell membrane integrity as opposed to cell scraping or trypsinisation which often resulted in compromised cell membranes. Samples were collected into BD FACS tubes which were centrifuged at 1300rpm for 5mins at room temperature and the supernatants discarded. Cells were washed once in ice-cold PBS and centrifuged again at 1300rpm for 5mins. The supernatant was discarded and the samples containing HS-5/MM cocultures were stained with either a CD38-FITC-

conjugated antibody or a CD38 IgG1-FITC isotype control antibody (both BD Biosciences), by adding 5ul antibody to 95ul PBS to the pelleted sample and incubating for 20mins at room temperature in the dark. After the incubation period, 400µl of propidium iodide (PI, Sigma-Aldrich; 50µg/ml PI + 50µg/ml RNAse A in PBS) was added to each sample and mixed thoroughly. Five thousand cells per sample were analysed immediately using a FACSCalibur™ flow cytometer (Becton Dickenson, NJ, USA) with CellQuest™ software. HS-5 cells were CD38 negative and MM cells were gated on their CD38 positivity using the analysis program FlowJo (version 7.5).

2.9 Analysis of cell cycle distribution using flow cytometry

At the end of the assay period, $1x10^6$cells/treatment for cell lines and at least $5x10^5$cells/treatment for primary cells were pelleted via centrifugation at 1300rpm for 5mins at room temperature. The medium was discarded and the cells were washed twice in ice-cold phosphate buffered saline (PBS). Cells were fixed in 5mls of 70% ethanol (Fisher Scientific, Leicestershire, UK) and incubated at 4°C for 30mins or stored at -20°C until further use (maximum 1week). The previously fixed cells were pelleted via centrifugation at 1300rpm for 5mins at room temperature. The supernatant was discarded and cells were washed once in ice-cold PBS. 500µl of PI/RNAse was added to each sample and mixed thoroughly. Ten thousand cells/sample for cell lines and at least 5000 cells/sample for primary cells were analysed immediately using a FACSCalibur™ flow cytometer (Becton Dickenson, NJ, USA) with CellQuest™ software. The percentage of cells in the sub-G1 (apoptotic fraction i.e. cells with a reduced PI stain but similar morphology (Darzynkiewicz, Li et al. 1994), G1, S and G2/M phases were determined using the analysis programs WinMDI (version 2.8) and FlowJo (version 7.5).

2.10 Sample preparation for western blot analysis

2.10.1 Cell treatment

Cell lines (1×10^6 in 5mls) or primary cells ($5x10^5$ in 5mls) were reset in fresh medium with or without HS-5 cells or in the sCD40L system, for 24hrs prior to the addition of drugs of interest for the required time.

2.10.2 Whole protein cell extraction

Cells were pelleted via centrifugation at 1300rpm for 5mins at room temperature. Medium was discarded and the cells were washed twice in PBS and re-pelleted at 4°C. The cells were resuspended in ice-cold lysis buffer [1 x PBS, 1% Triton X-100, 0.5% sodium deoxycholate, 0,1% sodium dodecyl sulphate (SDS), 1mM EDTA] made up to 500ml with de-ionised water, at pH 7.4. The protease inhibitor cocktail (Roche, Basel, Switzerland) was added to the lysis buffer at a 1:50 dilution prior to use. Samples were left on ice for 20mins and centrifuged at 20,000g for 5mins to remove insoluble cellular debris. The supernatant was transferred into fresh eppendorf tubes (Eppendorf UK Limited) and stored at -80^{o}C until protein quantification.

2.10.3 Protein quantification using the Bradford Reagent

The protein content of each lysate was determined by use of the BCA™ protein assay (Pierce, Illinois, USA). BCA is used for the colorimetric detection and quantitation of total protein and the assay uses the colorimetric reduction of Cu^{2+} to Cu^{1+} in an alkaline medium. Cu^{1+} is a purple reaction product formed by chelation of 2:1 molecules of BCA to Cu^{1+}. The absorbance is read at 562nm and is linearly related to increasing protein concentrations. 10ul of lysate was pipetted into a 96-well plate with 10ul of lysis buffer. The BCA reagent A (sodium carbonate, sodium bicarbonate, BCA and sodium tartrate in 0.1M sodium hydroxide) was mixed with BCA reagent B (4% cupric sulphate) in a 50:1 ratio and 160ul added to each well. The plate was incubated at 37^{o}C for 20mins and its absorbance measured. The protein content was determined by comparison with a standard concentration curve created by dilutions of bovine serum

albumin (BSA, 2mg/ml) from 0-20ug in lysis buffer and calculated by linear regression analysis.

2.11 Western bolt analysis

2.11.1 Protein electrophoresis and electroblotting onto PVDF membranes

20-40µg of cell protein was added to 1x NuPAGE® LDS sample buffer (Invitrogen™) and the samples were heated at 95°C for 10mins. Pre-cast SDS-PAGE gels (NuPAGE® Novex® Bis-Tris midi or mini gel system, Invitrogen™), were placed in a gel tank, running buffer (1x NuPAGE® running buffer, Invitrogen™) was added and the samples were loaded into the gel wells. In the first lane of each gel, the Novex® sharp standard protein molecular weight marker (3.5kDa -260kDa, Invitrogen™) was loaded. For blots that were to be developed using the Fuji Film image analyser (see below), a luminescent marker was loaded: MagicMark™ XP western protein standard (Invitrogen™) with bands between 20 and 220kDa. Electrophoresis of the gel was performed at a constant voltage of 200V for 30-60mins.

2.11.2 Transfer of proteins from the gel to the polyvinylidene fluoride membrane (PVDF)

Protein transfer was performed using the iBlot™ gel transfer device (Invitrogen™) for semi-dry blotting of proteins according to the manufacturers' instructions. It is a self-contained blotting unit with an integrated power supply. The device requires iBlot™ disposable gel transfer stacks with an integrated PVDF transfer membrane. Each transfer stack contains a copper electrode and appropriated cathode and anode buffers in a gel matrix. After completion of protein electrophoresis the gels were removed from the gel tank and placed on the anode stack, containing the PVDF membrane as the uppermost layer. Filter paper presoaked in distilled water, was placed on the gel and air bubbles were removed using a rolling device. The cathode stack was then placed on top of the filter paper and the transfer device closed and programmed to perform the protein transfer over 7mins.

2.11.3 Antibody probing of the PVDF membrane

The PVDF membrane was removed from the iBlot™ system and blocked in 1x tris(hydroxymethyl)aminomethane (Tris) buffered saline (TBS) [1L of 10x TBS; 24.2g Trizma® base (Sigma-Aldrich) and 80g NaCl made up with distilled water, pH adjusted to 7.6] with 0.1% (v/v) Tween-20®(Sigma-Aldrich) (TBS-T) to reduce non-specific antibody binding. Following 3x wash steps with TBS-T, the primary antibody was added either for 2hrs at room temperature or overnight at 4°C. The membrane was again washed three times and incubated with horseradish peroxidase (HRP)-conjugated secondary antibody. A horseradish peroxidase-conjugated goat anti-rabbit IgG1 (1:2000 dilution) was used as the secondary antibody in most cases, or an anti-mouse IgG1 (both Dako, Ltd. Cambridge, UK).

2.11.4 Antibodies used for protein detection

The primary antibodies used in western blot analysis are listed in table 2.1 on the next page. All antibodies were diluted in TBS-T.

Table 2.2 Primary antibodies used in western blotting experiments.

Primary Antibody	Molecular weight (kDa)	Supplier	Dilution	Source	Catalogue Number
Acetyl histone H3	17	Millipore	1:10,000	Rabbit	06-599
Histone H3	17	Cell Signaling	1:2000	Rabbit	9715
Acetylated α-tubulin	52	Sigma-Aldrich	1:3000	Mouse	T6793
β-actin	40	Cell Signaling	1:1000	Rabbit	4970
Akt	60	Cell Signaling	1:1000	Rabbit	9272
PARP	89, 116	Santa Cruz	1:1000	Rabbit	Sc-7150
Erk1/2	42, 44	Cell Signaling	1:1000	Rabbit	9102
GAPDH	36	Cell Signaling	1:1000	Rabbit IgG	2118
HSP27	27	Abcam	1:500	Rabbit	ab5579
HSP70	70	Cell Signaling	1:1000	Rabbit	4872
HSP90	90	Santa Cruz	1:200	Goat	Sc-27987
Mcl-1	40	Santa Cruz	1:1000	Rabbit	Sc-819
NF-κβ p65	65	Upstate	1:1000	Rabbit	06-418
p21	21	Santa Cruz	1:200	Rabbit	Sc-397
Phospho-Akt	60	Cell Signaling	1:1000	Rabbit	9271
Phospho-Erk1/2	42, 44	Cell Signaling	1:1000	Rabbit	9101
Phospho-p38 MAPK	43	Cell Signaling	1:1000	Rabbit	9211
p38 MAPK	43	Cell Signaling	1:1000	Rabbit	9212
Phospho-Stat3	79, 86	Cell Signaling	1:1000	Rabbit IgG	9145
Stat3	79, 86	Cell Signaling	1:1000	Mouse IgG2a	9139
α-tubulin	52	Cell Signaling	1:1000	Rabbit	2144
JNK/SAPK	46, 54	Cell Signaling	1:1000	Rabbit	9252

2.11.5 Visualisation of protein bands

The protein bands were visualised using an enhanced chemiluminescence (ECL) reagent (GE Healthcare UK Ltd., Little Chalfont, UK), which utilises the reaction when hydrogen peroxidase catalyses the oxidation of luminol in alkaline conditions. Immediately following oxidation, luminol is in an excited state which then decays to ground state via a light emitting pathway. PVDF membranes were incubated with ECL for 1min before the excess was blotted away and exposed to blue light sensitive autoradiography film, Hyperfilm (GE Healthcare UK Ltd., Little Chalfont, UK) for 5 to 20mins depending upon the strength of the bands. Development of the Hyperfilm was achieved by exposure to Kodak Developer followed by Kodak Fixer (Sigma-Aldrich). For most of the blots developed, a Fujifilm luminescent image analyser (Fujifilm LAS-4000, Tokyo, Japan) was used for visualisation of protein bands. Densitometric analysis was performed using Gelscan version 5.1 software (BioSciTech, Frankfurt, Germany). Values were normalized to the loading control.

2.12 Measurement of secreted cytokines in the MM/HS-5 system using the Meso Scale Discovery® (MSD) electrochemilumunescence assay

2.12.1 Principle of multi-cytokine measurement in the MSD assay

In collaboration with Meso Scale Discovery® we designed a custom cytokine assay measuring 7 human cytokines simultaneously in an MSD 96-well MULTI-SPOT®plate. The assay employs a sandwich immunoassay format where capture antibodies are coated in a single spot, on the bottom of the plate. When samples are incubated in the MULTI-ARRAY® or MULTI-SPOT®plate, each cytokine binds to its corresponding capture antibody spot. Cytokine levels were quantitated using a cytokine-specific detection antibody labeled with MSD SULFO-TAG™ reagent. The SULFO-TAG™ labels emit light upon electrochemical stimulation initiated at the electrode surfaces of the microplate (Figure 2.3). This luminescent signal is quantitated using the MSD AI2400 platform and a standard curve is generated. Cytokine levels in unknown samples were calculated by fitting the luminescence values to a linear regression equation.

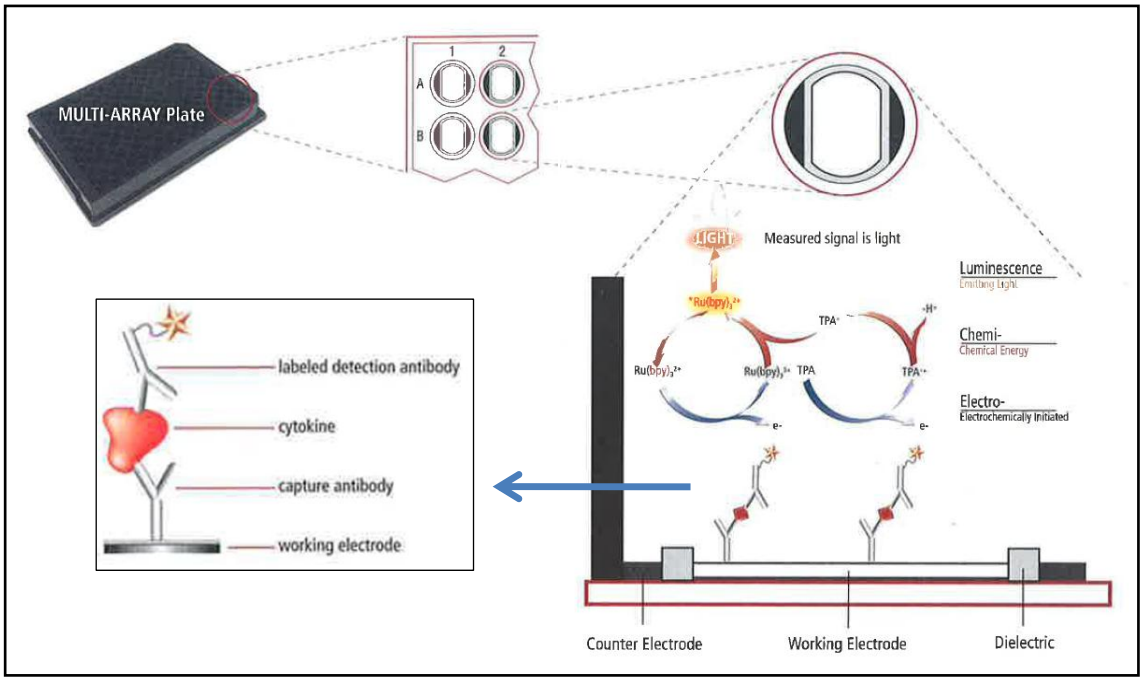

Figure 2.3 An example of a MULTI-SPOT®plate coated with 10 different capture antibodies. The antibodies are arrayed on the patterned working electrode and cytokines (analytes) are detected with antibodies labeled with SULFO-TAG™ reagent. The electrical energy generated by the SECTOR™ imager 2400, initiates a chemical reaction resulting in the generation of light. The luminescent signal is quantified using a standard curve and the MSD SI2400 platform.

2.12.2 Sample and reagent preparation

Cell culture supernatants collected from previously conducted MM/HS-5 co-culture experiments, were used in these experiments. They were stored at -80°C until their use in the MSD assays, when they were defrosted on ice and centrifuged at 3000rpm for 2mins at 4°C. Individual cytokine stocks were prepared by pipetting 5µl of the 50µg/ml calibrator into 20µl of sample matrix (standard culture medium) to give a 10µg/ml individual stock. A stock of combined calibrators was then prepared by combining the 10µg/ml individual stocks for each calibrator to generate a working stock solution in which each calibrator is a 1µg/ml. A 1x working detection antibody solution was prepared from a 50x concentration, that is, for each plate used, a 60µl aliquot of the stock detection antibody mix was added to 2.94ml of MSD antibody diluent. The assay read buffer was diluted 1 to 2 in deionised water to make a final

concentration of 2x MSD Read Buffer, so for each plate, 10ml of stock was added to 10ml deionised water.

2.12.3 Preparation of the calibration curve and the MSD plate

The combined working stock solution was diluted 1:100 to prepare a 10,000pg/ml combined high calibrator solution to be used as the highest value on the standard curve. The remaining standard solutions were then serially diluted 1:4 to give a standard range from 10,000pg/ml to 2.4pg/ml. 25µl of sample or standard was dispensed into separate wells of the MSD plate, in duplicate. The plate was sealed with an adhesive plate seal and incubated at room temperature with vigorous shaking (300-1000rpm) for 2hrs. This was followed by dispensing of 25µl detection antibody solution into each well of the plate which was sealed again and incubated at room temperature with vigorous shaking for a further 2hrs. The plate was then washed 3x with 0.05% PBS-Tween. 150Ml of 2x MSD read buffer was added to each well of the MSD plate and it was inserted into the SECTOR™ Imager for immediate analysis.

2.13 E_{max}modeling

The viability data were analysed using Graphpad PRISM® Software (Version 5.03), which fits the data to the sigmoid E_{max} concentration-effect model (Holford and Sheiner 1982) in order to identify the concentrations required to cause 50% of the maximum effect (EC_{50}). The model uses a modification of the following equation:

$$E_{pred} = E_{cont} - [E_{max} \times C^n / (EC_{50}^n + C^n)]$$

Where E_{pred} is the predicted effect (on viability), E_{cont} is the effect without the drug, E_{max} is the maximum effect attainable, C is the drug concentration, and n is the sigmoid factor which influences the steepness of the curve.

2.14 Combination interaction analysis

The combination data was analysed using Calcusyn software for dose-effect analysis (Chou and Talalay 1984). It is based on the multiple drug-effect equation of two drugs derived from enzyme kinetic models:

$$\mathbf{CI = (D)_1 / (D_X)_1 + (D)_2 / (D_X)_2}$$

Where: $(D)_1$ and $(D)_2$ are the concentrations of drug 1 and drug 2 that have x effect when used in combination and $(D_X)_1$ and $(D_X)_2$ are the concentrations of drug 1 and drug 2 that have the same x effect when used alone. Synergism is defined as a more than expected additive effect, and antagonism, as a less than expected additive effect. Combination Index (CI) values less than 1 indicates synergism, equal to 1 indicates additivity and greater than 1, antagonism.

2.15 Statistical analysis and acceptance criteria

Standard statistical methods such as mean and standard deviation are used to summarise data. Data are represented in graphical and tabular form. The paired t-test was used to compare the means of two groups and 2-way analysis of variance (ANOVA) was used for more than 2 groups of data. A p value <0.05 was considered significant and was denoted with an asterix (*). More significant P values were denoted as follows: $p<0.01$ = ** and $p<0.005$ = ***. The coefficient of variation (CV) for all replicates within an assay must be <20% for the assay to be accepted. And an R-value of all standard curves must be >0.95.

CHAPTER 3: Validation and use oftheCHO-CD40L *in vitro* primary culture system in Non-Hodgkin's lymphoma

3.1 Introduction

3.1.1 CD40

Malignant cell lines provide valuable preliminary data on the potential effectiveness of novel agents, and are useful to examine putative mechanisms of action, however, they have limitations. They have specific clinical characteristics that have enabled them to grow in culture, often have been grown for long periods of time and are likely to have evolved so will not necessarily resemble the original tumour or clinical situation. They are also unable to reflect patient tumour heterogeneity or *in vivo* growth conditions. Thus, an *in vitro* culture system using patient samples, which much more closely resemble the original tumour, is a valuable tool for investigating tumour biology and sensitivity to novel agents. B cell survival and proliferation in response to immune stimulation is dependent on CD40 activation and it is this knowledge that has been exploited to develop a culture system for the growth of malignant B cell lymphoma tumour cells.

CD40 is a 48-50kDa transmembrane glycoprotein cell surface receptor that belongs to the tumour necrosis factor (TNF) receptor superfamily (Kehry 1996). CD40 was first identified and functionally characterised on mature B-cells but is expressed throughout B-cell development, and on monocytes, dendritic cells, haematopoietic progenitor cells, endothelial cells and epithelial cells, as well as some B-cell malignancies and carcinomas (van Kooten and Banchereau 1997; Younes and Carbone 1999; Fiumara and Younes 2001). The ligand for CD40 (CD40L, CD154, or gp39) is a trimeric 33-39kDa type II transmembrane glycoprotein predominately expressed by activated CD4+ T-cells (Klaus, Choi et al. 1997). CD40L is also, however, expressed on activated B-cells, natural killer cells, monocytes, eosinophils, basophils, dendritic cells, platelets, endothelial cells and smooth muscle cells (Fiumara and Younes 2001).

3.1.2 CD40 responses in normal B cells

CD40-mediated stimulation of normal B-cells plays a key role in T-cell mediated B-cell activation and humoral immune responses. Cross-linking of CD40 with cells expressing CD40L promotes B-cell proliferation, immunoglobulin (Ig) production, Ig isotype switching, germinal centre formation and induction of B-cell memory. Mutations in the gene encoding CD40L cause an immuno-deficiency, X-linked hyper-IgM syndrome characterised by normal or elevated levels of IgM but no IgG, IgA, or IgE production and defects in germinal centre and memory cell formation (DiSanto, Bonnefoy et al. 1993; Korthauer, Graf et al. 1993). CD40 or CD40L knockout mice produce similar phenotypes that are unable to mount normal humoral immune responses (Klaus, Choi et al. 1997). Blocking interaction of CD40 and CD40L with soluble CD40 (which prevents CD40L binding to the native receptor) or monoclonal antibodies to CD40L prevents B-cell proliferation or Ig production in response to T-cell signals (Clark and Ledbetter 1994).

Ligation of CD40 by CD40L has been demonstrated to be important in B-cell proliferation. Banchereau *et al* demonstrated that culture of human B-cells with an anti-CD40 monoclonal antibody (CD40mAb), presented in a cross-linked fashion by transfected mouse fibroblast cells stably expressing human FcγRII/CDw32 Fc, were able to generate long-term normal B-cell lines (Banchereau, de Paoli et al. 1991). Addition of IL-4, which *in vivo* is produced by activated T cells, and selects for differentiation of the activated B cells into memory B cells with proliferative potential, strongly enhanced this cell proliferation. Thus in this system, the fibroblast line mimics follicular dendritic cells and the added cytokine would mimic germinal centre T cells (Banchereau, de Paoli et al. 1991; Banchereau and Rousset 1991; Rousset, Garcia et al. 1991). The first evidence that CD40 regulates apoptosis in normal B cells came from treatment of germinal centre cells with anti-CD40 monoclonal antibodies (mAbs)(Liu, Joshua et al. 1989). *In vitro* these cells rapidly undergo apoptosis, but treatment with anti-CD40 mAb induced long-term survival. Subsequent studies have demonstrated that CD40 activation rescues germinal centre B cells and peripheral blood B cells from spontaneous apoptosis when CD40 is activated by either CD40L transfection or anti-CD40 mAbs (Holder, Wang et al. 1993; Lomo, Blomhoff et al. 1997). CD40 ligation also

results in upregulation of surface molecules contributing to antigen presentation on dendritic cells and monocytes as well as on normal or malignant B cells.

3.1.3 CD40 responses in malignant B cells

Although CD40 is considered a survival factor for normal B-cells, in malignant cells, both suppression and induction of apoptosis have been observed (Schultze, Cardoso et al. 1995; Cardoso, Schultze et al. 1996). Ghia *et al* demonstrated that primary follicular lymphoma cells treated with soluble CD40L showed increased survival compared to cells cultured in media alone or in the presence of various cytokines (Ghia, Boussiotis et al. 1998). Johnson *et al* established primary cultures from isolated follicular lymphoma cells using a similar system to that of Bachereau (Johnson, Watt et al. 1993). Using a mouse fibroblast monolayer transfected with the CDw32 Fc receptor to present CD40 monoclonal antibody in the presence of IL-4, prolonged culture was possible. In mantle cell lymphoma, Anderson *et al* demonstrated that CD40 activation using a soluble CD40L trimer (huCD40LT) was able to induce proliferation of mantle cell lymphoma primary cultures, by inducing selective cell cycle progression and DNA synthesis (Andersen, Larsen et al. 2000). Castillo *et al* demonstrated that ligation of CD40, using an anti-CD40 monoclonal antibody, or a Jurkat cell line constitutively expressing CD40L, results in S phase entry and cell proliferation. IL-4 again enhanced these effects (Castillo, Mascarenhas et al. 2000). IL-10 too has been shown to enhance proliferation in the `CD40 system` in mantle cell lymphoma primary cultures (Visser, Tewis et al. 2000).

Conversely, CD40 activation has been shown to induce growth arrest and/or apoptosis in a number of malignant B-cell lines. Funakoshi *et al* demonstrated activation of CD40 resulted in growth inhibition of two human diffuse large B-cell lines and two EBV-induced human lymphoblastoid cell lines (Funakoshi, Longo et al. 1994). Conflicting effects have been found in the Burkitt's cell lines, Ramos and Daudi and in multiple myeloma cells with reports of both cell proliferation and growth inhibition (Pellat-Deceunynck, Amiot et al. 1996; Bergamo, Bataille et al. 1997; Baker, Eliopoulos et al. 1998; Lefterova, Marten et al. 2000; Teoh, Tai et al. 2000; Szocinski, Khaled et al. 2002). It is interesting, however, that no induction of apoptosis has been

demonstrated in primary cultures. Thus, the functional consequences of CD40 signalling appear to be highly dependent not only on the B-cell type being triggered but also the conditions in which it is triggered (Vonderheide, Dutcher et al. 2001).

3.1.4 Investigating the activity of bortezomib in primary NHL cells cultured in the CD40 system

The second aim was to use the system to investigate the sensitivity of these cultures to bortezomib and to correlate *in vitro* activity with clinical responses in patients treated on the phase II clinical trial. Bortezomib is the first in the class of proteasome inhibitors (PIs), which target the critical process of intracellular protein degradation or recycling through the proteasome. Bortezomib is approved for the treatment of relapsed or refractory mantle cell lymphoma in the United States and results presented here, in addition to studies that we have previously published (Strauss, Maharaj et al. 2006) confirm its efficacy in primary MCL cells cultured *in vitro*, taken from patients enlisted in the phase II trial.

3.2 Results

3.2.1 Effect of γ-irradiation on the growth of CHO-CD40L transfectants

Under normal culture conditions, non-transfected CHO cells characteristically grow quickly and double within 12hrs. Transfected cells are stressed due to being under constant selection pressure and thus CHO-CD40L cells have twice the normal doubling time of 24hrs. Even at this slower growth rate, expansion of CHO-CD40L cells over time would result in contamination of the B cells in the coculture system. It is thus essential to halt CHO-CD40L cell growth to allow for their use as nonreplicating, viable, metabolically active support cells which continually express CD40L thus promoting the selective expansion of the B cells of interest. An efficient way to do this is by treating them with γ-irradiation prior to their use in coculture assays.

Cells were harvested at 80% confluence and irradiated in anIBL 637 Cs137 Gamma Irradiator at 4 different doses according to the levels of shielding applied for each dose rate (refer to Chapter 2, table 2.1).When all samples were placed on the bottom shelf without any shielding (representing the highest dose rate), the time required to achieve the following doses were: 25Gy = 417sec, 50Gy = 833sec, 75Gy = 1250sec and 96Gy = 1600sec. Within an hour of being irradiated, 100ul of CHO-CD40L cells at a density of $2x10^5$cells/ml were seeded into 96-well plates and cultured in CHO cell media (refer to section 2.5.1 chapter 2 for media constituents). Cell growth was measured after 24hrs and 96hrs of culture at 37°C using the trypan blue dye exclusion assay. Cells were counted in triplicate wells and values averaged over 3 separate experiments.

Figure 3.1 shows that cells exposed to the highest radiation dose of 96Gy did not proliferate after 24hrs or 96hrs of culture compared to control cells which doubled and quadrupled in cell number, respectively. CHO-CD40L cells also doubled following 25Gy but a clear dose-dependent decrease in cell proliferation was apparent with higher radiation doses such that by 96hrs of culture cells had proliferated just 2.3-fold after 75Gy of radiation.

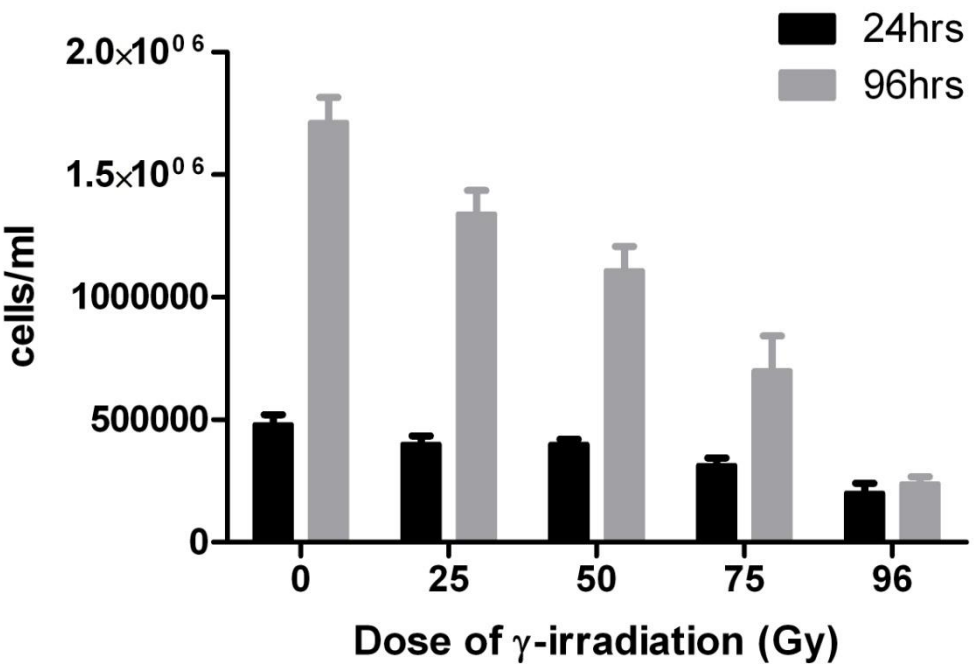

Figure 3.1 CHO-CD40L cells were irradiated at a range of doses from 25Gy up to 96Gy (Grays) for up to 1600sec in an IBL 637 Cs137 Gamma Irradiator. Cells were plated at 2x105cells/ml and cultured for 24hrs and96hrs in a humidified atmosphere at 37°C. Cell growth was measured in triplicate wells of the 96-well plate using the trypan blue dye-exclusion assay. Data points represent absolute cell numbers and the mean of 3 separate experiments.

3.2.2 Effect of irradiation on CD40L (CD154) expression

We then investigated the cell surface expression of CD154 on irradiated CHO-CD40L cells at 24hrs and 96hrs post-irradiation. CHO-CD40L cells were harvested at 80% confluence and exposed to the irradiation dose that was found in the previous experiment to fully halt cell growth, 96Grays. Cells were then cultured in CHO cell medium for 24hrs or 96hrs after which they were incubated for 30mins with an anti-CD154PE-conjugated antibody (clone TRAP1, Dako, Cambridge, UK). Following 20mins of cell fixation in 1.5% paraformaldehyde (PFA), samples were immediately analysed for CD154 expression via flow cytometry (BD FACSCalibur™, Becton Dickenson, BD Biosciences) and data was quantified using FlowJo software version 7.5.

As shown in figure 3.2, percentage expression of CD154 in control cells pre-culture (time 0hrs) was 90% (±1.4%, figure 3.2a), indicated by a right shift of the blue histogram from the negative isotype control (black histogram). After 24hrs of culture, this high level of expression was maintained at 85% (±2.6%, figure 3.2b) however had decreased to 66% (±1.1%, figure 3.2c) following 96hrs culture. Exposure to 96Gy irradiation did not significantly alter CD154 expression ($p>0.05$) at any stage of culture compared with the time-matched controls (figure 3.3a). Cells were subsequently analysed 5 days and 8 days post irradiation and CD154 expression was found to decrease to less than 50% (figure 3.3b). Results so far have shown that exposure to 96Gy of γ-irradiation render CHO-CD40L cells incapable of further proliferating for a period of up to 4 days in culture, whilst maintaining their ability to express CD40L as efficiently as non-irradiated control cells. This dosage was therefore used in all further coculture experiments.

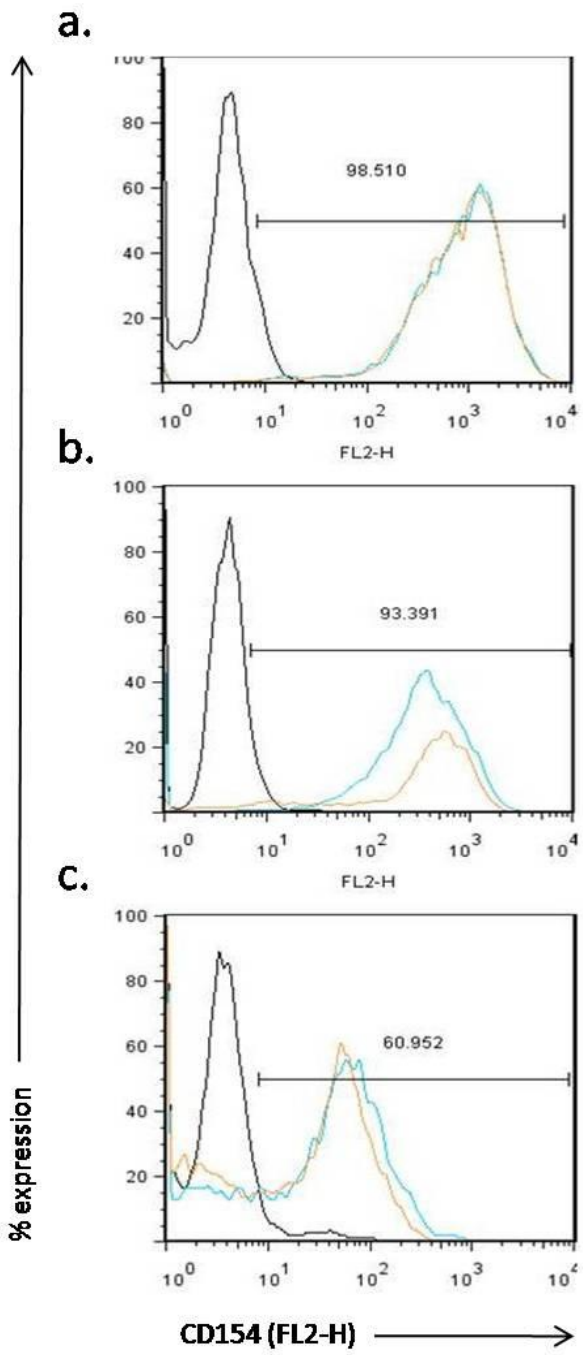

Figure 3.2 CD154 expression on CHO-CD40L cells a. untreated CHO-CD40L (blue histogram) and γ-irradiated (96Gy) (orange histogram) cells immediately after irradiation (0hrs), b. untreated CHO-CD40L and γ-irradiated (96Gy) cells 24hrs post-irradiation and c. untreated CHO-CD40L and γ-irradiated (96Gy) cells 96hrs (4 days) post-irradiation. 1x106cells/sample were harvested and exposed to an anti-CD154 PE-conjugated mAb for 30mins at RT followed by fixation in 1.5% PFA for 2hrs at 4°C. Samples were washed in ice-cold PBS then analysed for CD154 expression via for flow cytometry (BD FACSCalibur™, Becton Dickenson). Values represent the % expression in stained cells compared with a negative IgG1 isotype control (black histogram). Numbers inset are % positivity for irradiated samples at each time point.

a.

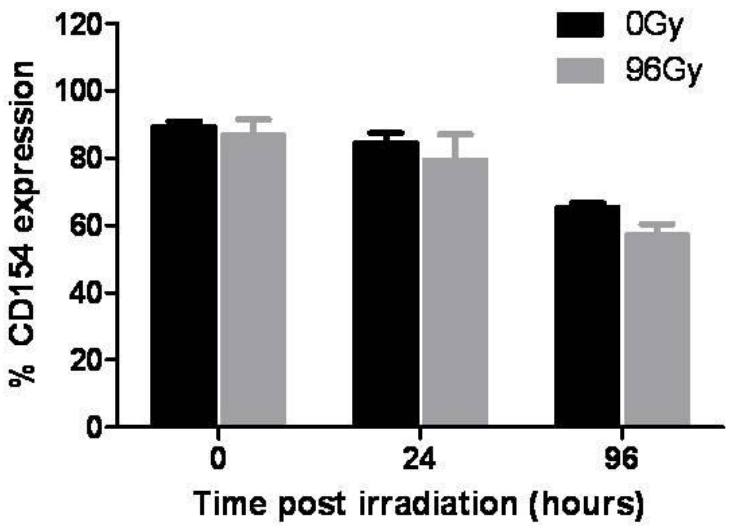

b.

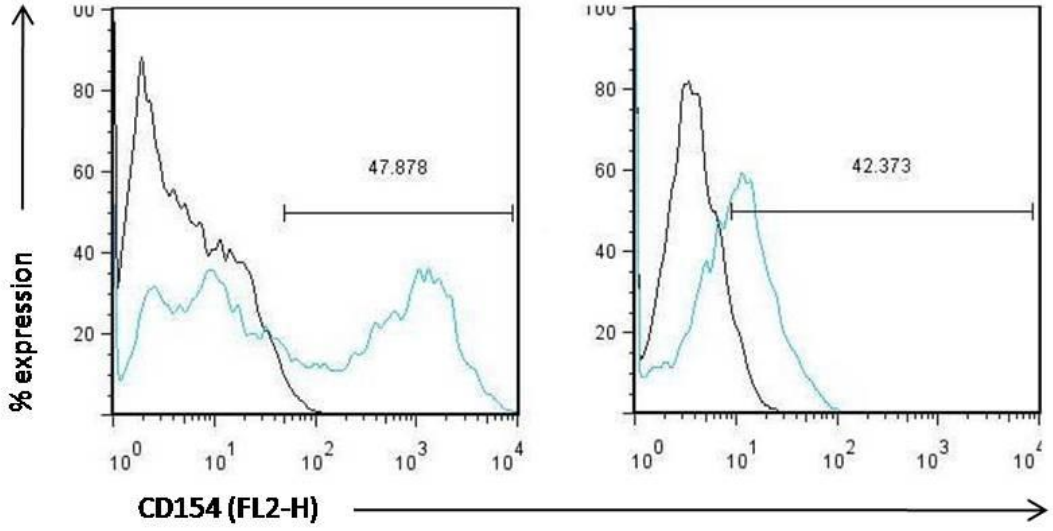

Figure 3.3 Summary of CD154 expression on CHO-CD40L cells. a. Values represent the mean ± S.D. % expression in stained cells relative to a negative IgG1 isotype control, for at least 2 independent experiments. b. Flow cytometric plots showing expression of CD154 after 5 days (blue histogram, left plot) and after 8 days of culture compared with the negative isotype control.1x106cells/sample were harvested and exposed to an anti-CD154 PE-conjugated mAb for 30mins at RT followed by fixation in 1.5% PFA for at least 2hrs at 4°C. Samples were washed in ice-cold PBS then analysed for CD154 expression via for flow cytometry (BD FACSCalibur™, Becton Dickenson).

3.3Effect of coculture in the CD40 system on the growth of normal PBMCs

We investigated the effect of the CD40 system on normal PBMCs isolated via density gradient centrifugation from pooled buffy coat samples collected from healthy donors (courtesy of the UK National Blood Service). PBMCs were cocultured in the CD40 system for 24, 48, 72 and 96 hours. At the end of each time point, the cells were assayed for viability and proliferation using trypan blue dye-exclusion assay (figure 3.4).

Results showed that viability of unstimulated cells decreased rapidly when cultured in medium alone, to just30% of their starting values after 96hrs (figure 3.4a) and this was accompanied by an equally dramatic reduction in total cell number (figure 3.4b). In contrast, cells cocultured in the CD40 system, maintained maximal cell viability over the entire culture period (figure 3.4a). After an initial 25% reduction in cell number over the first 48hrs, cell number quickly increased to 150% of starting values, indicative of an induction in cell proliferation, which was maintained at 96hrs.

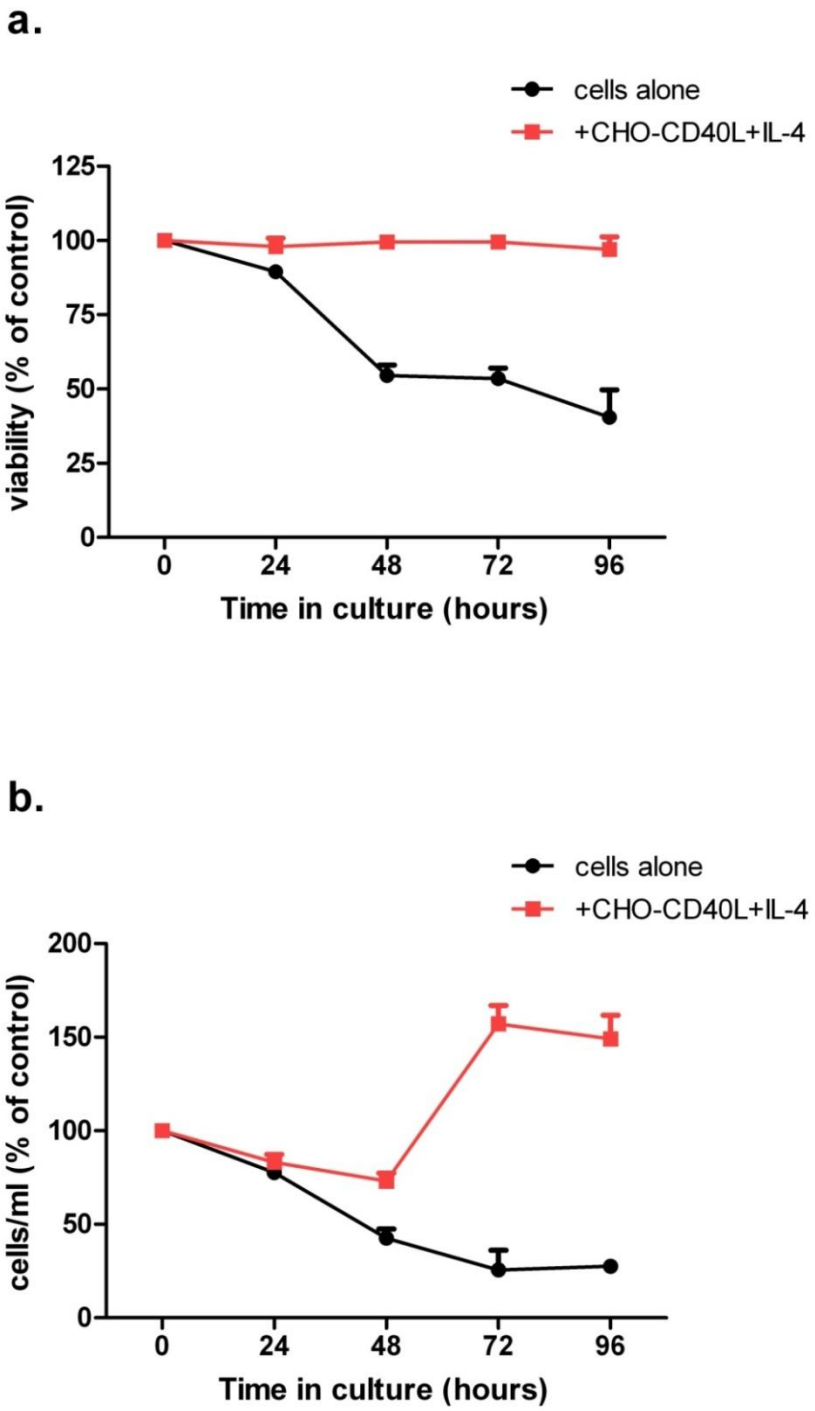

Figure 3.4 Growth of normal PBMCs in the CD40 system. PBMCs were isolated from 3 different buffy coat samples using Ficoll-Hypaque density gradient separation. Cells were cultured over a period of up to 96hrs in either media alone, or cocultured with CHO-CD40L + IL-4. After the indicated time points, cells were assessed for viability (a) and proliferation (b) using the trypan blue dye-exclusion assay. Data points represent the mean of 3 separate PBMC samples.

3.4 Effect of coculture in the CD40 system on the growth of primary MCL and FL cells

Results thus far showed that coculture in the CD40 system rescued normal PBMCs from spontaneous apoptosis *ex vivo* and induced their proliferation after 48hrs of culture for at least a further 48hrs, compared to cells cultured in media alone. Cell number and viability was optimal following 72hrs of coculture and CD40L was efficiently being presented, thus this time period was chosen for the next experiments investigating the effect of the CD40 system on growth of primary MCL and FL cells.

Cells from a total of 26 patient samples were cocultured in the CD40 system for 72hrs.All samples were used after resuscitation from liquid nitrogen storage and all samples with a cell viability of $\geq$ 50% on thawing were used. Sixteen of these were from patients with MCL (figure 3.5), 10 originating from peripheral blood, 5 from lymph node biopsy samples and 1 from pleural or ascitic fluid. Ten samples were obtained from patients with FL (2 from peripheral blood, 5 from lymph node biopsies, and 3 from pleural or ascitic fluid) (figure 3.6, table 3.1).Of the samples cocultured in the CD40 system, 21 (81%) samples grew successfully, defined as a cell viability of > 80% at 72hrs in control cells. Growth of all cocultured samples was compared to their growth in media alone, as controls (figures 3.5 and 3.6). The median viability in cocultured samples at day 3 was 91% compared to 53% for samples cultured in media alone.

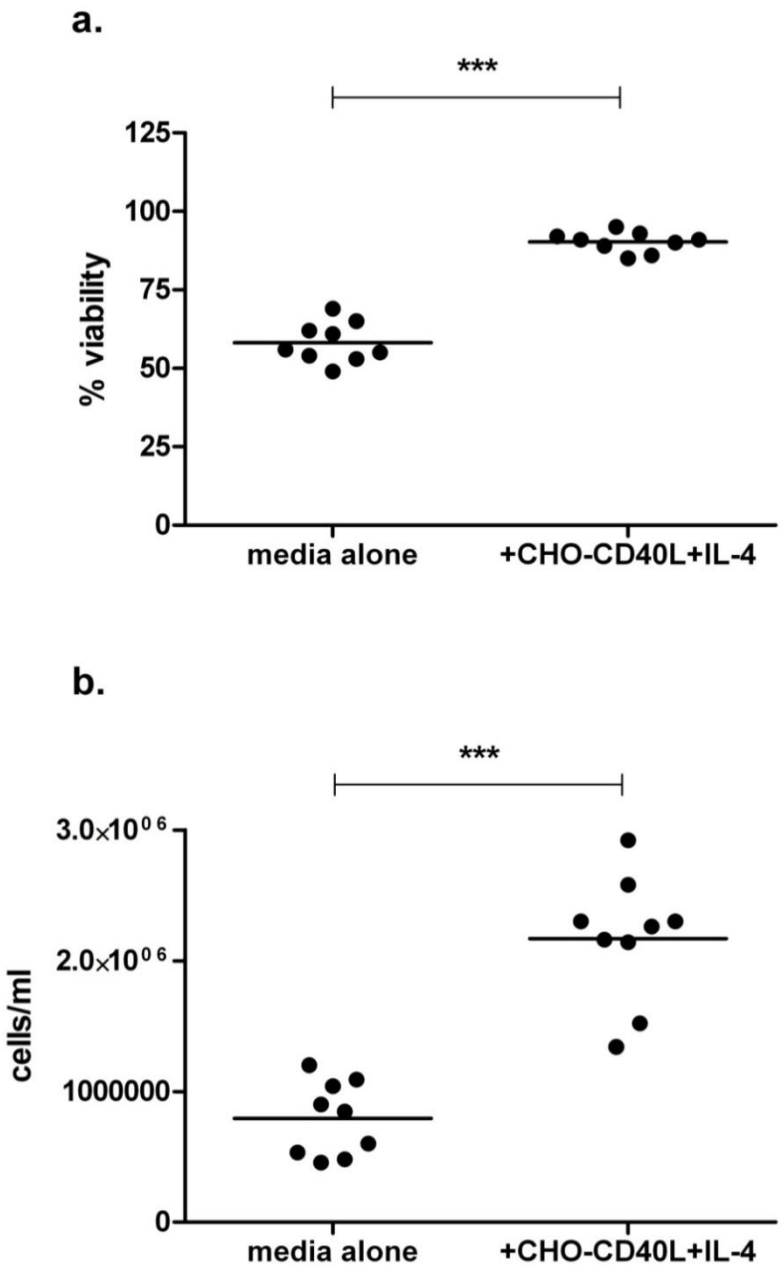

Figure 3.5 Viability (a) and cell proliferation (b) in primary MCL cells cultured for 72hrs either in media alone or cocultured in the CD40 system. Mononuclear cells were isolated from peripheral blood samples, ascites fluid or lymph node biopsies via density-gradient centrifugation on Ficoll-Hypaque. Cell suspensions were plated at a concentration of $1x10^6$cells/ml into 96-well plates either with media alone or in wells pre-coated with irradiated CHO-CD40L cells ($2x10^5$cells/ml). 5ηg/ml IL-4 was added to all coculture wells. After 72hrs, the trypan blue dye-exclusion was performed, counting cells in triplicate wells/treatment/sample. Horizontal lines indicate the mean of nine individual primary samples and *** indicates $p<0.005$ using the paired t-test.

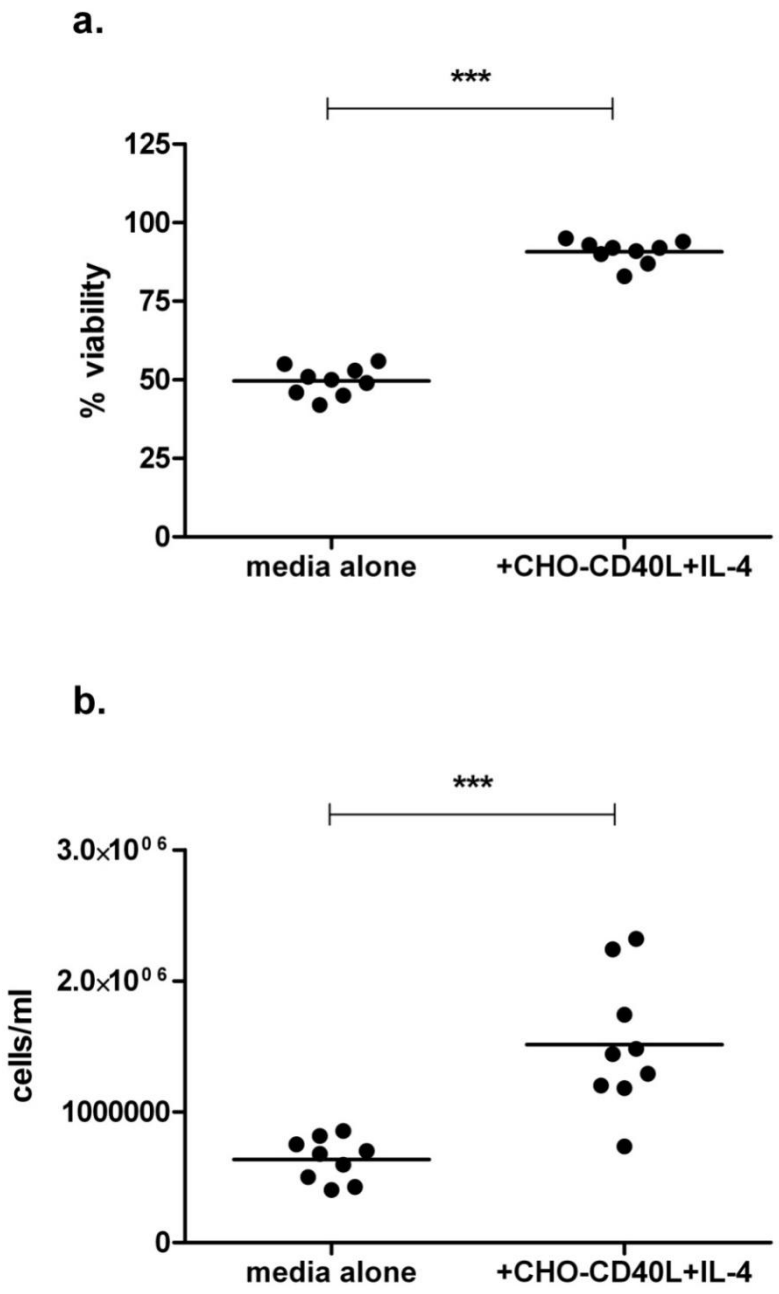

Figure 3.6 Viability (a) and cell proliferation (b) in primary FL cells cultured for 72hrs either in media alone or cocultured in the CD40 system. Mononuclear cells were isolated from peripheral blood samples, ascites fluid or lymph node biopsies via density-gradient centrifugation on Ficoll-Hypaque. Cell suspensions were plated at a concentration of $1x10^6$cells/ml into 96-well plates either with media alone or in wells pre-coated with irradiated CHO-CD40L cells ($2x10^5$cells/ml). 5ηg/ml IL-4 was added to all coculture wells. After 72hrs, the trypan blue dye-exclusion was performed, counting cells in triplicate wells/treatment/sample. Horizontal lines indicate the mean of nine individual primary samples and *** indicates $p<0.005$ using the paired t-test.

Table 3.1 Comparison of the characteristics of patient-derived cells cultured in standard medium or cocultured in the CD40 system.***P<0.001 for MCL and FL samples cocultured in the CD40 system versus the same samples cultured in media alone.

	-CD40 System		+CD40 System	
	MCL	FL	MCL	FL
# of samples cultured:	9	9	16	10
Peripheral blood	1	2	10	2
Lymph node	3	3	5	5
Pleural/ ascitic fluid	5	4	1	3
Median % viability at 72h (range)	56 (49-69)	50 (42-56)	91 (85-95)***	92 (83-95)***
Median cells/ml at 72h (range) *[Starting cells/ml = $1x10^6$]*	$8.5x10^5$ ($5x10^5$-$1x10^6$)	$6.8x10^5$ ($4x10^5$-$9x10^5$)	$2.3x10^{6***}$ ($1x10^6$-$3x10^6$)	$1.4x10^{6***}$ ($7x10^5$-$2x10^6$)
# of samples with >80% viability at 72hrs:	none	none	13	8
Peripheral blood	na	na	8	2
Lymph node	na	na	4	3
Pleural / ascitic fluid	na	na	1	3
Median CD19+ at 72h (range)	71 (66-75)	60 (56-64)	80 (68-87)	71 (63-91)
Median CD3+ at 72h (range)	33 (31-34)	35 (32-38)	15 (9-31)	24 (8-35)

3.5 Effect of the CD40 system on the immunophenotype of cells cultured in the CD40 system

Having confirmed that coculture for 72hrs in the CD40 system was sufficient to support cell growth of normal lymphocytes and primary FL and MCL samples, we then investigated whether this model system had any effect on cell phenotype following 72hr of coculture. Initially we monitored changes in cell surface expression of a panel of antigens (table 3.2) that together phenotypically define the disease of FL. We conducted this in 2 PBMC samples collected from the buffy coat of healthy donors and in 2 PBMC samples from patients with FL in the leukemic phase, over 72hrsof culture in the CD40 system (figures 3.7 and 3.8).

The antigens listed in table 3.2 below are those used in the routine diagnosis of patients with lymphoma, based on the WHO classification of Tumours of Haematopoietic and Lymphoid Tissues 2008 (Swerdlow, S. H., Campo, E., Harris, N. L., Jaffe, E. S., Pileri, S. A., Stein, H., Thiele, J. & Vardiman, J. W. E. (2008). ISBN: 9283224310).We compared the expression of each antigen at the indicated time points to their expression at time naught, before the start of the culture period. Cells were washed with PBS and exposed to antibodies for 30mins before re-washing & fixing in 1.5% paraformaldehyde (PFA) for 30mins. The samples were then analysed by flow cytometry on a FACSCalibur™ (FACScan, Becton Dickinson) and data was quantified using FlowJo software (version 7.5). Relative antigen expression was determined by setting markers for the antigen-labelled cell population and comparing them to markers set for the mouse IGg1 negative isotype control cells, thereby staging the cell population (figures 3.7 and 3.8).

Table 3.2 Cell surface antigens expressed by lymphoma cells. The following antibodies, all from Dako Products, Denmark, were used: CD19 (clone HD37) conjugated to mouse IgG1 phycoerythrin (PE), CD3 conjugated to mouse IgG1 fluorescein isothiocyanate (FITC), CD10 (Clone SS2/36), conjugated to mouse IgG1 FITC, CD38 (Clone AT13/5) and CD14 (Clone TUK4) both conjugated to mouse IgG1 RPE and finally Kappa (κ) and Lambda (λ) (both Clone HD37) antibody staining conjugated to rabbit IgG1 FITC and RPE respectively.

Antigen	Cell surface Expression
CD19-PE	Pan B cell marker, expressed throughout B cell development except on plasma cells
CD3-FITC	T cell marker (including all thymocytes and all NK cells)
CD14-FITC	Monocyte/macrophage marker
CD38-RPE	Mature germinal centre marker (lymphoplasmacytoid)
CD10-RPE	Immature germinal centre marker and memory B cells)
Lambda (λ)-RPE	Light chain restriction is a measure of cell clonality

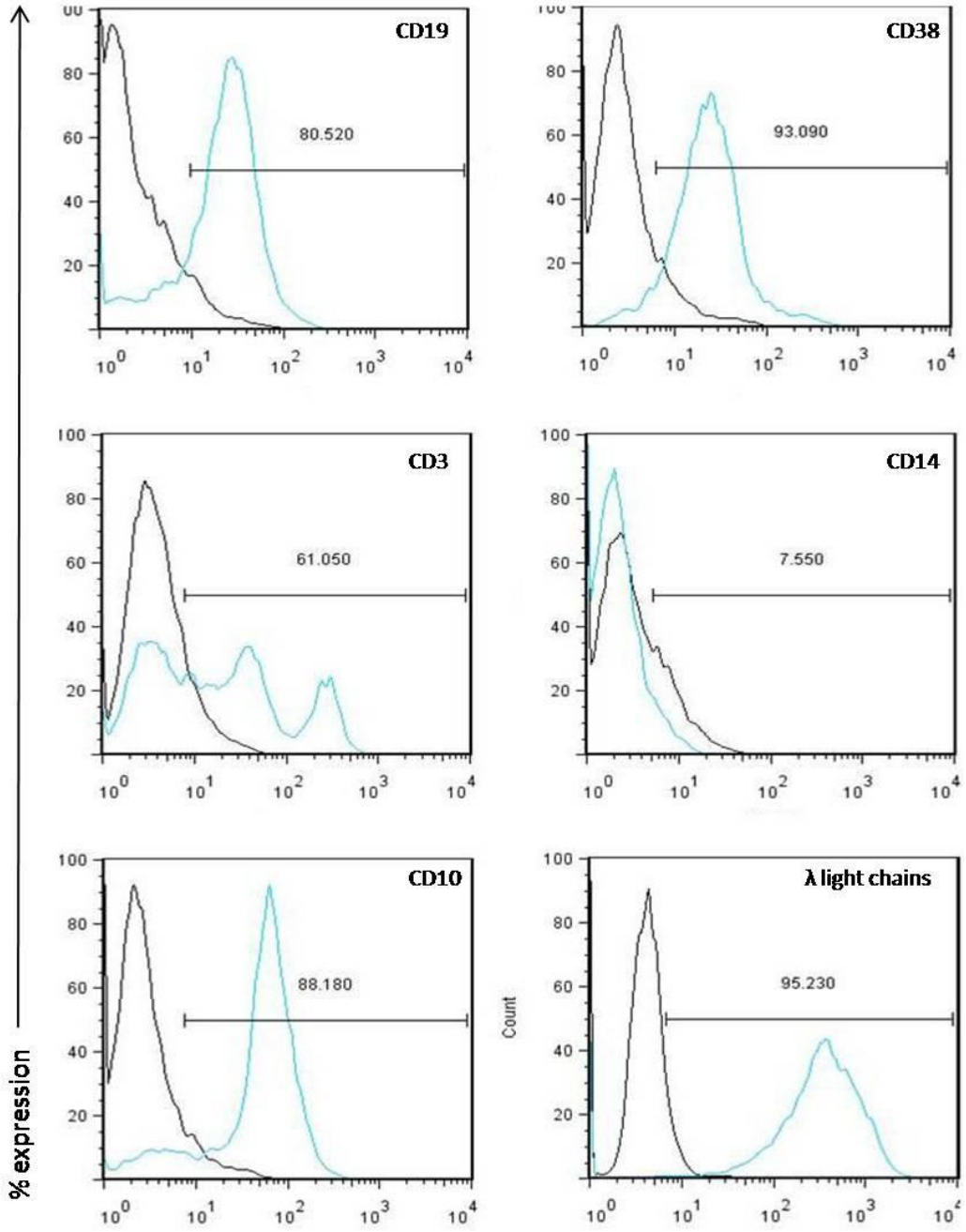

Figure 3.7 Example of the immunophenotypic marker profile for a patient with FL at the start of cell culture (day zero). Up to 1x10^{6}cells/sample were harvested, washed with PBS and exposed to antibodies for 30mins before re-washing & fixing in 1% paraformaldehyde (PFA) for 30mins. The samples were analysed by flow cytometry on a FACSCalibur™ (FACScan, Becton Dickinson) and data was quantified using FlowJo software (version 7.5). Relative % antigen expression was determined by setting markers for the antigen-labelled cell population (blue histogram) and comparing them to markers set for its mouse IGg1 negative isotype control (black histogram).Antigens were conjugated to PE (or RPE) and were resolved in the FL2-H fluorescence channel with the exception of CD3 and CD14 which were FITC-conjugated and measured in FL1-H.

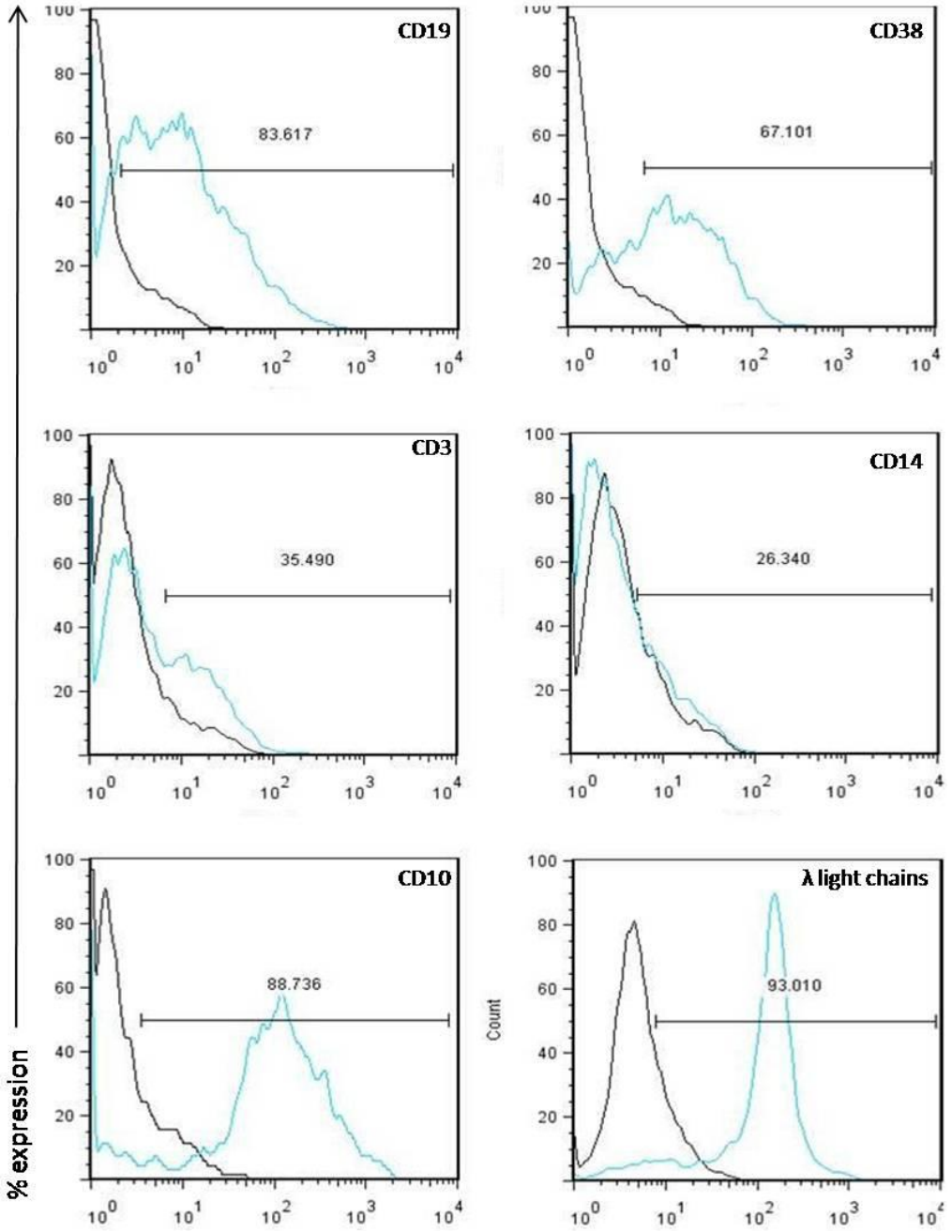

Figure 3.8 Example of the immunophenotypic marker profile for a patient with FL after 3 days of culture. Up to 1x10^{6}cells/sample were harvested, washed with PBS and exposed to antibodies for 30mins before re-washing & fixing in 1% paraformaldehyde (PFA) for 30mins. The samples were analysed by flow cytometry on a FACSCalibur™ (FACScan, Becton Dickinson) and data was quantified using FlowJo software (version 7.5). Relative % antigen expression was determined by setting markers for the antigen-labelled cell population (blue histogram) and comparing them to markers set for its mouse IGg1 negative isotype control (black histogram). Most antigens were conjugated to PE (or RPE) and were resolved in the FL2-H fluorescence channel with the exception of CD3 and CD14 which were FITC-conjugated and measured in FL1-H.

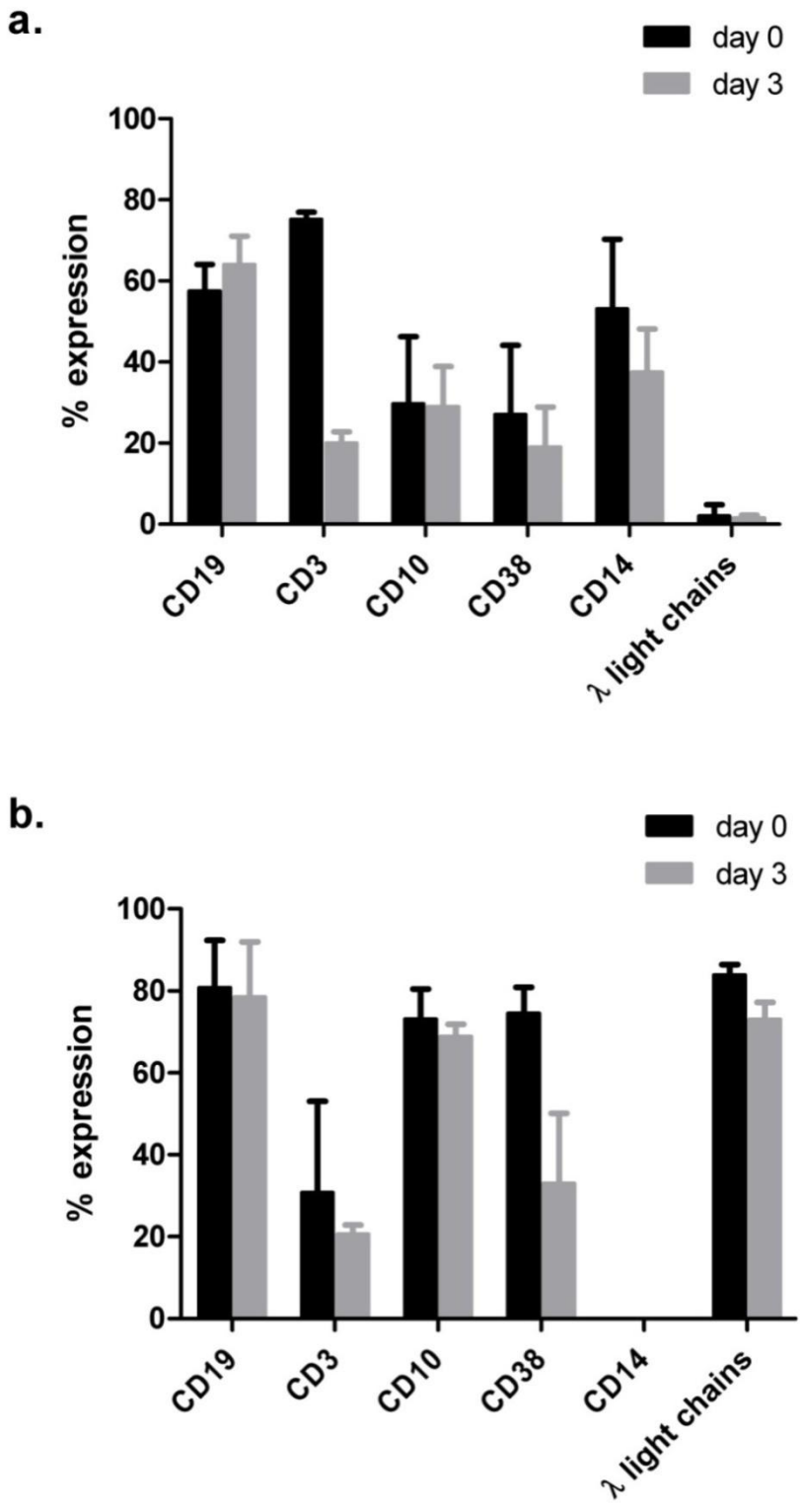

Figure 3.9 Antigen expression in (a) PBMCs from healthy donors and (b) PBMCs from patients with FL, at day 0 and following 72hrs of coculture in the CD40 system (day 3). Immunophenotyping percentages were compared to negative IgG1 isotype controls. Data points represent the mean ± S.D. of 2different samples.

Table 3.3 Summary table showing antigen expression in PBMCs from a healthy donor and cells from a patient with FL cultured for 3 days in the CD40 system. Percentage expression was compared to negative isotype controls. Data points represent the mean of 3 independent experiments. NA = not applicable, λ-light chain expression was undetectable in the normal PBMC sample.

	Normal PBMCs		FL	
Antibody (% expression)	**Day 0**	**Day 3**	**Day 0**	**Day 3**
CD19	58 ± 6.5	64 ± 7.1	81 ± 11.6	79 ± 13.4
CD3	75 ±1.7	20 ± 2.8	31 ± 22.3	21 ± 2.3
CD10	30 ± 16.6	29 ± 9.9	73 ± 7.3	69 ± 3.0
CD38	27 ± 17.1	19 ± 9.9	75 ± 6.4	33 ± 17.1
CD14	53 ± 17.2	38 ± 10.6	undetected	undetected
λ light chains	2 ± 2.8	2 ± 0.7	84 ± 2.6	73 ± 4.2
% viability Cells/ml	92 ± 3 $1x10^6 \pm 0$	90 ± 3 $1.69x10^6 \pm 9x10^4$	51 ± 1 $1x10^6 \pm 0$	76 ± 3 $1.82x10^6 \pm 6x10^4$

The summary figure 3.9 and table 3.3 above shows that at the time of culture, 58% of normal PBMCs were CD19 positive and this was maintained at 64% by day 3 confirming the expansion of B cells. There was no evidence of T cell or macrophage growth as expression of CD3 and CD14 decreased from 75% and 53% respectively to less than 20% and 38% by day 3. This suggested that depletion of these cells prior to cell use was unnecessary in the CD40 system. We continued to monitor CD19 and CD3 out to day 14 (data not shown) and found that CD19 expression gradually decreased from a peak of 73% at day 5 to 35% at day 14 and this was associated with a fewer number of B cells and increased cellular debris by day 14 when just 60% of cells were viable. In contrast, a high percentage of FL cells were CD19 positive at the time of culture (81%) and this was maintained at day 3. The T-cell population initially accounted for a third of the population (31%) and decreased to 21% at day 3. FL is a germinal centre lymphoma and thus was CD10 positive and light chain restricted throughout the culture period providing evidence for monoclonal expansion.

We then validated these initial findings in a larger cohort of FL and MCL samples when cultured in media only versus coculture in the CD40 system. From this point on, limited cell numbers meant that we were restricted to monitoring CD19 and CD3 expression, however, we found that this gave us a sufficient indication of maintenance of the B cell phenotype. There were no significant differences in the expression of CD19 and CD3 between cocultured and non-cocultured FL (figure 3.11a) and MCL samples (figure 3.11b), however, results did show a decrease in the B-cell phenotype (CD19+) associated with an increase in the T-cell population (CD3+) when samples were cultured in media alone over 72hrs. Examples of the CD19 and CD3 fluorescence plots in a MCL and a FL patient sample are shown in figure 3.10.

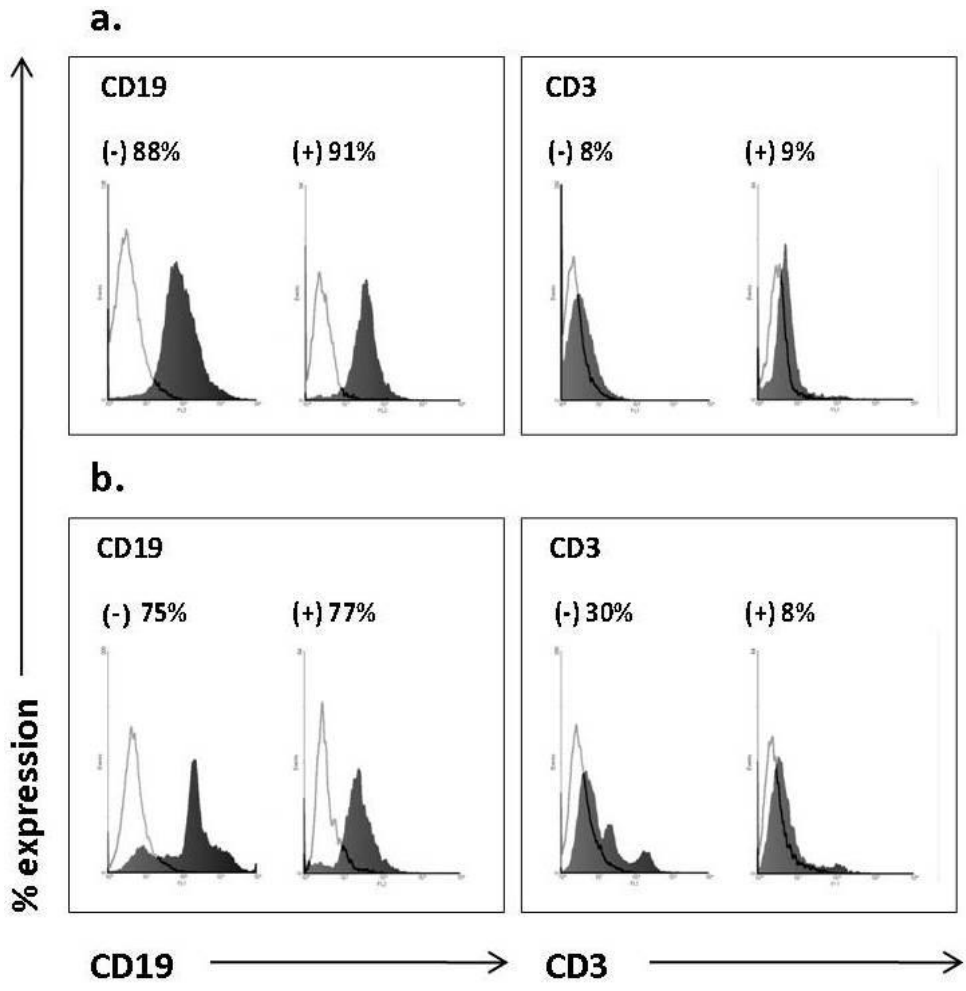

Figure 3.10 An example of immunophenotype analysis of isolated FL (a) and MCL (b) cells cultured in media alone (-) or in the CD40 system (+). Values are % positive cells for CD19 (B-cell, FL2-H) and CD3 (T-cell, FL1-H) markers (shaded histogram) compared to mouse IgG1 negative isotype controls (clear histogram).

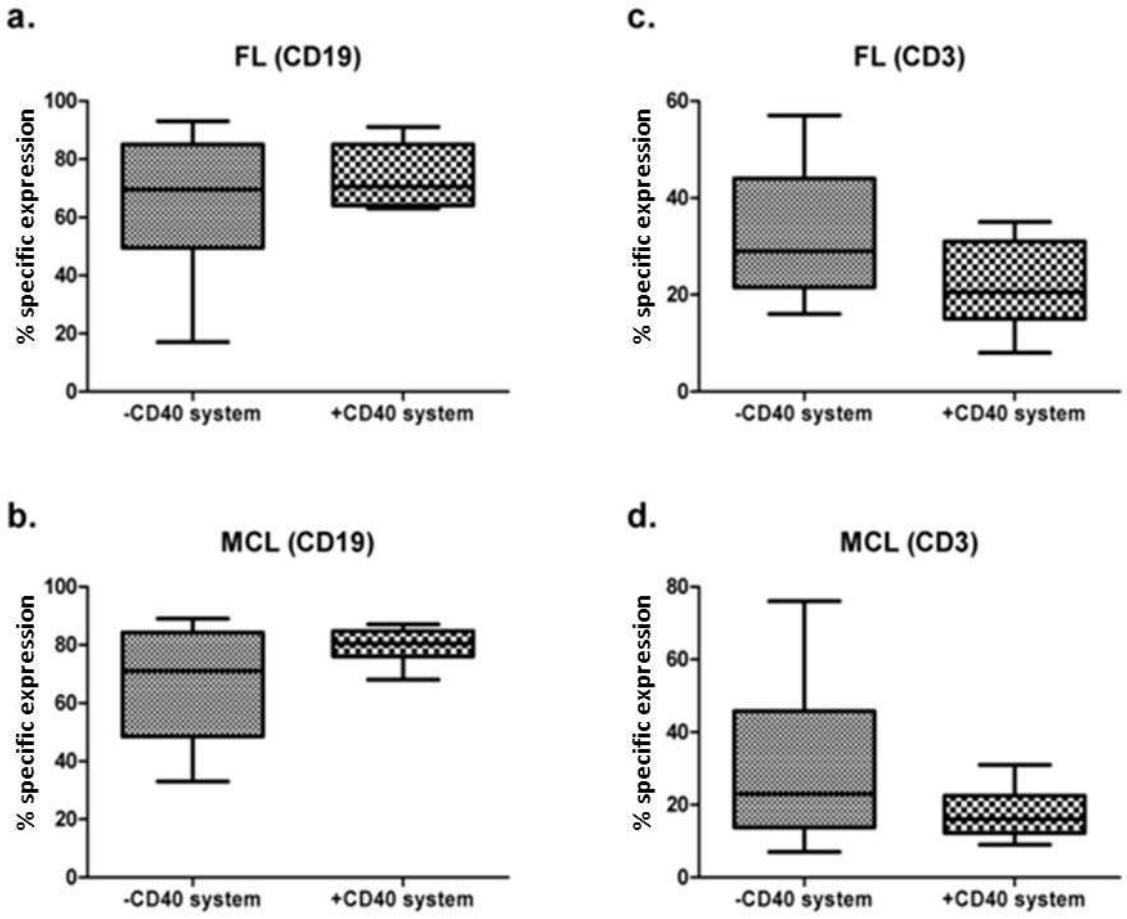

Figure 3.11 Mean CD19 and CD3 expression in FL (a, n=10) and MCL (b, n=16) primary cells cultured for 72hrs in media alone or in the CD40 system.

3.6 Use of the CD40 system: Investigating the activity of bortezomib (Velcade™) in primary MCL and FL samples

In this section, we demonstrate the use of the CD40 coculture system to determine the effectiveness of standard and novel treatments in NHL. We had the unique opportunity to work in conjunction with a multicentre phase II trial of bortezomib in patients with relapsed or refractory lymphoma in which St. Bartholomew's Hospital participated. Samples from 8 patients enlisted on this trial were used to investigate the activity of bortezomib used as a single agent and in combination with other agents, in the CD40 system. Importantly, we were able to relate *in vitro* activity with clinical responses in a few of these trial patients(Strauss, Maharaj et al. 2006).Samples from a total of 17 patients were successfully grown in the coculture system, nine from patients with MCL and 8 from patients with FL. On the basis of findings from the validation studies showing that B-cell growth and viability was maintained for at least 72hrs, and CD40L presentation was optimal at this time, this duration of culture was thus chosen for subsequent experiments using the CD40 system. Cells were cultured alone for 24hrs to establish cell growth at which time bortezomib was added at increasing concentrations and its effect examined 48hrs later (using the trypan blue dye exclusion assay).

3.6.1 Effect of bortezomib on primary samples from 2 different sites in a patient with MCL

A patient that had had a lymph node biopsy to confirm diagnosis also had pleural fluid drained for increasing respiratory symptoms. Immunocytochemistry confirmed this to contain mantle cells. The EC_{50} concentration was equal in both samples taken from different tissues (figure 3.12).

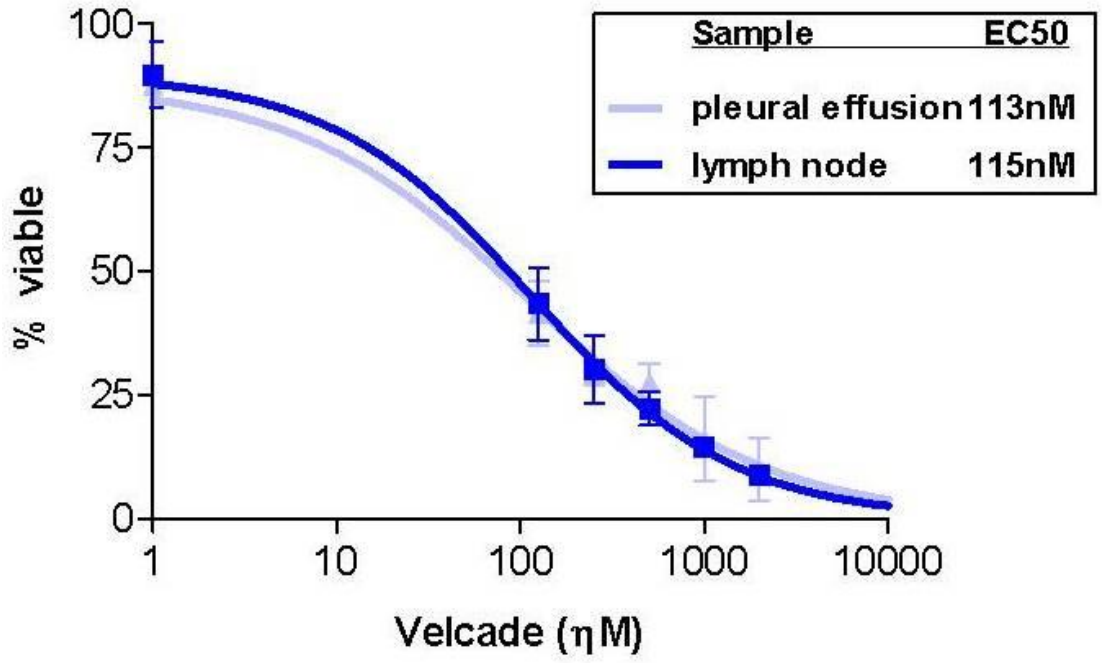

Figure 3.12 Concentration effect curves (with EC50 concentration) for samples from a lymph node and pleural effusion in the same patient with MCL cocultured in the CD40 system and treated with bortezomib for 48hrs. All data points are mean ± SD of at least two independent experiments.

3.6.2 Activity of bortezomib in primary MCL and in FL samples

The effect of 48 hours exposure to bortezomib was examined in 11 samples from 10 patients with MCL cocultured in the CD40 system. A dose-dependent reduction in cell viability was observed in all samples, but sensitivity varied from an EC_{50} of 113ηM in the most sensitive (#22) to resistance in one patient (#6), with an EC_{50} of 2207ηM. The median $EC_{50}$was 293ηM (table 3.4). Emax concentration curves for MCL samples are shown in figure 3.13a.

A dose-dependent reduction in cell viability was again observed in 8 samples from patient with follicular lymphoma cocultured in the CD40 system. An EC_{50} of 153ηM was obtained in the most sensitive; however, all other samples were markedly less sensitive, with a median EC_{50} of 1311ηM (figure 3.13b). This was significantly higher than that of the MCL samples (p=0.002) (table 3.4 and figure 3.14). Two samples from the same patient taken 6 months apart (#9 and #7) are shown, the patient having failed chlorambucil therapy in the interim. The sensitivity to bortezomib was reduced markedly in that time period, in that the sensitivity increased from 153ηM to 2213ηM.

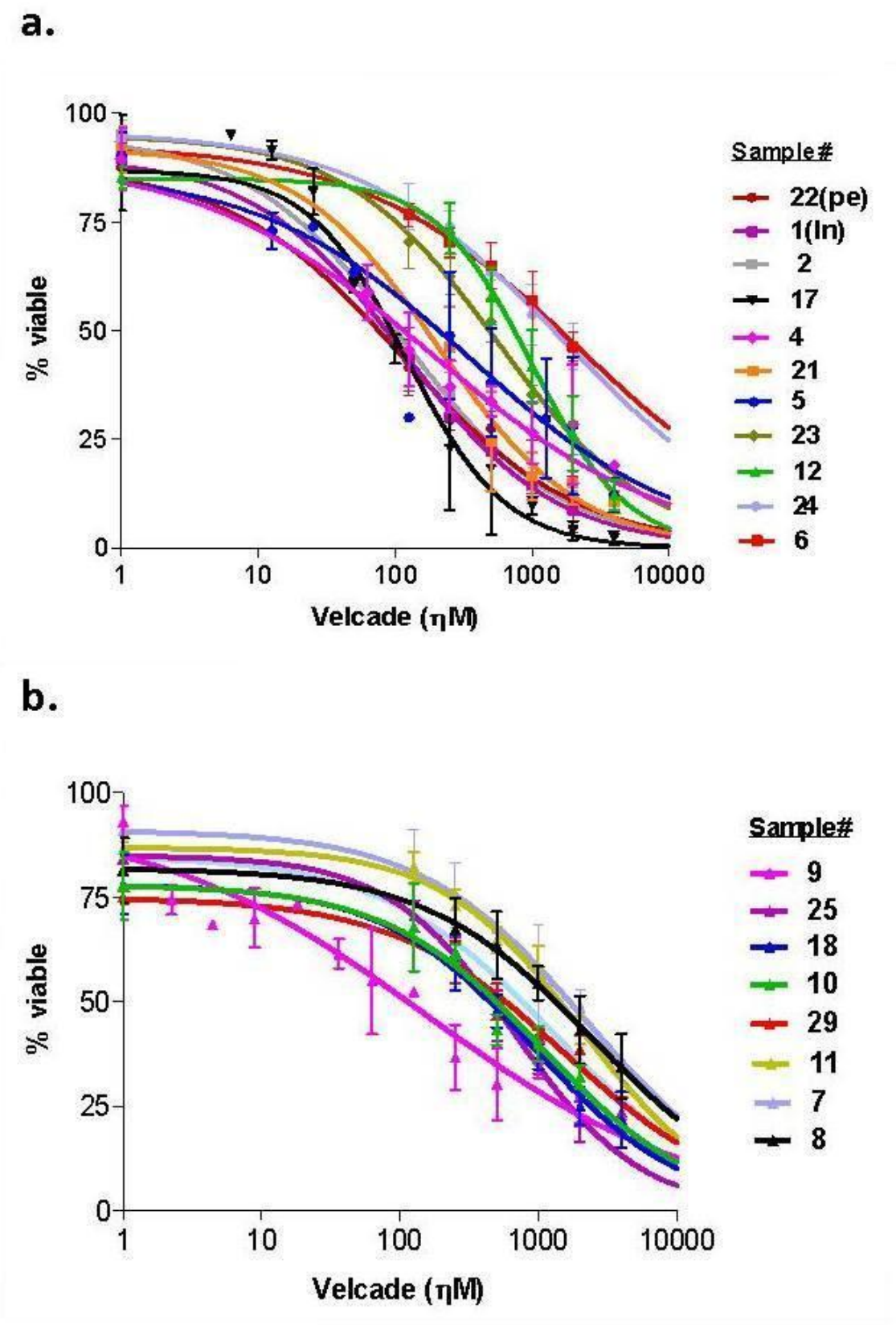

Figure 3.13 EC50 concentration effect curves for samples from patients with MCL (a) and FL (b) treated with bortezomib (n=11 and n=8, respectively). All data points are mean ± SD of at least two independent experiments and three where sufficient sample was available.

Table 3.4 EC50 values for the effect of bortezomib on primary MCL (n=10) and FL (n=8) primary samples cocultured in the CD40 system.**p= 0.002, MCL vs. FL.

Mantle Cell Lymphoma (MCL)			Follicular Lymphoma (FL)		
Patient#	**EC_{50} (nM)**	**(90 % CI)**	**Patient#**	**EC_{50} (nM)**	**(90% CI)**
22 (pe)	113	(90–140)	9	153	(108-215)
2	115	(97-138)	25	671	(600-750)
17	122	(99-148)	18	925	(770-1110)
4	179	(136-234)	10	1052	(850-1300)
21	209	(142-307)	29	1569	(1250-2000)
5	377	(265-518)	11	2026	(1750-2350)
23	557	(497-625)	7	2213	(1530-3200)
12	989	(880-1100)	8	2516	(1530-3150)
24	1657	(1310-2095)			
6	2207	(1655-2943)			
Median	**293****		**Median**	**1311****	

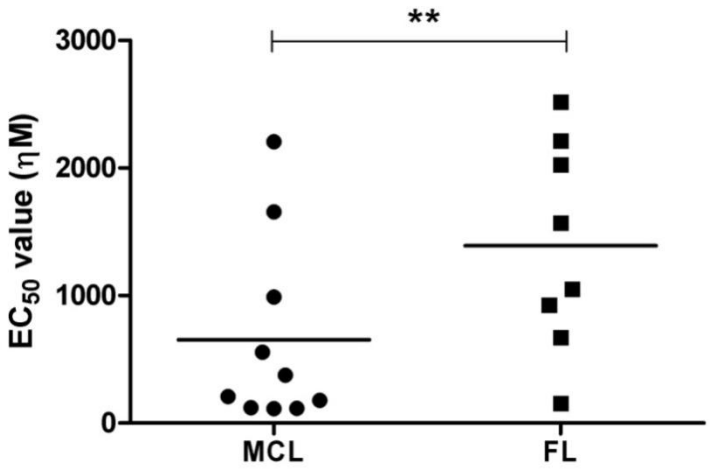

Figure 3.14 Scatter plot of the EC50 concentrations for bortezomib in samples cocultured in the CD40 system from patients with MCL (n=10) and FL (n=8). Median EC50 values are represented by the horizontal lines and were 293ηM and 1311ηM for MCL and FL samples, respectively. ** indicates p<0.005 using the paired t-test.

3.6.3 Correlation of EC_{50} with prior number of therapies

Patients with MCL and FL had both received a median of three prior therapies. There was no association between the prior number of therapies and response to bortezomib ($p > 0.05$, Mann-Whitney U test) (table 3.5).

Table 3.5 EC50 values and number of previous therapies received for MCL and FL patient samples used in the bortezomib *in vitro* sensitivity studies. Statistical analysis using the Mann Whitney U test showed no significant correlation between bortezomib sensitivity and prior number of therapies received in patients with MCL or FL ($p>0.05$).

Mantle Cell Lymphoma (MCL)			Follicular Lymphoma (FL)		
Patient#	# previous therapies	EC_{50} (ηM)	Patient#	# previous therapies	EC_{50} (ηM)
22 (pe)	5	113	9	0	153
2	1	115	25	5	671
3	3	122	18	0	925
4	3	179	10	2	1052
21	3	209	29	4	1569
5	3	377	11	7	2026
23	3	557	7	1	2213
12	1	989	8	5	2516
24	1	1657			
6	1	2207			
Median	**3**	**293**	**Median**	**3**	**1311**

3.7 Correlation of *in vitro* sensitivity in the CD40 system with clinical activity

3.7.1 Correlation of bortezomib *in vitro* sensitivity in MCL and FL samples with clinical response

EC_{50} concentrations were determined for samples from 8 patients treated on the phase II clinical study. The EC_{50} values ranged from 115ηM in the most sensitive to 477ηM (figure 3.15). The EC_{50} value was significantly associated with clinical response in all patients (table 3.6, Mann Whitney U test p=0.03). Patient #4 with an intermediate sensitivity initially responded to bortezomib (EC_{50} 179ηM), achieving a partial response (PR) after 4 cycles of therapy. He then had a treatment delay and 2 dose reductions due to excess toxicity and progressed towards the end of 8 cycles of therapy. This was documented on computerized tomography (CT) scanning on completion of the eighth cycle.

Table 3.6 Comparison of the *in vitro* bortezomib sensitivity and clinical activity in 8 patients treated on the phase II trial. For 2 patients (MCL #4 and MCL #5), samples were obtained at 3 different time points. PR = partial response and PD = progressive disease. In all samples, sensitivity correlated with clinical response (Mann Whitney U test p=0.03).

Sample #	Tumour type	EC_{50} (nM)	Clinical Response
1	MCL	115	PR
2	MCL	115	PR
3	MCL	122	PR
4	MCL	179	PR then PD
5	MCL	356	PD
6	MCL	2107	PD
7	FL	2211	PD
8	FL	2477	PD

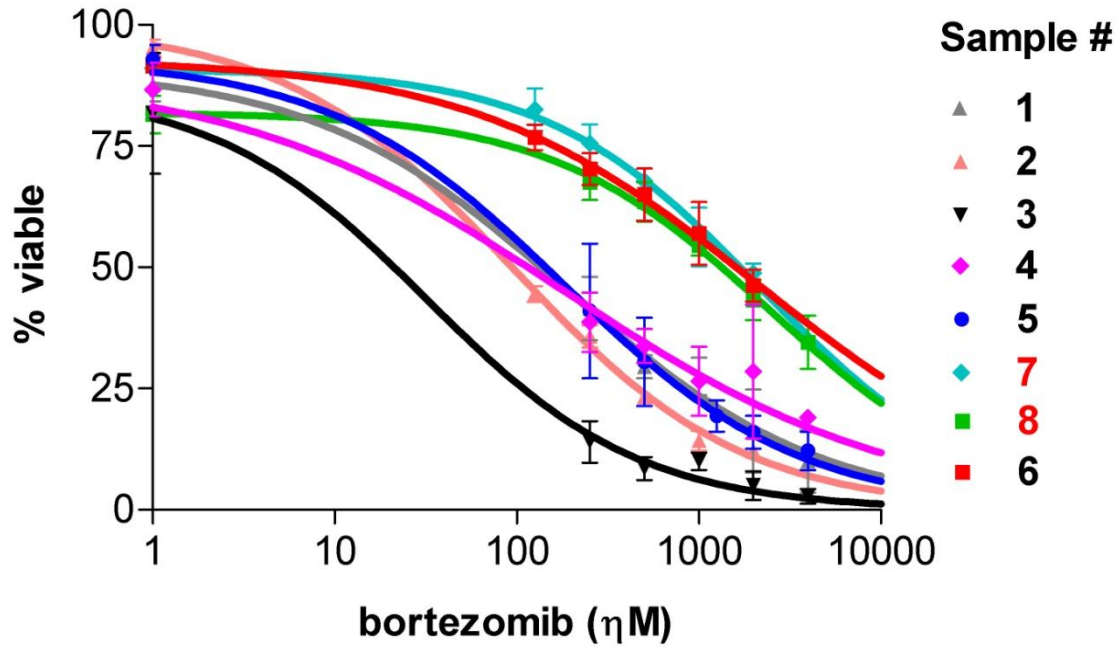

Figure 3.15 EC50 concentration effect curves for MCL (black sample #) and FL (red sample #) samples cocultured in the CD40 system from patients treated on the phase II clinical trial. Data points are the mean + SD of at least two separate experiments for each sample.

3.7.2 Correlation of *in vitro* sensitivity over time in two patients with MCL

Three samples were obtained from 2 patients with peripheral blood involvement before commencing bortezomib, on completion of therapy, and three months later. Patient #5 with an EC_{50} of 356ηM progressed after 2 cycles of therapy (table 3.6 and figure 3.16). The EC_{50} of the sample taken at this time and three months later were comparable at 356nM and 361nM. He was thus, initially resistant to bortezomib and retained this resistance. Patient #4 was initially sensitive to bortezomib in the *in vitro* primary culture system with an EC_{50} of 179nM and responded clinically to therapy as explained above (table 3.6). At the end of treatment, when he once again had a rising white blood cell count, the sample cultured had become less sensitive with the EC_{50} increasing to 325nM (p=0.03). Three months later, a further sample remained more resistant with an EC_{50} of 497nM (figure 3.16). It thus appeared that he had acquired resistance to the drug during therapy and perhaps a combination of this and a lower dose of bortezomib meant he progressed before the end of therapy.

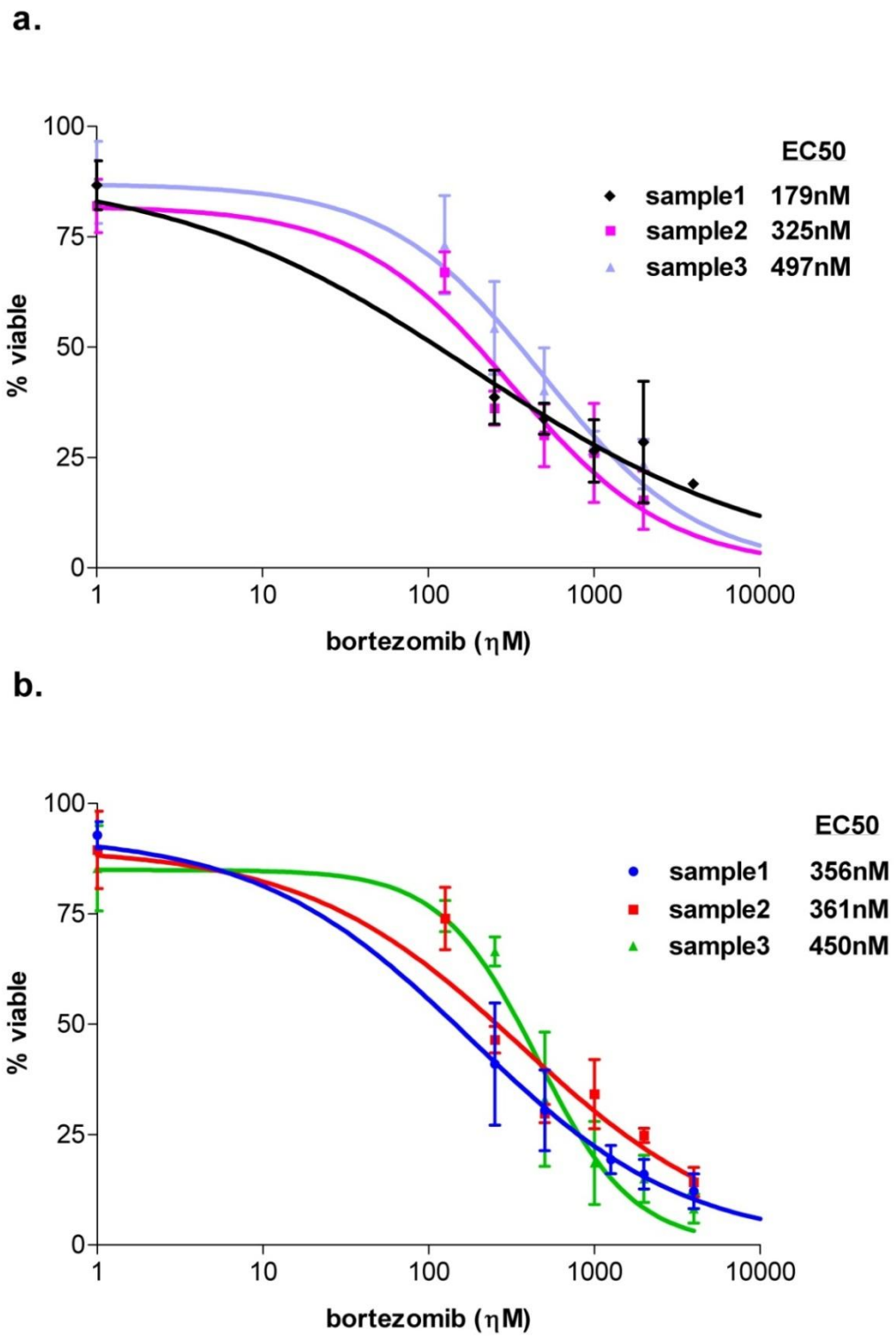

Figure 3.16 EC50 concentration effect curves for bortezomib 2 patients participating in the clinical trial. Three separate samples collected from patient #5 (a) and patient #4 (b) were collected prior to commencing therapy in the trial (sample1), on completion of treatment (sample2) and three months later (sample3). Data points are the mean + SD of at least three separate experiments for each sample.

3.8 Investigation of potential biological correlates with clinical activity

3.8.1 CD40 expression is associated with bortezomib sensitivity in different samples from 2 patients with MCL and 1 patient with FL

As CD40 ligation plays a role in B cell proliferation and survival, CD40 expression levels were examined firstly in the patient samples described in the previous section. A sample taken prior to therapy from patient #4 with initial bortezomib sensitivity (EC_{50} 179ηM) who responded clinically, had by the end of treatment acquired resistance (EC_{50} 325ηM) and three months later, a further sample remained more resistant at 497nM (table 3.8 and figure 3.17a, b, c). This was associated with a decrease in expression of the CD40 receptor from 79% in sample 1 to 45% and 19% in samples 2 and 3, respectively. Similarly, patient #5 with an EC_{50} of 356nM progressed after 2 cycles of therapy (EC_{50} 361ηM) and three months later become more resistant (EC_{50} 450ηM) which was associated with a decrease in CD40R expression from 52% in sample 1 to 45% in sample 2 and finally to 31% in sample 3 (table 3.8; figure 3.17d,e,f). Similarly, a follicular lymphoma sample (patient #9 EC_{50} 153ηM) was initially sensitive to bortezomib prior to therapy and subsequently acquired resistance (EC_{50} 2213ηM), which was associated with a dramatic decrease in CD40R expression from 79% to 14% 6 months later (table 3.8 and figure 3.17g and h).

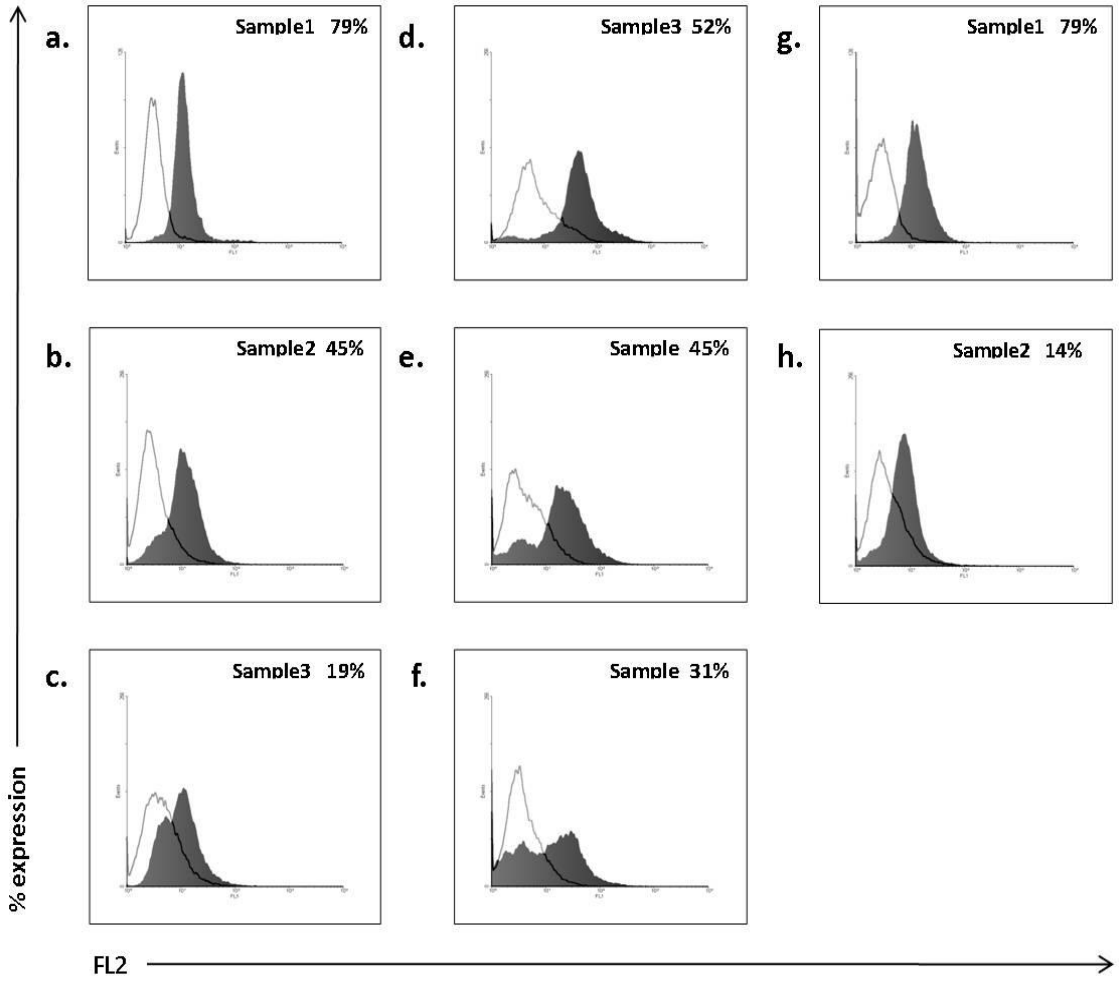

Figure 3.17 CD40 expression in 3 samples from MCL patient #4 (a, b, c) and MCL patient #5 (d, e, f). Samples were collected prior to commencing therapy in the clinical trial (sample1), on completion of treatment (sample2) and three months later (sample3). Two samples from FL patient #9 (g, h) taken prior to commencing therapy (sample1) and 6 months later (sample2). Percentages are CD40 expression (shaded histogram) relative to negative mouse IgG1 isotype control (clear histogram).

Table 3.7 Expression of CD40 receptor in samples taken from 2 MCL patients and 1 FL patient enlisted on the phase II trial.

Patient #	Malignancy	EC50 ηM (95% CI)	% CD40R expression
4 - sample1	MCL	179 (136-234)	79
4 - sample2	MCL	325 (261-404)	45
4 - sample3	MCL	497 (409-603)	19
5 - sample1	MCL	356 (250-509)	52
5 - sample2	MCL	361 (270-484)	45
5 - sample3	MCL	450 (373-453)	31
9 - sample1	FL	153 (108-215)	79
9 - sample2	FL	2211 (1531-3193)	14

3.8.2 Correlation of CD40 expression with bortezomib sensitivity in MCL patients

Basal CD40 expression was again examined to determine whether the observed association between *in vitro* sensitivity to bortezomib and expression of CD40 in 3 patients, was a consistent finding across a larger cohort of samples (figure 3.18a). Interestingly, CD40 expression correlated well with sensitivity to bortezomib in 10 MCL patient samples (Spearmen's correlation coefficient p=0.002) but not in 6 FL patient samples (p=0.42) (figure 3.18a). The culture system uses CD40 ligation as a basis for cell proliferation, thus it was possible that a greater CD40 expression at baseline would result in more successful proliferation of cells with a greater number of dividing cells possibly explaining the increase in sensitivity. Thus, the correlation between CD40 expression and cell proliferation was also examined and no relation was found in either mantle cell or follicular lymphoma cultures (figure 3.18b).

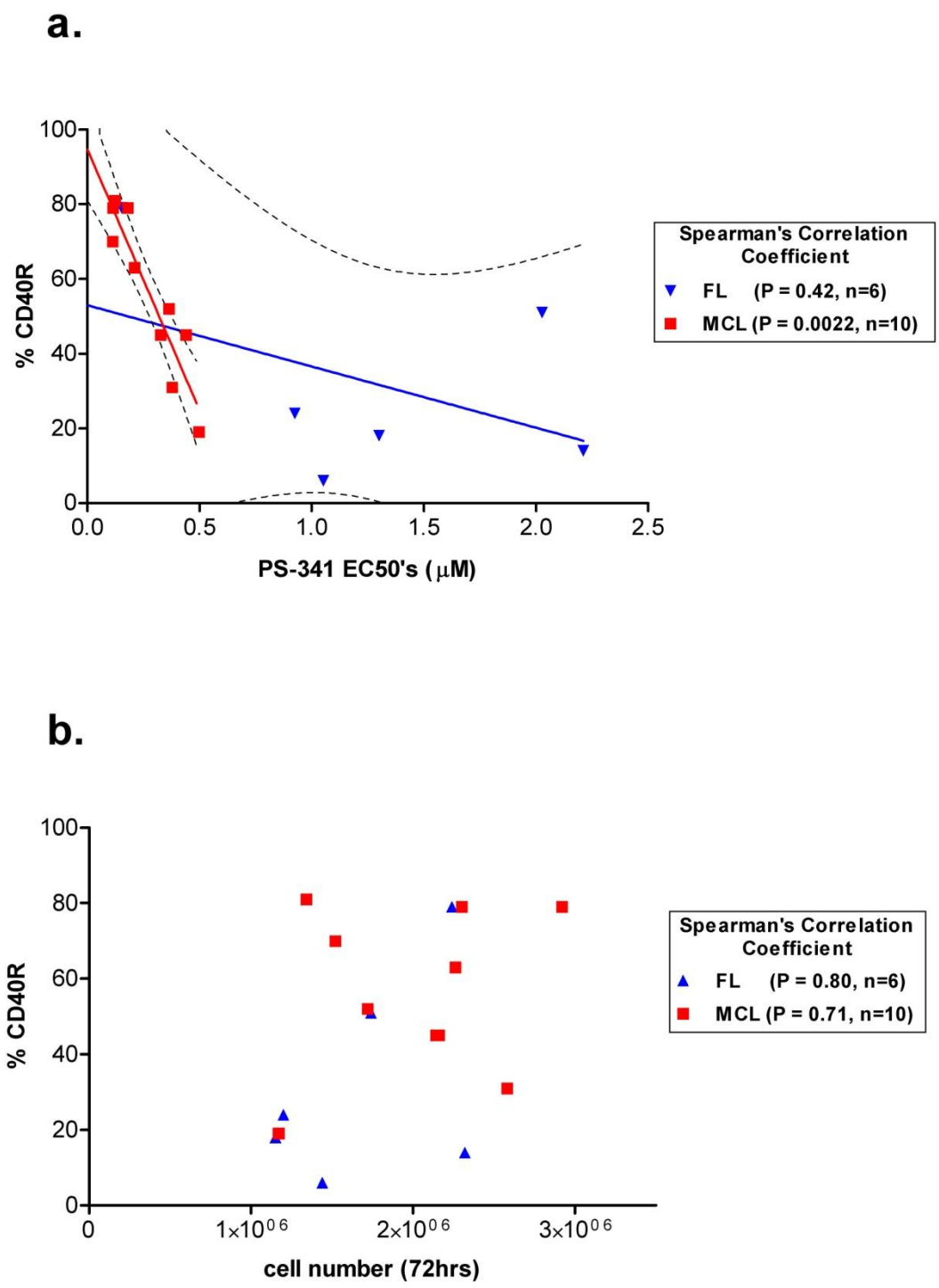

Figure 3.18 a. CD40 expression correlates with sensitivity to bortezomib in mantle cell lymphoma (MCL) but not follicular lymphoma (FL) p=0.002 and p=0.42 respectively. b. CD40 expression does not correlate with cell number at 72hrs (day 3) in MCL or FL p=0.71 and p=0.8, respectively.

3.9 Effect of bortezomib on the cell cycle distribution of primary MCL and FL cells cultured in the CD40 system

The effect of bortezomib on cell cycle distribution was examined in 5 primary cocultures three samples were from patients with MCL sensitive to bortezomib and two samples from patients with FL more resistant to bortezomib. Figures 3.19 and 3.20 below shows an example of one of the MCL and FL samples respectively, where a dose-dependent increase in the sub-G1 (or apoptotic) fraction occurred according to sensitivity of the samples to bortezomib. There was a consequent decrease in other phases of the cell cycle, apart from the S-phase which appeared to increase with increasing drug dose. When the cell cycle distribution was analysed in 5 different MCL patient samples, the latter observation was again noted (figure 5.21) and this is in agreement to findings in NHL cell lines, where S-G2/M arrest was observed.

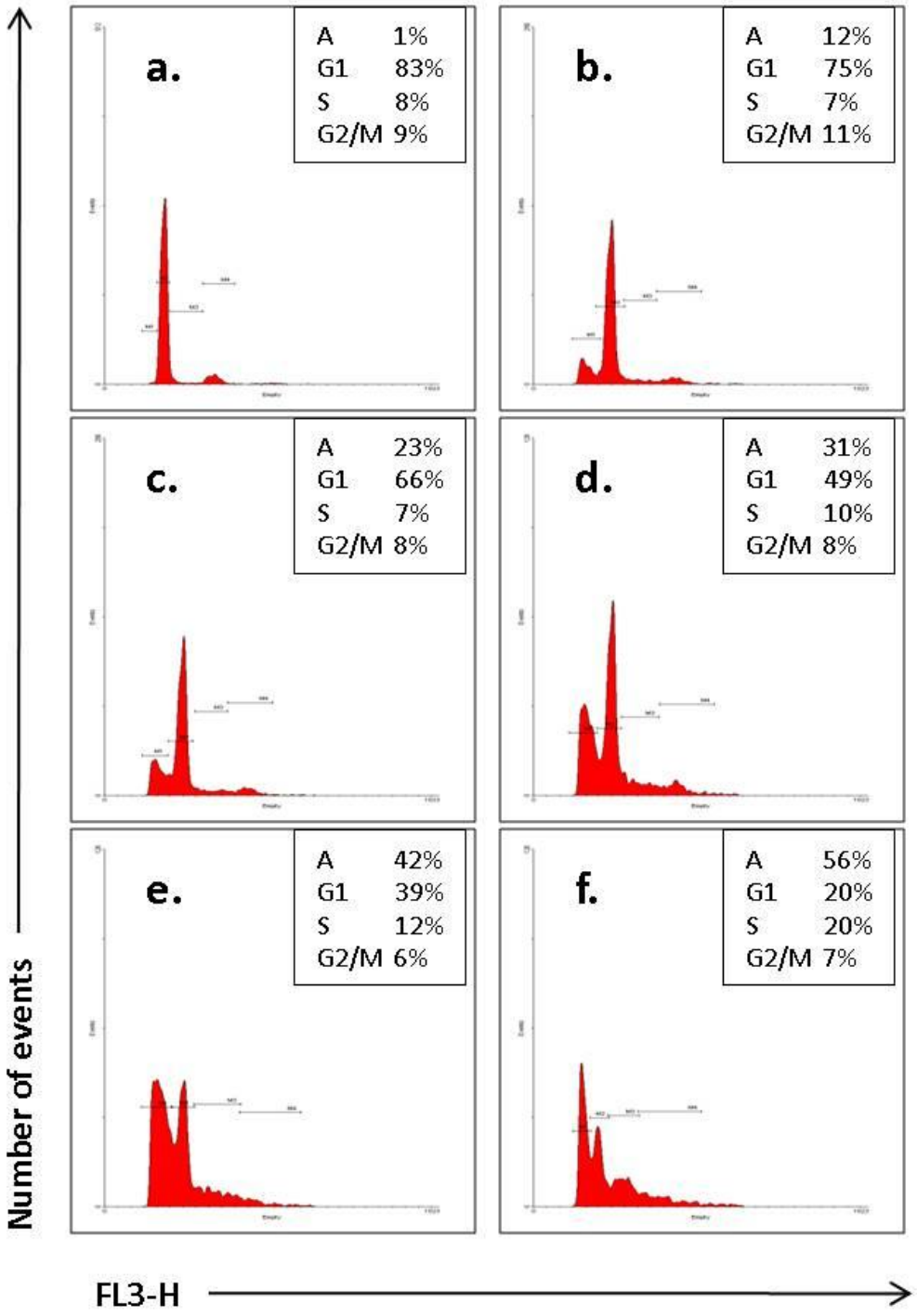

Figure 3.19 Example of the effect of increasing concentrations of bortezomib on cell cycle distribution in a primary coculture from a patient with MCL (#4, sample2): EC50 = 325ηM (CI:261-404ηM). a. Control cells at 72hrs, b. treated with 125ηM bortezomib, c. treated with 250ηM bortezomib, d. treated with 500ηM bortezomib, e. treated with 1000ηM bortezomib and f. treated with 2000ηM bortezomib. Markers indicate phases of the cell cycle i.e. M1=sub G1, M2=G1, M3=S and M4=G2/M. Values indicate the % of cells within each marker. CI = confidence interval

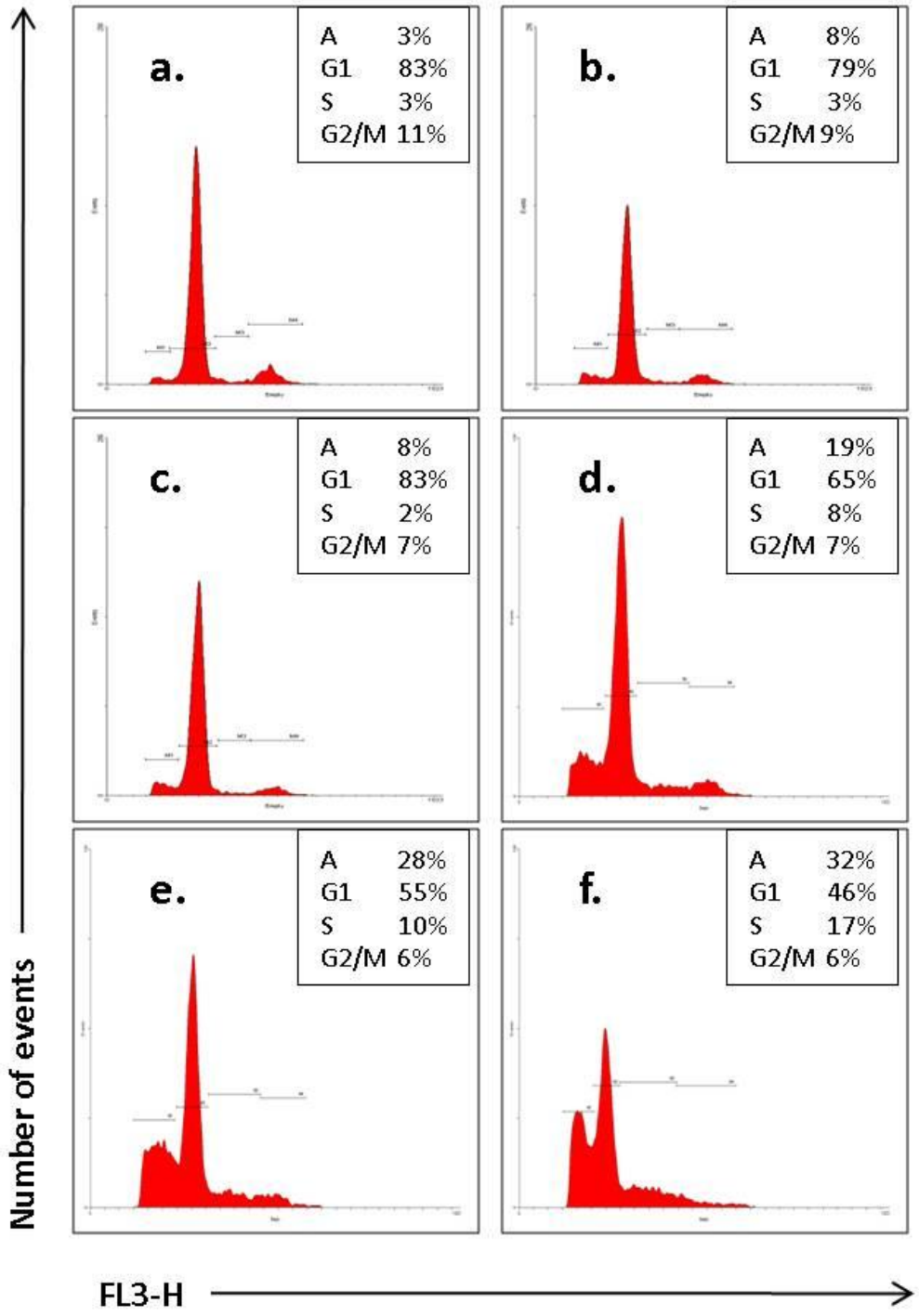

Figure 3.20 Example of the effect of increasing concentrations of bortezomib on cell cycle distribution in a primary coculture from a patient with FL (#11) EC50 = 2026ηM (CI: 1750-2350ηM). a. Control cells at 72hrs, b. treated with 125ηM bortezomib, c. treated with 250ηM bortezomib, d. treated with 500ηM bortezomib, e. treated with 1000ηM bortezomib and f. treated with 2000ηM bortezomib. Markers indicate phases of the cell cycle i.e. M1=sub G1, M2=G1, M3=S and M4=G2/M. Values indicate the % of cells within each marker. CI = confidence interval.

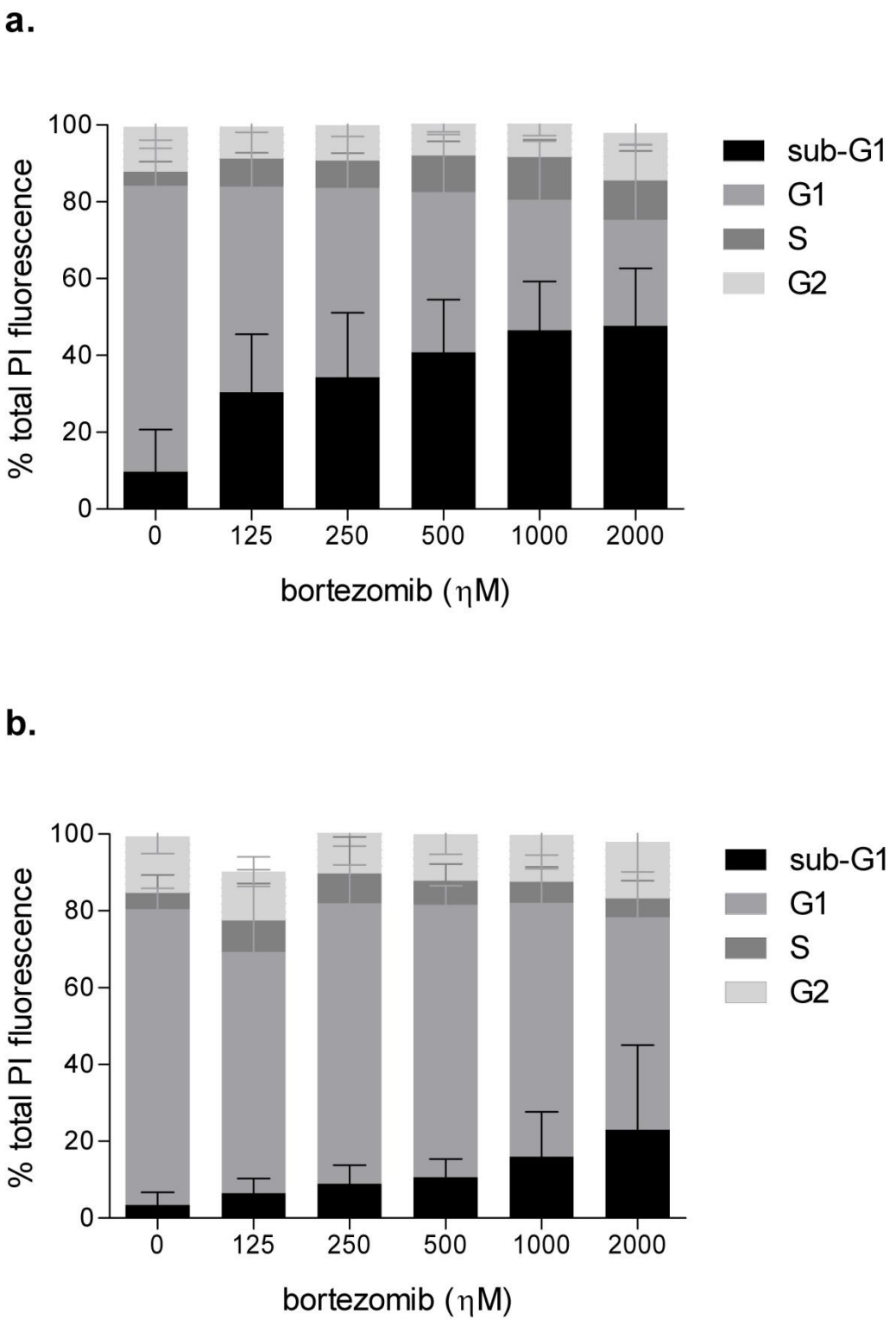

Figure 3.21 Summary bar charts showing the effect of increasing concentrations of bortezomib (up to 2μM) on cell cycle distribution in primary patient cocultures a. patients with MCL and b. patients with FL. Data are the mean + SD of 5 different patient samples.

3.10 Discussion

Cell lines provide only preliminary evidence of the efficacy of novel agents. Studies of these agents are greatly benefited by having an *in vitro* system for culturing cells isolated from patients as this more closely mirrors what is occurring *in vivo.* A number of investigators have demonstrated that growth of cells isolated from indolent lymphomas is possible using CD40 ligation to induce proliferation. These studies used a 'CD40 system' to examine the role of the microenvironment and factors that may be important in mediating resistance to apoptosis, as well as progression of the disease (Johnson, Watt et al. 1993; Ghia, Boussiotis et al. 1998; Castillo, Mascarenhas et al. 2000; Visser, Tewis et al. 2000). The system however, also provides a novel means of studying new treatment strategies. The aims of this investigation were to validate the primary culture system as a method of growing cells from patients with lymphoma and subsequently to examine its use to investigate the effect of bortezomib and correlate *in vitro* sensitivity with clinical findings.

Initial validation studies involved establishing the effect of irradiation on the transfected fibroblastic Chinese hamster ovary (CHO) cells which were used as non-proliferating support cells providing CD40L in the coculture system. Both mitomycin C and γ-irradiation have been used to prepare such 'feeder layers'. Both treatments inhibit DNA replication by slightly different mechanisms: whereas mitomycin C cross-links with DNA, γ-irradiation leads to DNA strand breaks (Malinowski, Pullis et al. 1992). A key study in the field showed that expansion of normal B cells was 100x more potent using γ-irradiated feeder cells compared to mitomycin C-treated cells (Roy, Krzykwa et al. 2001). This was attributed to a significant reduction in both cellular metabolism and the level of CD154 expression observed in mitomycin C-treated feeder cell, but not in γ-irradiated cells. Thus mitomycin C treatment has limitations when cells have to express stably a key ligand required to stimulate proliferation of cocultured target cells. Irradiation was therefore our chosen method as it is a more efficient way to inhibit CHO cell growth whilst preserving their metabolic and antigen presentation abilities.

Indeed initial results showed that even though CHO-CD40L cell proliferation was halted after treatment with 96Gy of γ-irradiation, their ability to present CD154 antigen was maintained at levels comparable to that of untreated cells. Expression of CD154 post irradiation was dependent on time spent in culture as the fluorescence signal halved by day 8 from 90% of cells expressing the ligand to just 42%.This indicated that if the system were to be used for long-term culture of B cells, they would require transferring to freshly irradiated CHO-CD40L-coated plates at least every 4 days when presentation of CD40 ligand was maintained at a moderately high level of 70%.

As a control B cell population, we chose to use normal peripheral blood mononuclear cells (PBMCs) isolated from healthy donors as opposed to using isolated tonsillar cells, as the latter are germinal centre B cells which would be comparable to follicular lymphoma but not to mantle cell lymphoma. Growth of normal PBMCs was greatly enhanced in the CD40 system over a 96 hour culture period. Viability was maintained at almost 100% and after an initial reduction in cell number over the first 48hrs, proliferation was induced to 150% of control values. In contrast, cells cultured in media alone showed a marked decline in viability and cell number with almost all cells dead at 72hrs.

The individual contribution of the CD40L-transfected cells or of interleukin-4 (IL-4) was not investigated immediately due to time constraints on generating the validation data. The phase II trial of bortezomib had already begun and patient samples were becoming available for *in vitro* testing. Therefore, the combined effect of CD40L and IL-4 was investigated in a total of 9 mantle cell and 9 follicular lymphoma samples over a 72hr culture period. Within this time frame, we could be confident that CD40L was sufficiently expressed in the media and that with co-stimulation provided by IL-4 at least normal B cells could be stimulated to proliferate. Viability of both mantle and follicular lymphoma cells was increased to over 90% after 72hrs coculture in the CD40 system whereas, the same samples cultured in media alone, underwent a decrease in viability. Cell proliferation reflected this, as MCL cell doubled and cell number increased significantly in FL samples compared with their culture in media alone. MCL samples were more responsive to stimulation in this system compared to FL cells,

which is likely due to constitutive activation of NFκB in MCL rendering it more sensitive to the effects of activation of this pathway via CD40L stimulation.

Studies with immunophenotype analysis on PBMCs from healthy blood donors, and PBMCs from 2 patients with follicular lymphoma in the leukaemic phase demonstrated that the isolated cells maintained good viability and retained close phenotypic resemblance to the original tumour sample cells for the 3 day culture period. This confirmed that drug sensitivity assays could be conducted within a 3 day period whilst remaining phenotypically unchanged. Further monitoring of some of these samples showed that this was continued for approximately one week (data not shown). The primary samples studied were obtained from clearly involved lymph nodes by excisional biopsy or from circulating blast cells (n=6, requiring leukopheresis in four samples), with median percent CD19 positive cells before and after culture of 73% and 78%, respectively, suggesting that the majority of cells cultured were lymphoma B-cells. Furthermore, CD3 positive T cells did not expand in the culture system thus T cell depletion of samples was not required.

In total, growth of 26 samples was attempted, of which 21 (81%) produced consistent reproducible high viability until day three with maintenance of the B cell phenotype. The lack of growth in some samples was due to low viability on thawing and in others growth was not possible despite good viability and CD19 expression on day 0. Visser*et al* report that 13 of 16 mantle cell samples proliferated well in the CD40 system but that addition of IL-10 provided additional proliferation in 10 of 13 samples, whilst IL-4 only had an additional effect in 4 cases (Visser, Tewis et al. 2000). It is thus possible that the use of other cytokines may increase the number of samples that proliferate well enough for investigation. Nonetheless, a sufficient number of samples were grown to allow investigation of the effects of bortezomib.

Bortezomib treatment of all primary cultures resulted in a dose-dependent loss of cell viability, however, there was a difference between mantle cells and follicular cells, with median EC_{50} values of 293ηM and 1311ηM respectively, p=0.002. Sensitivity to bortezomib was independent of the site or tissue sampled in one patient who provided

lymph node tissue and pleural fluid, the EC_{50} values being 113ηM and 115ηM respectively. In one patient two samples taken six months apart were analysed. The sample was initially sensitive to bortezomib with an EC_{50} of 153ηM. Six months later, after failing chlorambucil, further cells were collected. This time the cells were resistant to bortezomib with an EC_{50} of 2213ηM. It is noteworthy that normal lymphocytes are less sensitive to proteasome inhibition than chronic lymphatic leukaemia–derived lymphocytes, suggesting that low *in vitro*EC_{50}values, reflecting sensitivity to bortezomib, are not a result of normal cell contamination (Masdehors, Omura et al. 1999).

It is well known that malignant tumours acquire resistance to therapy following multiple treatments, thus the number of previous therapies was examined to ascertain whether this influenced sensitivity to bortezomib. Both sets of patients had received a median of three prior therapies and so this could not explain the difference in sensitivity observed between MCL and FL.

The *in vitro* sensitivity of patient samples was correlated with clinical response in eight patients treated on the phase II clinical trial. In all patients, sensitivity to bortezomib correlated with clinical response. Measurement of bortezomib concentration *in vivo* is difficult as the drug is rapidly cleared from the vascular compartment, but it is thought that the clinically achievable dose of bortezomib *in vivo* is 100 to 200ηM. The results presented here corroborate that, as only patients with an EC_{50} of up to 179ηM achieved a clinical response. Samples from 2 patients with MCL were collected at different time intervals. These came from patients being treated on the clinical trial of bortezomib, with samples being taken prior to bortezomib therapy, on completion of therapy and three months later. The EC_{50} of the patient who progressed on therapy started at greater than 200ηM and did not change over that time period.

Another patient MCL#4 with a low EC_{50} of 179ηM on the *in vitro* primary culture system achieved a PR after 4 cycles of therapy. At the end of treatment, after a delay and 2 dose reductions for toxicity, the patients lymphoma cells had become less sensitive with the EC_{50} increasing to 325ηM (p=0.03). Three months later, a further

sample remained more resistant at 497nM. It thus appeared that he had acquired resistance to the drug during therapy and perhaps a combination of this and a lower dose of bortezomib meant he progressed before the end of therapy.

Although the mechanism by which bortezomib causes cell death has not been fully elucidated, NF-κB signalling is still thought to be important and contribute to this. Pham *et al* demonstrated constitutive NFκB activity in MCL cell lines and primary cultures, which was inhibited by bortezomib and resulted in cell death by apoptosis (Pham, Tamayo et al. 2003). Similarly, Heckman *et al* demonstrated constitutive NFκB activity in two other t(14;18) B cell lines (DHL-4 and DHL-6) and demonstrated inhibition of NFκB prevented cell growth, but evidence of constitutive NFκB activity has not been demonstrated in follicular lymphoma primary cultures (Heckman, Mehew et al. 2002).

We conducted preliminary investigations into NFκB activity in a small number of primary follicular lymphoma samples and results indicated a low level of NFκB activity compared to mantle cell samples (data not shown). On the other hand, bortezomib-mediated induction of apoptosis in MCL cell lines was found to be independent of constitutive NFκB or Akt activity, instead mediated via Noxa (Rizzatti, Mora-Jensen et al. 2008). Cell line work previously conducted in our lab using a t(14;18) cell line characterised by follicular lymphoma (DHL-7) demonstrated that, although some inhibition of NFκB occurred, it was less marked than that caused by the equipotent concentrations of the specific NFκB inhibitor Bay 11-7082. It was therefore not sufficient to explain cell death and other mechanisms of action may be important in this subtype of lymphoma.

Examination of CD40 expression in untreated primary culture samples revealed a significant correlation of expression with sensitivity to bortezomib in mantle cell lymphoma samples only, that was not a function of B cell proliferation. It is thus possible that CD40 signalling provides a more important growth signal in MCL than in FL, which is mediated by activation of NFκB. Inhibition of NFκB with bortezomib is thus able to result in apoptosis more readily than in follicular lymphoma where this signal is

perhaps less important. These findings could be further validated using immunohistochemical staining of paraffin biopsy specimens as all trial patients had biopsies prior to treatment. Proteins stained for would include CD40; Bcl-2 family members including Bcl-2, Bax and Bak and the NFκB family members, c-Rel and Rel-A, including their localisation as the presence of nuclear staining would provide evidence of constitutive NFκB activation. This may help explain the difference in bortezomib activity in MCL and FL samples.

CD40 expression in patient samples has not been correlated with outcome specifically in FL or MCL, however, a recent study carried out on a total of 114 patients with NHL (100 of which had completed 4 cycles of CHOP) reported a significant negative correlation between CD40 expression, detected via flow cytometry, and disease stage. The authors concluded that CD40 expression be used to predict disease outcome in NHL as expression is increased in responding patients (Soliman, Fathy et al. 2009). Similarly in DLBCL, CD40 expression (positive in 76% of patients) identified a favourable subgroup of patients with a greater time to treatment failure ($p=0.027$) and overall survival ($p=0.0068$) (Szocinski, Khaled et al. 2002; Linderoth, Jerkeman et al. 2003). Activation of CD40 in aggressive lymphoma cell lines however, causes apoptosis found to be via induction of Bax, rather than cell proliferation as seen in the more indolent lymphomas (Szocinski, Khaled et al. 2002)thus, it would be interesting to examine CD40 expression in these diseases and attempt to correlate it with outcome. It would be expected that the majority would be positive but if relative expression could be quantified differences in outcome might be observed.

As the proteasome also effects many regulators of the cell cycle, and differences in cell cycle effects were observed preciously in our lab in the sensitive (DHL-7) and resistant cell lines (DHL-4), the effect of bortezomib on cell cycle distribution was examined in primary cocultures. A dose-dependent increase in the sub G1 (apoptotic) fraction was observed which correlated with sensitivity to bortezomib and an observableS-G2/M arrest was evident in primary MCL samples in keeping with the cell line studies. To examine these effects more fully, immunoblotting of cell cycle proteins is necessary; however, these experiments did suggest that differing effects on cell cycle regulation

are insufficient to explain the different sensitivities to bortezomib observed between these MCL and FL samples.

Work presented in this chapter has thus far has indicated that our CD40 coculture model suitably sustains the growth of primary NHL cells *in vitro* and this has enabled investigations into their bortezomib sensitivity. We have noted an important differential sensitivity to the drug where MCL patients were more sensitive than FL samples, which corroborate *in vivo* observations. Furthermore, *in vitro* sensitivity correlated with CD40 expression, thus CD40 could potentially act as a clinical biomarker for response to bortezomib. Most importantly, we were able to demonstrate for the first time that bortezomib *in vitro* activity can predict clinical response. We next used this model to investigate bortezomib in combination with standard chemotherapy (doxorubicin), and with a novel targeted approach (HDAC inhibition). The aim of these combination studies was to increase the efficacy of the already approved agents; thereby improving treatment outcomes for patients with NHL.

CHAPTER 4: Investigating bortezomib in combination therapy in NHL cells cocultured in the CHO-CD40L model

4.1 Introduction

In addition to its single agent activity, bortezomib has demonstrated a valuable role in increasing sensitivity of malignant cells to other chemotherapy. Given the lack of significant additive toxicity, bortezomib may therefore be appropriate as part of combination therapy in NHL treatment. Current phase I, phase II and phase III studies are exploring the integration of bortezomib into regimens including rituximab-cyclophosphamide-doxorubicin-vincristine, and prednisone (R-CHOP), R-EPOCH, rituximab-cyclophosphamide-predinisone and fludarabine (Dreyling 2010; Tilly and Dreyling 2010). We have now investigated the use of bortezomib in combination with a standard cytotoxic doxorubicin, or with a novel histone deacetylase inhibitor (HDACi) UCL67022, in the NHL CD40 coculture model.

4.1.1 Histone deacetylase in cancer therapy

Epigenetic therapy has an increasing role for the treatment of cancers. The acetylation status of histones is controlled by a balance in activity of histone acetyl transferases (HATs) and histone deacetylases (HDACs) that alter the spatial binding of DNA and functionally effect gene transcription. HATs transfers an acetyl group to histone tails whereas HDACs remove this group (Cress and Seto 2000). HDAC inhibitors represent an exciting new class of anti-cancer agents and have widespread effects both inside and outside of the genome. Proteins outside of the genome include cytoskeletal proteins (e.g. tubulin (Palazzo, Ackerman et al. 2003)), molecular chaperones (e.g. HSP90 (Kovacs, Murphy et al. 2005)) and transcription factors , NFκB (Chen, Fischle et al. 2001)). These proteins are acetylated by a post-translational modification event that regulates their function. Four main classes of HDAC have been described to date (Minucci and Pelicci 2006). HDAC6 (class 2) is unique by its two active HDAC domains and ubiquitin binding zinc finger that participates in the aggresomal pathway of protein degradation (Kawaguchi, Kovacs et al. 2003).

4.1.2 A novel HDACi, UCL67022

Through collaboration between Barts Cancer Institute and University College London, novel HDAC inhibitors have been formulated, synthesized and investigated. The lead compound, UCL67022 has a hydroxamic acid terminal group, and a bifurcated cap. This extra side chain increases the polarity of the molecule, which increases binding avidity to the active site, and alters interactions with amino-acids outside the pocket. This is believed to confer it greater potency than vorinostat the most clinically advanced hydroxamic acid, and it also changes interactions with amino acids outside the binding pocket which may allow differential interaction between classes of HDACs. We investigated the activity of UCL67022 in comparison with vorinostat in a panel of DLBCL and MCL cell lines and then in primary DLBCL, MCL, FL and CLL samples cultured in the CD40 system. Its activity in combination with bortezomib was then studied in both the cell lines and primary cocultured samples.

4.1.3 Investigating the use of soluble CD40 ligand

In chapter 1.3.2 we observed that a soluble trimeric form of CD40 ligand has also been shown to increase survival of MCL cells similarly to that induced by fibroblasts transfected to express the Fc receptor or the membrane-bound ligand, and that this was enhanced by the addition of IL-4 (Castillo, Mascarenhas et al. 2000). CLL cells also receive growth signals from CD40 activation, and studies have shown it to rescue B-CLL cells from spontaneous apoptosis as well as from fludarabine- and Fas-induced apoptosis (Kitada, Zapata et al. 1999). Therefore, in an effort to simplify the CHO-CD40L model and circumvent problems associated with attachment of B-cells to the irradiated fibroblast monolayer, we abrogated the need for the fibroblasts by replacing it with a recombinant human soluble CD40 ligand (sCD40L).

4.2 The effect of combining bortezomib and doxorubicin in primary MCL and FL samples cocultured in the CD40 system.

We investigated the effect of combining bortezomib with a standard of care agent, doxorubicin in the same primary mantle cell lymphoma and follicular lymphoma samples as used in the previous experiments.

4.2.1 Effect of doxorubicin on primary MCL and FL samples cultured in the CD40 system

All primary cocultured samples were markedly less sensitive to doxorubicin than bortezomib in this system, and all required micromolar doses to induce cell death (figure 4.1). Out of 10 primary cocultured mantle cell lymphoma samples, the median EC_{50} values was 5.2μM with a range from 2.3 μM to 13.7 μM (figure 4.1a and table 4.1). One sample was less sensitive (MCL#6) than the others, with viability of over 50% at 10μM, and for an additional sample (MCL#3) an EC_{50} value could not be calculated which is indicative of drug resistance (table 4.1).

Again, micromolar doses were required to induce cell death in all follicular lymphoma samples. Out of the 8 primary cocultured samples tested, the median EC_{50} value was 5.7μM which ranged from 1.1μM to 25μM (figure 4.1b and table 4.1). Two samples showed less sensitivity compared with the others, to high concentrations of doxorubicin (FL#25 and FL#10, figure 4.1b), and a further two samples displayed doxorubicin resistance as EC_{50} values were unattainable for them (FL#29 and FL#11). Notably, the data shows that there was no significant difference in doxorubicin sensitivity between MCL and FL primary cocultured samples, a clear contrast to the bortezomib data (figure 4.2, p=0.27).

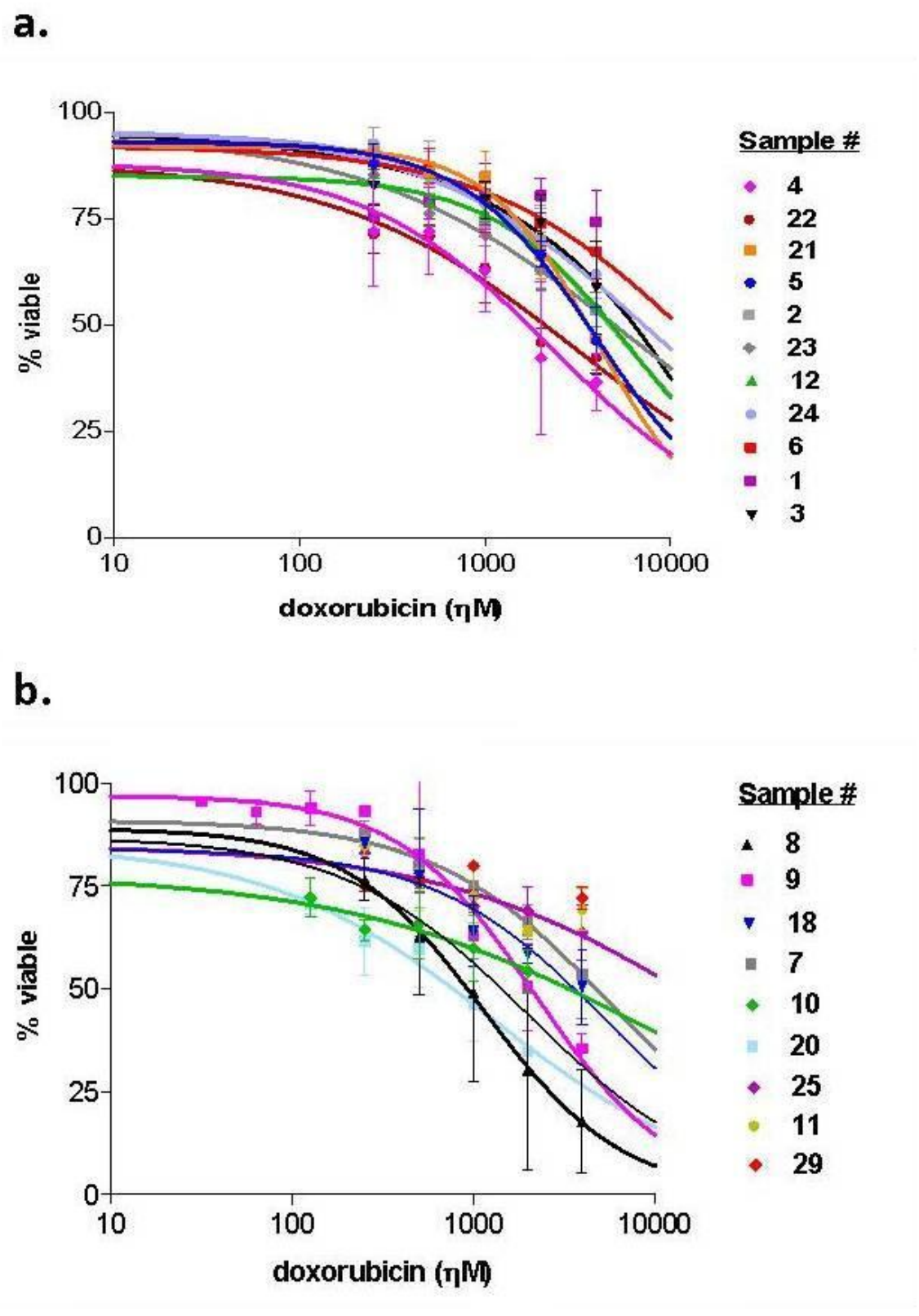

Figure 4.1 EC50 concentration curves for samples from patients with MCL (a) and FL (b) treated with doxorubicin (n=11 and n=9, respectively). Viability was determined using the trypan blue assay. Data points represent mean ± S.D. of at least two independent experiments.

Table 4.1 EC50 values for the effect of doxorubicin on primary cells cultured from patients with MCL (n=10) and FL (n=8).

Mantle Cell Lymphoma (MCL)			Follicular Lymphoma (FL)		
Patient#	EC_{50} (µM)	(90 % CI)	Patient#	EC_{50} (µM)	(90% CI)
22 (pe)	3.1	(2.4–4.1)	9	2.2	(1.7-2.9)
2	5.2	(3.4-8.1)	25	25	(8.3-76.2)
4	2.3	(1.8-3.1)	18	5.5	(2.6-11.4)
21	4.0	(3.4-4.8)	10	11	(850-1300)
5	4.0	(3.5-4.7)	29	No EC_{50}	-
23	5.9	(4.6-7.9)	11	No EC_{50}	-
12	6.6	(4.4-9.8)	7	5.9	(4.2-8.4)
24	8.1	(4.4-12.6)	8	1.1	(0.8-16.0)
6	13.7	(7.7-24.5)			
3	No EC_{50}	-			
Median	**5.2**		**Median**	**5.7**	

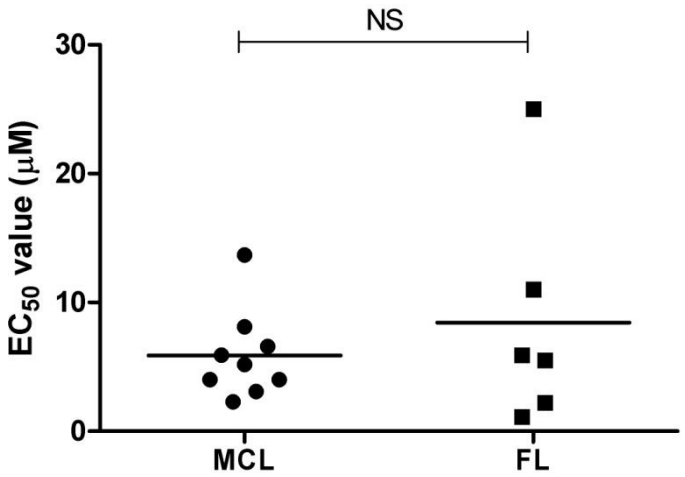

Figure 4.2 Scatter plot of EC50 concentrations for doxorubicin in samples cultured in the CD40 system from patients with MCL (n=10) and FL (n=8). Median EC50 values are represented by horizontal lines and were 5.2µM and 5.7µM for MCL and FL samples, respectively. There was no significant difference between MCL and FL patient EC50 values (p=0.27 paired t-test).

4.2.2 Effect of combining bortezomib with doxorubicin in primary MCL and FL samples cultured in the CD40 system

Simultaneous exposure to a combination of increasing concentrations of bortezomib and doxorubicin in both mantle cell (n=6) and follicular (n=8) primary cocultures revealed greater cell kill than doxorubicin alone. In the majority of experiments, however, this was primarily due to the effect of bortezomib on cell viability (figures 4.3 and 4.4). The effect of the combination was within the range of what would be expected when the effect of doxorubicin and bortezomib were added; thus when samples were analysed for interaction of the drugs in combination using calcusyn dose-effect software (Chou-Talalay), additivity was observed but no synergistic interactions were found (figure 4.5). In addition, bortezomib was not able to induce doxorubicin sensitivity in samples that were resistant to doxorubicin cell kill, which again is likely due to the effect on cell kill being attributable to that of bortezomib alone. The effects of scheduling were not examined in this system.

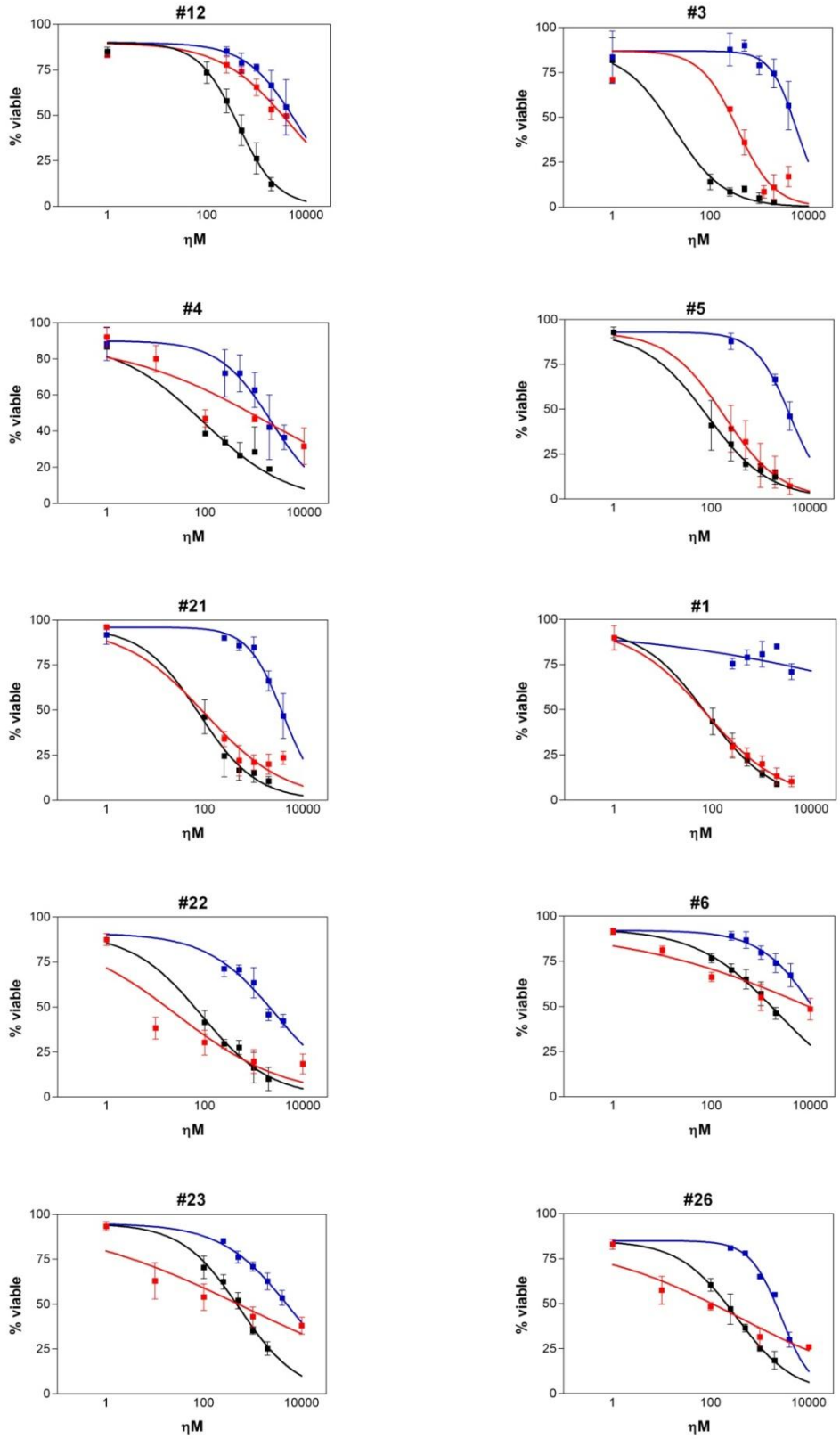

Figure 4.3 Effect of the combination of bortezomib and doxorubicin on cell viability in MCL primary cocultures. Data points are the mean + SD of at least two separate experiments for each sample. Black = bortezomib, blue = doxorubicin, red = combination.

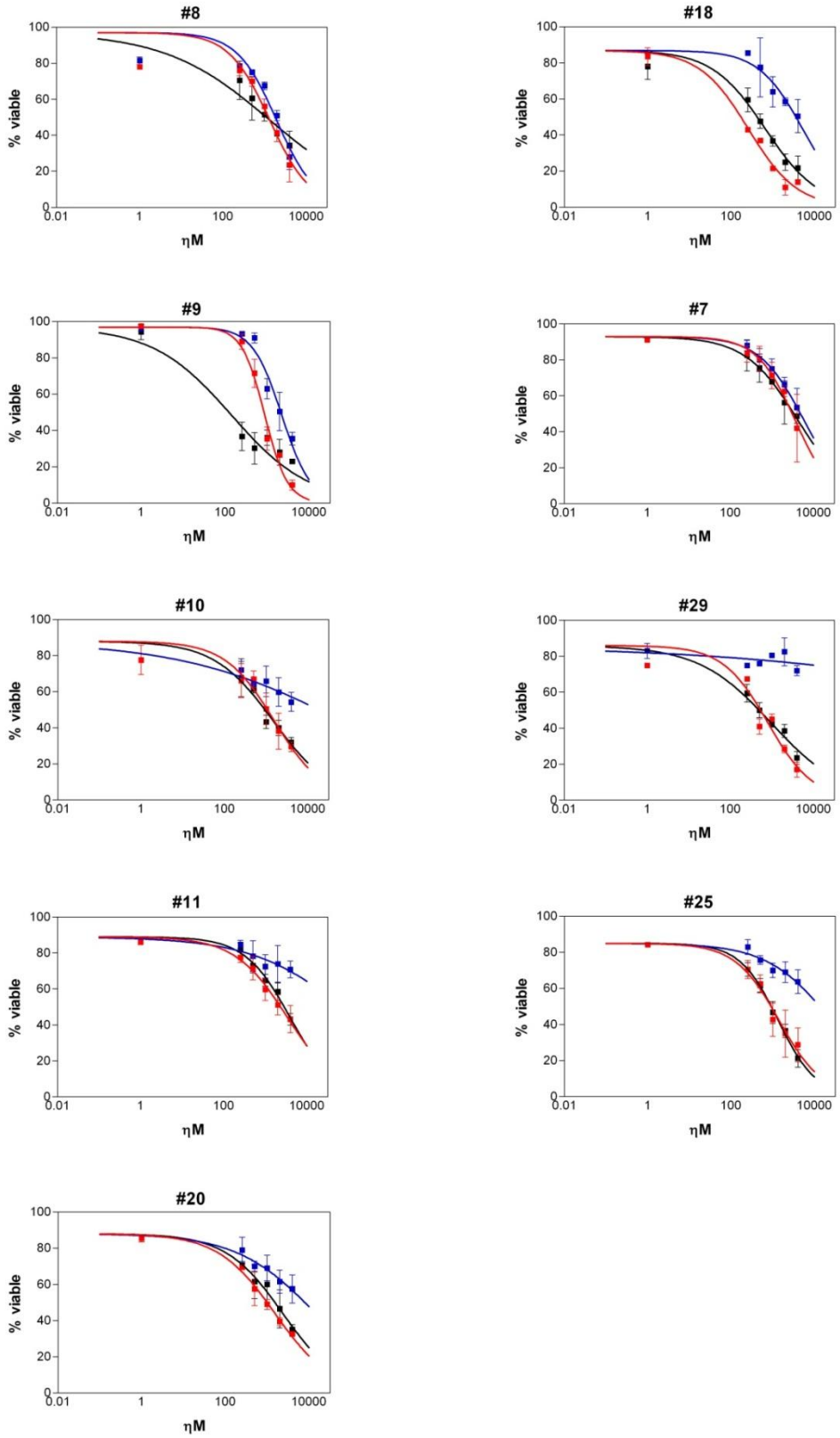

Figure 4.4 Effect of the combination of bortezomib and doxorubicin on cell viability in FL primary cocultures. Data points are the mean + SD of at least two separate experiments for each sample. Black = bortezomib, blue = doxorubicin, red = combination.

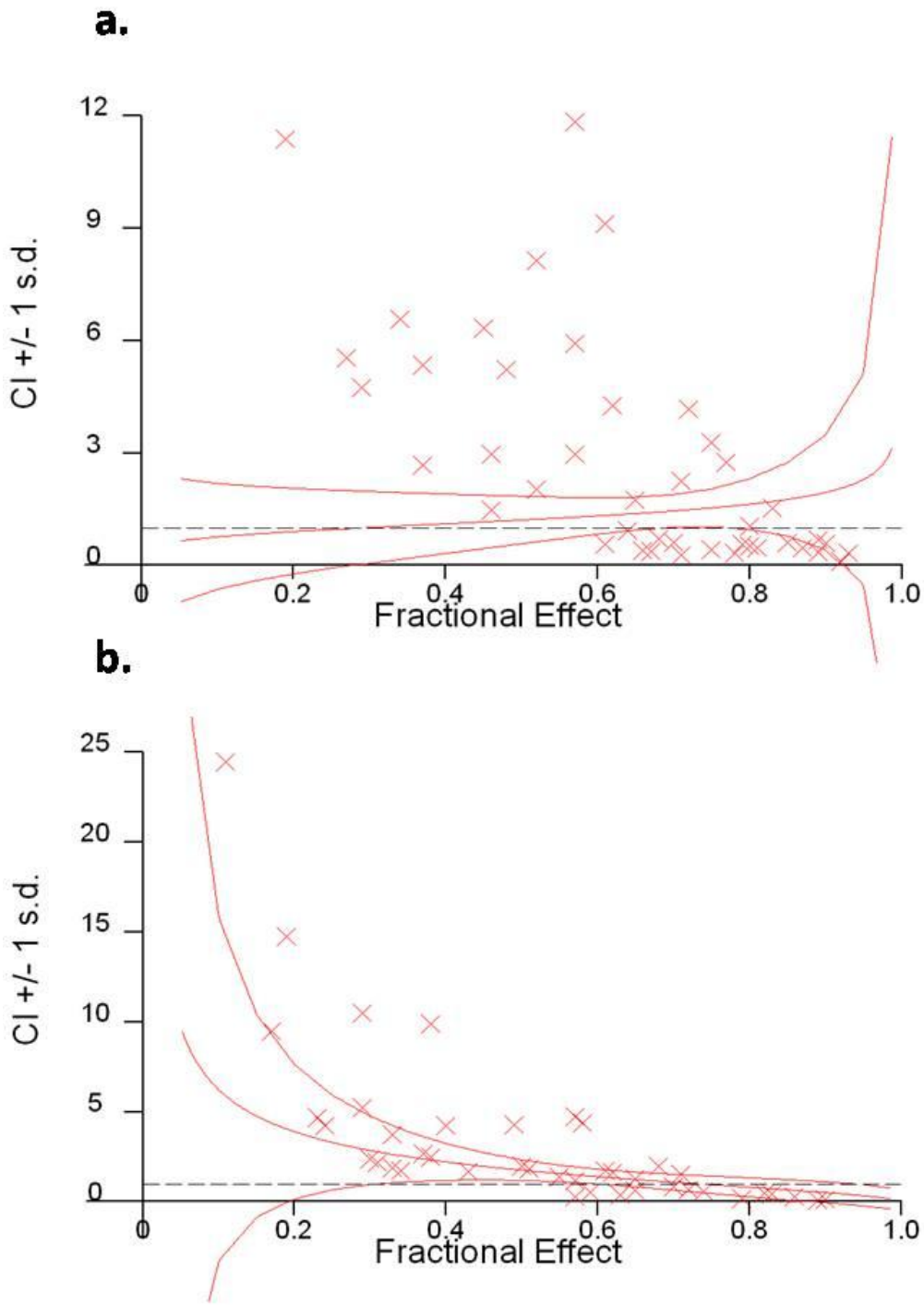

Figure 4.5 Calcusyn plots showing the combination index (CI) values for the combination of bortezomib and doxorubicin as a function of the fractional effect (cell viability) in (a) MCL and (b) FL primary cocultures. Data points are the mean of at least two separate experiments for each sample, depicted as the fraction of cells affected compared to untreated controls. Dashed line is the line of additivity at CI=1. CI<1 indicates synergism and CI>1 indicates antagonism. The horizontal line indicates the mean of all values and the curved red lines indicate the 95% confidence intervals.

4.3 Effect of a novel histone deacetylase inhibitor, UCL67022 on primary MCL and FL samples cultured in the CD40 system

Primary samples used in this section were different to those studied previously due to lack of remaining sample material. In addition to this, we used a new cytotoxicity assay, the ATP assay (Lonza, UK) and the reasons for this are outlined below.

4.3.1 Use of the ATP bioluminescence assay

The ATP assay is based on the bioluminescent measurement of ATP and utilises the enzyme luciferase which catalyses the formation of light from ATP and luciferin. The assay is a measure of a cells ability to generate ATP (or its metabolic activity), as cells lose viability they lose the ability to generate ATP and the ATP concentration in each well therefore reflects both cell number and cell viability, and is thus represented as viable cell number. The ATP assay is therefore a more sensitive measure of cell viability than the trypan blue assay, as loss of the ability to generate ATP is an early event leading to apoptotic cell death. Further advantages of using the ATP assay is that it is far less labour-intensive, lacks user subjectivity and it is semi-automated, therefore is more reproducible, accurate and robust an assay than trypan blue exclusion.

A slight modification to the ATP assay protocol was necessary when assaying primary cocultures (see section 2.8.2, chapter 2 for a more detailed description). This involved transferring the lymphocyte suspensions from the original coculture plates into fresh 96-well plates before beginning the assay. In this way, the adherent CHO monolayer was discarded along with the original plates and there was no CHO-contamination present in the assay plate. Any contribution to the ATP signal in treatment wells from CHO cells was negligible and was relative to that present in control untreated wells.

4.3.2 The activity of UCL67022 and vorinostat in NHL and MCL cell lines

DLBCL cell lines (SUD-4, CRL, DoHH2, DHL-4, DHL-5, DHL-6 and DHL-7) and MCL cell lines (JEK0-1 and GRANTA-519) were cultured for 24 hours in B cell medium after which vorinostat and UCL67022 were added at increasing concentrations and their effect examined 48 hours later using the ATP assay. Both drugs showed potent *in vitro* activity which was concentration-dependent (figure 4.6), even in the p53 mutated cell line GRANTA-519. EC_{50} values for viable cell number ranged from 0.38-1.29μM for vorinostat and 0.28-1.01μM for UCL67022. Notably, the novel UCL compound was 20-fold more potent than vorinostat (median EC_{50} values 0.05μM and 0.93μM, respectively, $p<0.005$) (table 4.2). This was illustrated as a shift to the left of the UCL67022 dose response curve (figure 4.6b).

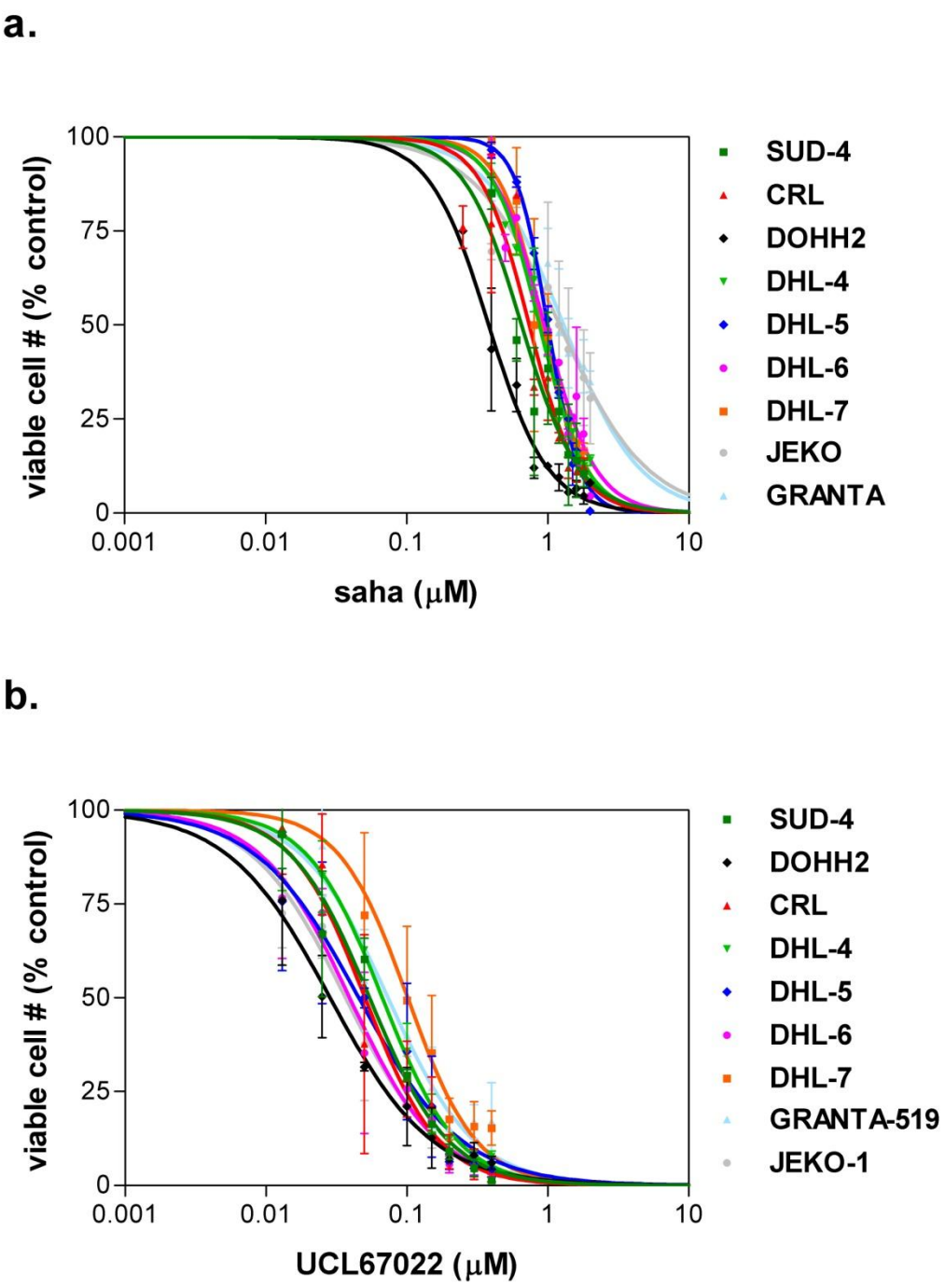

Figure 4.6 (a) vorinostat and (b) UCL67022 activity in a panel of DLBCL cell lines and MCL cell lines (GRANTA-519 and JEKO-1). Cells were incubated with for 24hrs and varying drug concentrations were then added up to 2μM for 48hrs. Viable cell number was assessed using the ATP assay. Data points represent the mean of 3 separate experiments.

Table 4.2 EC50 values for activity of vorinostat (vorinostat) and UCL67022in DLBCL (n=7) and MCL (n=2) cell lines. ***p= 0.0001, vorinostat vs. UCL67022.

Cell line characteristics		SAHA		UCL67022	
Cell line	**Malignancy**	**EC_{50} (µM)**	**(95% CI)**	**EC_{50} (µM)**	**(95% CI)**
SUD-4	DLBCL	0.65	(0.50-0.78)	0.05	(0.05-0.06)
CRL	DLBCL	0.74	(0.64-0.87)	0.03	(0.02-0.03)
DoHH2	DLBCL	0.38	(0.34-0.43)	0.05	(0.04-0.07)
DHL-4	DLBCL	0.88	(0.84-0.92)	0.07	(0.06-0.07)
DHL-5	DLBCL	1.00	(0.97-1.03)	0.05	(0.04-0.06)
DHL-6	DLBCL	0.95	(0.88-1.03)	0.04	(0.03-0.05)
DHL-7	DLBCL	0.93	(0.82-1.04)	0.10	(0.08-0.13)
JEKO-1	MCL	1.21	(0.95-1.54)	0.04	(0.03-0.05)
GRANTA-519	MCL	1.29	(1.11-1.51)	0.07	(0.06-0.09)
Median (µM)		**0.93**		**0.05*** **	

4.3.3 The activity of UCL67022 and vorinostat in primary MCL and FL samples cultured in the CD40 system

The effect of 48 hours exposure to vorinostat and UCL67022 was examined in cocultured samples taken from 5 different patients (2 MCL, 2 DLBCL and 1 FL). Samples were cultured in the CD40 system for 24hrs and drugs were added at 3 different concentrations (0.5µM, 1µM and 2µM) for a further 48hrs. A concentration dependent reduction in cell viability was observed in all samples in response to both compounds (figure 4.7). Sensitivity varied in response to vorinostat from an EC_{50} value of 1µM in the most sensitive (MCL#3) to the least sensitive DLBCL#41 with an EC_{50} value 9µM. This sample was also less sensitive to UCL67022 compared with the others (EC_{50} 6µM). However, the primary samples were always more sensitive to UCL67022 than to vorinostat (median EC_{50} 1.4µM vs. 6.0µM) (figure 4.8 and table 4.3). Although the primary samples tested displayed a 4.3 fold difference in sensitivity to the two drugs, this did not reach statistical significance (figure 4.8).

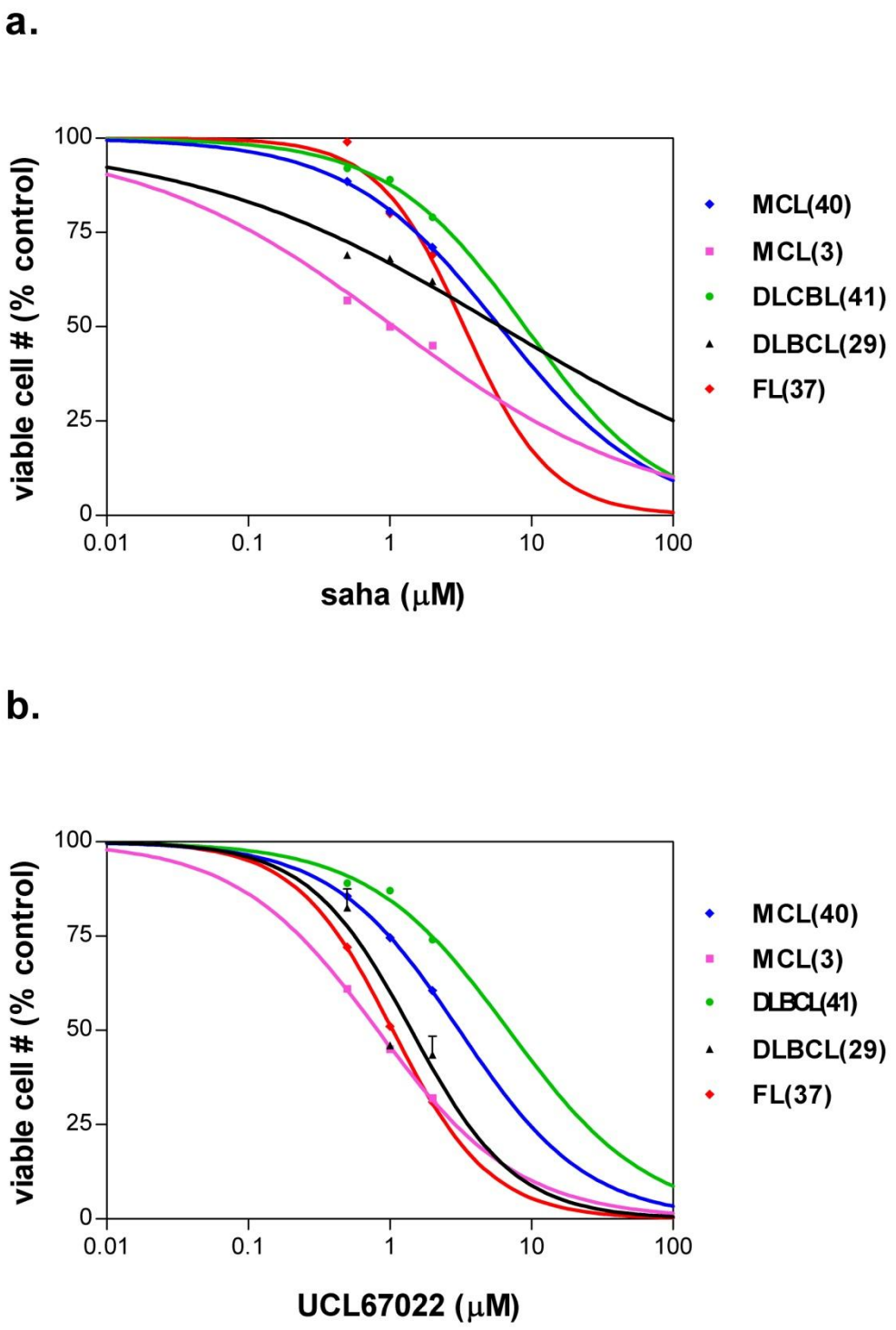

Figure 4.7 EC50 concentration effect curves for samples from patients with MCL, FL, CLL and DLBCL treated with (a) vorinostat and (b) UCL67022. Cells were incubated in coculture plates for 24hrs and exposed to 3 drug concentrations up to 2μM for 48hrs. Viable cell number was measured using the ATP assay and data points represent results from at least one experiment per patient sample.

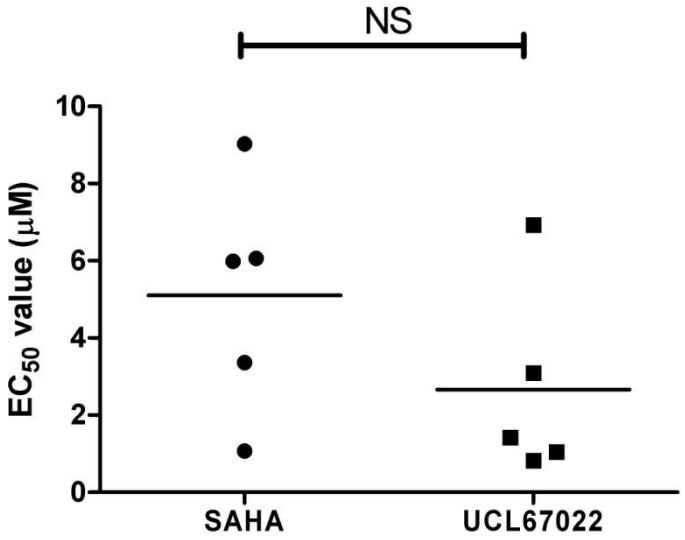

Figure 4.8 Scatter plot showing EC50 values for primary cocultures treated with vorinostat and UCL67022 (2 x MCL, 2 x DLBCL and 1 x FL). Cells were incubated in coculture plates for 24hrs and exposed to 3 drug concentrations up to 2µM for 48hrs. Viable cell number was measured using the ATP assay and data points represent results from at least one experiment per patient sample. NS = not significant (p=0.06).

Table 4.3 EC50 values for effect of vorinostat (vorinostat) and UCL67022 in primary cocultures from patients with MCL (n=2), FL (n=1) and DLBCL (n=2).

Patient information		SAHA		UCL67022	
ID#	Malignancy	EC_{50} (µM)	(95% CI)	EC_{50} (µM)	(95% CI)
40	MCL	5.99	(0.83-43.10)	3.10	(1.35-7.10)
3	MCL	1.07	(0.53-2.17)	0.82	(0.75-0.90)
41	DLBCL	9.03	(2.96-27.56)	6.93	(1.38-34.76)
29	DLBCL	6.06	(0.48-76.80)	1.42	(0.97-2.08)
37	FL	3.36	(0.93-12.14)	1.05	(1.01-1.09)
Median (µM)		**6.0**		**1.4**	

4.3.4 The effect of UCL67022 and vorinostat on histone acetylation

Following 24hrs incubation with vorinostat and UCL67022, acetylation of histone H3 was demonstrated in the DHL-7 cell line via western blot analysis (figure 4.9). This occurred with concentrations as low as 0.1µM UCL67022, and was more pronounced at 0.3µM and above. Clear changes in acetylated α-tubulin from 0.1µM confirmed HDAC6 inhibitory activity and of note, there were no changes in total histone H3, confirming that the increase in acetylated histone H3 was attributable to increased acetylation rather than increased histone H3 protein. Notably, a 10-fold higher concentration of vorinostat was required to achieve the same effect, thus confirming the marked difference observed in their EC_{50} values (4.4µM for UCL67022 vs. 95µM for vorinostat in DHL-7 cells).

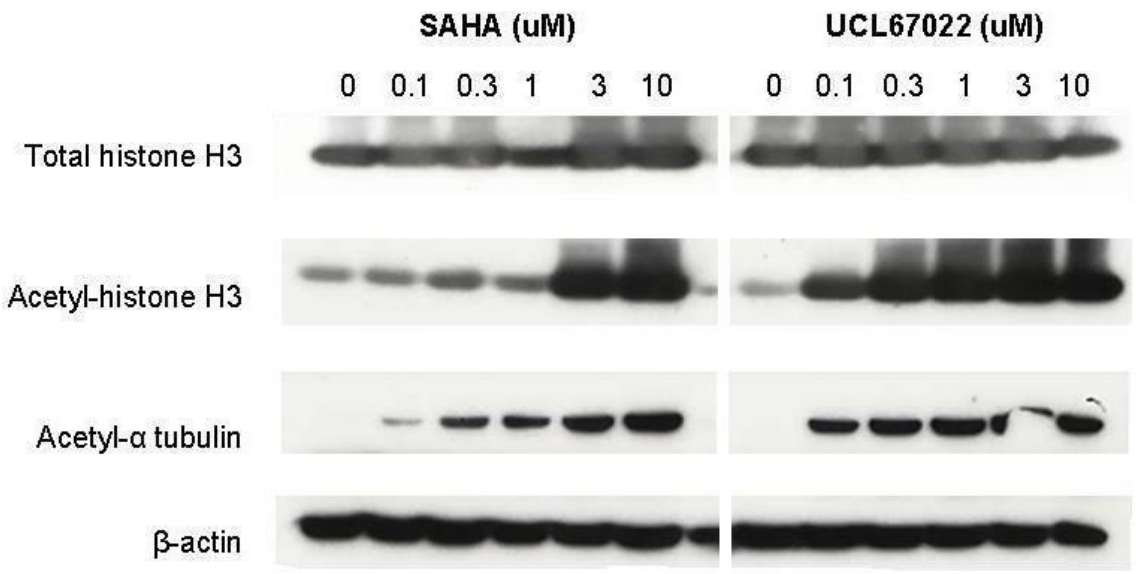

Figure 4.9 Western blots of DHL-7 whole cell lysates following 24hrs exposure to vorinostat (saha) and UCL67022. Blots were probed for total histone H3, acetylated histone H3, acetylated α-tubulin and β-actin.

4.4 Effect of combining bortezomib and HDAC inhibition in primary NHL samples cultured in the CD40 system

4.4.1 Combining bortezomib with vorinostat

Whilst examining the single agent activity of vorinostat and UCL67022 in the 5 primary NHL samples, we also investigated the simultaneous combination of either vorinostat or UCL67022 with bortezomib (figures 4.10 and 4.12). Samples were cultured in the CD40 system for 24hrs prior to the addition of 3 doses of each compound: and 0.5μM, 1μM and 2μM vorinostat or UCL67022 with 0.125μM, 0.25μM and 0.5μM bortezomib. EC_{50} values were generated from dose response curves using linear regression analysis and Graphpad PRISM® software and combination data was analysed using Calcusyn software for dose-effect analysis in order to generate combination index (CI) values (tables 4.4 and 4.5), thus providing a semi-quantitative measure of the effect of the combination. In figures 4.11 and 4.13 the same data is presented as that shown in figures 4.10 and 4.12, but as individual CI plots. Combination index values < 1, = 1, and > 1 indicates synergism, additivity and antagonism, respectively (tables 4.4 and 4.5).

Overall, the dose response curves for the effect of the bortezomib – vorinostat combination displayed a shift to the left when bortezomib was added to vorinostat, indicative of lower EC_{50} values required to achieve the same effect elicited by vorinostat alone (figure 4.10). This sensitizing effect of bortezomib was confirmed by calcusyn analysis which generated CI plots displaying a synergistic to additive to antagonistic interaction with increasing concentrations of bortezomib (figure 4.11). Upon closer inspection of the CI values, a clear synergy was evident at 0.125μM bortezomib, but this was less evident at the highest dose of vorinostat (2μM) (table 4.4). DLBCL#41 was not responsive to the combination instead it produced an antagonistic interaction at all doses of vorinostat tested.

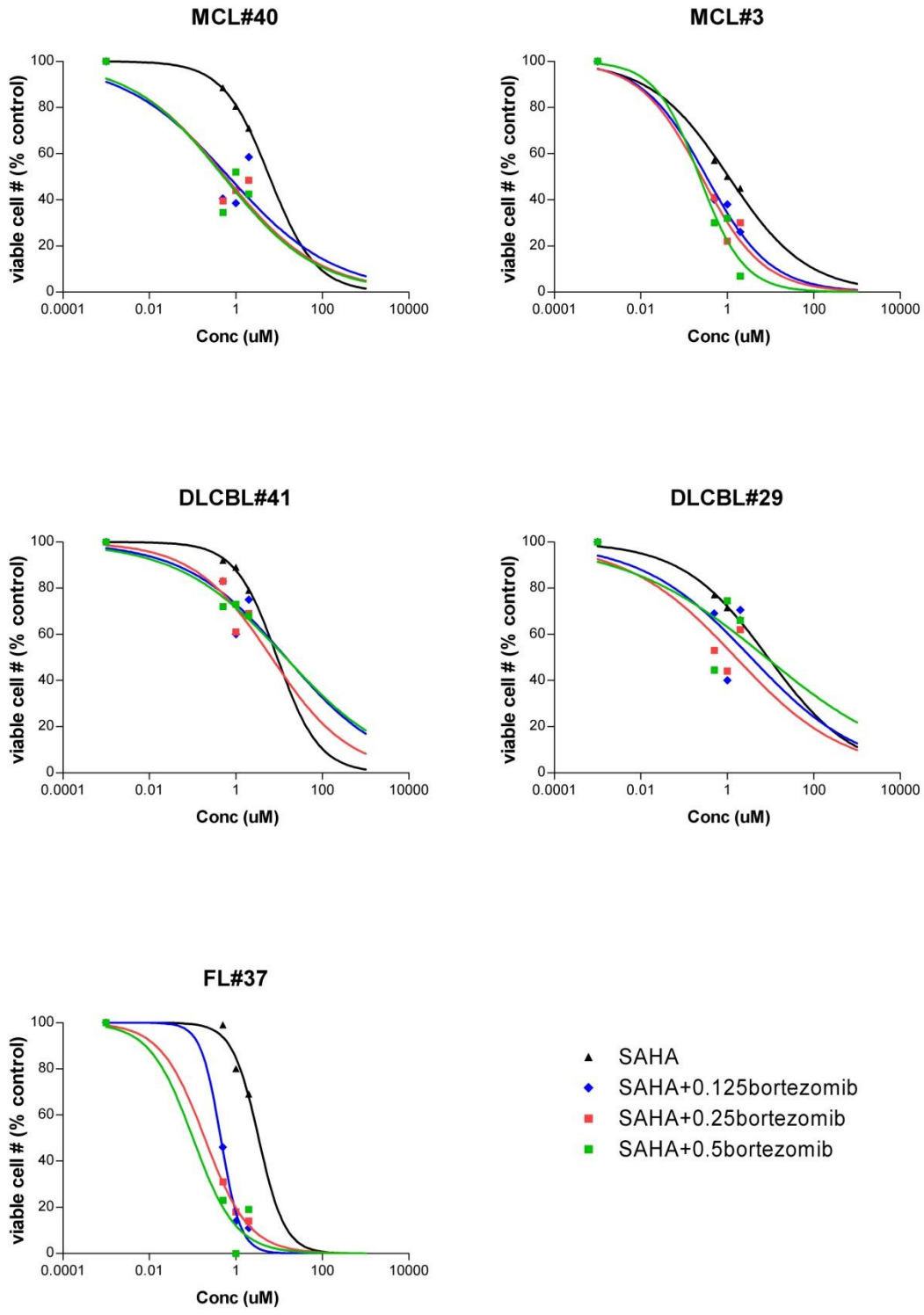

Figure 4.10 Simultaneous combination of bortezomib and vorinostat in 5 primary cocultures: 2xMCL, 2xDLBCL and 1xFL. The dose response curves show the mean of at least 1 experiment. Concentrations of vorinostat used were 0.5µM, 1µM and 2µM.

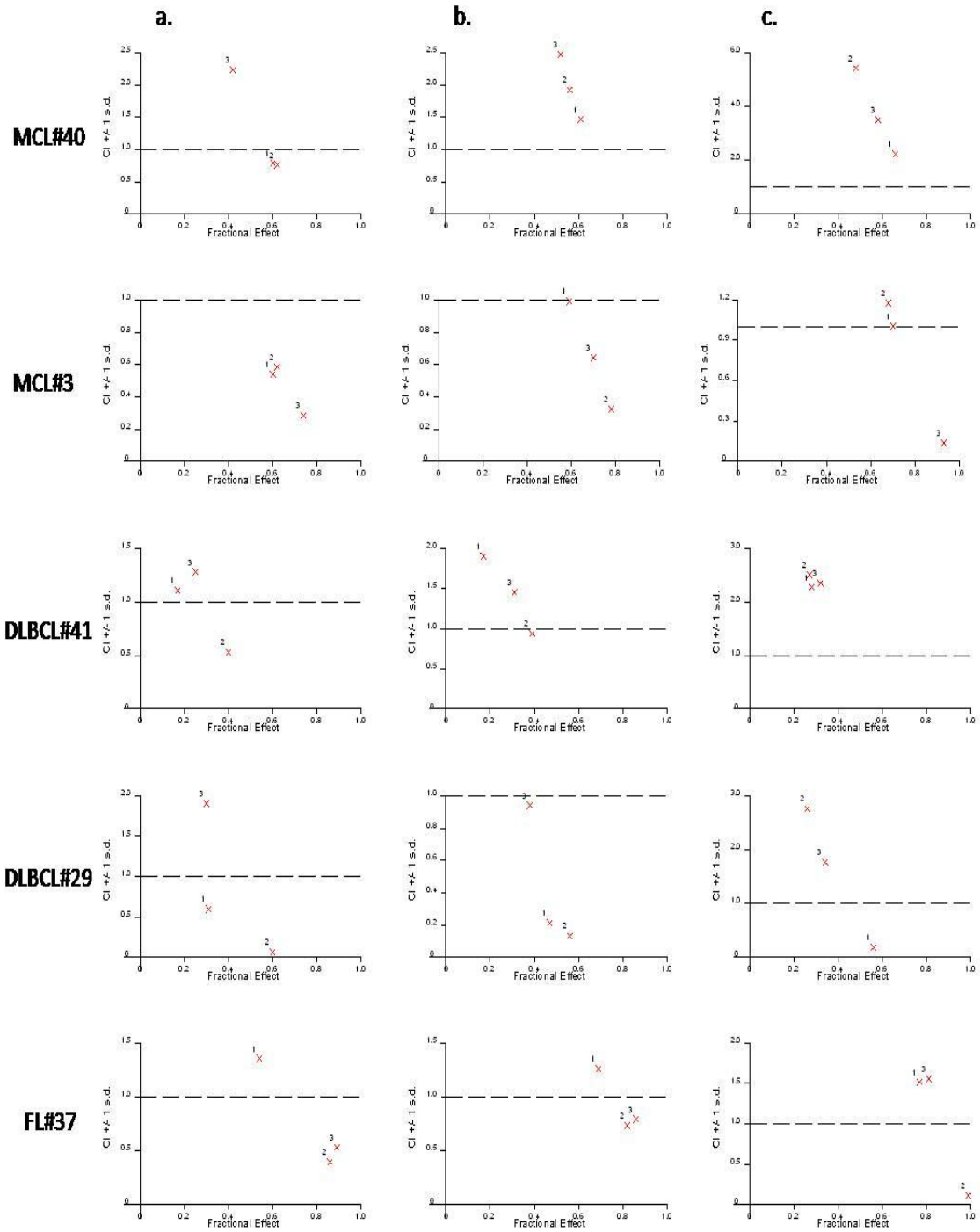
a.
b.
c.
MCL#40
MCL#3
DLBCL#41
DLBCL#29
FL#37
CI +/- 1 s.d.
Fractional Effect

Figure 4.11 Simultaneous combination of bortezomib and vorinostat in 5 primary cocultures: 2xMCL, 2xDLBCL, and 1xFL. The calcusyn combination index (CI) plots shows fraction of cells affected compared to untreated controls at increasing doses of vorinostat: (0.5μM, 1μM and 2μM) combined with increasing doses of bortezomib (a 0.125μM, b 0.25μM and c 0.5μM). Numbers indicate the number of combinations processed. Dashed line is the line of additivity at CI=1. CI<1 indicates synergism and CI>1 indicates antagonism.

4.4.2 Combining bortezomib with UCL67022

DLBCL#41 was also resistant to the UCL67022 – bortezomib combination although CI values were lower indicating a less antagonistic response (table 4.5). Interestingly, DLBCL#29, which was 4-fold more sensitive to UCL67022 than to vorinostat, responded synergistically to the combination of UCL67022 with bortezomib in contrast to the lack of synergy shown with vorinostat (figure 4.13). Again, the lowest dose combination (0.125μM bortezomib + 0.5μM UCL67022) was the most effective at producing synergy (table 4.5). There were no differences in the pattern of combination interaction between vorinostat and UCL67022 except that CI values for UCL67022 were lower than vorinostat (median CI 0.19-0.90 vs. 0.52-1.41 respectively) which corresponded with its increased potency.

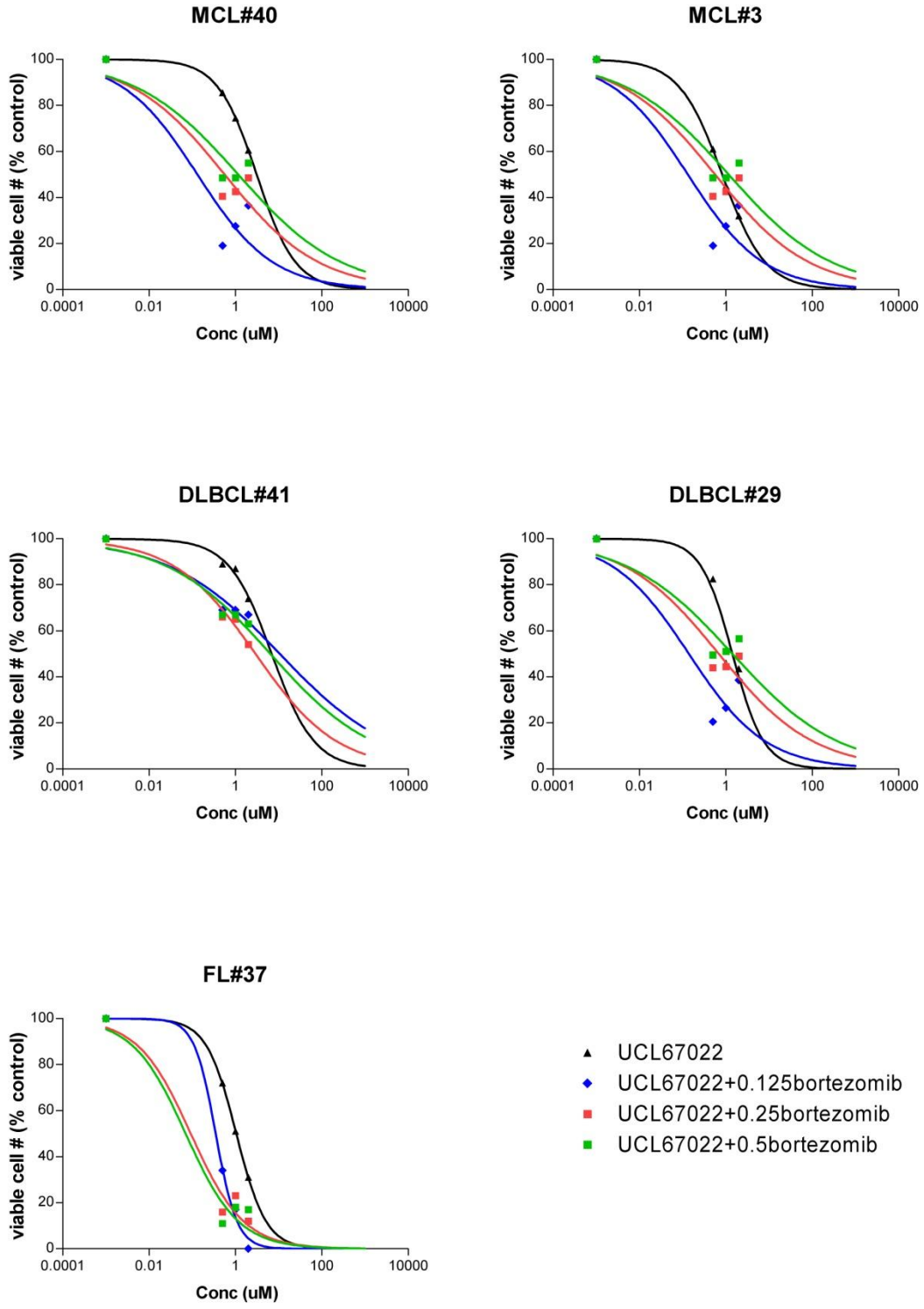

Figure 4.12 Simultaneous combination of bortezomib and UCL67022 in 5 primary cocultures: 2xMCL, 2xDLBCL and 1xFL. The dose response curves show the mean of at least 1 experiment. Concentrations of UCL67022 used were 0.5µM, 1µM and 2µM.

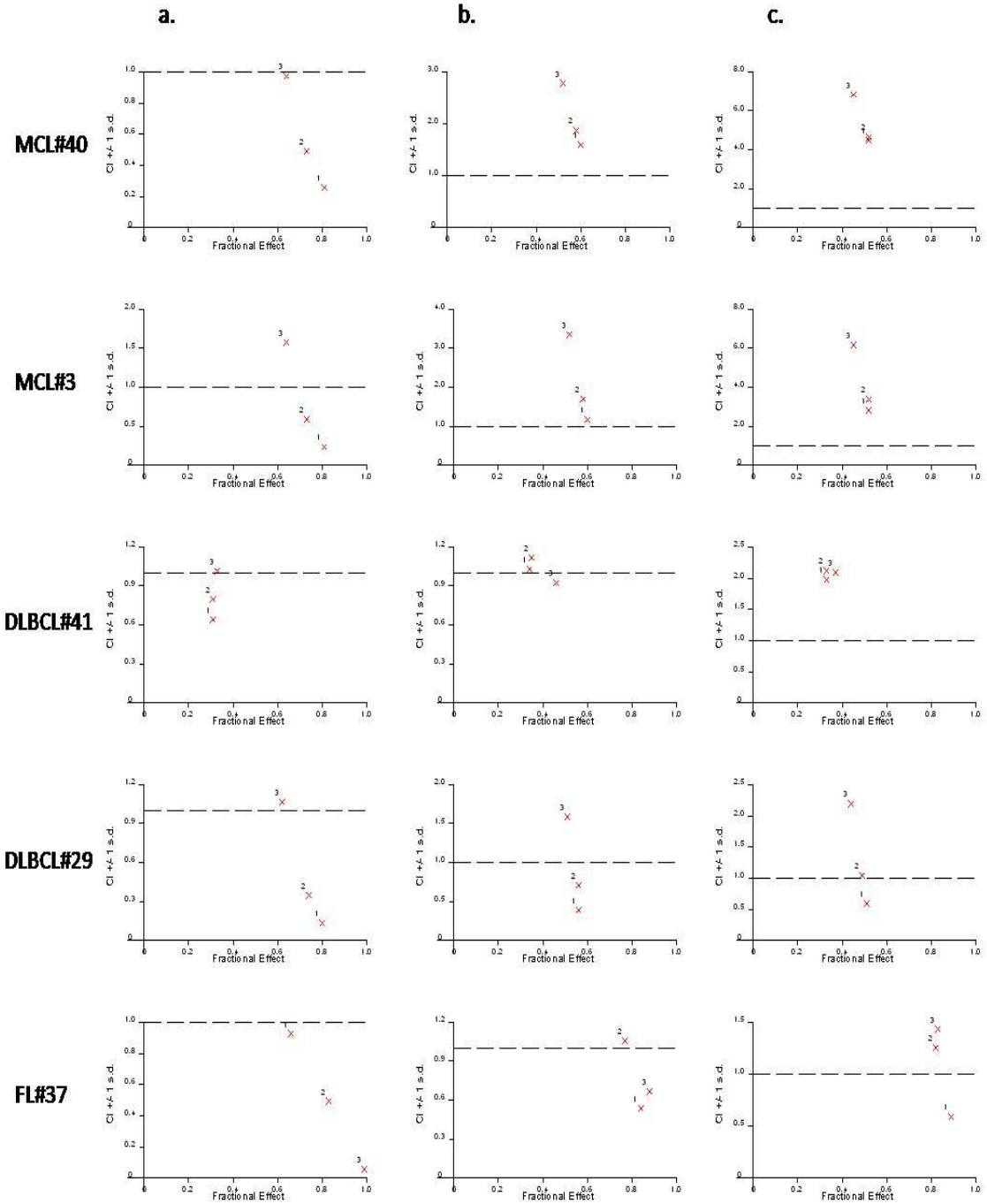
a.
b.
c.
MCL#40
MCL#3
DLBCL#41
DLBCL#29
FL#37
CI +/- 1 s.d.
Fractional Effect

Figure 4.13 Simultaneous combination of bortezomib and UCL67022 in 5 primary cocultures: 2xMCL, 2xDLBCL, and 1xFL. The calcusyn combination index (CI) plots shows fraction of cells affected compared to untreated controls at increasing doses of UCL67022: (0.5µM, 1µM and 2µM) combined with increasing doses of bortezomib (a 0.125µM, b 0.25µM and c 0.5µM). Numbers indicate the number of combinations processed. Dashed line is the line of additivity at CI=1. CI<1 indicates synergism and CI>1 indicates antagonism.

Table 4.4 EC50 values for the effect of vorinostat and bortezomib as single agents and in combination. Combination index (CI) values for 0.125µM bortezomib with 0.5µM, 1µM and 2µM vorinostat are shown in cocultures from patients with MCL (n=2), FL (n=1) and DLBCL (n=2). CI values < 1, = 1, and > 1 indicates synergism, additivity and antagonism, respectively.

Patients		EC_{50} values (µM)		CI values bortezomib + saha (µM)		
ID#	**Malignancy**	**bortezomib**	**saha**	**0.125 + 0.5**	**0.25 + 1**	**0.5 + 2**
40	MCL	0.12 (0.04-0.29)	5.99 (0.83-43.1)	0.40	0.45	1.41
3	MCL	0.20 (0.08-0.53)	1.07 (0.53-2.17)	0.40	0.45	0.36
41	DLBCL	0.41 (0.29-0.57)	9.03 (2.96-27.56)	3.01	1.13	3.08
29	DLBCL	1.56 (0.31-7.95)	6.06 (0.48-76.80)	1.38	0.49	2.39
37	FL	0.10 (0.04-0.29)	3.36 (0.93-12.14)	0.52	0.12	0.13
	Median (µM)	0.20	5.99	0.52	0.45	1.41

Table 4.5 EC50 values for the effect of UCL67022 and bortezomib as single agents and in combination. Refer to legend above**.**

Patients		EC_{50} values (µM)		CI values bortezomib + UCL (µM)		
ID#	**Malignancy**	**bortezomib**	**UCL67022**	**0.125 + 0.5**	**0.25 + 1**	**0.5 + 2**
40	MCL	0.12 (0.04-0.29)	3.10 (1.35-7.10)	0.17	0.38	0.90
3	MCL	0.20 (0.08-0.53)	0.82 (0.75-0.90)	0.17	0.38	0.90
41	DLBCL	0.41 (0.29-0.57)	6.93 (1.38-34.76)	1.69	2.30	3.21
29	DLBCL	1.56 (0.31-7.95)	1.42 (0.97-2.08)	0.19	0.36	0.98
37	FL	0.10 (0.04-0.29)	1.05 (1.01-1.09)	0.39	0.21	0.02
	Median (µM)	0.20	1.42	0.19	0.38	0.90

4.5 Use of soluble CD40 ligand

4.5.1 Titration of soluble CD40L

Before addition of the sCD40L, it was ligated to a cross-linking enhancer (1µg/ml), which enables CD40 activation to occur at levels achieved with the membrane-bound CD40L (Holler, Tardivel et al. 2003). See figure 2.1 (chapter 2) for an illustration of how its activity is increased in the presence of the enhancer ligand. Figure 4.14 below shows the titration of sCD40L in PBMC samples collected from two different donors and in PBMCs from 2 patients with CLL. This dose-finding experiment confirmed that 100ηg/ml of the ligand was sufficient to induce growth of normal as well as malignant leukemic cells under these conditions.

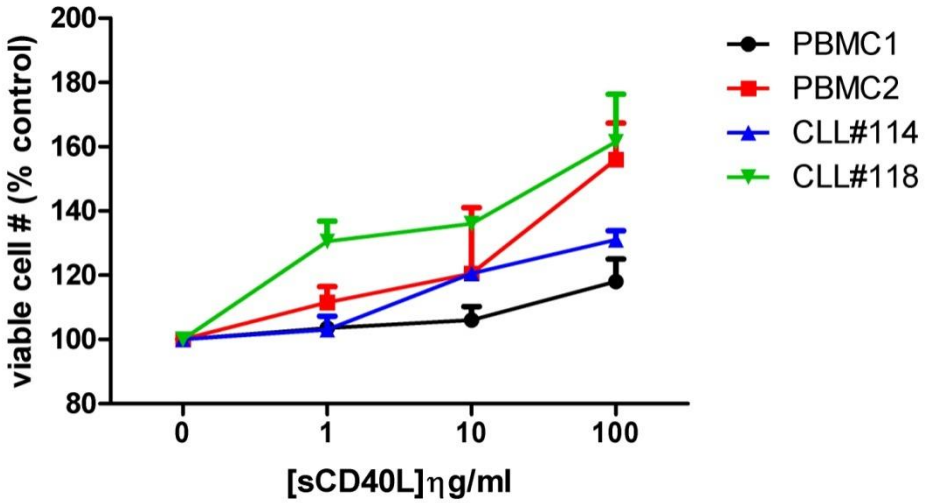

Figure 4.14 Stimulation of B cells with a recombinant human soluble CD40L (sCD40L). Dose dependent co-stimulation of normal PBMCs from 2 donors and mononuclear cells isolated from peripheral blood samples taken from 2 patients with CLL, in the presence of 1µg/ml of a cross-linking enhancer ligand. Mononuclear cells were harvested via density gradient centrifugation on Ficoll-Hypaque and incubated in 96-well plates (105cells/ml in 100µl B cell media supplemented with 10% human serum). Viable cell number was measured using the ATP Vialight Plus assay following 72hrs incubation of cells with varying concentrations of sCD40L (all pre-incubated with 1µg/ml of enhancer). Data points represent mean ± S.D. of at least two independent experiments.

4.5.2 The individual effects of IL-4, sCD40L and IL-4+sCD40L on the growth of primary MCL, FL and CLL samples

We then tested the ability of 100ηg/ml sCD40L to stimulate growth in a larger sample of primary cells including NHL (4xMCL and 2xFL) and CLL (n=8) cells. Isolated B-cells were washed in B-cell culture mix and resuspended at a concentration of $5x10^5$cells/ml in fresh medium supplemented with 5ηg/ml recombinant human IL-4. 100μl/well of this mix was plated into 96-well plates and 100ηg/ml sCD40L (pre-incubated with enhancer at 1μg/ml) was added along with IL-4 as usual at 5ηg/ml. The effect of the sCD40L+IL-4 combination was measured using the ATP assay after 72hr culture of primary MCL, FL and CLL cells, and this was compared to the effect of their culture in control standard media, or in media supplemented with IL-4, or in media supplemented with sCD40L (figure 4.15).

Significant increases in cell growth were observed upon supplementation of media with IL-4 or with sCD40L. The combination of sCD40L+IL-4 resulted in variable responses where more efficient stimulation of cell growth was observed in some primary samples and additive or minimal effects observed in others. Overall however, the individual cytokines synergized to produce enhanced cell growth which reached significance in CLL cells ($p=0.002$ for IL-4 vs. IL-4+sCD40L and $p=0.009$ for sCD40L vs. IL-4+sCD40L figure 4.15c). The limited number of FL samples did not allow for statistical analysis to be applied (figure 4.15b).

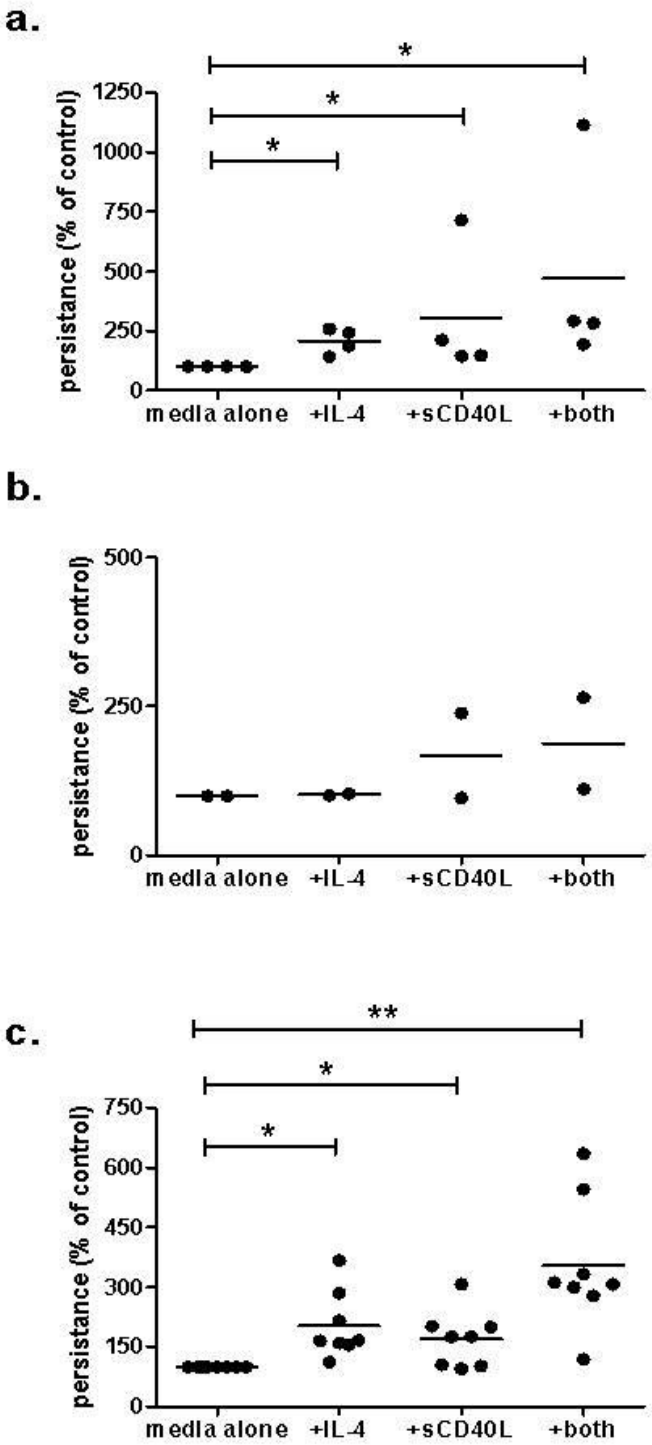

Figure 4.15 Growth of primary MCL (a), FL (b) and CLL (c) in the sCD40L system. Samples were cultured in B cell media (+10% human serum), or supplemented with 5ηg/ml IL-4, or with 100ηg/ml sCD40L (+1μg/ml enhancer), or with IL-4 (5ηg/ml) and sCD40L (+1μg/ml enhancer). Cells were cultured in 96-well plates for 72hrs and assayed for viable cell number using the ATP Vialight Plus cytotoxicity assay. Horizontal lines represent the mean of n=4 primary MCL, n=2 primary FL and n=8 primary CLL samples. *$p<0.05$ and **$p<0.01$ using the paired t-tests.

4.6 Discussion

The mechanisms of proteasome inhibition are very complex by nature (because they affect many pathways) and not fully understood. Despite this, the mechanism of action of bortezomib and of other investigational proteasome inhibitors such as carfilzomib, marizomib, ONX-0912, and MLN9708 are distinct from those of other NHL treatments, making them attractive options for combination therapy. Preclinical evidence suggests that proteasome inhibitors have additive and/or synergistic activity with a large number of agents both *in vitro* and *in vivo*, from cytotoxics to new agents, supporting a growing number of combination studies currently underway in NHL patients.

We therefore studied the effect of combining bortezomib with the commonly used cytotoxic, doxorubicin. Although the addition of bortezomib to doxorubicin increased cell death, this was wholly due to the effect of bortezomib and no synergy was demonstrated. This is disappointing as marked synergy between bortezomib and doxorubicin has been observed in multiple myeloma primary cultures, in particular a patient sample with doxorubicin resistance, where a subtoxic dose of bortezomib (2ηM) reduced the IC50 from 150 to 26ηM (Mitsiades, Mitsiades et al. 2003). Indeed several on-going clinical trials are investigating combinations of bortezomib with doxorubicin and dexamethasone in patients with newly diagnosed or relapse/refractory myeloma (Berenson, Yellin et al.; Lee, Kim et al. 2012). We did not find evidence of consistent synergy in any of the samples at any dose of the drugs, and neither were combined effects greater in samples more sensitive to either agent. In addition, subtoxic or low concentrations of bortezomib were unable to sensitise cells to the effects of doxorubicin. We did not investigate the effects of scheduling and it is possible that different combination schedules may induce synergy and change the outcome.

We next studied the effects of a novel small molecule inhibitor of histone deacetylase (HDAC), UCL67022, as a single agent and in combination with bortezomib. Epigenetic therapy has emerged as a new concept in the treatment of cancers and research into the effects of histone deacetylation, a well known epigenetic modification, has given rise to various HDAC inhibitors that may have a beneficial role in lymphoma treatment.

UCL67022, representing a new class of hydroxamate-based HDAC inhibitor, demonstrated potent (nanomolar) activity in a range of NHL cells lines and potent (low micromolar) activity in 5 primary NHL samples cultured in the CD40 model. No difference in sensitivity to UCL67022 was observed between the DLBCL and MCL cell lines or between the different NHL subtypes in the primary samples, indicating that the mechanism of action is different to that of bortezomib (where MCL cells showed greater sensitivity) and does not involve the proteasome.

Importantly, UCL67022 was clearly more potent than vorinostat, the most clinically progressed HDAC inhibitor; and this effect was evident in both cell lines (20-fold greater potency) and in primary samples (4.3-fold greater potency). Its increased potency correlated with increased inhibition of HDAC activity as demonstrated by changes in acetylated histone H3. This was associated with a corresponding increased acetylation of the non-histone substrate, α-tubulin, which is mediated by HDAC6 and so confirmed its HDAC6 inhibition (class II HDAC). These acetylation changes occurred at approximately 10-fold lower concentrations than vorinostat, confirming the increased potency of the drug. Further knockdown studies are required to clarify the particular sub-class specificity of UC67022 but preliminary work has demonstrated its potency to both HDAC1 and HDAC6 (class I and class II HDACs, data not shown).

There is now ample evidence establishing the rationale for examining HDACis in combination with proteasome inhibition. Studies with the most clinically progressed HDACis, vorinostat and panabinostat, have revealed synergistic interactions with bortezomib in NHL cells, and have suggested a mechanism involving enhanced generation of reactive oxygen species (ROS), increased caspase-3, -8 and -9 activity and marked reduction in proteasome and NFκB activity (Heider, von Metzler et al. 2008; Bhalla, Balasubramanian et al. 2009; Rao, Nalluri et al. 2010). This was consistently observed using different HDACis such as the broad spectrum hydroxamic acid PCI-2478 (Bhalla, Balasubramanian et al. 2009) and vorinostat in combination with next generation proteasome inhibitors such as carfilzomib (Dasmahapatra, Lembersky et al. 2010).

Furthermore, HDAC6 knockdown has been found to confer greater sensitivity to proteasome inhibition than wild type cells (Kawaguchi, Kovacs et al. 2003). Based on its potent HDA6 inhibition, this suggests a potentially greater synergistic effect with the combination of UCL67022 and bortezomib than has been previously observed with vorinostat. Our results demonstrated a synergistic interaction when a subtoxic dose of vorinostat was combined with lower than EC_{50} values of bortezomib in primary NHL samples, in agreement with previous studies. A novel finding however, was the enhanced synergistic interaction between bortezomib and UCL67022, which corresponds with its increased potency compared with vorinostat. We would have liked to confirm these results in more primary samples but were limited by low sample availability. Despite this limitation, this study has demonstrated for the first time the ability of low doses of a novel HDACi, UCL67022, to synergise with low doses of bortezomib in primary DLBCL, MCL and FL cells cultured in a CD40-based tumour-microenvironment model.

We did not investigate the mechanism for the observed synergy, however, our studies in multiple myeloma (not shown here) have also shown effects on caspase activation and increased ER stress as described above. In addition, we demonstrated abrogation of bortezomib-induced aggresome formation (Maharaj, L; Popat, R et al. manuscript submitted; Popat R, Maharaj L. EHA 2008) and this has been associated with increased expression of NOXA and CHOP and induction of lethal unfolded protein response (UPR) (Dasmahapatra, Lembersky et al. 2010; Rao, Nalluri et al. 2010). These observations support further evaluations of the i*n vivo* efficacy of the combination of UCL67022 with bortezomib in NHL.

In a final set of experiments, we investigated the effect of replacing the fibroblastic CHO feeder layer with a recombinant human soluble from of the CD40 ligand (sCD40L). Results showed that this revised model proved effective at stimulating cell growth in primary MCL, FL and CLL samples however, this result only reached significance in the CLL samples (n=8 samples). This was likely due to the limited number of FL (n-2) and MCL (n-4) samples that were available for investigation, and therefore its further validation in different NHL subtypes is required. This alteration to the original model

represents a potential improvement as it is simple to apply, is more reproducible and can be easily standardised. Furthermore, our subsequent work using this new model has successfully identified novel PI3Kδ inhibitors with potent activity in CLL patient samples, some of which have been selected for further development in human clinical trials (data not shown). Its use has also enabled us to demonstrate the greater efficacy of the dual PI3Kα/δ inhibitor, GDC-0941, than the most clinically progressed, PI3Kδ inhibitor, GS-1101 in MCL patients (Iyengar, Clear et al. 2013). We have therefore explored the use of the sCD40L model in our next set of experiments described in the following chapter.

CHAPTER 5: Validation and use of an *in vitro* primary multiple myeloma/bone marrow stromal cell coculture model

5.1 Introduction

Multiple myeloma (MM) is a plasma-cell malignancy characterized by accumulation of malignant cells in the bone marrow and production of a monoclonal immunoglobulin (M protein). Treatment strategies for MM have changed substantially over the past 10 years following the introduction of bortezomib and the immunomodulatory drugs (IMiDs), thalidomide and lenalidomide. Although these drugs have improved patient survival, the disease is still incurable in the majority of patients. There is therefore an unmet need for novel treatment strategies (Kumar, Rajkumar et al. 2008; Kastritis, Zervas et al. 2009; Lonial and Cavenagh 2009; Chanan-Khan, Borrello et al. 2010).

5.1.1 Multiple myeloma cell line models

As with lymphoma and leukaemia cell lines, human multiple myeloma cell lines (HMCLs) are readily available and provide a basic model for investigating the effects of cytotoxic agents with the advantage of continuous proliferation. They are often well characterised in terms of cytogenetic abnormalities and drug responsiveness. For example, the commonly used MM1.S cell line was isolated from a patient that exhibited dexamethasone sensitivity and has been extensively studied to examine the mechanism of dexamethasone-mediated apoptosis (Chauhan, Pandey et al. 1997; Chauhan, Auclair et al. 2002; Rees-Unwin, Craven et al. 2007). Other examples are RPMI 8226 (a standard MM line) and U266 (an IL-6-dependent cell line demonstrating autocrine signalling in MM). The above described HMCLs were used in initial validation studies presented in this chapter.

Despite the advantages outlined above, MMCLs may not be representative of the heterogeneity found in tumours from MM patients as they tend to arise from cases of advanced disease or from extramedullary sites. Often the clones are highly mutated and have complex cytogenetic abnormalities seen in patients with poor prognosis. In

addition, as MMCLs are able to proliferate exponentially in culture medium, they are no longer completely dependent on the bone marrow microenvironment (BMM) for growth and survival. Therefore, assays using MM cells isolated from patient bone marrow aspirates are more likely to give an accurate representation of the disease process that affects the majority of patients. As demonstrated in previous chapters, using patient-derived samples allows the correlation of drug sensitivity with patient characteristics and clinical response, and is more reflective of the heterogeneity of their disease processes. Thus patient-derived MM cells provide a more accurate indication of the likely clinical benefit of a drug than cell lines. Patient-derived MM cells were therefore obtained and used in experiments presented in this chapter.

5.1.2 Development of an *in vitro* primary culture model for the growth of MM cells

Upon isolation of patient-derived MM cells, their viability often rapidly falls despite culture medium supplementation, which limits their use in drug sensitivity assays. Based on findings presented in the previous chapter which demonstrated a stimulatory effect of soluble CD40L (sCD40L) on the growth of NHL and CLL cells, we firstly sought to investigate whether this model (using the ATP assay to assess cell growth) would also support the growth of MM cells *in vitro* and maintain cellular viability long enough to assess drug activity in MM cells. CD40 is commonly expressed on human MM cells (van Kooten and Banchereau 2000; Eliopoulos and Young 2004) but not on normal, terminally differentiated plasma cells (van Kooten and Banchereau 2000; Tong and Stone 2003), thus providing a rationale for its use as a stimulatory ligand in MM.

In parallel with the above experiments, we investigated growth in the same samples cultured under the same conditions but using the guava Viacount assay instead of the ATP assay. As described in chapters 1.6.4 and 2.8.3, the guava assay provides a more complete and accurate evaluation of the assayed cells due to its simultaneous measurement of both cell proliferation and cell viability. It thus has the advantage of allowing differentiation between cytotoxic or cytostatic drug effects. Results from both assays were compared in order to identify the most accurate endpoint test to use in future experiments.

5.1.3 An *in vitro* MM microenvironment model

As described in detail in chapter 1.4, MM cells are dependent on cell-to-cell contact with supportive bone marrow stromal cells (BMSCs) in their microenvironment for their proliferation, migration, metastases and survival; all hallmarks of malignancy. BMSCs are considered the most important element promoting MM cell growth and drug resistance (Hideshima, Mitsiades et al. 2007) and by incorporating this aspect into our *in vitro* culture model, we can give a more accurate representation of *in vivo* drug effects. The second set of experiments thus explores the effects of adhesion of MM cells to BMSCs on MM cell growth. BMSCs may be obtained either from immortalized cell lines (e.g. HS-5 described in section 1.4.5) or grown from BM aspirates of patients with MM. The latter would more likely give a better representation of the disease process, however due to the limited availability of BM samples; we have primarily used the HS-5 cell line as the basis of our model. Again, these experiments were conducted using both the ATP and guava assays in order to find the most accurate and robust model.

5.1.4 Investigating the activity of current anti-MM therapies and their optimisation when used in combination

Due to the known supportive influence of the BMM on MM cell growth, a sought after feature of drugs under development for MM is to demonstrate activity in a microenvironment model. Bortezomib has been shown to maintain cytotoxicity to MM cells in the presence of BMSCs (Hideshima, Richardson et al. 2001) whereas the effects of dexamethasone are abrogated (Chauhan, Pandey et al. 1997; Cheung and Van Ness 2001; Frassanito, Cusmai et al. 2001). As melphalan is “standard of care” for elderly MM patients and bortezomib has also now been incorporated into standard treatment regimes, we have evaluated bortezomib as well as melphalan and the most commonly used MM agent, dexamethasone, in the BMM model validation and cytokine secretion studies described in this chapter. Bortezomib in combination with melphalan is efficacious for patients with multiple myeloma (MM), both in the untreated (San Miguel et al, 2008) and relapsed (Popat et al, 2009) setting. Responses are high, but as only a minority achieve a complete response and toxicities are observed, there is a need to optimise the combination. The most common schedule (San Miguel et al,

2008) is based on historical regimens with bortezomib for days 1, 4, 8 and 11 and oral melphalan from days 1–4. We have investigated this combination in order to determine the optimal schedule of bortezomib and melphalan in the BMM model using HMCLs and patient-derived MM samples.

5.1.5 Investigating the activity of the novel HDAC inhibitor, UCL67022 in MM

We also studied activity of the novel HDACi UCL67022 in the BMM model as this agent demonstrated potent activity in primary cocultured NHL cells described in the previous chapter. HDACis such as vorinostat have also demonstrated promising activity in MM. Vorinostat has exhibited potent *in vitro* activity against HMCLs, including cells resistant to conventional/novel anti-MM agents (Mitsiades, Mitsiades et al. 2003). It is associated with antiproliferative and/or proapoptotic molecular sequelae, including suppression of transcripts for growth factors and/or their receptors; caspase inhibitors; oncogenic kinases; DNA synthesis/repair enzymes and proteasome subunits. Vorinostat is also reported to overcome the protective effects of IL-6 and BMSCs (Mitsiades, Mitsiades et al. 2003). The ability of UCL67022 to overcome bortezomib resistance was recently studied in our group by Dr. Rakesh Popat, and these findings together with those presented here, in the next chapter and in chapter 4, have been recently submitted for publication.

5.1.6 Investigating Hsp90 inhibition in MM and its effect in combination with current anti-MM therapies

Hsp90 is a molecular chaperone that facilitates the folding and stability of numerous signalling molecules that control the growth and survival of cancer cells (Allegra, Sant'antonio et al. 2011). It also plays a crucial role in chaperoning immunoglobulins, including M protein, and interruption of this chaperoning activity leads to accumulation of mis/un-folded proteins (Davenport, Moore et al. 2007). Thus MM cells may be particularly sensitive to Hsp90 inhibition due to their large amount of immunoglobulin production. Hsp90 is also involved in the stabilisation of multiple client proteins involved in apoptosis and tumour angiogenesis, and its inhibition leads to combinatorial inhibition of multiple proliferative signal transduction pathways

(Mitsiades, Mitsiades et al. 2006). We therefore investigated the effects of Hsp90 inhibition using a novel non-ansamycin, non-purine, and non-resorcinol Hsp90 inhibitor agent, KW2478 (Nakashima, Ishii et al. 2010), in our *in vitro* primary MM model.

In gene expression profiling and protein validation studies performed separately to work presented here, an association was found between resistance to bortezomib and the expression of Hsp90, in NHL cell lines (data not shown). We therefore hypothesised that the activity of bortezomib may be enhanced in MM by concurrent Hsp90 inhibition. As further rationale for this combination, the large production of immunoglobulin in MM cells may also render them more sensitive to proteasome inhibition; thus resulting in accumulation of mis/un-folded proteins, which may be further enhanced by use of Hsp90 inhibitors. In a seemingly counterproductive effect, bortezomib treatment typically induces upregulation of Hsp90 (Mimnaugh, Xu et al. 2004; Mitsiades, Mitsiades et al. 2006), as part of induction of the UPR terminal response to proteasome-induced ER stress (Meister, Schubert et al. 2007). This further warrants the use of Hsp-90 inhibition with bortezomib.

KW-2478 has shown potent Hsp90 inhibitory activity in a binding affinity assay (IC_{50} 3.8ηmol/L)), and antiproliferative activity in HMCLs, associated with the degradation of Hsp90 client proteins including cyclin D1 and c-Maf, both IgH translocation products. IgH translocations are observed in around 65% and 75% of patients with intramedullary and extramedullary myeloma respectively (Bergsagel and Kuehl 2001), and their presence increases the stage of disease. KW-2478 has also shown anti-myeloma activity in both subcutaneous and orthotopic models, associated with a decrease in Hsp90 client proteins and a reduction in serum M protein (Nakashima, Ishii et al. 2010). This compound is now undergoing clinical evaluation (in a phase I/II trial in which Barts is participating, NCT01063907) in patients with relapsed and/or refractory MM. Here we present data demonstrating the single agent activity of KW-2478 and the efficacy of its combination with bortezomib and with melphalan in patient-derived MM samples, grown in our stromal coculture model.

5.2 The growth of myeloma cells cultured in the CD40 system

5.2.1 The CD40 system does not affect the growth of HMCLs and patient-derived MM cells.

As demonstrated in the previous chapter, the CD40 system using soluble CD40 ligand proved effective at stimulating growth of lymphoma and leukaemia cells, when using the ATP assay to assess viable cell number. As CD40 has also been shown to stimulate growth of myeloma cells, we investigated the effects of culture in the CD40 system on MM cell growth.

A set of 3 HMCLs (MM1.S, RPMI8226 and U266) and three patient-derived plasma cell samples (MM#1, MM#2 and MM#3) was used in the following experiments. We used a negative plasma cell selection (CD138+) technique fully described in the methods chapter 2.2.2. The main advantage of this technique compared to using a positive selection technique, was that the resultant cells were not antibody-labelled and thus not inadvertently activated. Furthermore, the MM cells were enriched to >90% purity and there was a trend for a higher efficiency in terms of the cell number yield. Optimisation of this procedure was performed in the lab prior to the work detailed in this thesis and therefore is not reported on here.

For the CD40 system, the same concentrations of ligand and cytokine as used in chapter 4 were used in this section that is, 100ηg/ml sCD40L (+ 1µg/ml enhancer) + 5ηg/ml IL-4. HMCLs were cultured at $1x10^5$cells/ml and primary patient cells at $2x10^5$cells/ml for 24hrs, 48hrs and 72hrs. Note, that figure 5.1 shows the effects of CD40 stimulation using the ATP assay as a measure of viable cell number calculated and expressed relative to media-alone controls. Figure 5.2 and 5.3 shows the effects of CD40 stimulation using the guava viacount assay as a measure of cell viability and of cell number, respectively.

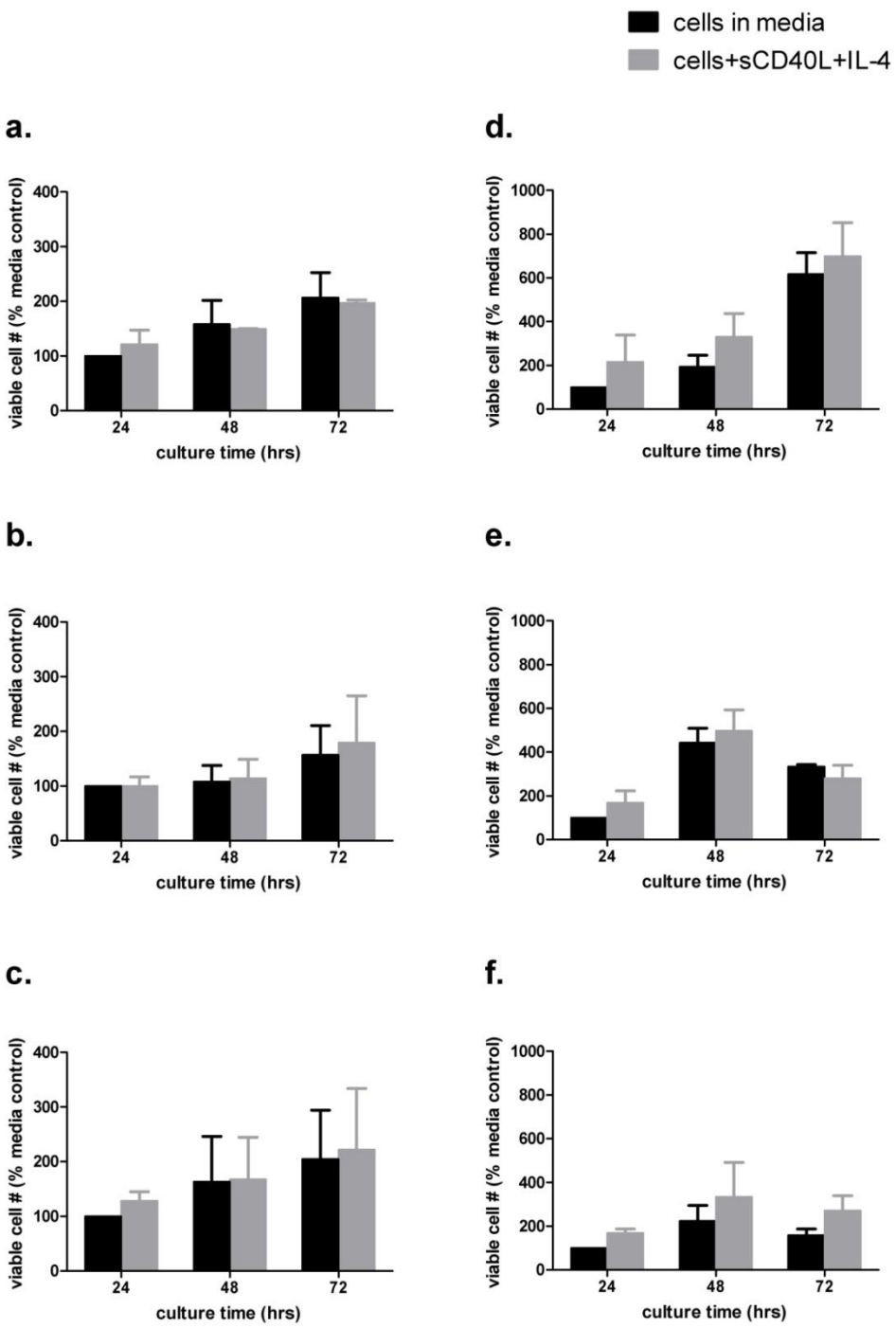

Figure 5.1 Effect of culture in the CD40 system on HMCL and primary MM cell viability using the ATP assay (a) MM1S (b) RPMI8226 and (c) U266 (d) MM#1, (e) MM#2 and (f) MM#3. HMCLs were plated at 1x105cells/ml and primary MM cells at 2x105cells/ml into 96-well plates either with media alone or with 100ηg/ml sCD40L (+ 1μg/ml enhancer) + 5ηg/ml IL-4. Following 24hrs, 48hrs and 72hrs the ATP assay was performed, and luminescence was measured in triplicate wells. Data points represent mean viable cell number ± S.D relative to media-alone controls for 2 experiments per sample.

The doubling times of the MM1S, RPMI8226 and U266 HMCLs are all approximately 72hrs, and this was confirmed using the ATP assay (figure 5.1a, b and c) and the guava assays (figure 5.3 a, b and c) when cells were cultured in media alone. Whilst the CD40 system induced some increases in the growth of the HMCLs compared to their growth in media alone, this effect did not reach statistical significance. Importantly this result was comparable between both assays (figures 5.1, 5.2 and 5.3 a, b and c).

Cell growth in the 3 primary MM samples was variable. According to the ATP assay results, MM#1 responded well to culture in medium alone and expanded by 6-fold over 72hrs (figure 5.1d). In contrast, MM#2 and MM#3 displayed an initial increase in growth over 48hrs followed by a loss of cells by 72hrs (figures 5.1e and f). CD40 stimulation elicited some increases in cell growth (MM#1 and MM#3) but again this effect did not reach significance (figures 5.1 and 5.3 d, e and f).

On closer inspection of the guava assay results, a moderate improvement in primary MM cell viability was observed in response to CD40 stimulation (figure 5.2 d, e and f), although again was not significant. This effect was not observed in the HMCLs, likely due to the fact that they were seeded at maximal viability and therefore there was no room for any increase in viability (figure 5.2 a, b and c). In contrast, the viability of the primary cells tended to remain low after 24hrs of culture (MM#1=36% ± 11%; MM#2=50% ± 10% and MM#3=51% ± 8%). This may also explain their apparent improvement in viability, especially of sample MM#1. Therefore, culture in the CD40 system produced minor increases in cell growth in HMCLs and although some improvement in primary MM cell viability was observed, it did not offer any growth advantage under the present culture conditions. Notably, the ATP assay and the guava assay produced similar results.

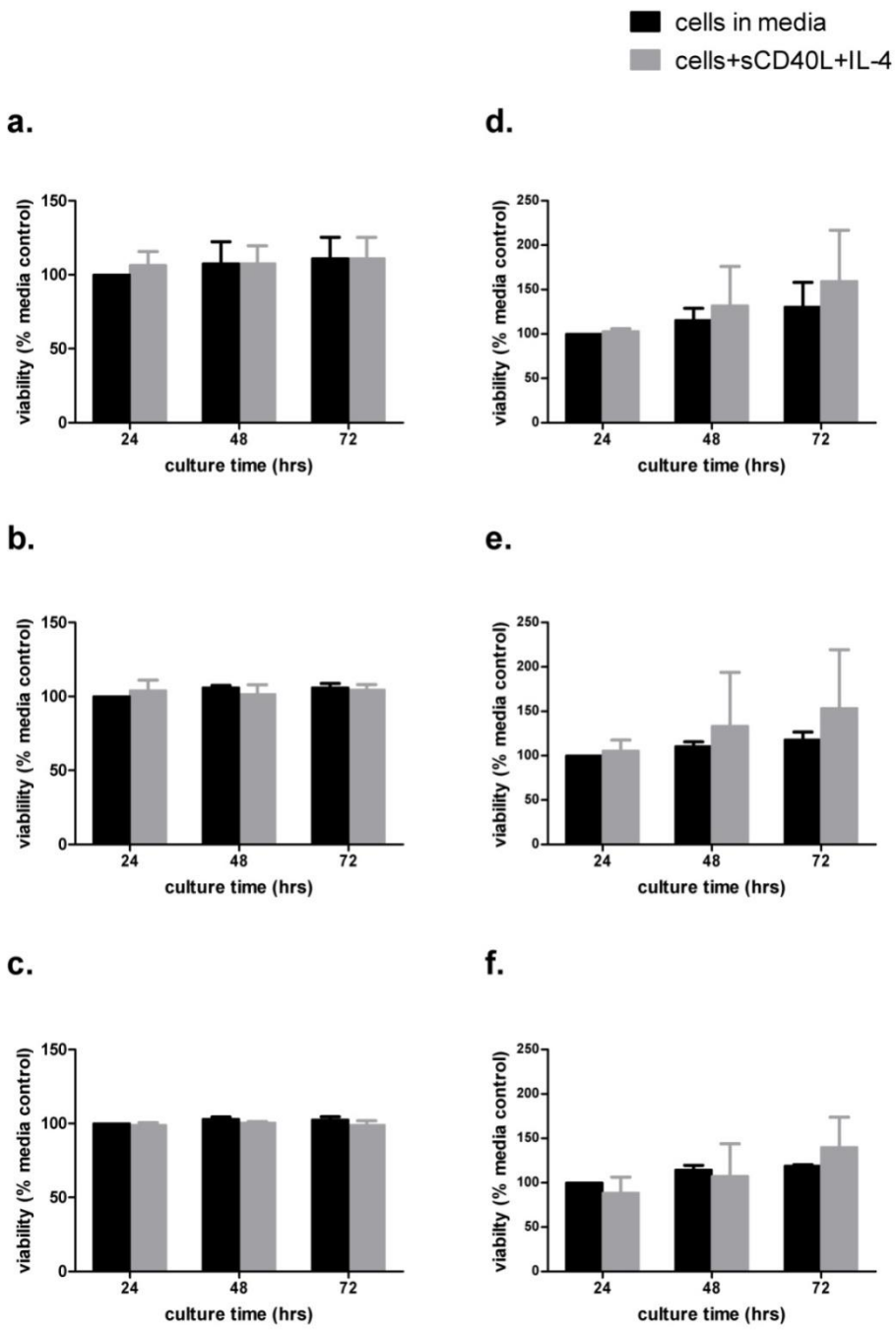

Figure 5.2 Effect of culture in the CD40 system on HMCL and primary MM cell viability using the guava assay (a) MM1S (b) RPMI8226 and (c) U266 (d) MM#1, (e) MM#2 and (f) MM#3. HMCLs were plated at 1x105cells/ml and primary MM cells at 2x105cells/ml into 96-well plates either with media alone or with 100ηg/ml sCD40L (+ 1μg/ml enhancer) + 5ηg/ml IL-4. Following 24hrs, 48hrs and 72hrs the guava Viacount assay was performed, and % viability measured in triplicate wells. Data points represent mean % viability ± S.D. relative to media-alone controls for 2 experiments per sample. No significant difference between treatments was detected in either HMCLs or primary MM samples.

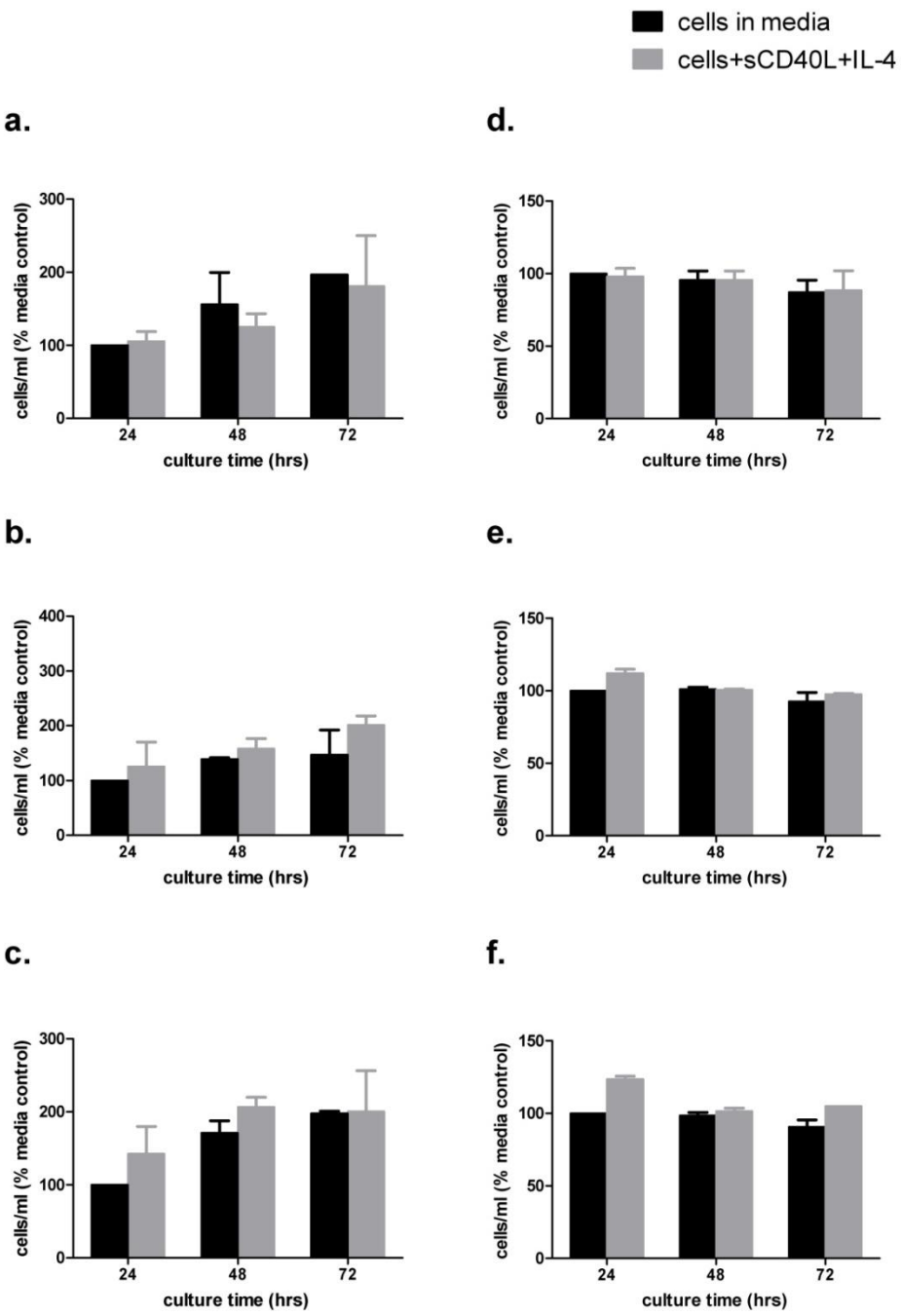

Figure 5.3 Effect of culture in the CD40 system on HMCL and primary MM cell proliferation using the guava assay (a) MM1S (b) RPMI8226 and (c) U266 (d) MM#1, (e) MM#2 and (f) MM#3. HMCLs were plated at 1x105cells/ml and primary MM cells at 2x105cells/ml into 96-well plates either with media alone or with 100ηg/ml sCD40L (+ 1μg/ml enhancer) + 5ηg/ml IL-4. Following 24hrs, 48hrs and 72hrs the guava Viacount assay was performed and cell number was measured in triplicate wells. Data points represent mean cells/ml ± S.D. relative to media-alone controls for 2 experiments per sample. No significant difference between treatments was detected in either HMCLs or primary MM samples.

5.3 The growth of myeloma cells cocultured with HS-5 BMSCs

5.3.1 HS-5 coculture significantly induces the growth of HMCLs and patient-derived MM cells.

Alongside the experiments described above, we investigated the effects of MM coculture with HS-5 BMSCs in the same HMCLs and primary MM samples. The HS-5/MM coculture method has been fully described in chapter 2.7. Briefly, MM cell suspensions were layered over a pre-adhered HS-5 monolayer for a period of 72hrs. Optimisation experiments (not shown here) showed that after this time period there was negligible contribution from the HS-5 cells to the overall viable cell number count (ATP assay) or viability and cell number count (guava assay) obtained in the cocultures. These preliminary experiments also identified an optimum HS-5 96-well plate seeding density of 2,500cells/ml. This cell concentration was used in all experiments presented in this chapter.

No significant effects on HMCL cell growth were observed when they were cocultured with HS-5 BMSCs compared to their growth in media alone (figures 5.4 and 5.5a, b and c). In contrast, growth of primary MM samples was significantly enhanced after 72hrs ($p<0.001$, figures 5.4d, e and f). Values for % viable cell number were in fact unexpectedly 60,000-80,000-fold higher compared to control values for MM#1 and MM#2 via the ATP assay. This was confirmed by a significant enhancement of cell viability (MM#1 and MM#2, figure 5.5d, e and f) and cell proliferation ($p<0.05$ MM#1 and MM#3, $p<0.01$ MM#2, figure 5.6d, e and f) using the guava assay, where more moderate increases were observed. A trend towards this effect was also evident in the MM1.S cells and this reached statistical significance in both RPMI 8226 and U266 cell lines after 72hrs (figure 5.6b and c).

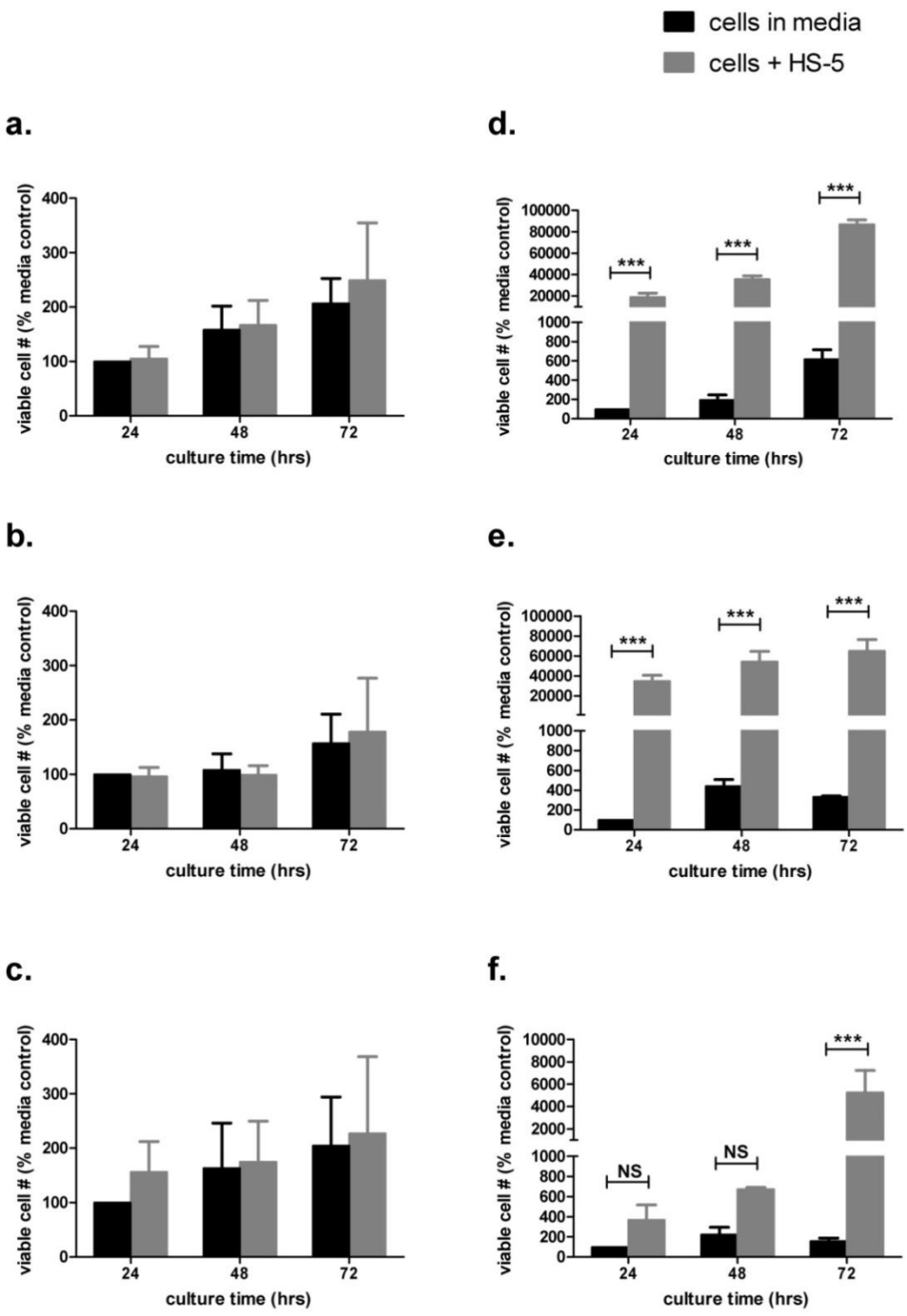

Figure 5.4 Effect of culture in the HS-5 system on HMCL and primary MM cell viability using the ATP assay (a) MM1S (b) RPMI8226 and (c) U266 (d) MM#1, (e) MM#2 and (f) MM#3. HMCLs were plated at 1x105cells/ml and primary MM cells at 2x105cells/ml into 96-well plates either with media alone or with a pre-adhered layer of HS-5 cells seeded at 2x104cells/ml. Following 24hrs, 48hrs and 72hrs the ATP assay was performed, and luminescence was measured in triplicate wells. Data points represent mean viable cell number ± S.D. to media-alone controls for 2 experiments per sample. NS = no significant difference and *** indicates $p<0.001$ (2way ANOVA + Bonferroni post-test).

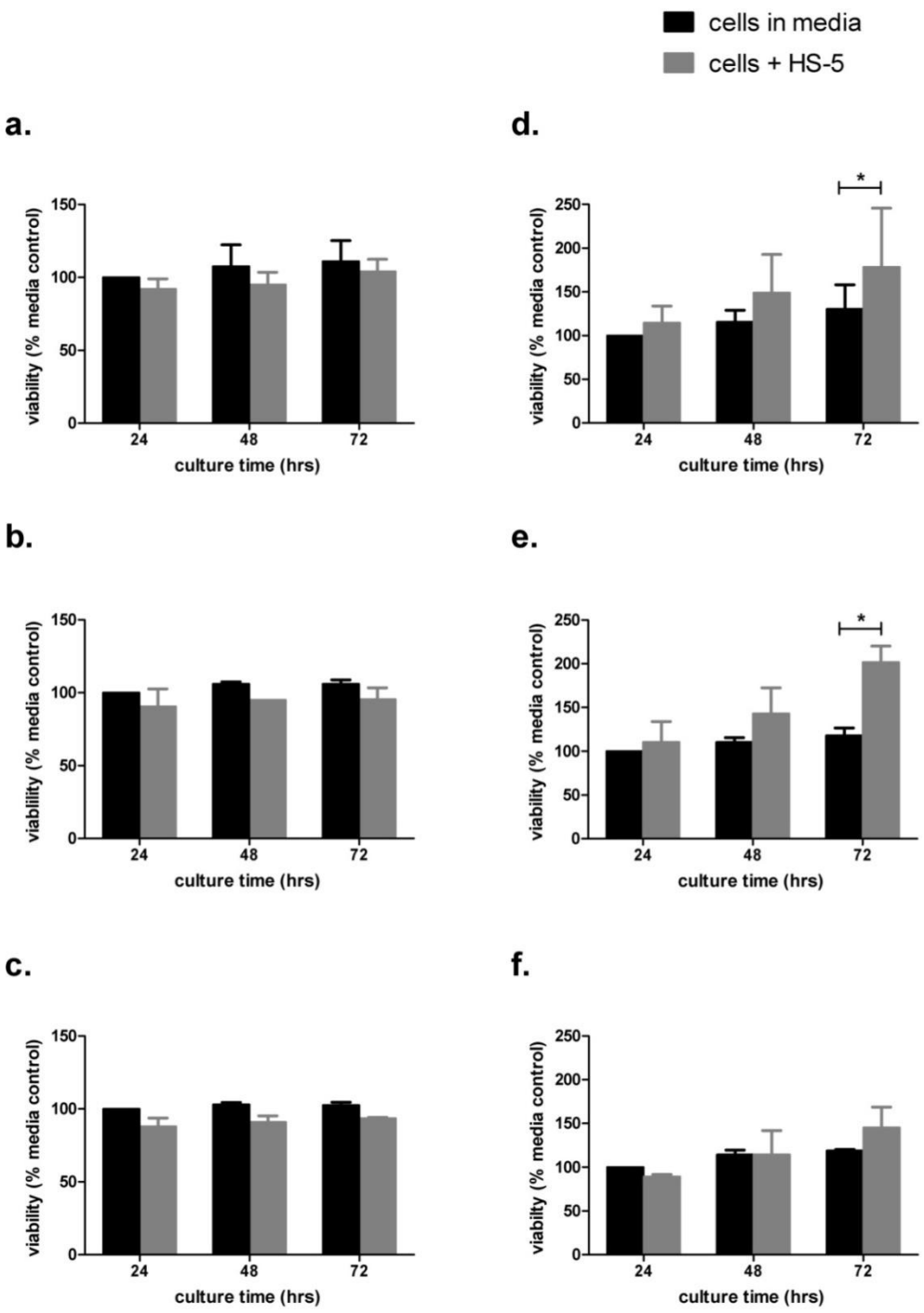

Figure 5.5 Effect of culture in the HS-5 system on HMCL and primary MM cell viability using the guava assay (a) MM1S (b) RPMI8226 and (c) U266 (d) MM#1, (e) MM#2 and (f) MM#3. HMCLs were plated at 1x105cells/ml and primary MM cells at 2x105cells/ml into 96-well plates either with media alone or with a pre-adhered layer of HS-5 cells seeded at 2x104cells/ml. Following 24hrs, 48hrs and 72hrs the guava Viacount assay was performed, and viability was measured in triplicate wells. Data points represent mean % viability ± S.D. relative to media-alone controls for 2 experiments per sample. *p<0.05 (2way ANOVA and Bonferroni post-test).

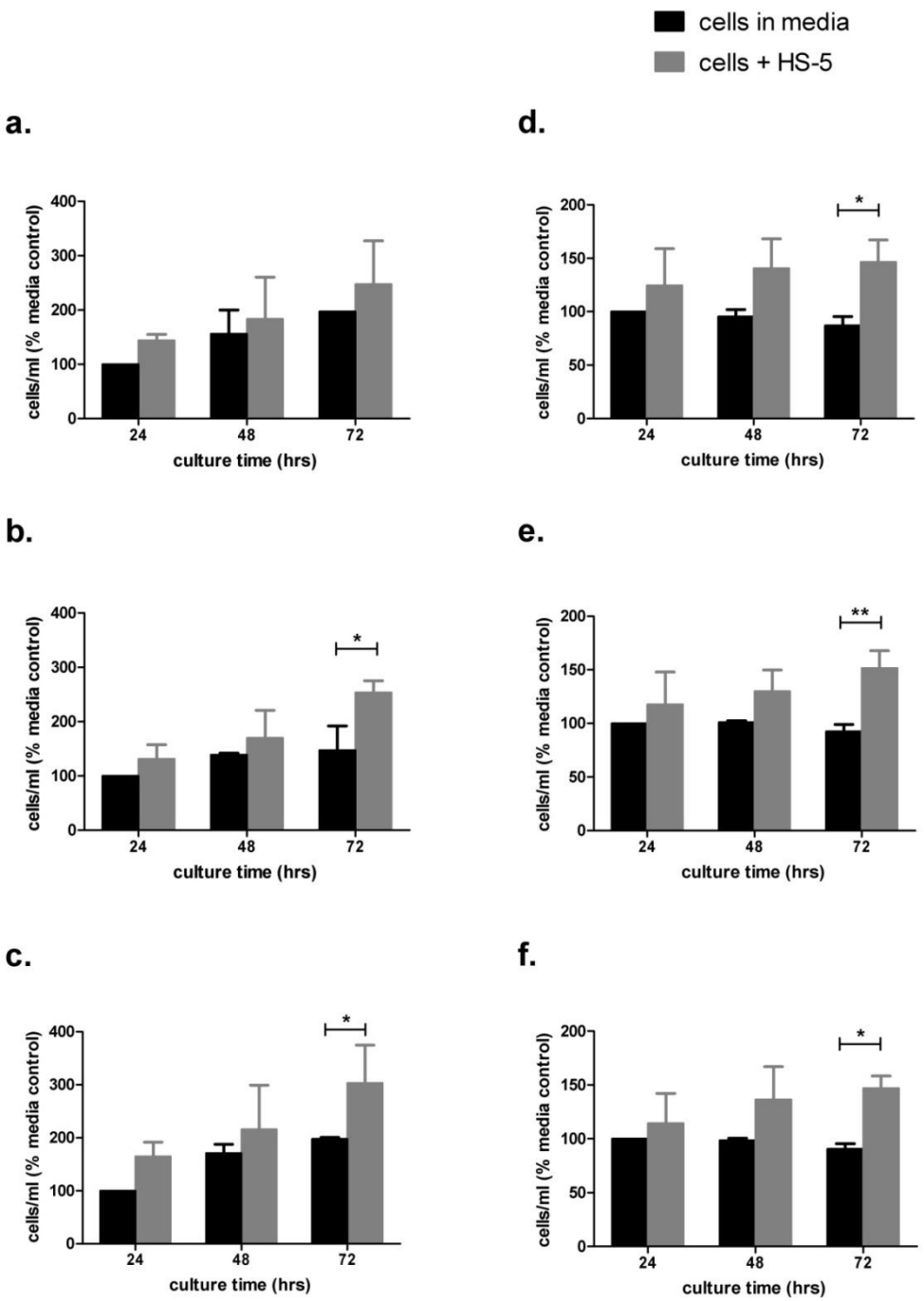

Figure 5.6 Effect of culture in the HS-5 system on HMCL and primary MM cell proliferation using the guava assay (a) MM1S (b) RPMI8226 and (c) U266 (d) MM#1, (e) MM#2 and (f) MM#3. HMCLs were plated at 1x105cells/ml and primary MM cells at 2x105cells/ml into 96-well plates either with media alone or with a pre-adhered layer of HS-5 cells seeded at 2x104cells/ml. Following 24hrs, 48hrs and 72hrs the guava Viacount assay was performed, and cell number was measured in triplicate wells. Data points represent mean cells/ml ± S.D. relative to media-alone controls for 2 experiments per sample. *p<0.05 **p<0.01 (2way ANOVA and Bonferroni post-test).

In conclusion, coculture of a limited number of primary MM cells in the HS-5 model conferred a proliferative advantage over culture in media alone or in the CD40 system for a period of 72hrs. Results also showed that the influence of HS-5 cells on cell proliferation (summarised in figure 5.7) was more accurate when the guava assay was used compared with the ATP assay, and the former was therefore selected for use in all subsequent experiments.

In order to strengthen the statistical significance of these results, the HS-5 coculture model was tested in a larger cohort of primary MM samples (n=16) and its effects on cell viability and cell proliferation is shown in figures 5.8a and 5.8b, respectively. Overall viability significantly increased from a median (± S.D.) of 39% (± 12.51) in media alone, to 54% (± 11.52) with HS-5 coculture ($p<0.0001$). Similarly, total cell number increased from a median (± S.D.) of 65,352 (± 21,687) to a 76,687 (± 22,070). It is important to note that this model does not significantly increase MM cell proliferation but rather is highly effective at prolonging cell survival, under these conditions.

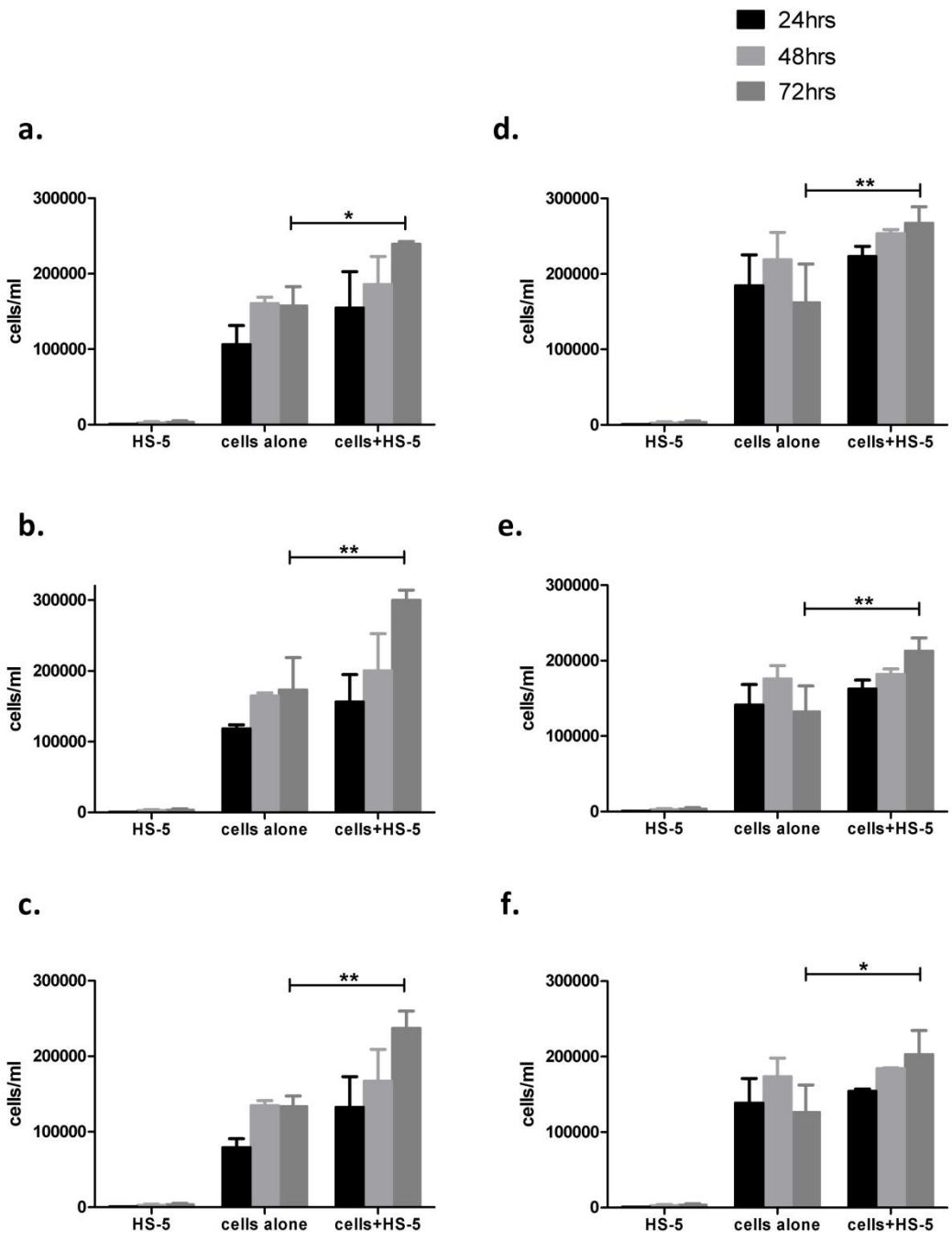

Figure 5.7 MM cell proliferation in the HS-5 system using the guava assay. HMCLs (a) MM1S (b) RPMI8226 and (c) U266 were plated at 1x105cells/ml and primary MM cells (d) MM#1, (e) MM#2 and (f) MM#3 at 2x105cells/ml into 96-well plates either with media alone or with a pre-adhered layer of HS-5 cells seeded at 2x104cells/ml (growth of which is shown in the 3 leftmost bars on each graph). Following 24hrs, 48hrs and 72hrs the guava Viacount assay was performed, and cell number was measured in triplicate wells. Data points represent mean ± S.D. for 3 experiments per sample. *p<0.05 **p<0.01 (2way ANOVA and Bonferroni post-test).

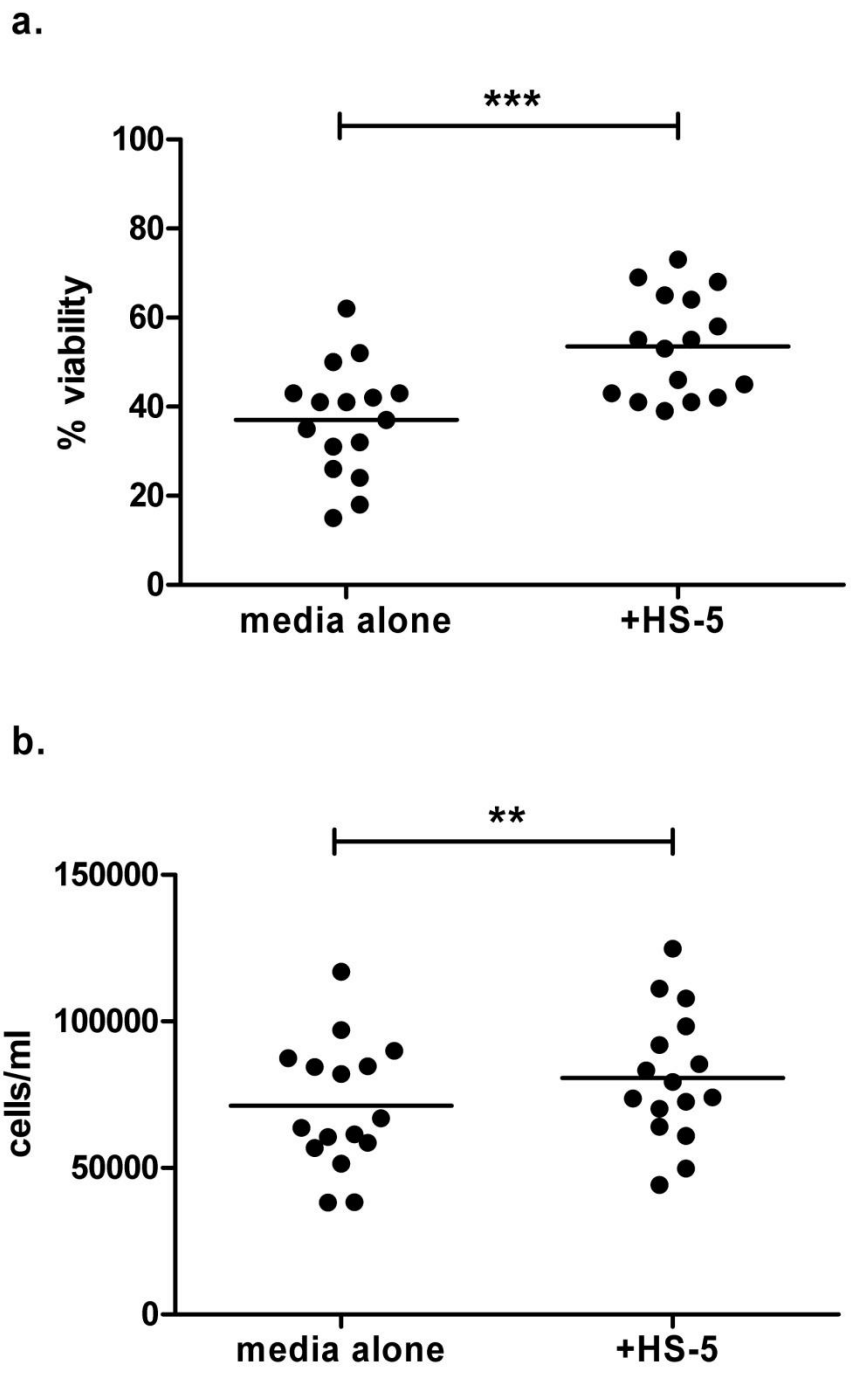

Figure 5.8 Primary MM cell growth (a. viability and b. proliferation) in the HS-5 system after 72hrs. Cells were plated at 1x105cells/ml into 96-well plates either with media alone or with a pre-adhered layer of HS-5 cells seeded at 2x104cells/ml. Following 72hrs the guava Viacount assay was performed, and total cell number was measured in triplicate wells per time point per sample. Horizontal lines represent the mean of 16 different primary samples. **p<0.01 and ***indicates p<0.001 using the paired t-test.

5.4 Investigating drug activity in the HS-5 microenvironment model

5.4.1 The standard MM therapies: dexamethasone, melphalan and bortezomib and the novel agent UCL67022 display differing abilities to overcome the growth effects of HS-5 stroma

Bortezomib has been demonstrated to maintain cytotoxicity to MM cells in the presence of BMSCs (Hideshima, Richardson et al. 2001) whereas the effects of dexamethasone are abrogated (Chauhan, Pandey et al. 1997; Cheung and Van Ness 2001). Dexamethasone and melphalan are standard of care for patients with MM, and in the last 5 years, bortezomib has been incorporated into the treatment regime. Thus, we have tested dexamethasone, melphalan and bortezomib in our coculture model in order to validate the method. As HDACis have demonstrated promising activity in MM, and in NHL (described in the previous chapters using the CD40 model), we investigated its activity in our MM stromal model.

Data presented here compares the effects of these 4 agents on the growth of MM1.S cells and on primary MM samples when cultured in media alone or in the presence of HS-5 stroma. We chose to limit our cell line investigations to the use of MM1.S cells as they are sensitive to dexamethasone therefore, any resistance observed upon coculture would be directly attributable to HS-5 cells. New primary samples were used in these experiments as no remaining cells were available from previously used samples. Cells were cultured in either media or with HS-5 stroma for 24hrs after which each drug was added at varying concentrations (up to 10ηM for bortezomib or up to 10μM for all 3 other agents). Cell viability was determined after 48hrs of drug exposure using the guava viacount assay. Data was analysed via Graphpad PRISM® software and a linear regression model was used to generate sigmoidal dose-response curves and EC_{50} values (see the chapter 2.7 and 2.14 for a full description).

Bortezomib was highly potent in both MM1.S cells and in 5 different primary MM samples as indicated by EC_{50} values in the low nanomolar range (table 5.1. and figures 5.9 and 5.10). Notably, there was no discernible difference in the activity of bortezomib when MM cells were cultured in the presence of HS-5 stroma, suggesting

that bortezomib retains its activity in the BMM, in agreement with previous findings alluded to above. In contrast, mean EC_{50} values for melphalan increased significantly from 256µM to 291µM in the same 5 primary samples ($p<0.05$, figure 5.10), suggesting a failure of melphalan to overcome stroma-induced resistance. This effect was most striking with dexamethasone where HS-5 coculture clearly mediated drug resistance (in MM1.S mean EC_{50} values 0.6µM to 8.2µM, $p<0.05$ and in 2 of 5 primary MM samples mean EC_{50} values 0.01µM to 614µM, $p<0.05$, table 5.1 and figures 5.1 and 5.2). Again this was in accordance with previous studies thus confirming the validity of our HS-5/MM model.

Finally, results indicated that UCL67022 also maintained cytotoxicity in the presence of HS-5 stroma as there was no significant change in EC_{50} values (table 5.1). Importantly, HS-5 stroma showed minimal sensitivity to bortezomib and UCL67022 at concentrations that were toxic to MM cells suggesting a therapeutic window (figure 5.11).

Table 5.1 EC50 values (µM with 95% confidence intervals) for the MM1.S cell line and primary MM samples treated with dexamethasone (n=2), melphalan (n=5), bortezomib (n=5) and UCL67022, (n=2) for 48hrs in media alone or in the HS-5 coculture model. *p<0.05 for cells cultured in media vs. cells cocultured with HS-5. NA =not applicable as CI values could not be generated by the software.

	EC_{50} values (µM) (95% CI)			
Drug treatments	**- HS-5**		**+ HS-5**	
	MM1.S	**Primary MM**	**MM1.S**	**Primary MM**
Dexamethasone	0.6 (0.3-1.2)	0.01 (NA)	8.2* (3.9-17.5)	613.6* (NA)
Melphalan	7.24 (5.4-9.8)	255.6 (12.7-5153)	14.6 (9.9-21.5)	291.4* (4.5-18906)
Bortezomib	0.007 (0.006-0.008)	0.01 (0.004-0.03)	0.007 (0.006-0.008)	0.012 (0.006-0.02)
UCL67022	0.1 (NA)	202.1 (138.8-294.2)	0.1 (NA)	262.0 (190.2-360.9)

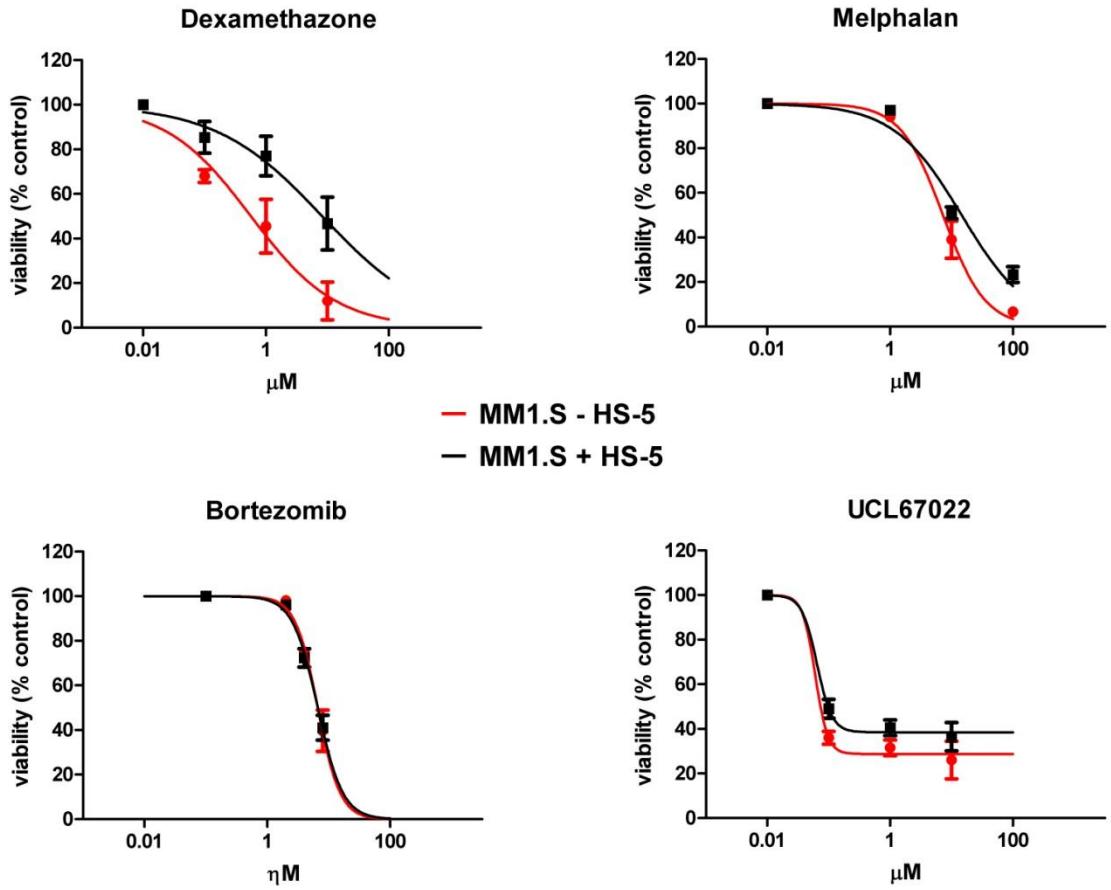

Figure 5.9 Sensitivity of MM1.S to standard (dexamethasone, melphalan and bortezomib) and novel (UCL67022) therapy when cultured in media alone (red) or in the HS-5 system (black). Cells were cultured at 1x105cells/ml alone or with HS-5 cells at 2x104cells/ml. After 24hrs drugs were added for a further 48hrs and % viability was measured using the guava Viacount assay. EC50 curves were generated via linear regression analysis using Graphpad PRISM™ software. Data points represent the mean ± S.D. of 3 independent experiments.

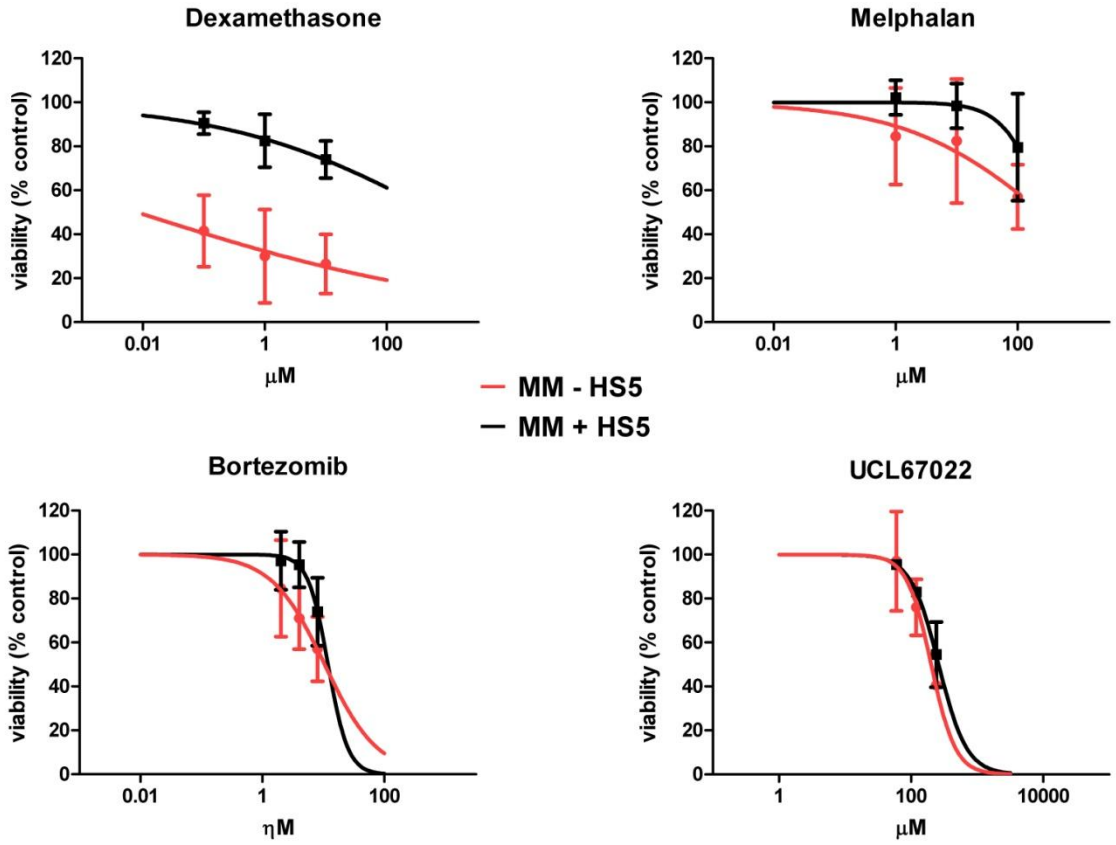

Figure 5.10 Sensitivity of primary MM to standard (dexamethasone, melphalan and bortezomib) and the novel (UCL67022) therapy when cultured in media alone (red) or in the HS-5 system (black). Cells were cultured at 1x105cells/ml alone or with HS-5 cells at 2x104cells/ml. After 24hrs drugs were added for a further 48hrs and % viability was measured using the guava Viacount assay. EC50 curves were generated via linear regression analysis using Graphpad PRISM™ software. Data points represent the mean ± S.D. of 2 (UCL, dexamethasone) or 5 (melphalan, bortezomib) separate MM samples.

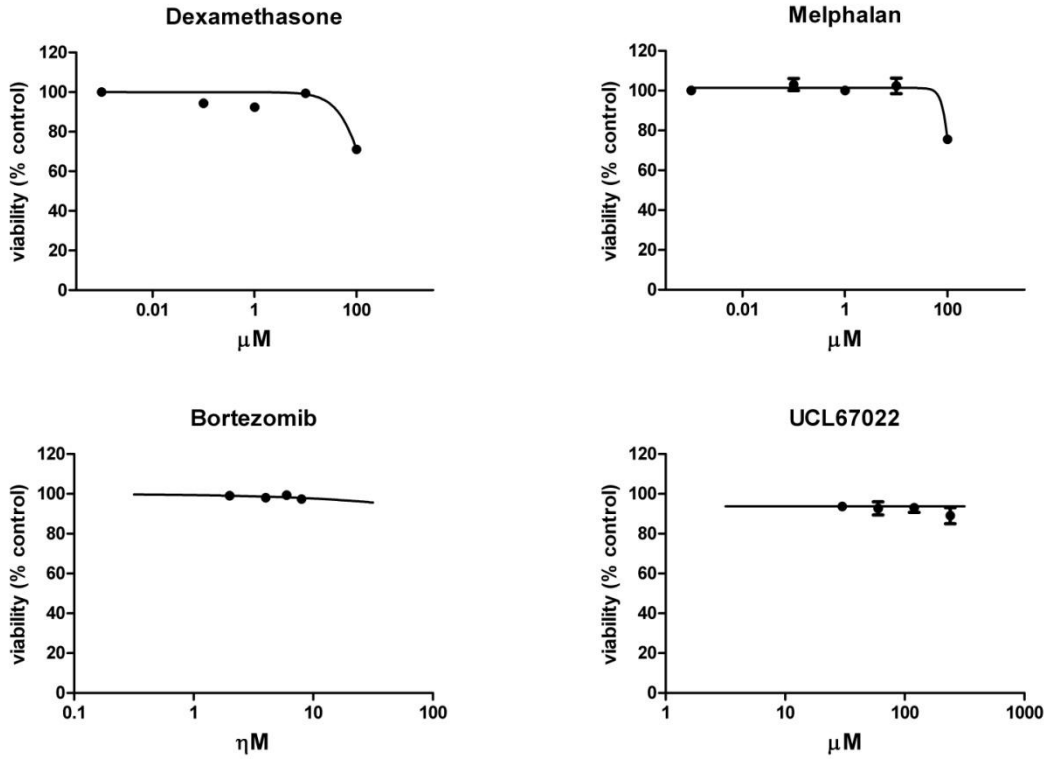

Figure 5.11 Standard therapies (dexamethasone, melphalan and bortezomib) and novel (UCL67022) therapy have minimal effect on HS-5 stroma cultured at 2x104cells/ml. Drugs were added after 24hrs cell culture for a further 48hrs. Cell viability was measured using the guava Viacount assay and curves were generated via linear regression analysis using Graphpad PRISM® software. Data points represent the mean ± S.D. of 3 independent experiments.

5.4.2 The combination of bortezomib and melphalan is highly synergistic and is schedule dependent in MM cells cultured in the HS-5 model

As described in the introduction, the combination of bortezomib with melphalan is efficacious for patients with MM, but as only a minority achieve a complete response and toxicities are observed, there is a need to optimise the combination. We have therefore investigated this combination in order to determine the optimal schedule of administration in our HS-5/MM model in MM1.S cells and the 5 primary samples used in the single agent studies. Bortezomib and melphalan were tested as single agents for 24hr and 48hr exposures and concurrently, three combination schedules were investigated: the simultaneous administration of bortezomib and melphalan for 48hrs (schedule 1); bortezomib for 24hrs prior to melphalan for a total bortezomib exposure of 48hrs (schedule 2); and melphalan for 24hrs prior to bortezomib for a total melphalan exposure of 48hrs (schedule 3).

For the combinations, a sensitising concentration of bortezomib was used: half its EC_{50} value in MM1.S cells (4ηM) and this was combined with 3 increasing doses of melphalan: 1μM, 10μM and 100μM. Viability was determined as usual using the guava viacount assay. In order to assess the effect of the combinations compared with the effect of each drug on its own; the combination data was converted to % cell kill relative to untreated controls. This was plotted against the predicted % cell kill, calculated by adding together the single agent % cell kill data for each drug at the appropriate time point. These data is presented in the observed versus expected bar charts in figure 5.12. Results indicated a clear effect of scheduling for example, when cells were exposed to schedule 2 (bortezomib prior to melphalan), observed cell kill was significantly greater than the cell kill expected on combining the single agent data (figure 5.12b, $p<0.05$ at 1μM melphalan in MM1.S cells and at all melphalan doses in the primary samples). The effect was most striking however, when cells were exposed to schedule 3 (melphalan prior to bortezomib). Figure 5.12c shows that all concentrations of melphalan in combination with bortezomib produced highly significant increases in cell kill (in MM1.S $p<0.005$ at 1μM, $p<0.01$ at 10μM and $p<0.05$ at 100μM and in primary MM $p<0.01$ at 1 and 10μM and $p<0.05$ at 100μM).

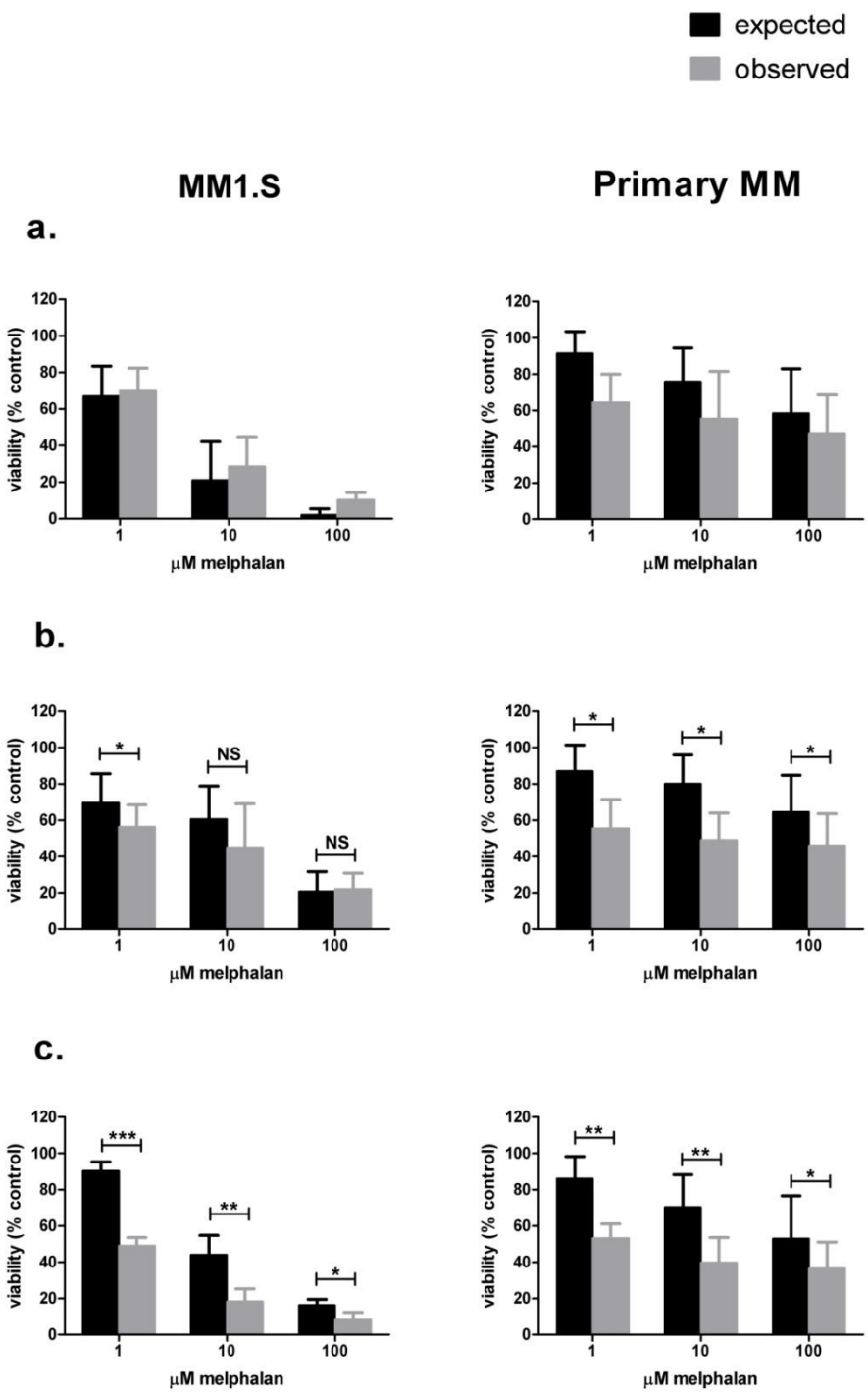

Figure 5.12 Combination of bortezomib (4ηM) with melphalan (1μM, 10μM and 100μM) in MM1.S and primary MM samples. Cells were cultured in the HS-5 system for 24hrs and exposed to drugs for an additional 48hrs. Three schedules were investigated (a) simultaneous exposure, (b) bortezomib pre-treatment followed by melphalan and (c) melphalan pre-treatment followed by bortezomib. Viability was calculated using the guava Viacount assay. Data represents mean ± S.D. of 3 independent experiments for MM1.S and of 5 separate primary MM samples. *p<0.05, **p<0.01 and ***p<0.005

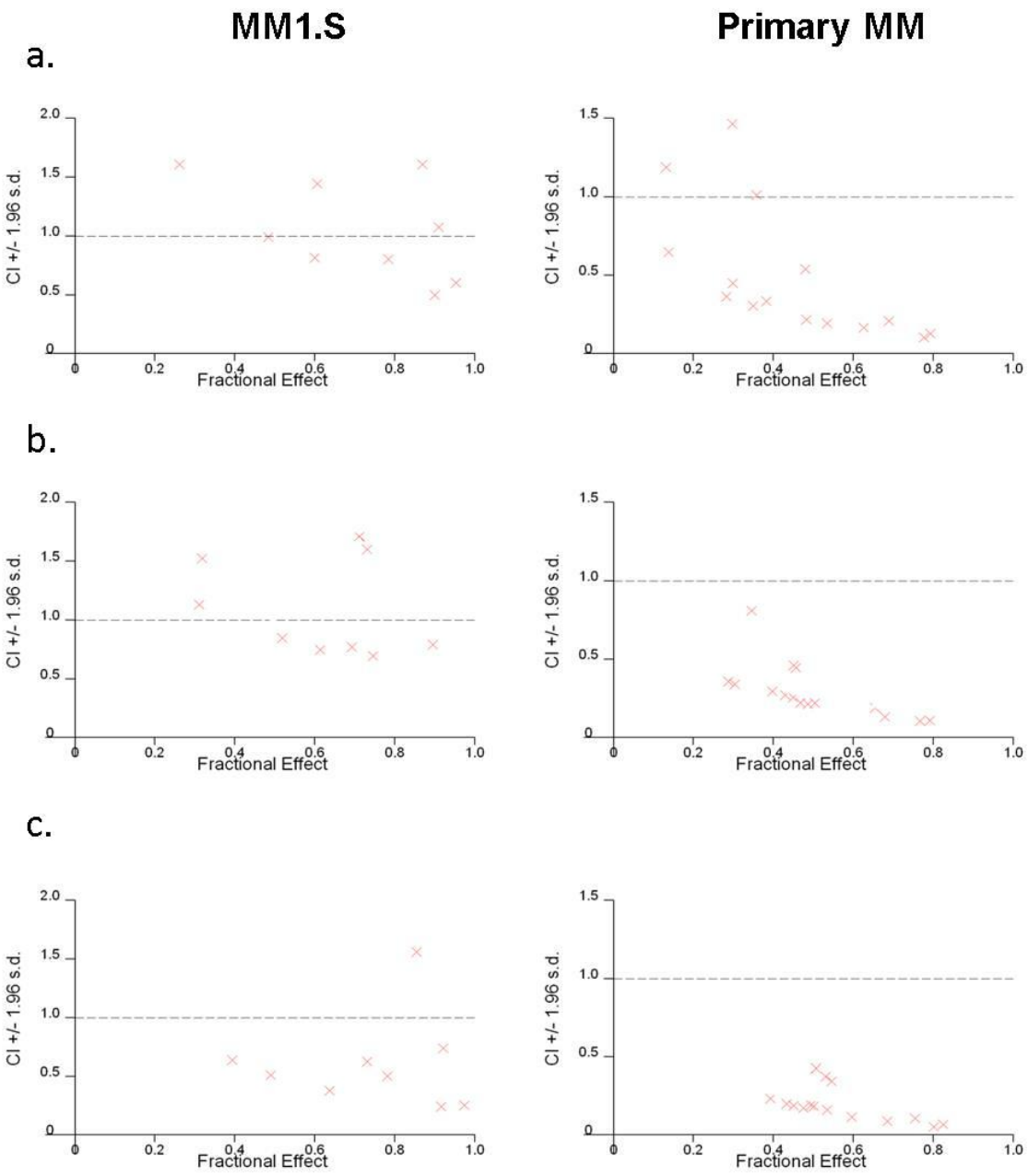

Figure 5.13 Calcusyn plots showing CI values for the combination of bortezomib (4ηM) with melphalan (1μM, 10μM and 100μM) in MM1.S and in primary MM samples. Cells were cultured in the HS-5 system for 24hrs and exposed to drugs for an additional 48hrs. Three schedules were investigated (a) simultaneous exposure, (b) bortezomib pre-treatment followed by melphalan and (c) melphalan pre-treatment followed by bortezomib. Viability was determined using the guava Viacount assay and data points show CI values of 3 independent experiments for MM1.S and 5 separate primary MM samples. Dashed line is the line of additivity at CI=1. CI<1 indicates synergism and CI>1 indicates antagonism.

Calcusyn analysis was performed to formally evaluate the interaction between the two drugs (figure 5.13). For both the MM1.S and primary MM samples, synergistic cytotoxicity (indicated by CI values <1) was generated with schedule 3 as shown in figure 5.13c. Primary MM cells displayed additive to synergistic interactions with the other administration schedules and in MM1.S cells mostly additive interactions were observed (figures 5.13a and b). The combinations became more synergistic at lower concentrations of melphalan (1μM and 10μM) as these were associated with lower CI values, shown in table 5.2 below.

Table 5.2 Combination index (CI) values for MM1.S and 5 primary MM samples cultured in the HS-5 system and treated with the combination of bortezomib and melphalan using 3 different schedules: simultaneous exposure; bortezomib pre-exposure and melphalan pre-exposure. A fixed dose of bortezomib of 4ηM was used with increasing concentrations of melphalan. Experiments were performed in triplicate and were repeated 3 times for MM1.S and once for each of the 5 primary samples. CI values are colour coded and show that CI<1 indicates synergism, CI=1 indicates additivity and CI>1 indicates antagonism.

MM cells	Bortezomib (ηM)	Melphalan (μM)	Simultaneous exposure		Bortezomib pre-exposure		Melphalan pre-exposure	
			CI	S.D.	CI	S.D.	CI	S.D.
MM1.S	4	1	1.14	0.42	0.91	0.20	0.51	0.13
	4	10	0.92	0.48	1.00	0.46	0.46	0.20
	4	100	1.10	0.50	1.37	0.50	0.85	0.66
Primary MM (n=5)	4	1	0.35	0.18	0.25	0.09	0.18	0.04
	4	10	0.45	0.44	0.23	0.07	0.14	0.06
	4	100	0.67	0.56	0.26	0.16	0.40	0.28

>1 =1 <1

5.4.3 A novel Hsp90 inhibitor, KW-2478 retains its activity in the MM/HS-5 microenvironment model

As described in the introduction, Hsp90 inhibition leads to accumulation of mis/un-folded proteins and therefore could enhance the anti-myeloma activity of bortezomib. Previous work carried out in our group demonstrated that expression of heat shock family proteins such as Hsp90, Hsp27 and Hsp70 was associated with bortezomib resistance in lymphoma cell lines cultured in the CD40 system, and several studies have already reported synergistic anti-MM activity with combinations of Hsp90 inhibitors and bortezomib (Duus, Bahar et al. 2006; Mitsiades, Mitsiades et al. 2006; Sydor, Normant et al. 2006; Wright 2010).

Taken together, these studies provided a rationale for examination of the effects of a novel second-generation Hsp90 inhibitor, KW-2478 in our MM coculture model. The anti-tumour activity of the KW-2478 has been demonstrated in an MM xenograft model and in an orthotopic MM model (Nakashima, Ishii et al. 2010) and a phase I study of KW-2478 in combination with bortezomib in patients with relapsed and/or refractory multiple myeloma, is currently on-going. We therefore investigated its activity firstly in MM1.S cells cultured under standard culture conditions in order to determine an effective dose range in which to test the agent in primary MM samples. We then investigated the activity of KW-2478 in 10 primary MM samples cultured in the HS-5 model.

MM1.S cells were exposed to KW-2478 at 6 non-zero concentrations (0.01 – 10μM) after which changes in cell number and viability were assessed using the guava viacount assay. The effect of KW-2478 (shown in figure 5.14a) was more cytostatic than cytotoxic indicated by a lower EC_{50} value for its effect on cell number compared with cell viability (0.45μM (95% CI 0.40-0.51) vs. 2.06μM (95% CI 0.62-6.88)). In contrast to the previous studies using bortezomib and melphalan, an effect was also observed on HS-5 cells, but at the higher concentrations of 2μM and 20μM at which KW-2478 induced HS-5 cytostasis (figure 5.14b). When 10 primary MM samples were exposed to 3 increasing concentrations of KW-2478, variable effects were observed with some samples showing clear drug effects at 0.5 or 2μM KW-2478, but others

showing little or no effect on either cell viability or proliferation at 20µM KW-2478 (figure 5.15). The drug continued to show equivalent activity in primary MM cells cocultured with HS-5 cells (p values with vs. without HS-5 cells by Wilcoxon matched pairs signed ranks test 0.92 at 0.5 µM, 0.07 at 2.0 µM and 0.16 at 20.0 µM KW-2478) (figure 5.15). Importantly, no activity in normal PBMCs from healthy donors was observed at concentrations up to 10µM (see appendices).

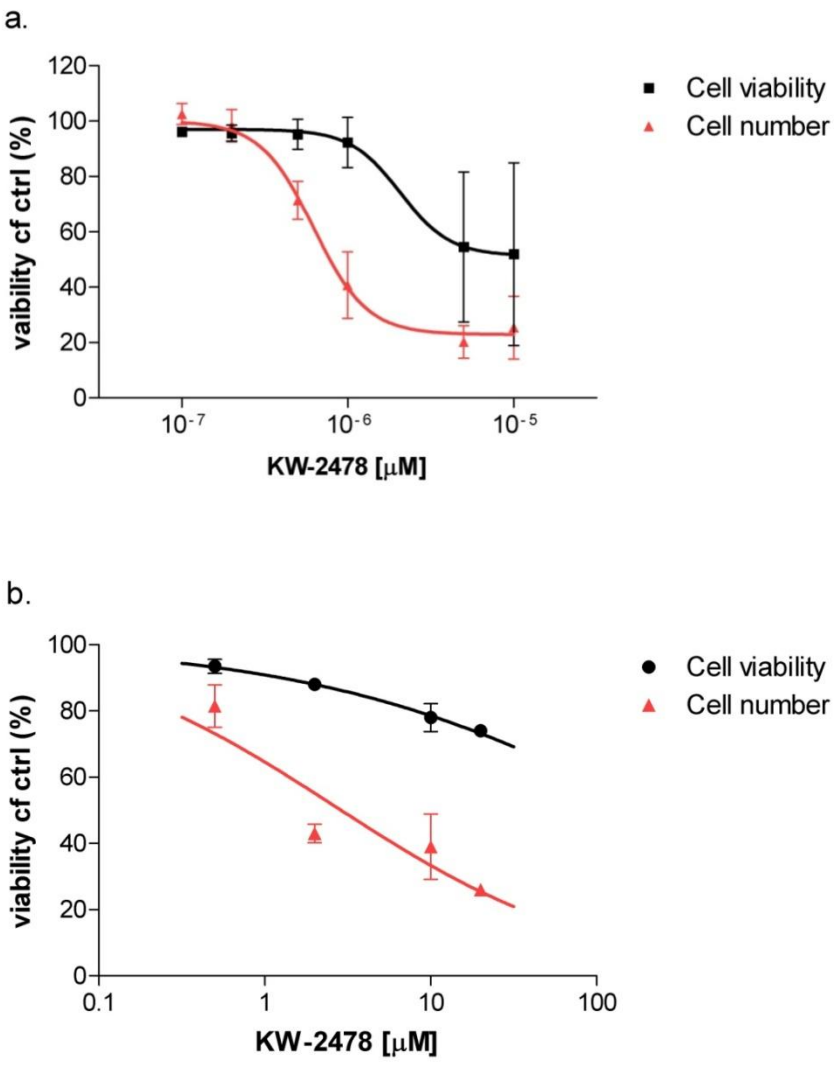

Figure 5.14 Effect of KW-2478 on cell viability and cell proliferation of (a) MM1.S cells and (b) HS-5 cells cultured in standard medium. MM1.s Cells were initially cultured for 24hrs prior to the addition of drug at varying concentrations (0.01µM to 10µM) for a further 48hrs. The guava Viacount assay was used to calculate cell viability and proliferation and these are represented as a % of control values. Results show the mean ± S.D. from 3 independent experiments conducted in triplicate.

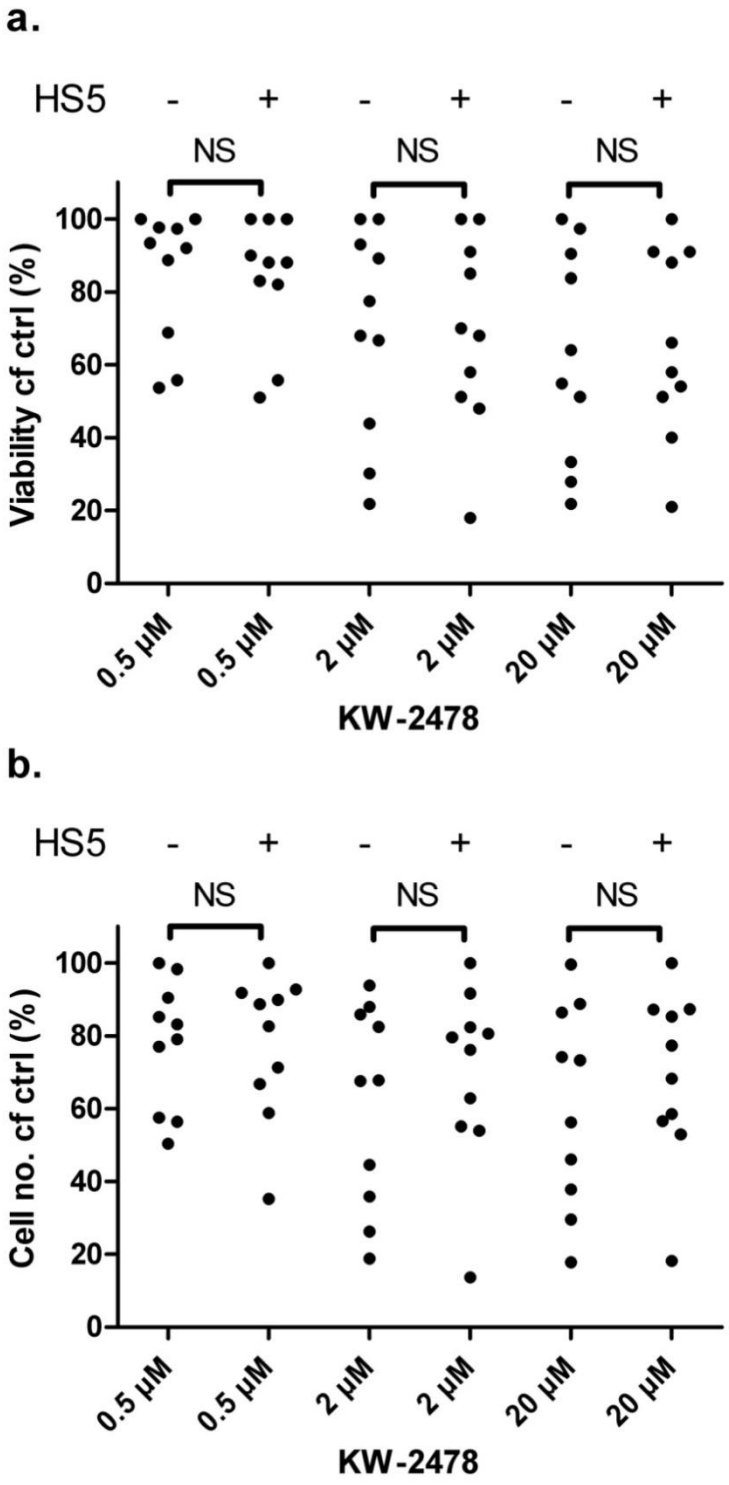

Figure 5.15 Effect of KW-2478 on (a) cell viability and (b) cell number in primary MM samples cultured in standard medium or in the HS-5 microenvironment model. Cells were cultured either with or without HS-5 cells for 24hrs prior to the addition of drug at 0.5µM, 2µM and 20µM for a further 48hrs. The guava Viacount assay was used to calculate cell viability and proliferation represented as a % of control values. Experiments were conducted once in each of 10 primary MM samples.

5.4.5 Treatment with KW-2478 was associated with inhibition of its client proteins and in the induction of apoptosis in MM1.S cells

In order to assess the molecular consequences of Hsp90 inhibition in MM1.S cells, we performed western blotting analysis to identify changes in proteins stabilised by this molecular chaperone, specifically: Akt, ERK1/2 and the IGF-1 receptor. We chose these proteins as they are involved in key proliferative signalling pathways (PI3K/Akt and MAPK) in MM (described in chapter 1.5). We also investigated changes induced by KW-2478 in expression of the apoptotic protein caspase-3 and in the phases of the cell cycle. We also probed for changes in the Hsp90 co-chaperone, Hsp70, as its activation is an indicator of the cellular stress response to Hsp90 inhibition, and this was observed in the lymphoma studies referred to above. For these experiments, protein lysates and total protein extracts were prepared from MM1.S cells before and after treatment with varying concentrations of KW-2478 from 0.1μM to 10μM for 24hrs (figure 5.16). The cell cycle distribution of MM1.S was determined following 48hrs of treatment with similar drug doses from 0.1μM to 5μM (figure 5.17).

We observed detectable effects of Hsp90 inhibition on the client proteins ERK1/2, Akt and IGF-1 after 24hrs in MM1.S cells. Starting at concentrations of KW-2478 as low as 0.1μM (figure 5.16), expression of these proteins decreased in a dose-dependent manner suggesting their degradation. The most striking observation was a strong upregulation in Hsp70 expression, indicating clear inhibition of Hsp90 starting from 0.5μM (figure 5.16). Results also showed a dose-dependent decrease in caspase-3 (indicative of its cleavage) which implied an induction of apoptosis. This was confirmed via examination of the cell cycle distribution of MM1.S cells shown in figure 5.17, where we noted a dose-dependent increase in the sub-G1 (or apoptotic) fraction. This was reflected in a subsequent decrease in other phases of the cell cycle.

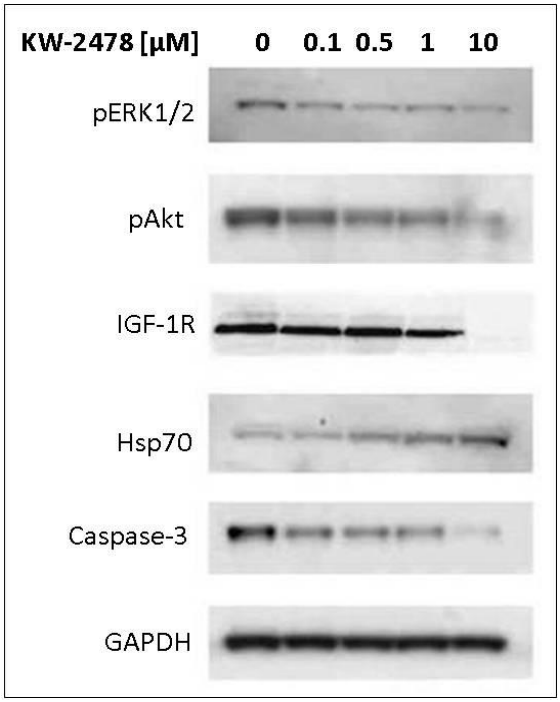

Figure 5.16 Example of the effect of KW-2478 on changes in protein expression in MM1.S cells following a 24hr exposure. 20µg of whole cell lysates were prepared and subjected to a 4%-12% NuPAGE gel electrophoresis. PVDF membranes were probed for phosphorylated and total proteins as detailed in chapter 2.11.

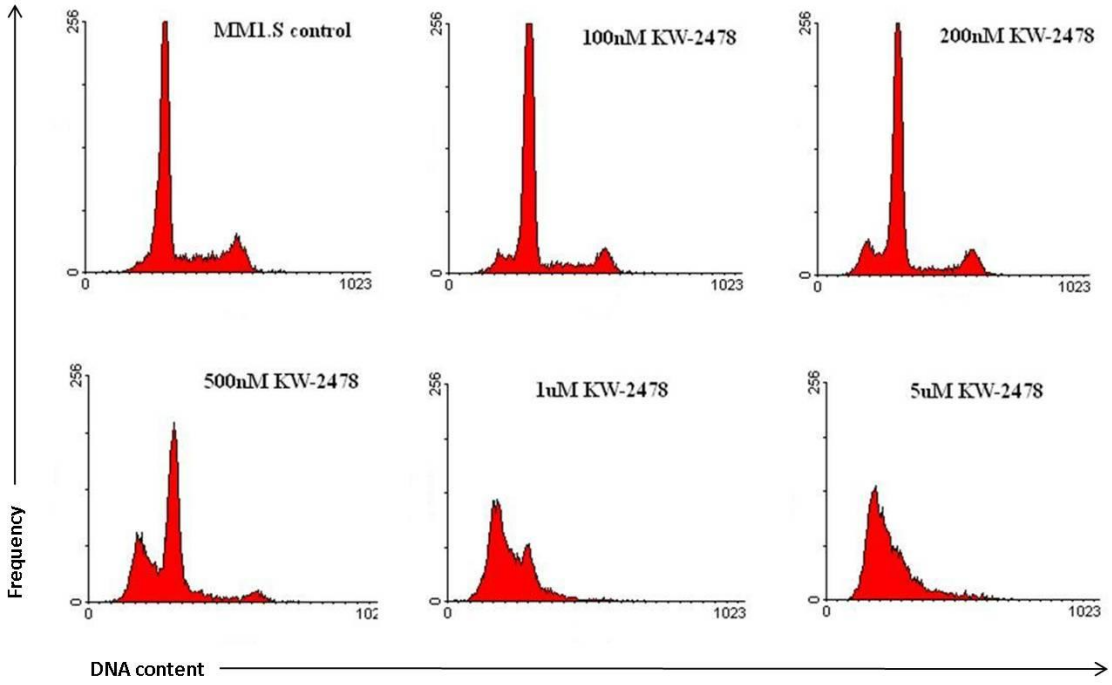

Figure 5.17 Example of the effect of increasing concentrations of KW-2478 (100ηM to 5µM) on the cell cycle distribution of MM1.S cell cultured in standard medium.

5.4.6 Treatment with KW-2478 was associated with inhibition of Akt and the activation of Hsp70 in primary MM cells

In a similar series of experiments, we now assessed changes in Hsp70 after exposure to KW-2478 (at 0.5, 5 and 10µM) in 4 of the 10 primary MM samples previously studied. These 4 samples were those with a sufficient number of cells remaining to extract enough lysate for immunoblotting experiments. In agreement with results from the MM1.S experiments, all samples studied showed a decrease in Akt activation (shown by a dose-dependent decrease in phosphorylated Akt), and a marked increase in Hsp70 expression after 24hrs exposure to KW-2478 (at concentrations as low as 0.5µM, figure 5.18). A decrease in an Hsp90 client protein was also apparent in each sample, in some samples showing a concentration dependent effect up to 10µM KW-2478, even if the Hsp70 response was maximal at 0.5µM KW-2478. We would have liked to increase the number of primary samples studied but were limited by the availability of sample. Nonetheless, it is noteworthy that the clearest decrease in an Hsp90 client protein was seen in the most sensitive sample (% viability at 2µM KW-2478 of 19% (#4)) with a minimal decrease in the least sensitive sample (86% (#1)). Viability in the remaining samples at 2µM were 45% (#2) and 82% (#3).

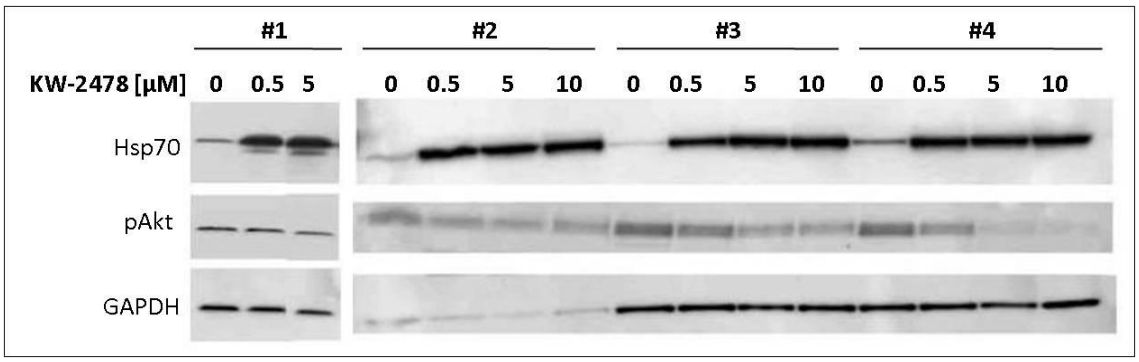

Figure 5.18 Effect of KW-2478 on protein expression in 4 primary MM samples following 24hrs exposure. 40µg of whole cell lysates were prepared and subjected to a 4%-12% NuPAGE gel electrophoresis and immunoblotting. Cells were probed for phospho-Akt, Hsp70 and GAPDH as a loading control.

5.5 KW-2478 in combination with bortezomib and with melphalan

5.5.1 KW-2478 sensitises some primary MM cells to the effects of bortezomib

We next assessed the effect of Hsp90 inhibition combined with proteasome inhibition (using bortezomib), in our panel of 10 primary MM samples. As already mentioned, interruption of Hsp90 chaperoning activity and inhibition of the proteasome are both mechanisms leading to accumulation of mis/un-folded proteins in myeloma cells. Therefore, it is logical to assume that the activity of bortezomib may be enhanced by its combination with Hsp90 inhibitors (Hsp90i). Furthermore, as bortezomib has been associated with stimulation of the cytoprotective ER stress response, its combination with Hsp90 inhibition could potentially lead to a synergistic interaction.

For these experiments, we evaluated the effects of 1 and 2μM KW-2478 combined with 3 or 6ηM bortezomib on the viability of the 10 primary samples cocultured in the MM/HS-5 model. Results showed that KW-2478 significantly increased the activity of bortezomib, at all the combinations studies except at the lowest doses of each drug i.e. 1μM KW-2478 with 3ηM bortezomib (figure 5.19). It is noteworthy that whilst an overall synergistic effect was demonstrated in the 10 samples studied, not all primary samples showed an increased effect with the combinations, an observation most apparent in several samples at 3ηM bortezomib (figure 5.19).

In order to more formally evaluate the interaction between the two drugs, calcusyn analysis was performed. Results shown in figure 5.20 suggests that the combinations produced a synergistic response in 5 out of 10 samples (#7, #8, #12, #31 and #39), an additive response in 3 samples shown in figure 5.21a (#5, #32 and #34) and antagonism in 2 samples shown in figure 5.21b (#2 and #33). There were no obvious correlations between response of the samples to the combinations and their sensitivity to bortezomib or KW-2478.

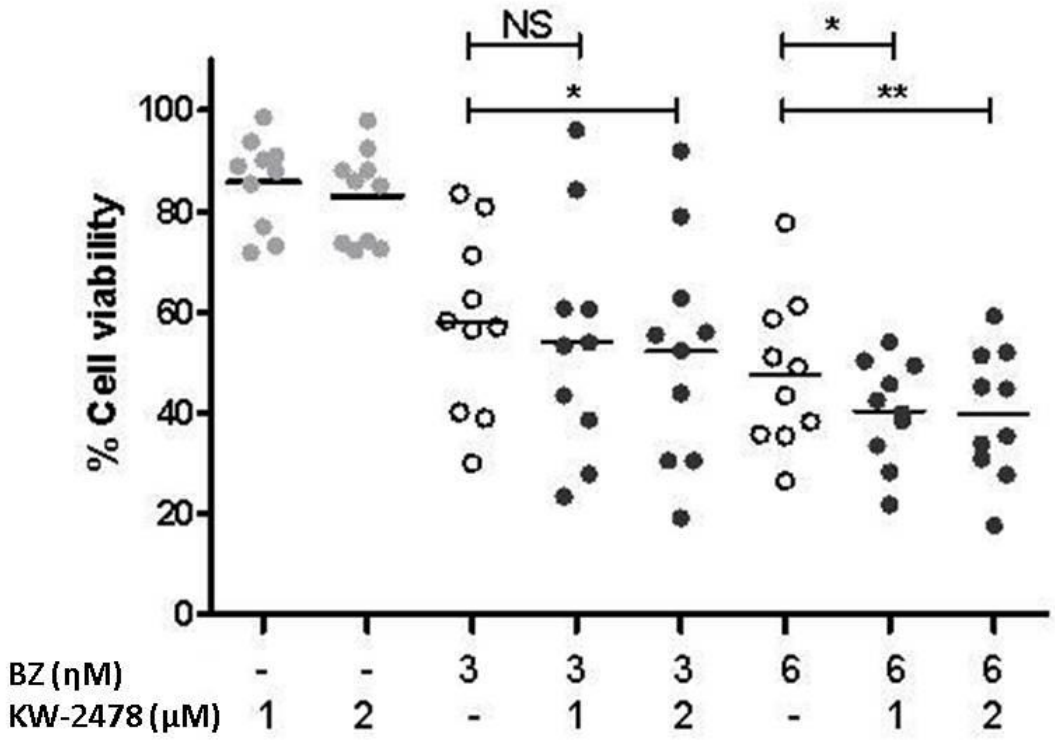

Figure 5.19 Effect of the simultaneous combination of KW-2478 (1 and 2μM) with bortezomib (3 and 6ηM) in 10 primary MM samples cultured in the HS-5 model.MM cells were cocultured with HS-5 cells for 24hrs and exposed to drugs for an additional 48hrs. Horizontal lines represent the mean % viability of all 10 samples. Open circles indicate individual effects of bortezomib and closed circles indicate effects of the combinations. *indicates $p<0.05$ and **indicates $p<0.01$ using the paired t-test.

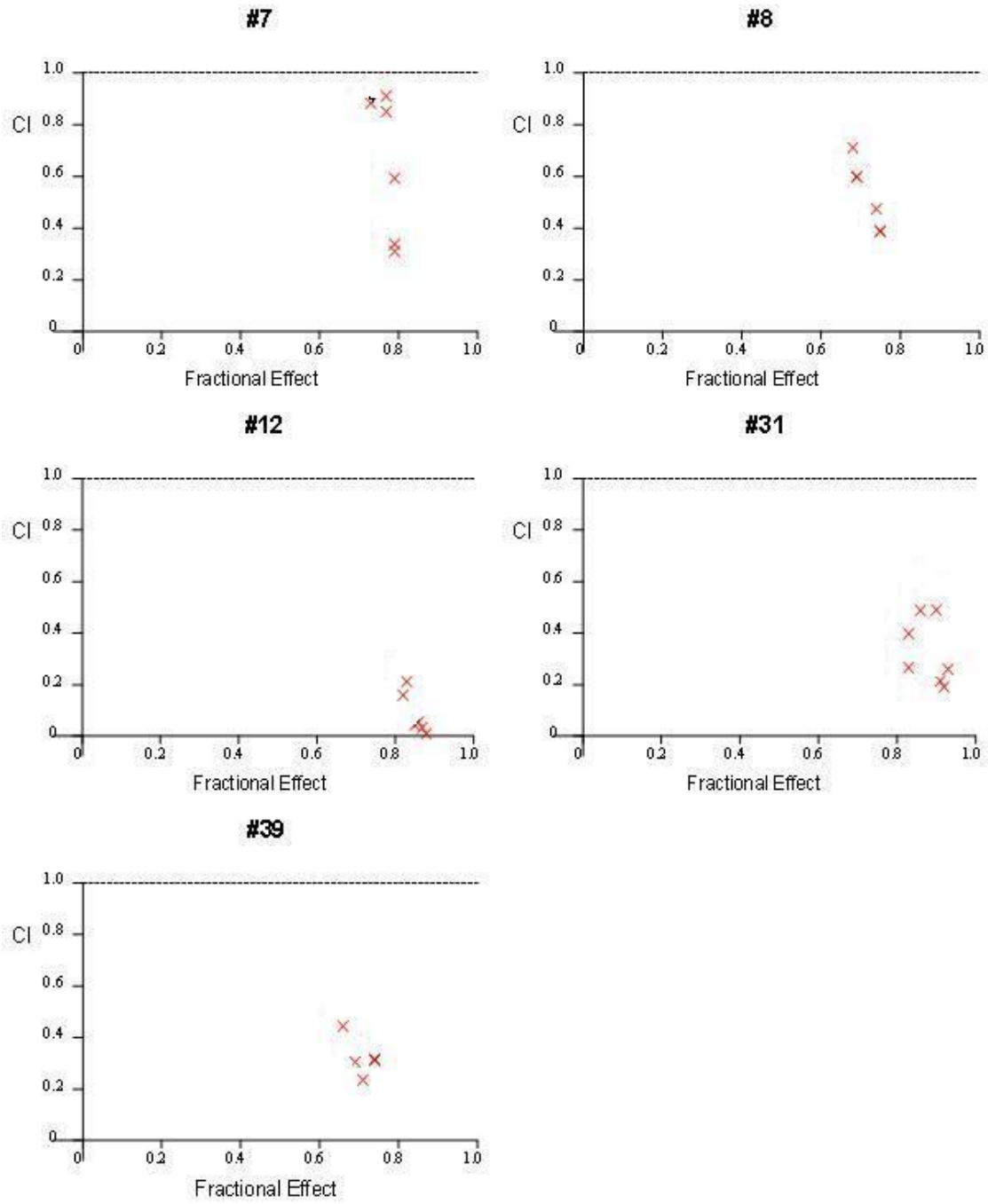

Figure 5.20 Calcusyn analysis of the simultaneous combination of KW-2478 (1 and 2µM) with bortezomib (3 and 6ηM) in 5 primary MM samples where synergy was observed (CI values <1). Samples were cultured in the HS-5 model and treated for 48hrs with both drugs. Data (x) depicted as the fraction of cells affected compared to untreated controls and shows 4 combinations (and 2 replicates for some samples). Dashed line is the line of additivity at CI=1. CI>1 indicates antagonism.

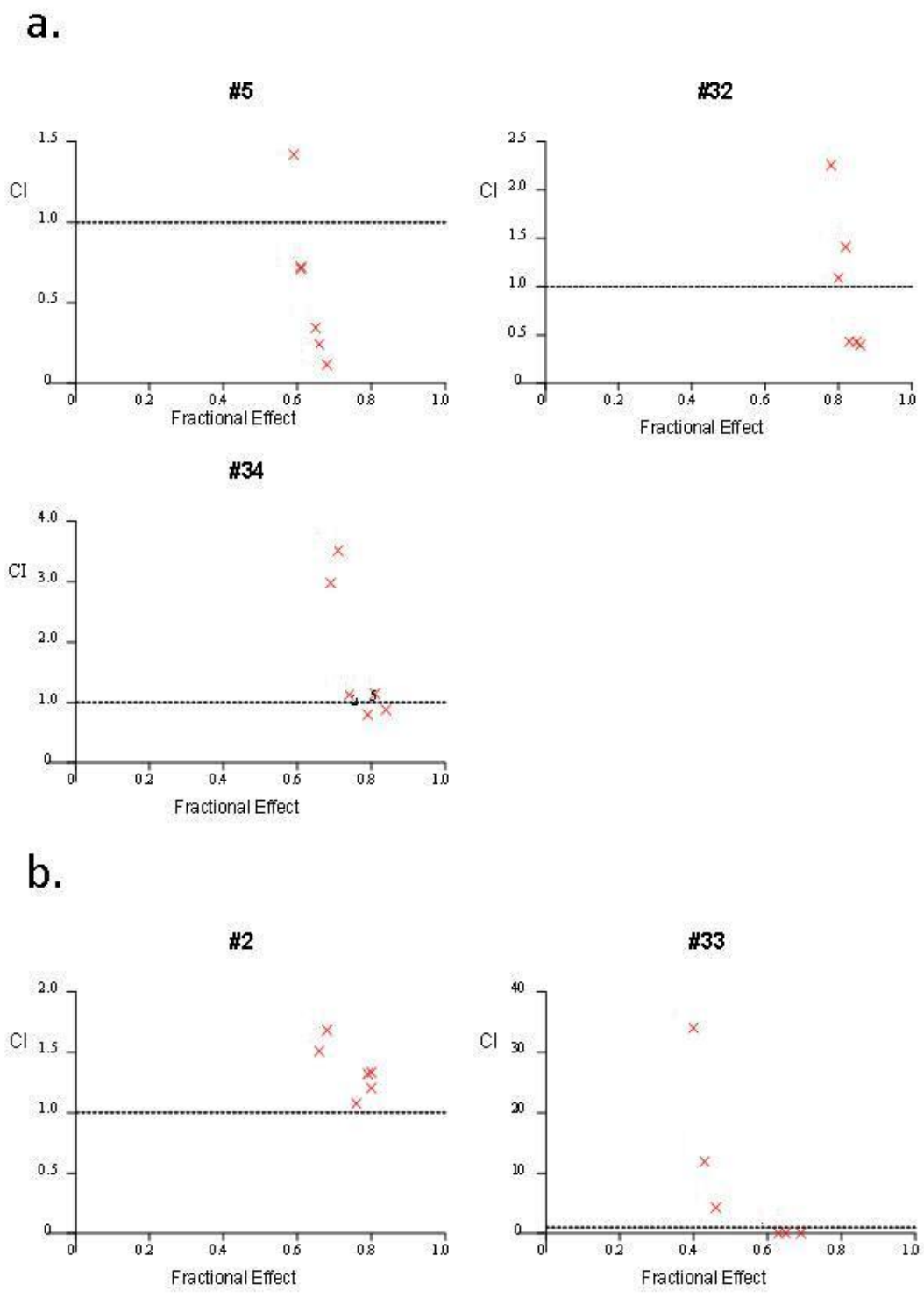

Figure 5.21 Calcusyn analysis of the simultaneous combination of KW-2478 (1 and 2μM) with bortezomib (3 and 6ηM) a. 3 primary MM samples where additivity was observed (CI values =1) and in b. 2 samples where antagonism was observed (CI values>1). Samples were cultured in the HS-5 model and treated for 48hrs with both drugs. Data (x) depicted as the fraction of cells affected compared to untreated controls and 4 combinations (some samples with 2 replicates). Dashed line is the line of additivity at CI=1.

5.5.2 KW-2478 is more effective at sensitising primary MM cells to the effects of melphalan

Given the results produced with the melphalan – bortezomib combinations presented in section 5.4.2, we next investigated the anti-MM activity of the combination of melphalan with KW-2478 in our panel of 10 primary MM samples cultured in the HS-5 model.

Results showed that treatment with KW-2478 (1 and 2μM) increased the activity of melphalan (1 or 10μM), an effect that was statistically significant in all combinations studied shown in figure 5.22. Importantly, and in contrast to results with the KW-2478 – bortezomib combinations, all primary samples showed an increased effect with the KW-2478 – melphalan combinations and this was most apparent at 2μM melphalan (combined with the equivalent concentration of KW-2478 shown in figure 5.22).

When calcusyn analyses was applied to the data, the combination of KW-2478 with melphalan resulted in a predominantly synergistic interaction in 7 of the 10 primary MM samples (figure 5.23 overall CI <0.75) and additivity in the remaining 3 samples (#5, #8 and #39) (figure 5.24 overall CI 0.75-1.25). Notably, no antagonism was observed in any samples and in several samples a marked synergistic effect was observed (figure 5.23).

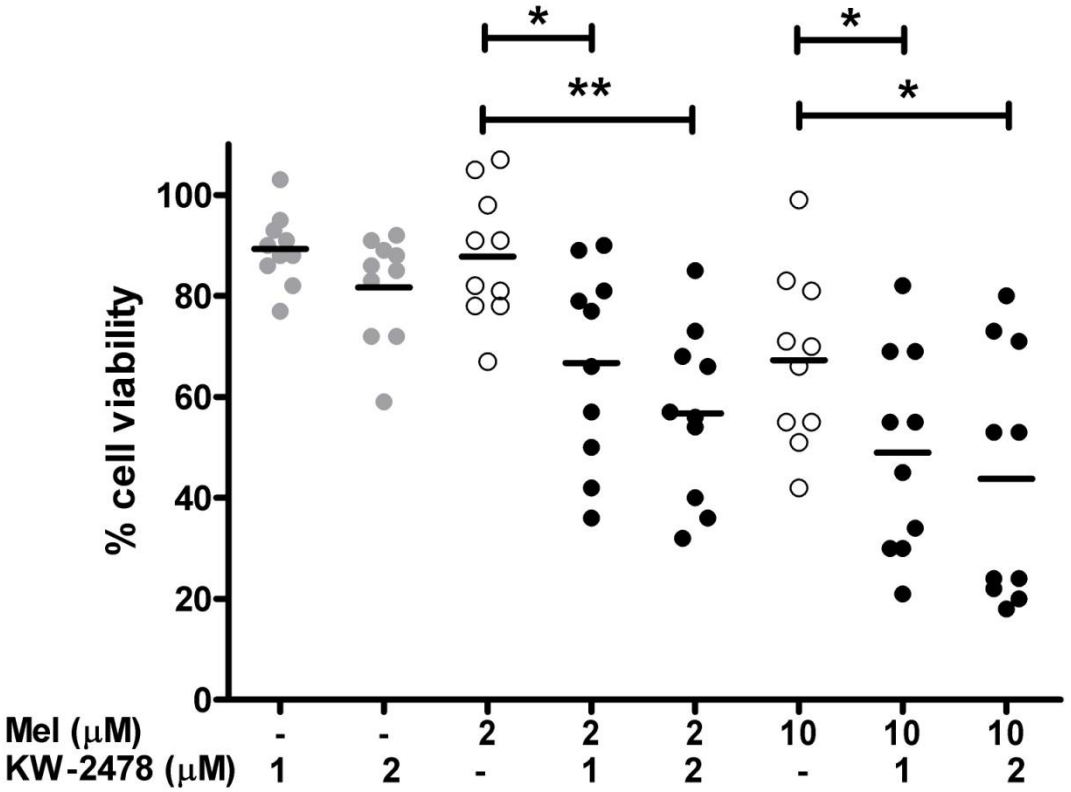

Figure 5.22 Effect of the simultaneous combination of KW-2478 (1 and 2μM) with melphalan (2 and 10μM) in 10 primary MM samples cultured in the HS-5 model. MM cells were cocultured with HS-5 cells for 24hrs and exposed to drugs for an additional 48hrs. Horizontal lines represent the mean % viability of all 10 samples. Open circles indicate individual effects of melphalan and closed circles indicate effects of the combinations. *indicates $p<0.05$ and **indicates $p<0.01$ using the paired t-test.

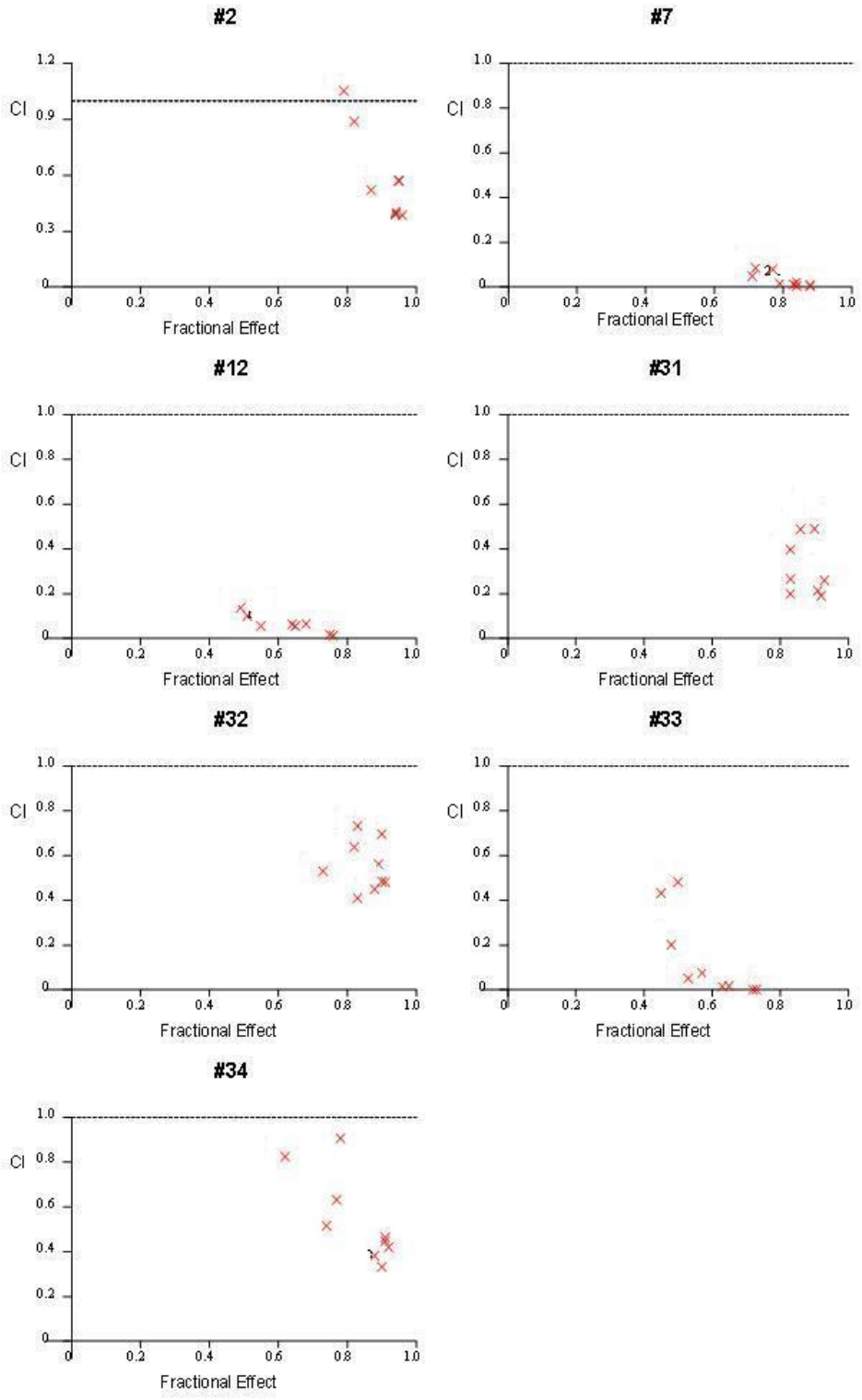

Figure 5.23 Calcusyn analysis of the simultaneous combination of KW-2478 (1 and 2µM) with melphalan (2 and 10µM) in 7 primary MM samples where synergy was observed (CI values<1). Samples were cultured in the HS-5 model after treatment with both drugs for 48hrs. Data (x) depicted as the fraction of cells affected compared to untreated controls and shows 4 combinations and 2 replicates. Dashed line is the line of additivity at CI=1. CI>1 indicates antagonism.

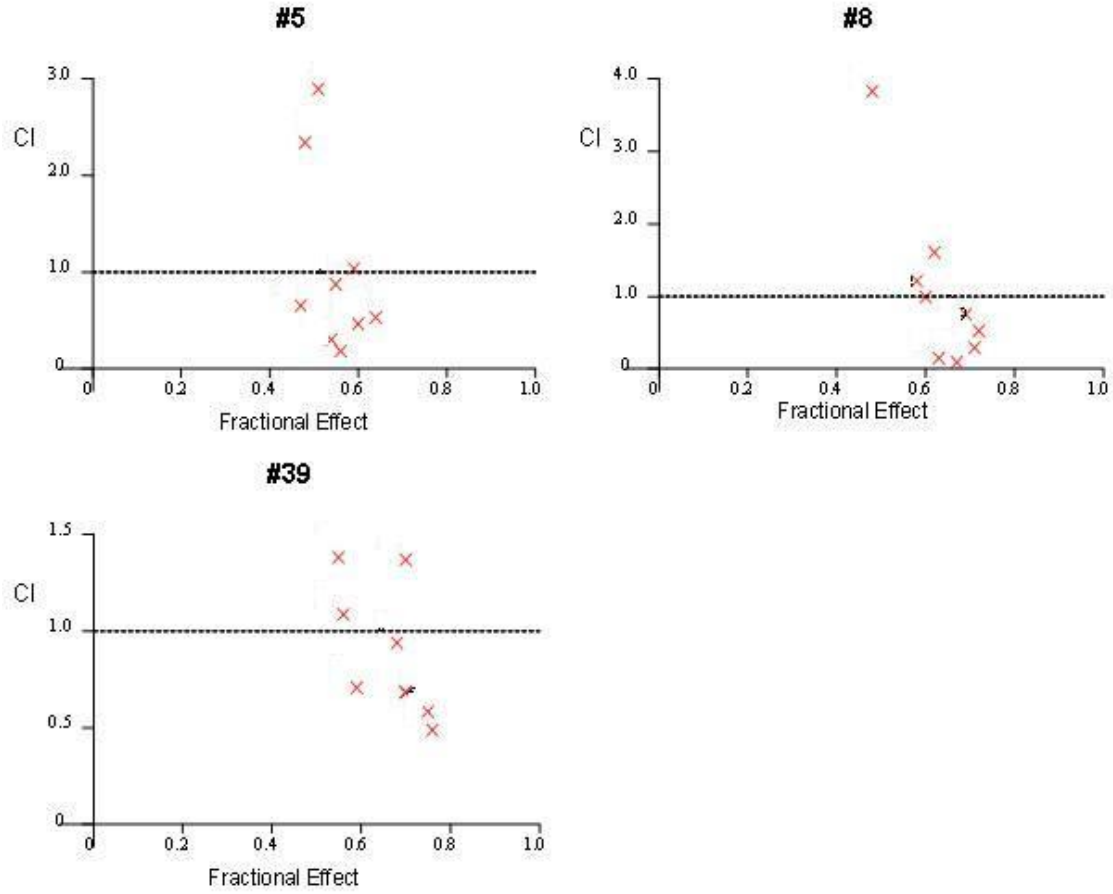

Figure 5.24 Calcusyn analysis of the simultaneous combination of KW-2478 (1 and 2µM) with melphalan (2 and 10µM) in 3 primary MM samples where additivity was observed (CI values=1). Samples were cultured in the HS-5 model after treatment with both drugs for 48hrs. Data (x) is depicted as the fraction of cells affected compared to untreated controls and shows 4 combinations and 2 replicates. Dashed line is the line of additivity at CI=1. CI<1 indicates synergy and CI>1 indicates antagonism.

5.6 Discussion

The first aim of this part of the project was to validate a method for the *in vitro/ex vivo* culture of patient-derived MM cells. This was initially conducted in 3 commonly used HMCLs and in 3 primary MM samples, cultured either in the CD40 model (used previously in chapters 2 and 3) or in a MM/HS-5 coculture model, using 2 different cell viability assays to assess effects on MM cell growth. Results indicated that the guava viacount assay was superior to the ATP assay as it was a more reliable measure of cell growth compared with the ATP assay and it provided information not only on cell viability but also on cell proliferation. A second important finding was that coculture with HS-5 stroma protected primary MM cells from spontaneous apoptosis ($p<0.001$, n=16 samples) and this was associated with an increase in cell proliferation ($p<0.01$). Based on these findings, we were able to standardise our MM model by selecting an endpoint assay (the guava viacount assay) and a reproducible method of growing MM cells in a 2-dimentional stromal coculture model.

CD40 stimulation in our MM cells did not result in cell growth in contrast to its growth-promoting effect in our NHL coculture model (chapters 3 and 4). This was surprising given that CD40 is expressed at high levels on the surface of MM cells (Pellat-Deceunynck, Bataille et al. 1994) where its activation is known to induce MM cell proliferation and migration (via PI3K/AKT and NFκB signaling pathways and secretion of IL-6 and VEGF from BMSCs (Urashima, Chauhan et al. 1995; Tai, Podar et al. 2003)). Although some increases in cell viability upon CD40 stimulation was observed, this did not reach statistical significance and it is possible that increasing the sample size may have increased the significance of these results. Unfortunately we were unable to answer this question in more primary cells due to limited sample availability.

Of note, varying effects of CD40 stimulation in patient-derived MM cells has been reported in the literature and appears to be associated with their TP53 mutation status: in the absence of wtp53-like activity cells proliferate however, in the presence of functional wt-like p53 activity, cells undergo growth arrest. In support of this, RPMI

8226 cells, which have a p53 missense mutation at codon 285, have been shown to undergo cell proliferation in response to CD40 stimulation (Teoh, Tai et al. 2000). However, our studies revealed no significant effects of CD40 stimulation on HMCLs irrespective of their p53 status (U266 and MM1.S are both wtp53). Mutations in the p53 gene are detected in approximately 13% of MM patients and are specifically associated with the more advanced and clinically aggressive acute/leukaemic forms of MM (in 43% of these cases) (Neri, Baldini et al. 1993). Unfortunately, we do not have information on the p53 status of our MM samples however, 9 out of 16 were obtained from patients with aggressive/late stage disease, thus potentially a quarter of our samples should respond to CD40. As we investigated the effects of CD40 stimulation in just 3 samples, we are unable to arrive at a firm conclusion regarding CD40-mediated MM cell growth based on these results.

In contrast, the majority of samples responded to HS-5 stimulation, thus supporting our use of stromal cell coculture in our MM model. The rationale for investigating BMSCs in a MM primary culture model is that they are well known to provide growth signals produced in the *in vivo* BMM (as explained in the introduction and in detail in chapter 1.4.2). Furthermore, adhesion to HS-5 cells (via expression of fibronectin; collagen types I, III and IV and vascular cellular adhesion molecule (VCAM-1) leads to cell proliferation via secretion of proinflammatory cytokines such as IL-6 (Uchiyama, Barut et al. 1993; Torok-Storb, Iwata et al. 1999). The net result is the emergence of CAM-DR and resistance to FAS-mediated cell death (Dalton 2002; Shain, Landowski et al. 2002). Therefore, use of a model incorporating effects mediated by BMSCs would allow us to examine the effects of microenvironment-induced resistance to commonly used cytotoxics and to novel therapies.

Bortezomib has already been shown to retain its cytotoxicity in MM cells cultured in the presence of BMSCs (Hideshima, Richardson et al. 2001) whereas the effects of dexamethasone are abrogated (Chauhan, Pandey et al. 1997; Cheung and Van Ness 2001; Frassanito, Cusmai et al. 2001). Furthermore, RPMI 8226 cells become resistant to the effects of doxorubicin and melphalan upon adherence to fibronectin (Damiano, Cress et al. 1999). We therefore investigated bortezomib, dexamethasone and

melphalan in our MM model in order to firstly confirm these previous findings, and to secondly investigate their more effective utilisation when given in combination with each other or with novel agents such as UCL67022 (which showed potent activity in the NHL coculture model in chapter 4) and KW-2478, a novel Hsp90 inhibitor that has already demonstrated potent activity in HMCLs and efficacy in mouse models of the disease (Nakashima, Ishii et al. 2010).

In agreement with earlier studies, bortezomib was highly potent in primary MM samples when cultured in the HS-5 model. Melphalan in contrast, did not retain its activity in the presence of HS-5 stroma and this was exemplified with dexamethasone whose activity was completely abolished in both the dexamethasone-sensitive MM1.S and in primary MM cells, thus confirming the previously reported findings. In contrast, and importantly, UCL67022 retained its activity in the HS-5 stromal model and these data in addition to data produced by Dr. Rakesh Popat has been recently submitted for publication. Reassuringly, none of the drugs studied had significant effects on HS-5 BMSCs at concentrations that were toxic to MM cells, suggesting a therapeutic window.

We next investigated improving the efficacy of current treatment combinations, specifically that of bortezomib and melphalan, in our stromal/microenvironment model. This combination is clinically active in patients with MM both in the untreated and relapsed setting (San Miguel, Schlag et al. 2008; Popat, Oakervee et al. 2009) however, as complete responses are only achieved in a minority of patients with accompanying high toxicities, there is a need to optimise the schedule. Results from our combination studies (reported in a recent publication (Popat, Maharaj et al. 2012)) showed a highly synergistic effect (CI values<0.3) when primary cells were pre-treated with melphalan for 24hrs followed by bortezomib for 24hrs (total melphalan treatment of 48hrs). All of the 5 samples tested were obtained from MM patients at relapse that had not been previously treated with bortezomib. Two of these patients were subsequently treated with bortezomib and with melphalan and achieved at least a partial response, thus confirming the efficacy of this schedule in MM patients.

There is *in vitro* evidence that the schedule of bortezomib administration may be important from other published studies. Synergistic effects were seen with combinations of doxorubicin or melphalan, but with doxorubicin synergy was most marked when the cells were previously exposed to chemotherapy (Mitsiades, Mitsiades et al. 2003). In pancreatic cancer, maximal apoptosis was seen when cells were pre-incubated with gemcitabine (Fahy, Schlieman et al. 2003) and in MCL, pre-incubation with cytarabine was the more effective schedule (Weigert, Pastore et al. 2007). Furthermore, bortezomib, when administered 24hrs before high dose melphalan in the context of autologous transplantation, demonstrated increased cytotoxicity compared to bortezomib 24hrs after (Lonial and Cavenagh 2009). Therefore, other studies have demonstrated the advantages of scheduling with this combination however, detailed scheduling analysis has until now (Popat, Maharaj et al. 2012) not been investigated. Our results warrant the further clinical evaluation of the melphalan pre-treatment schedule, such synergy may allow lower drug doses to be used thus reducing treatment-related toxicities.

Additional data produced Dr. Rakesh Popat in our lab has suggested a mechanism for this schedule dependency: Melphalan induces double stranded DNA breaks following formation of inter-strand cross-links (ICLs) (Spanswick, Craddock et al. 2002). Bortezomib prevents ICL repair by inhibition of DNA protein kinases (Mitsiades, Mitsiades et al. 2003) and the Fanconi anaemia complex (Yarde, Oliveira et al. 2009). Consequently, when bortezomib administration follows melphalan, cells sustain irreversible damage leading to apoptosis. On the other hand, bortezomib pre-exposure results in the rise in anti-apoptotic molecules such as Mcl-1, Akt and heat shock proteins as a result of proteasome inhibition which may render cells more resistant to cell death and subsequently decrease the effect of melphalan administered 24hrs later (Popat, Maharaj et al. 2012).

In relating this data to the clinical setting, a limitation is that in our culture model, cells were continuously exposed to each drug whereas in an *in vivo* system, the drugs would undergo metabolism thus decreasing their bioavailability or concentration inside the cells. However, these findings could have larger implications due to the high number of

clinical trials currently investigating bortezomib in combination with a variety of cytotoxic drugs, where knowledge of the optimum schedule would enable administration of the most effective therapy. For example, the combination of bortezomib, melphalan and prednisolone has been demonstrated to improve progression free survival of elderly patients with MM when compared to melphalan and prednisolone (San Miguel, Schlag et al. 2008).

The final set of experiments investigated the effects of Hsp90 inhibition in MM cells using a novel agent, KW2478. As outlined in the introduction, interruption of the chaperoning activity of Hsp90 leads to accumulation of mis/un-folded proteins in MM cells (Davenport, Moore et al. 2007). Furthermore, as Hsp90 is involved in the stabilisation of multiple client proteins involved in apoptosis and tumour angiogenesis, inhibition of Hsp-90 in MM leads to combinatorial inhibition of multiple proliferative signal transduction pathways (Mitsiades, Mitsiades et al. 2006). Therefore Hsp90 inhibition represents an attractive target in MM.

KW-2478 demonstrated potent activity in primary MM samples which was fully maintained in the presence of stromal cells. Importantly, normal PBMCs from healthy donors were not sensitive to KW-2478, although the drug did have effects on BMSCs which may explain its high activity in our model. The existence of a therapeutic window (lack of activity in normal PBMSCs) suggests that KW-2478 is likely to maintain its effect *in vivo*, and results from the on-going phase I/II clinical trial in patients with relapsed and/or refractory MM are awaited in order to confirm this hypothesis. In addition to this, we demonstrated a sensitising effect of KW-2478 to the effects of bortezomib in primary MM cells, suggesting that resistance to bortezomib can be overcome by Hsp90 inhibition with KW-2478. We propose the following mechanism for this effect based on subsequent research in our lab not reported here. Many cellular proteins are targeted for degradation in the proteasome. When combined with a proteasome inhibitor, Hsp90 inhibition can overload the protein degradation machinery and lead to accumulation of unfolded protein and consequent stress response (UPR).

This mechanism is supported by recent findings from Roue et al who demonstrated that resistance to bortezomib can be overcome by Hsp90 inhibition with IPI-504, a geldanamycin analogue (Roue, Perez-Galan et al. 2010), associated with depletion of Grp78. However, investigations into signal transduction carried out by others in the lab, showed that KW-2478 induced neither accumulation of ubiquitinated proteins nor stress response proteins such as CHOP or Grp78. Therefore, the underling mechanism mediating the effects observed may be different from those reported previously. This may be explained by a difference in drug treatment regimen; for the signal transduction studies, a 3hr pulse treatment was used whilst others used continuous treatment, therefore, mechanisms other than Grp78 inhibition or CHOP induction may be important with pulse drug treatments. These studies did however show the induction of Noxa (a BH3-only protein that is considered a key mediator of bortezomib induced apoptosis) with the KW-2478 - bortezomib combination, and this is consistent with previous findings (Qin, Ziffra et al. 2005; Gomez-Bougie, Wuilleme-Toumi et al. 2007; Wang, Mora-Jensen et al. 2009). Importantly, KW-2478 enhanced bortezomib dependent Noxa induction in a dose dependent manner, in parallel with caspase activation and apoptosis. Therefore, Noxa induction could be one of the mechanisms underlying the combinatorial effects observed and these data, including that presented in this chapter, have been reported in a recent publication (Ishii, Seike et al. 2012).

In addition, our studies demonstrated that KW-2478 dramatically increased the expression of Hsp70 both in MM1.S cells and in primary MM samples, thus confirming the inhibition of Hsp90 (as a compensatory stress response). Furthermore, this was also found in the combination studies (discussed above) in particular with a homologue of Hsp70, Hsp70B. This indicated that Hsp70B could be a surrogate biomarker to monitor the combinatorial effect, which may provide useful information in future clinical trials.

Collaboration with Kyowa Hakko Kirin Co. Ltd led to evaluation of the combination of bortezomib with KW-2478 in a NCI-H929 s.c. inoculated model and an OPM-2/GFP orthotopic model, using a twice-weekly administration schedule similar to the clinical

administration schedule of bortezomib. In both mouse models, the combination of KW-2478 and bortezomib showed beneficial activities, thus supporting and confirming our results. The enhanced anti-tumour activity observed in the OPM-2/GFP orthotopic model may be particularly informative, as this model is considered to be more relevant to the pathological condition in MM. Overall, these data provide compelling evidence for further investigation of the KW-2478 - bortezomib combination in the clinic, specifically suggesting a twice-weekly administration schedule (Ishii, Seike et al. 2012). Furthermore, the combination of another Hsp90 inhibitor, 17-AAG, and bortezomib has already been investigated in a Phase II study, and has demonstrated significant and durable responses with acceptable toxicity in patients with relapsed and refractory MM (Richardson, Badros et al. 2010). Since KW-2478 has superior physicochemical (such as lower solubility) and toxicological properties to 17-AAG, the combination of KW-2478 and bortezomib is expected to be more promising. A Phase I/II study of KW-2478 in combination with bortezomib is currently on-going in MM patients, results of which are awaited..

Given the synergy produced with the melphalan – bortezomib combinations (section 5.4.2), we next investigated the anti-MM activity of the combination of melphalan with KW-2478. As expected, synergistic effects were observed in primary samples cultured in the stromal model when exposed to low dose melphalan and KW-2478. Again, work was done in addition to that presented here, which aimed to characterise the molecular mechanism responsible for the synergy produced. Results showed that KW-2478 treatment resulted in decreases in key client proteins such as Grp78, p-Akt including total Akt, c-Raf and also one of the major receptors for growth factors in MM, IGF-1R (data now shown). Furthermore, a huge induction of Hsp70 with the melphalan - KW-2478 combination was observed; thus adding strength to this finding.

Results from a subsequent *in vivo* study (courtesy of Kyowa Hakko Kirin) demonstrated that this combination was also effective in an animal model as it resulted in an additive reduction of tumour growth compared to the animal groups that received single agents only. To further evaluate the effect of the combination *in vivo* another indicator to quantitatively monitor the progression of MM was used by measuring levels of

paraprotein M in the serum of each individual at the end of the experiment (Blade, Samson et al. 1998). This method was used as an indication of the ability of KW-2478 to cause a partial remission (PR) by reducing serum M protein levels. It was found that only the combination treatment caused a <50% reduction in the serum M protein showing that this combination gave a much better response than the single agents over 28 days in SCID mice (data currently in preparation for publication). These results collectively provide strong evidence for the further clinical evaluation of the combination of KW-2478 and melphalan in MM.

In conclusion, we have validated a method for the *ex vivo* culture of primary MM cells using the BMSC line, HS-5. This allowed us to relate *in vitro* drug activity to *in vivo* effects by mimicking the myeloma BMM. Using this model, we were able to identify an optimum schedule for the administration of the combination of bortezomib with melphalan (pre-exposure to melphalan followed by bortezomib exposure) which will hopefully be used to inform future clinical trials. Furthermore, we have also identified KW-2478 as a potent Hsp90 inhibitor which sensitises MM cells to bortezomib and melphalan both in our stromal model and in studies conducted separately using *in vivo* models of the disease. These findings suggest further evaluation of Hsp70 as a prognostic marker for the effect of Hsp90 inhibition when used in combination therapy. Given that we have now demonstrated the validity an applicability of this model in identifying new more effective therapies, we next sought to characterise the nature of the interactions occurring in our stromal/MM model. This is the focus of studies described in the next chapter.

CHAPTER 6 Investigating drug resistance in the multiple myeloma bone marrow microenvironment model

6.1 Introduction

Despite recent advances in MM therapy using dose-intensified regimens and new molecular targeted compounds such as immunomodulatory drugs (IMiDs) or proteasome inhibitors (bortezomib), the disease still remains incurable. This is due to the development of resistance to the available chemotherapeutic regimens and patients eventually die of disease progression.

In the bone marrow, both the myeloma cells and stromal cells secrete cytokines and interact through adhesion molecules, activating the stromal cells that further support the growth and survival of the myeloma cells. It has also been shown that myeloma cells in the BMM are much less sensitive to chemotherapeutic drugs (Damiano, Cress et al. 1999; Nefedova, Landowski et al. 2003). This mechanism of drug resistance is referred to as cell adhesion–mediated drug resistance (CAM-DR) and it has been shown for a variety of cancers such as MM, acute and chronic leukaemia, lymphoma, lung and breast cancer (Dalton 2003; Hazlehurst, Landowski et al. 2003). Presented in this chapter are present experiments designed to use the HS-5 model to more closely mimic the nature of MM/BMSC interactions in order to investigate the development of drug resistance caused by tumour cell adhesion in the BMM.

6.1.1 Use of an adhesion - transwell - conditioned media model to examine the impact of soluble factors on drug resistance in MM

Firstly, we aimed to investigate the relative contributions of the bone marrow stroma (HS-5 cells) and of soluble factors in the BMM (in coculture supernatants) to survival and drug resistance conferred to MM cells in our coculture model. In order to achieve this aim, we designed 3 different culture platforms: MM cells cocultured in direct contact with HS-5 monolayers (direct adhesion model); or MM cells separated from stroma by a 0.4µm-thick micropore membrane that interrupts cell-to-cell contact but

allows the passage of culture medium (transwell model (TM)); or MM cells cultured in medium harvested from 14-day HS-5 cultures (conditioned medium model (CM)).

As a measure of cell viability in these experiments we used a double staining propidium iodide (PI)/CD38 technique coupled with flow cytometry. PI was used as the viability stain and CD38 was used as a MM-specific surface marker. CD38 is the most characteristic and specific surface marker for MM cells, which importantly is not expressed on HS-5 cells (Roecklein and Torok-Storb 1995). Thus, CD38/PI double staining is able to specifically distinguish the MM cells in a mixed sample containing MM and HS-5 cells.

For these experiments we focused our drug studies on bortezomib and melphalan and their simultaneous combination (present in the previous chapter and in our recent publication (Popat, Maharaj et al. 2012)). These drugs were used to validate the models used here and to correlate results with those produced using the original guava adhesion model presented in chapter 5.

6.1.2 Investigating signal transduction associated with drug resistance in the MM/HS-5 model

As mentioned above, our MM/HS-5 coculture model allows us to study cell adhesion-mediated drug resistance in MM. This begins with an alteration in the activation of intracellular signalling pathways, for example, MM cells have been shown to become independent of the IL-6/STAT-3 pathway in the presence of BMSCs (Chatterjee, Honemann et al. 2002). It is important to note that the biological consequences of adhesion of MM cells to either BMSCs or to extracellular matrix (ECM) proteins such as integrins or fibronectin can differ greatly as they interact with different groups of receptors and ligands. For example, CAM-DR can occur in response to MM cell adhesion to cell surface integrins, resulting in activation of the HMG-CoA/GG-PP/Rho/Rho-kinase pathway; which can be therapeutically targeted (Schmidmaier, Baumann et al. 2004).

We therefore focused our studies on three signal transduction pathways that are important in MM/BMSC interactions, all of which are induced by stimulation of the IL-6 receptor (IL-6R/gp180). These are: 1) the jun-activated kinase (JAK) pathway, which activates STAT-3 and to a lesser extent STAT-1 (Catlett-Falcone, Landowski et al. 1999); 2) the phosphatidyl 3-kinase (PI3K)/Akt pathway that leads to NFκB, forkhead (FKHR) and GSK-3β activation (Tu, Gardner et al. 2000; Hideshima, Nakamura et al. 2001); and 3) the mitogen-activated protein kinase (MAPK) pathway (Nishimoto, Shima et al. 1997; Heinrich, Behrmann et al. 1998; Hirano, Ishihara et al. 2000).

The MAPK pathway has also been implicated in conferring resistance to bortezomib and dexamethasone (Yasui, Hideshima et al. 2007) and we therefore investigated the effects of these drugs on signal transduction in our model. To add to our initial investigations on the activity of melphalan and UCL67022 in MM, (refer to chapter 5) we now studied their effects on these intracellular signalling pathways. For these experiments we used MM1.S and primary MM cells cultured in the presence or absence of BMSCs.

6.1.3 Profiling cytokines produced in the MM/HS-5 model and investigating their modulation by bortezomib and melphalan

The IMiDs thalidomide, lenalidomide and bortezomib have been shown to reduce secretion of vascular endothelial growth factor (VEGF) and IL-6 in MM/BMSC cocultures, which may lead to a reduction in tumour angiogenesis and drug resistance (Gupta, Treon et al. 2001; Hideshima, Richardson et al. 2001). Based on these observations, we next sought to investigate the effects of bortezomib, melphalan and UCL67022 on soluble factors secreted in our MM/BMSC coculture model.

On reviewing the current literature, we restricted study to a list of 5 pro-inflammatory cytokines, osteoclastogenic and angiogenic factors that we could investigate in cytokine profiling experiments. These were: interleukin-6 (IL-6), interleukin-8 (IL-8), and the soluble receptor for IL-6 (sIL-6R); macrophage inhibitory protein-1alpha (MIP-1α) and VEGF. These factors are implicated in contributing to a favourable pathologic microenvironment protecting MM cells from chemotherapy (as discussed in chapter 1

section 1.5 and 1.6.). For these experiments, supernatants from drug-treated cocultures were harvested and used in a customised Meso Scale Discovery® (MSD), ELISA-based assay; details of which are described further in this chapter and in chapter 2.13.1 and figure 2.3.

6.1.4 Investigating cytokine neutralisation in the MM/HS-5 model

In a final set of experiments we aimed to further test the theory that soluble factors play a role in resistance to chemotherapy. We did this by examining the effect of cytokine neutralisation on drug response in MM/HS-5 cocultures. The cytokines targeted in these experiments were based on results from the experiments outlined above.

6.2 Direct adhesion or soluble factor-mediated drug resistance

6.2.1 A CD38/PI flow cytometry method can be successfully used to quantify MM cell growth in the MM/HS-5 model

The double staining CD38/PI flow technique allowed MM cells in MM/HS-5 cocultures to be easily distinguished from HS-5 stroma and this is demonstrated by an example of the gating strategy employed during the flow analysis shown in figure 6.1. HS-5 cells were observed as the larger cell population depicted in the forward scatter versus side scatter graphs (figure 6.1). Use of a CD38 negative IgG1 isotype control antibody allowed the determination of the relative CD38 positivity of all cells contained in the sample and PI positivity was calculated relative to untreated control samples. HS-5 cells were consistently CD38 negative, as indicated by less than 5% of them staining positive for CD38 which was similar to that of the negative isotype control. In contrast, all MM cells tested stained positive (>90%) for CD38 thus confirming the validity of this method. We therefore continued to use it in all subsequent experiments.

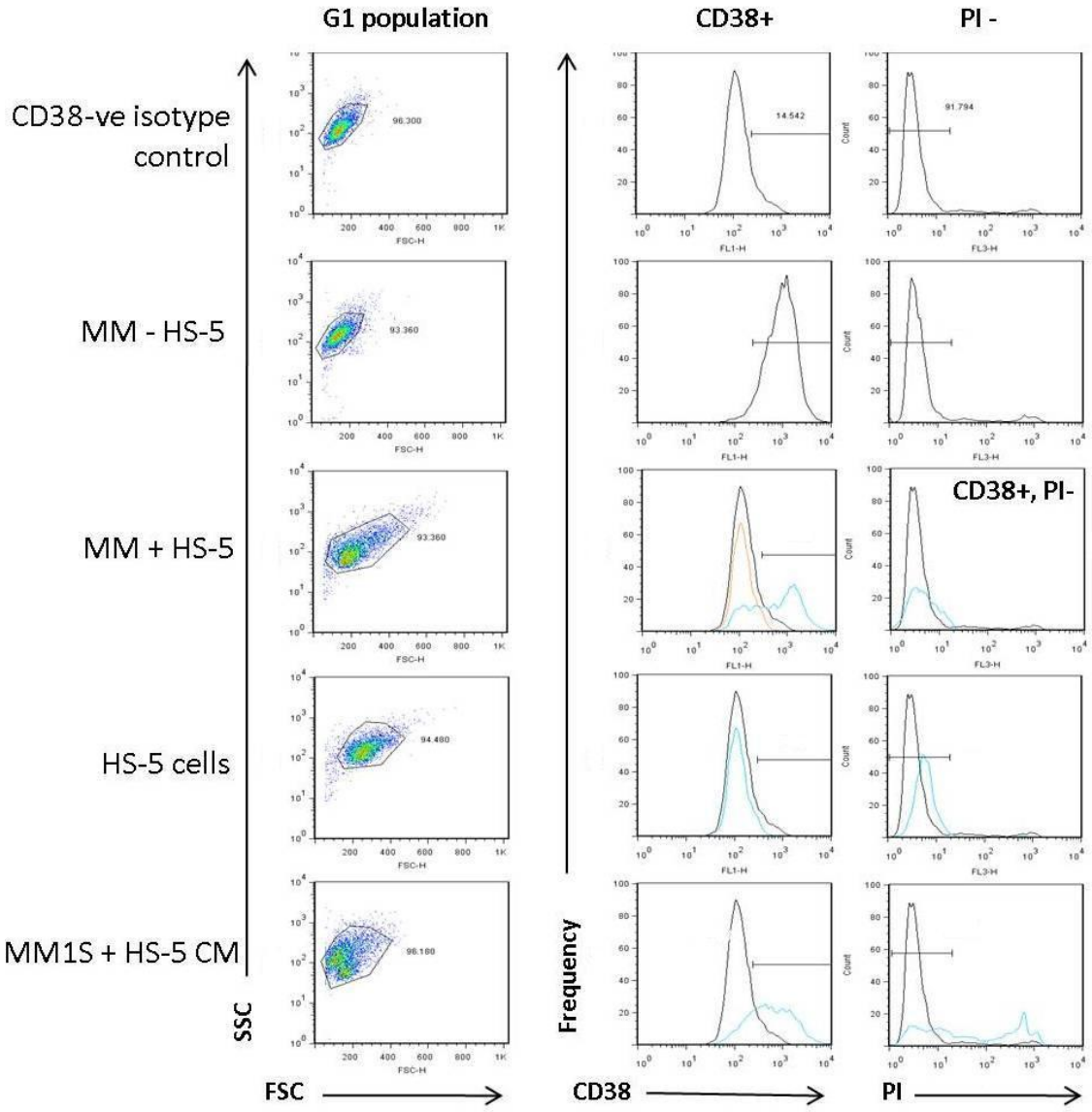

Figure 6.1 Forward scatter (FSC) and side scatter (SSC) gating of CD38/PI double-stained MM and HS-5 cells using flow cytometry.MM cells were discriminated from HS-5 cells by their strong CD38 positivity relative to its negative IgG1 isotype control. HS-5 cells were consistently CD38 negative (<95% stained positive). Viable cells were PI negative based on gating untreated control MM1.S or HS-5 cells cultured under the same conditions.

6.2.2 Soluble factors contribute to resistance of MM1.S cells to bortezomib and melphalan in the MM/HS-5 model

We used the adhesion-transwell-conditioned medium/CD38/PI models in order to firstly confirm the single agent drug activity results from the HS-5 coculture assays (presented in chapter 5) and secondly, to investigate whether activity of bortezomib and melphalan and the synergy produced by their combination was related to effects on different components of the microenvironment addressed in these models.

We used 2 doses of bortezomib (4ηM and 8ηM) and 2 doses of melphalan (10μM and 100μM) for assessment of the single agent effects and the lowest dose of each agent in three different combination schedules: simultaneous exposure to both agents (S1); bortezomib 24hrs prior to melphalan (S2) and melphalan 24hrs prior to bortezomib (S3). Cell viability was assessed via CD38/PI double staining following 48hr drug incubations. In figure 6.2 histogram plots from a representative experiment in MM1.S cells is shown and overall results are summarised in figure 6.14.

Results showed that bortezomib-induced cell death was attenuated in MM1.S cells cultured in the adhesion model ($p<0.05$), however, a dose-dependent decrease in cell viability was maintained (as shown in figure 6.3). A similar effect occurred at 4ηM bortezomib in both the TW and CM models, however in these 2 models, the effect of 8ηM bortezomib was not significantly difference between cells cultured with or without HS-5 cells (figure 6.3). This suggested that in the current model, resistance to bortezomib in MM1.S cells was mediated by direct adhesion to BMSCs and that factors present in the soluble compartment contributed to this effect. The activity of melphalan at 10μM was also attenuated in all 3 models, but the significance of this effect was greater in the TW model ($p<0.01$) and most striking in the CM model ($p<0.001$). At the higher dose of melphalan (100μM) activity was retained, however it tended to be less effective in the CM model (although this effect did not reach significance). This result may be suggestive of a greater role for soluble factors in promoting resistance to melphalan compared to bortezomib in MM1.S cells.

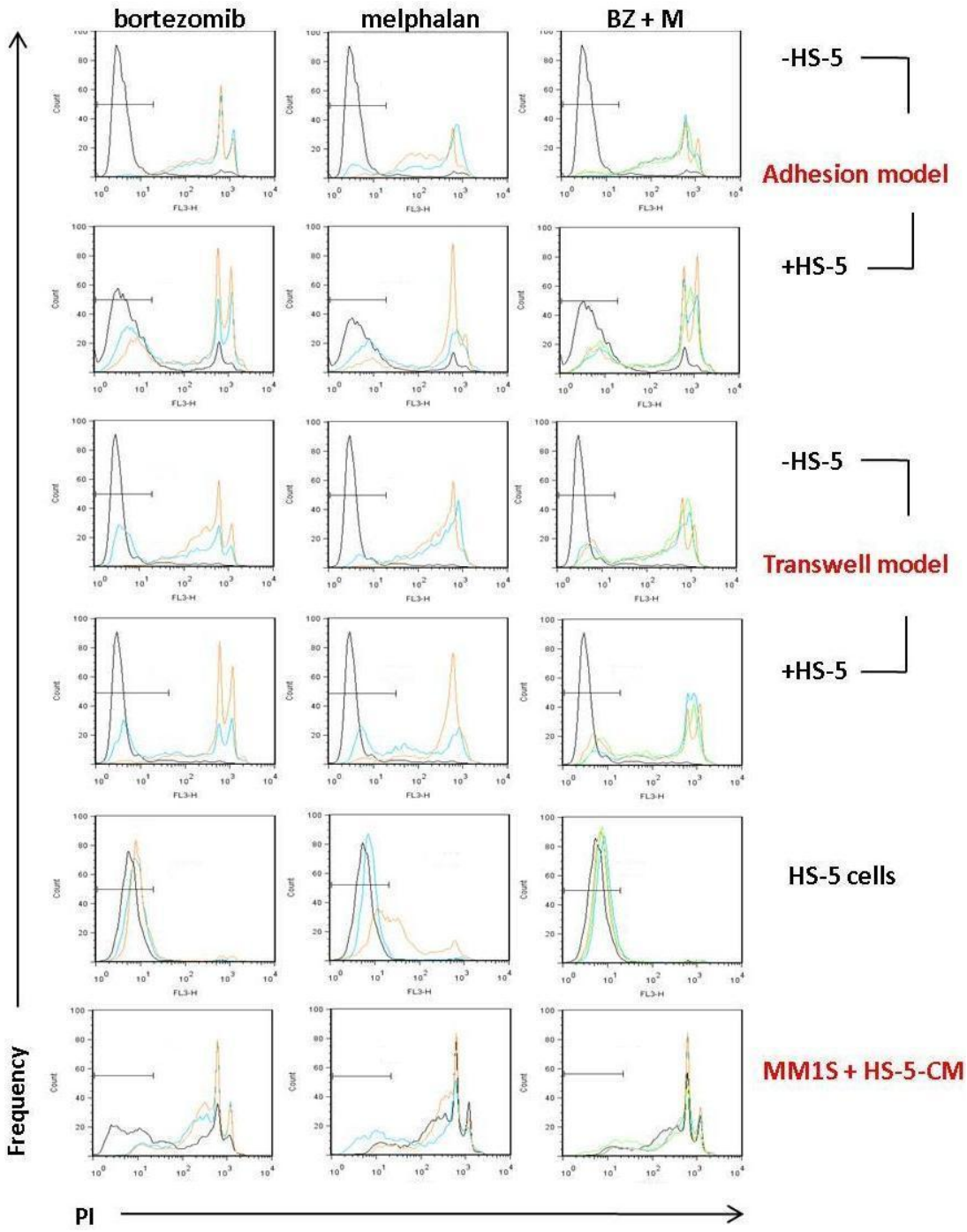

Figure 6.2 A representative experiment showing the viability of MM1.S cells treated with bortezomib (BZ 4ηM, 8ηM) with melphalan (M 10μM and 100μM) or with 3 combination schedules of BZ (4ηM) and M (10μM):simultaneous exposure (S1); bortezomib 24hrs prior to melphalan (S2) and melphalan 24hrs prior to bortezomib (S3). Treatments were assessed under 3 culture conditions: direct contact (adhesion model), or indirect contact (transwell model), or with HS-5-conditioned medium (CM model). Viability of HS-5 cells is also shown and was assessed using CD38/PI double-staining via flow cytometry. Black histogram = control untreated; blue histogram = lower dose or S1; orange histogram = higher dose or S2 and green histogram = S3. A total of at least 3 independent experiments in MM1.S cells were completed.

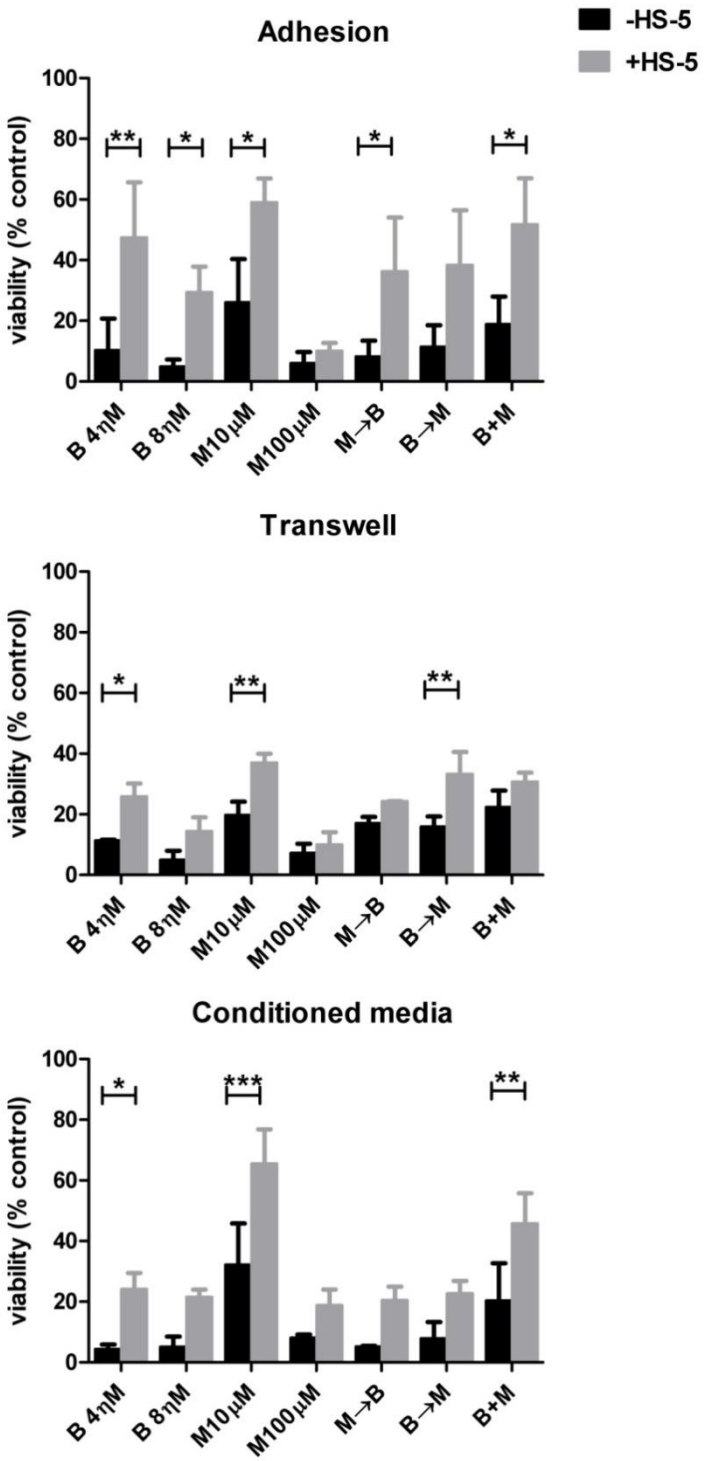

Figure 6.3 Viability of MM1.S cells treated with bortezomib (B 4ηM, 8ηM) with melphalan (M 10μM, 100μM) or with 3 combination schedules of 4ηM B and 10μM M: simultaneous exposure (S1); bortezomib 24hrs prior to melphalan (S2) and melphalan 24hrs prior to bortezomib (S3). Treatments were assessed under 3 culture conditions: direct contact (adhesion model), or indirect contact (transwell model), or with HS-5-conditioned medium (CM model). Data shows mean % viability relative to controls ± S.D. for 3 independent experiments. *indicates $p<0.05$, ** $p<0.01$ and ***$p<0.005$ using the paired t-test.

Of note, whereas bortezomib was non-toxic to HS-5 cells, 100µM melphalan resulted in HS-5 cytotoxicity as illustrated below. This effect was also observed in the previous chapter (figure 5.11), and is now more pronounced using the CD38/PI technique.

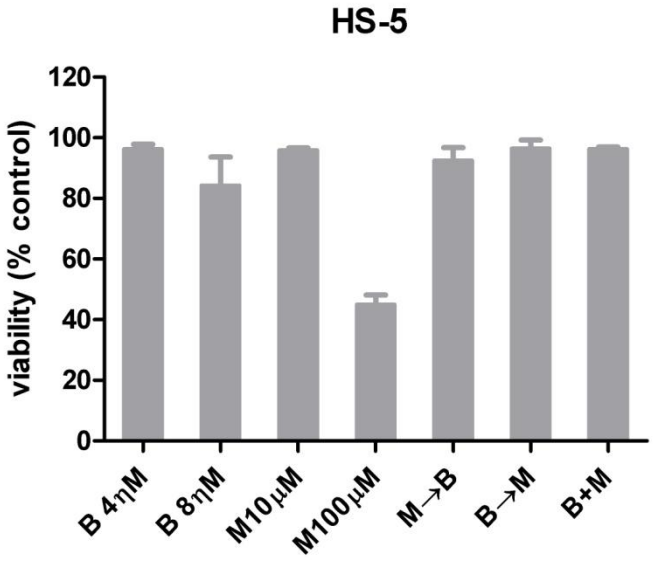

Figure 6.4 Viability of HS-5 cells treated with bortezomib (B 4ηM, 8ηM) with melphalan (M 10µM, 100µM) or with 3 combination schedules of B (4ηM) and M (10µM): simultaneous exposure (S1); bortezomib 24hrs prior to melphalan (S2) and melphalan 24hrs prior to bortezomib (S3). Data shows mean % viability relative to controls ± S.D. for 2 independent experiments.

A difference in activity was observed between the combination schedules. The melphalan pre-treatment tended to be more effective at decreasing the viability of MM1.S cells than the bortezomib pre-treatment or the drugs given simultaneously (which was the least effective combination) (figure 6.3). These data supports our previous findings in the guava model indicating the superiority of the melphalan pre-treatment combination schedule. In addition, it has shown that both HS-5 stroma and soluble factors appear to promote resistance to the effects of the bortezomib-melphalan combination. Overall, use of this system demonstrated a clear role for both direct stromal adhesion (CAM-DR) and soluble factors in mediating drug resistance in MM1.S cells.

6.2.3 The effects of soluble factors are more pronounced in primary MM cells cultured in the MM/HS-5 model

Due to limited sample availability, we were restricted to investigating bortezomib and melphalan at one concentration each (4ηM bortezomib and 10μM melphalan) and their simultaneous combination (at the same concentrations), in three of the 5 primary samples previously investigated in chapter 5.

Results demonstrated that, in contrast to MM1.S cells, indirect drug resistance occurring as a result of soluble factors (environment-mediated drug resistance (EM-DR)) accounted for much of the observed drug resistance. This is shown in figure 6.5, and is indicated by an increase in significance of the difference in viability of cells cultured in the adhesion model compared with the TW model and the CM model (i.e. p values in adhesion < TW < CM). Furthermore, this result was the same for all drug treatments suggesting that soluble factors conferred protection to primary MM cells from the effects of bortezomib and melphalan. Of note, the viability of these co-cultured primary MM cells after 48hrs (less than 60% viable) tended to be lower than the HMCLs which were consistently over 85% viable.

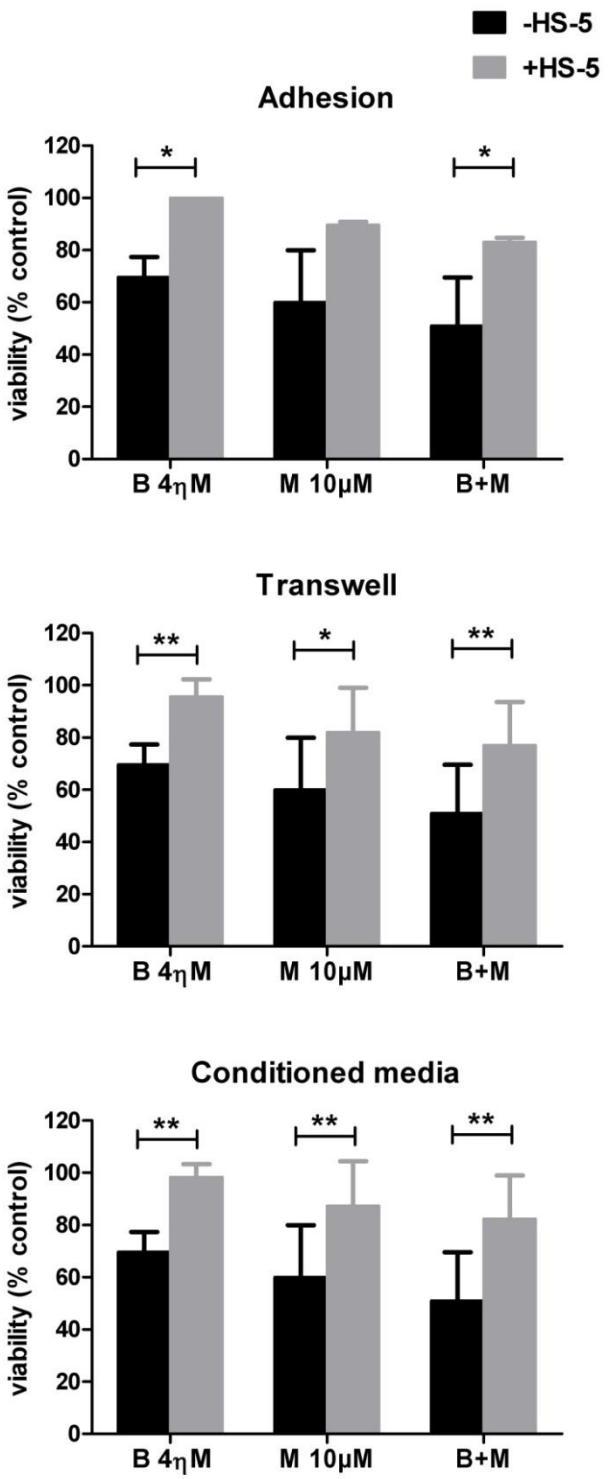

Figure 6.5 Viability of primary MM cells treated with bortezomib (B 4ηM, 8ηM) with melphalan (M 10μM, 100μM) or with 3 combination schedules of B (4ηM) and M (10μM): simultaneous exposure (S1); bortezomib 24hrs prior to melphalan (S2) and melphalan 24hrs prior to bortezomib (S3). Treatments were assessed under 3 culture conditions: direct contact (adhesion model), or indirect contact (transwell model), or with HS-5-conditioned medium (CM model). Data shows mean % viability relative to controls ± S.D. for 3 separate samples. * indicates $p<0.05$ and **indicates $p<0.01$ using the paired t-test.

6.3 Intracellular protein changes associated with drug resistance in the HS-5 coculture model

Results from the adhesion, transwell and conditioned media models suggested that soluble factors produced in the bone marrow microenvironment may confer drug resistance to MM cells. We investigated this further by studying the activation of intracellular signaling pathways involved in MM cell survival and implicated in mediating chemoresistance, such as the JAK/STAT-3, PI3K/Akt and the MAPK pathways. These pathways are known to be induced by microenvironmental growth factors, the most important of which is IL-6.

Changes in the expression of key pathway proteins were analysed by western blotting firstly in MM1.S cells following exposure to bortezomib (4ηM and 8ηM) and to melphalan (10μM and 100μM) for 24hrs. Secondly, we were able to analyse signal transduction in a primary MM sample (patient #1) in which sufficient cells were available. The primary cells were treated with 60μM UCL67022 and with dexamethasone (10 and 100μM) and lysates prepared after 24hrs. Drug effects were determined in MM monocultures and in MM/HS-5 cocultures.

6.3.1 Bortezomib and melphalan are ineffective at blocking the activation of cell survival pathways in MM1.S cells

The most striking effect of MM1.S coculture with HS-5 cells was activation of STAT-3 and ERK1/2, (lane 1 and 5, respectively, figure 6.6). This was indicated by expression of phosphorylated STAT-3 and ERK1/2 in MM1.S+HS-5 cocultures but not in MM1.S-HS-5 monocultures. Flow cytometry analysis (shown in figure 6.8) confirmed that this was not due to a lack of expression of the IL-6 receptor in MM1.S monocultures, stimulation of which leads to STAT-3 activation. Therefore, STAT-3 activation in MM1.S cocultures could be attributed to the presence of HS-5 stroma. Quantification of the expression of phosphorylated proteins relative to expression of total proteins via densitometry analysis, confirmed that bortezomib downregulated the expression of phospho-STAT-3 in MM1.S cocultures, however this result did not reach significance

(figure 6.7). Melphalan was more effective at doing this and completely abolished STAT-3 activation at 100μM. In contrast, ERK1/2 activation was not abrogated by bortezomib or melphalan; in fact its phosphorylation appeared to be enhanced by drug treatment (figures 6.6 and 6.7).

P38 MAPK was constitutively activated in MM1.S monocultures (lane 3, figure 6.6)) and was upregulated in coculture. This was associated with a loss in the ability of melphalan to suppress its activation (at 100μM $p<0.005$, figures 6.6, 6.7). In a similar manner, melphalan (100μM) effectively induced PARP cleavage in monocultures, but this did not occur under coculture conditions. Bortezomib demonstrated no effect on activation of the P38 MAPK pathway or on PARP cleavage.

Taken together, these results suggest that 1) the activity of bortezomib in MM1.S cells is most likely unrelated to its effects on the signal transduction pathways investigated in this model; 2) melphalan was effective at inhibiting JAK/STAT-3 signaling, but it was ineffective at blocking signaling via the MAPK pathways, which resulted in protection from melphalan-induced apoptosis in MM1.S cocultures; and 3) it is unlikely that the synergy observed with the combination of bortezomib and melphalan is due to an effect on intracellular signalling.

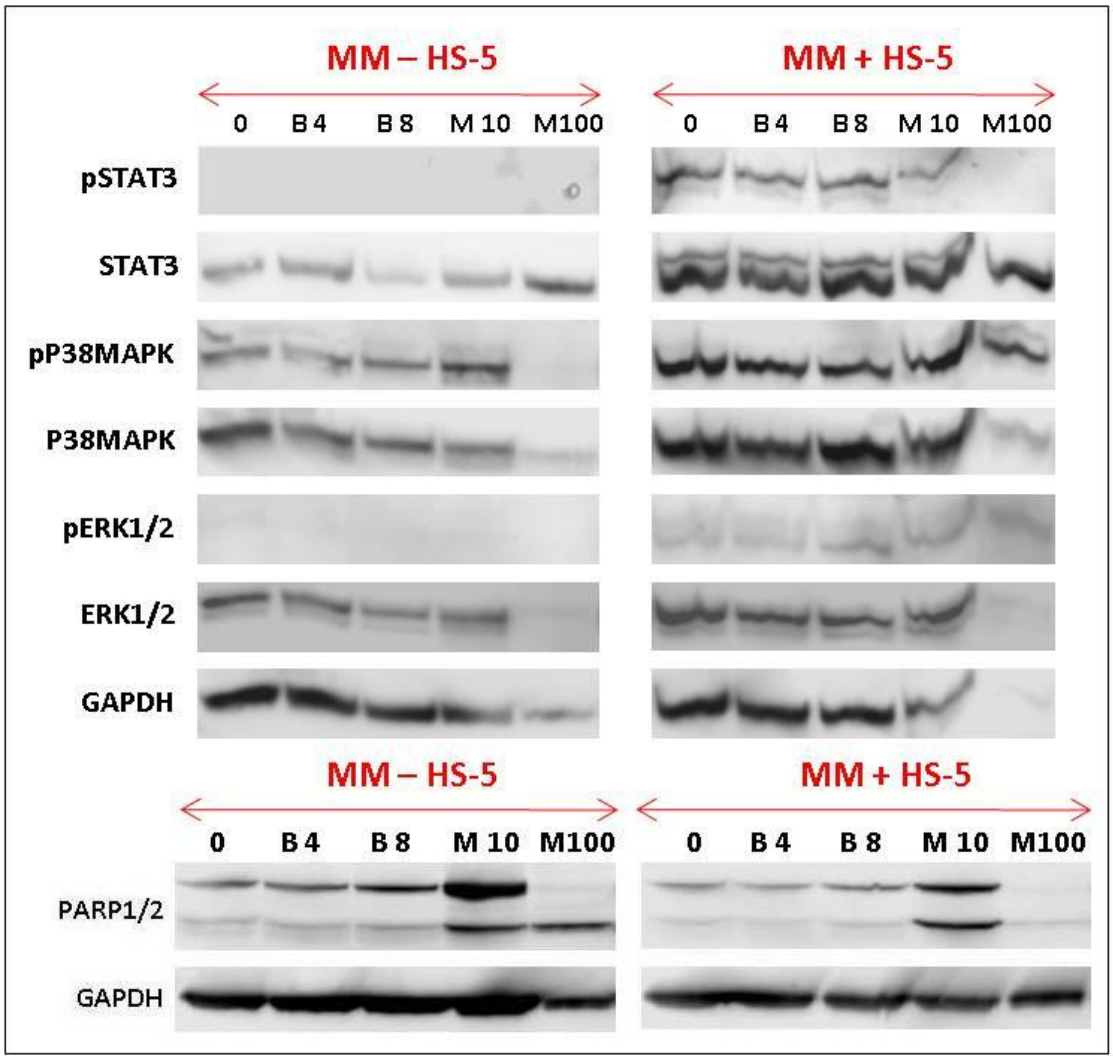

Figure 6.6 Effect of HS-5 stroma on pathway activation in MM1.S cells treated with bortezomib ('B' at 4ηM, 8ηM) and melphalan ('M' at 10μM, 100μM). Cells were cultured alone or with HS-5 cells for 24hrs and exposed to drugs for an additional 24hrs. 20μg of whole cell lysates were prepared and subjected to a 4%-12% NuPAGE gel electrophoresis and immunoblotting. For a detailed list of antigens probed for see chapter 2, section 2.11.4. Data from a representative experiment is shown and the experiment was repeated once.

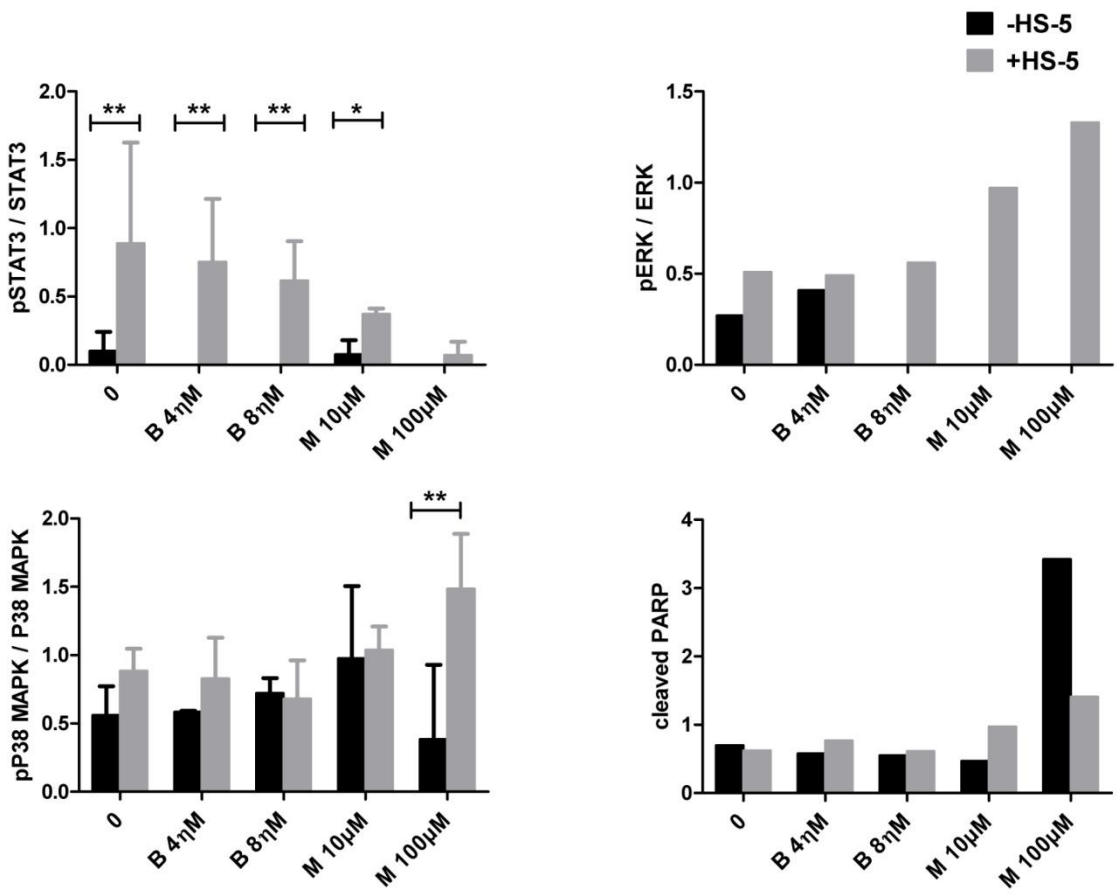

Figure 6.7 Densitometry quantification of western blot data in MM1.S cells treated with bortezomib ('B' at 4ηM and 8ηM) and melphalan ('M' at 10μM and 100μM) for 24hrs. Gelscan software was used to calculate fold change of phosphorylated proteins relative to total protein expression. Error bars show mean ± S.D. of 2 separate experiments. *indicates $p<0.05$ and **indicates $p<0.005$ using the paired t-test.

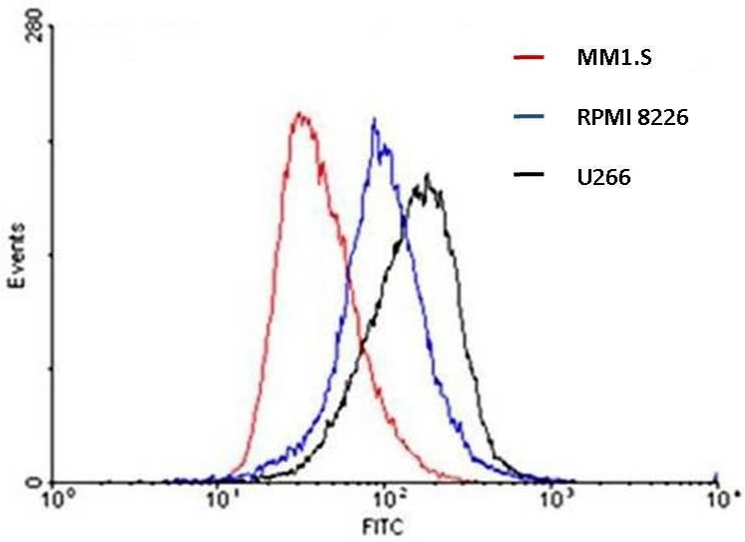

Figure 6.8 A representative experiment showing basal IL-6Rα expression in HMCLs (MM1.S, RPMI 8226 and U266) measured by flow cytometry using indirect staining via a FITC-labelled secondary antibody. All HMCLs stained positive for IL-6R expression compared to a negative isotype IgG1 control (not shown).

6.3.2 Primary MM displays constitutive activation of cell survival pathways which is more effectively inhibited by UCL67022 than dexamethasone

We next investigated signaling transduction in a primary MM sample (patient #1) treated with UCL67022 (60μM) and dexamethasone (100μM), under the same culture conditions. Importantly and in contrast to that observed in MM1.S cells, STAT-3 was constitutively activated in this sample and this was unaffected by coculture (figure 6.9). The MAPK pathways (P38 and ERK), the PI3K/Akt pathway (Akt) and NFκB were also constitutively activated in the primary cells, in accordance with previous reports (Catlett-Falcone, Landowski et al. 1999; Hsu, Shi et al. 2004).

Both dexamethasone and UCL67022 effectively abolished STAT-3 activation in mono- and in cocultures (indicated by the absence of phospho-STAT-3 at 60μM UCL67022 and at 100μM dexamethasone, figures 6.9 and 6.10). Similarly, both drugs maintained the ability to downregulate phospho-Akt and subsequent expression of active NFκB (p65) (lanes 3 and 9, respectively, figure 6.20). In contrast, whilst UCL67022 blocked P38 MAPK activation under coculture conditions (lane 5) it was ineffective against MAPK signaling via ERK1/2 (lane 7). Dexamethasone was also less effective in the presence of

stroma on signalling via the MAPK pathways (P38 and ERK1/2). In summary, these data in a primary MM sample suggests that dexamethasone-resistance conferred to MM cells by the stromal microenvironment may occur via the MAPK pathway. Furthermore, STAT-3 and MAPK signaling appears to contribute independently to MM cell survival and drug resistance; as both UCL67022 and dexamethasone were able to block signaling via STAT-3, but not via the MAPK pathway.

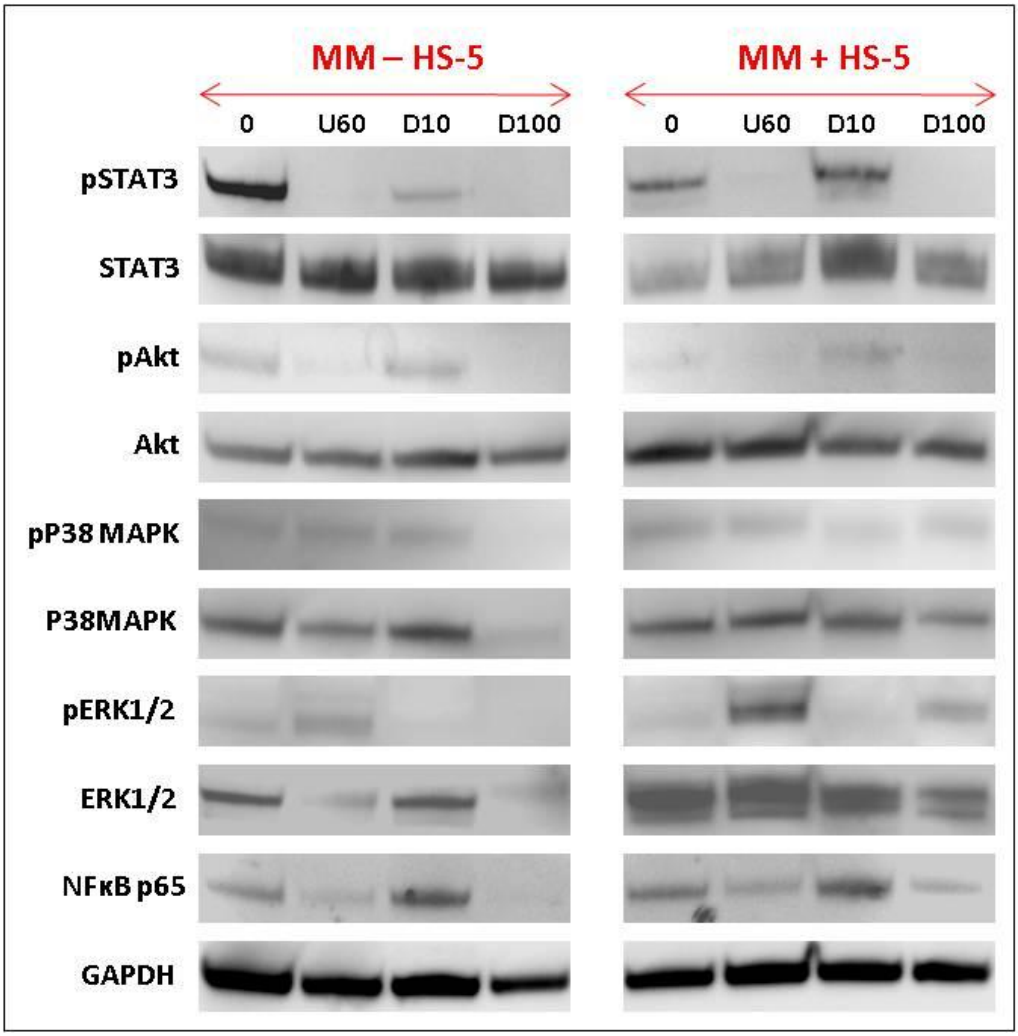

Figure 6.9 Effect of HS-5 stroma on intracellular signaling in a primary MM sample treated with dexamethasone ('D' at 10μM and 100μM) and UCL67022 ('U' at 60ηM). Cells were cultured alone or with HS-5 cells for 24hrs and exposed to drugs for an additional 24hrs. 40μg of whole cell lysates were prepared and subjected to a 4%-12% NuPAGE gel electrophoresis and immunoblotting. For a more detailed list of the antibodies used see chapter 2, section 2.11.4. This experiment was performed once due to a lack of available sample.

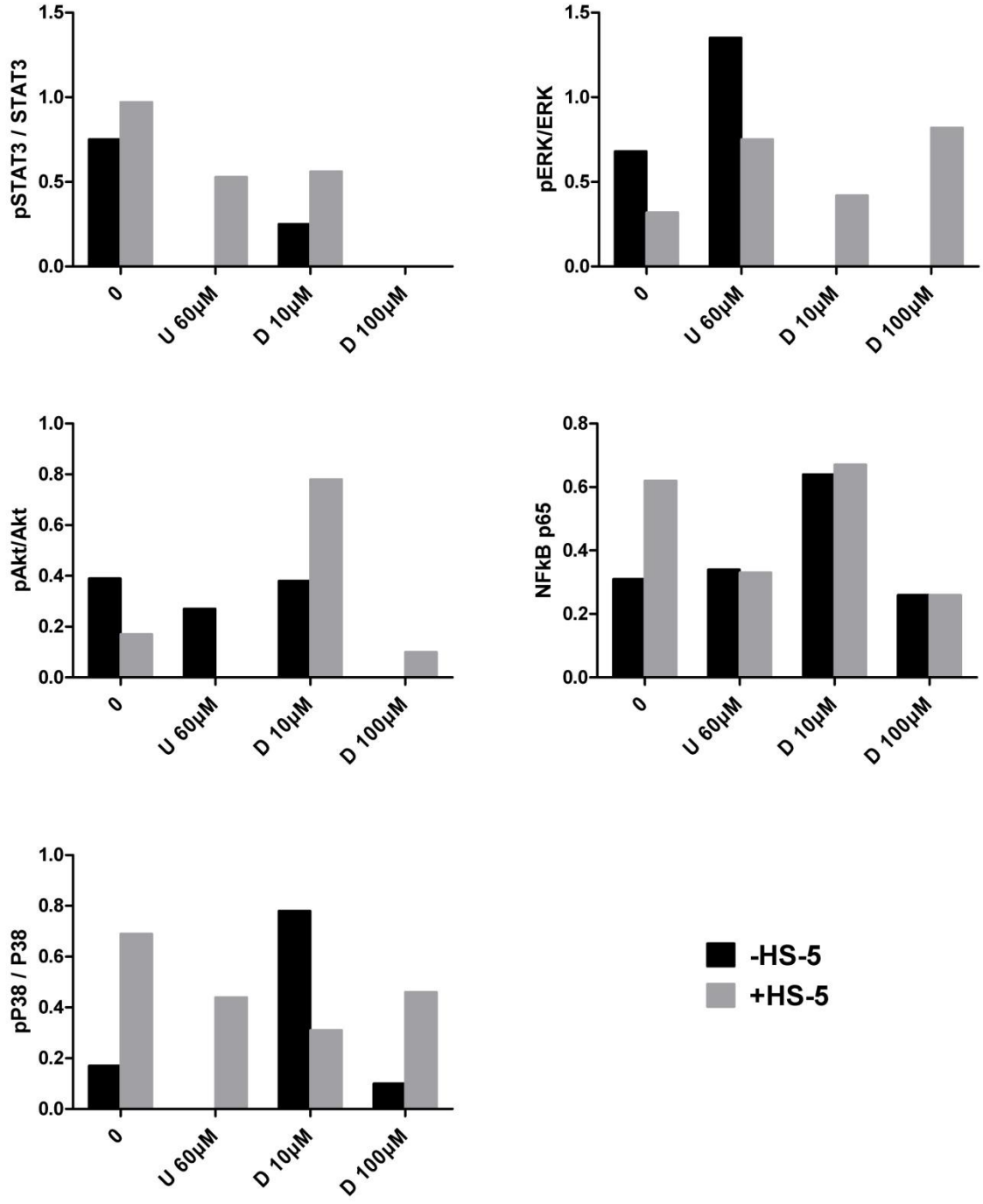

Figure 6.10 Densitometry quantification of western blot data for the effect of HS-5 stroma on in primary MM cells treated with dexamethasone ('D' at 10µM and 100µM) and UCL67022 ('U' at 60ηM) for 24hrs. Gelscan software was used to calculate fold change of phosphorylated proteins relative to total protein expression.

6.4 Cytokine profiling in the HS-5 coculture model

We have so far demonstrated that resistance to two of the most efficacious chemotherapies used in the treatment of patients with MM, melphalan and bortezomib, may be in part, mediated by soluble elements present in the stromal/MM milieu. We therefore set up a series of experiments to firstly confirm that soluble factors are present in the MM/HS-5 cocultures and to quantify their levels using a multiplexed ELISA assay; and secondly to investigate their role in MM cell survival and drug resistance by correlating their levels with drug sensitivity. Lastly, we used the coculture model to investigate whether external manipulation of growth factors, using cytokine neutralising antibodies, could offer a potential therapeutic benefit in the treatment of MM.

6.4.1 The MSD assay is an effective means of measuring cytokine levels in primary cell culture supernatants

In collaboration with Meso Scale Discovery® (MSD) we customized a sandwich immunoassay ELISA plate where capture antibodies were coated in a single spot, on the bottom of the plate (see chapter 2.13.1 figure 2.3). Incubation of samples (cell culture supernatants) in the MULTI-SPOT®plate, initiates the binding of each cytokine to its corresponding capture antibody spot. Cytokine levels were detected using a cytokine-specific detection antibody labelled with an MSD SULFO-TAG™ reagent which emits light upon electrochemical stimulation initiated at the electrode surfaces of the microplate. This luminescent signal was quantified and levels of cytokines in unknown samples were calculated using standard curves generated by linear regression analysis.

As shown in figure 6.11, standard curves for IL-6, IL-6R, IL-8, MIP-1α and VEGF were linear within a detection range of 10pg/ml up to approximately 10,000pg/ml (all R-values were > 0.95). This suggested that the assays could accurately measure all 5 cytokines relative to standards and within acceptable limits for precision, which was indicated by less than 20% variation in replicates from the mean values (table 6.2).

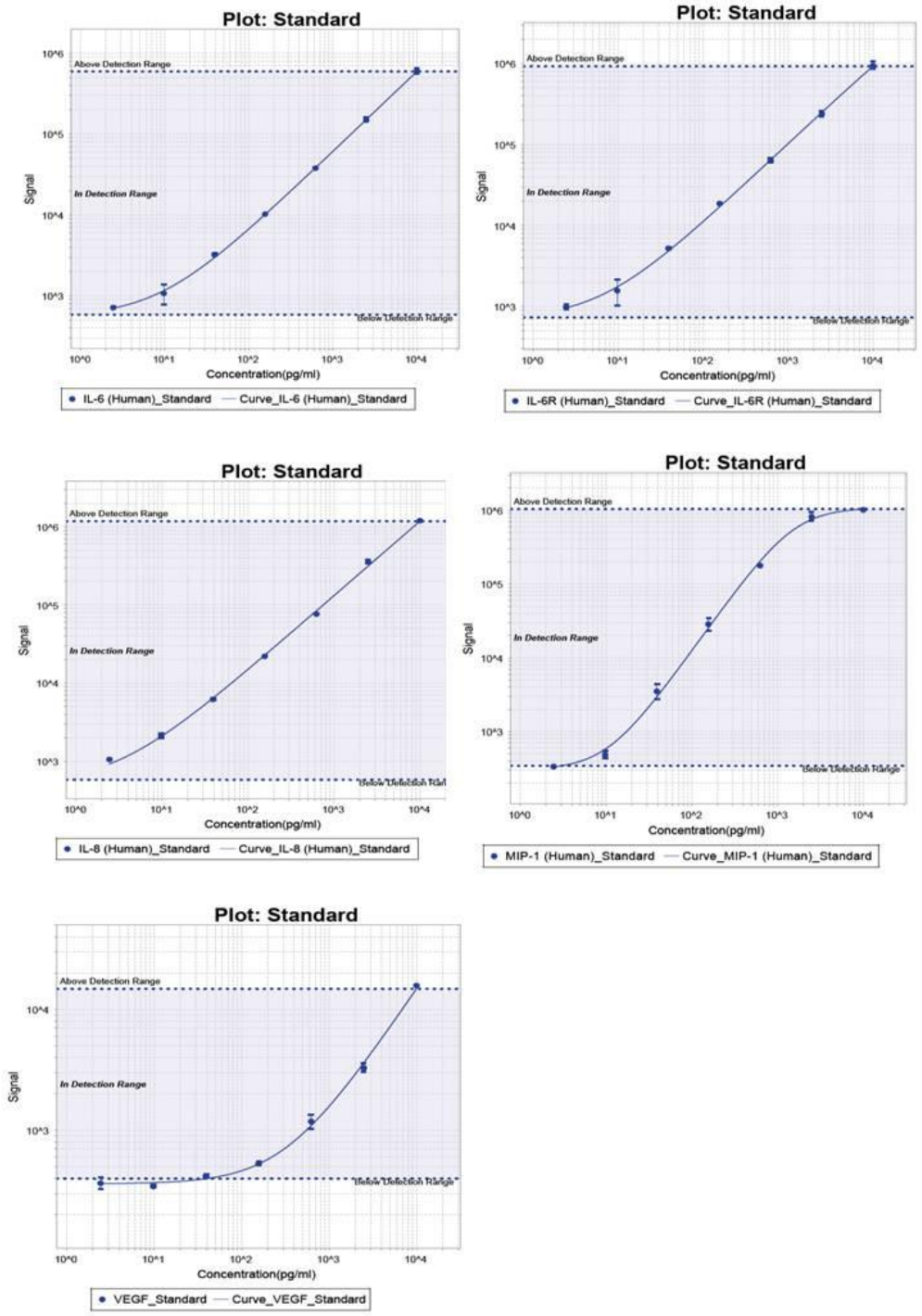

Figure 6.11 Standard curves for cytokines measured in the MSD assay. Cytokines from top left to right were: IL-6, sIL-6R, IL-8, MIP-1α and VEGF. Briefly, stock solutions of cytokine standards were diluted in culture medium to give a range from 10,000pg/ml to 2.4pg/ml. 25µl of standards or samples were dispensed in duplicate into the 96-well plate prior to a 2hr incubation with vigorous shaking at RT. This was followed by dispensing of 25µl detection antibody and a further 2hr incubation at RT. Read buffer was added and the plate was analysed in the SECTOR™ Image analyser.

Table 6.1 Summary table showing the accuracy and precision of the MSD assay method in detecting concentrations of cytokines in cell culture supernatants from HS-5/MM cocultures.

	Measured values (mean ± S.D.)				
[standards] pg/ml	IL-6	IL-6R	IL-8	MIP-1$^{\alpha}$	VEGF
10000	10416 ± 534	11158 ± 1583	11215 ± 1503	10140 ± 17	11505 ± 1947
2500	2483 ± 16	2629 ± 222	2587 ± 281	2620 ± 329	2557 ± 419
625	603 ± 18	549 ± 94	545 ± 88	587 ± 30	558 ± 11
156	154 ± 6	153 ± 7	160 ±	162 ± 15	155 ± 5
39	41 ± 4	44 ± 1	44 ± 17	40 ± 4	42 ± 6
9.8	9 ± 1	10 ± 2	10 ± 2	9 ± 1	10 ± 1
2.4	3 ± 1	3 ± 0	3 ± 2	3 ± 0	3 ± 0
0	0	0	0	0	0

6.4.2 IL-6, IL-8 and VEGF are detected at high levels in the MM/HS-5 model

The supernatants used in this study were harvested from the original guava cocultures described in the previous chapter, and stored at -80°C for later use. We measured the soluble factors described above in several samples: 1) HS-5 monocultures, 2) MM1.S monocultures, 3) 5 primary MM monocultures (P1-P5), 4) MM1.S/HS-5 cocultures and 5) 5 primary MM/HS-5 cocultures. These samples were treated with either bortezomib, melphalan or their combination (3 schedules: simultaneously, bortezomib-pre exposure or melphalan pre-exposure) for 48hrs.

As illustrated in figures 6.12 and 6.13, negligible levels of IL-6R and MIP-1α (<10pg/ml) were detected in all samples across all treatments, suggesting that these factors do not play an important role in our BMM model. In contrast, dramatically higher levels of IL-6 and IL-8 were detected in primary MM cocultures (mean of 5 samples IL-6=1226pg/ml and IL-8=1322pg/ml) compared to negligible levels (<10pg/ml) in MM1.S or primary MM monocultures. Furthermore, these cytokines were measured in HS-5 monocultures at levels 10-fold lower than that measured in the cocultures (IL-

6=123pg/ml and IL-8=244pg/ml). This suggested that IL-6 and IL-8 were secreted by HS-5 cells and upregulated upon adhesion to MM cells in a predominantly paracrine manner.

VEGF was more variably secreted in primary supernatants. It was detected at high levels in HS-5 monocultures (298pg/ml) and in 2 out of 3 primary MM monocultures (patient #2, 113pg/ml and #3, 240pg/ml), and adhesion of MM cells to stroma resulted in its upregulation in 2 out of 3 samples (patient #3, 686pg/ml and #4, 482pg/ml). This suggests a predominantly autocrine mechanism for VEGF production in myeloma cells, which could be attributed to differences in their intrinsic biology and as such would explain some of the heterogeneity observed in VEGF secretion.

Of note, there were some differences between MM1.S cells and the primary samples: 1) there were higher levels of IL-6R and VEGF in MM1.S monocultures compared with primary MM. In fact VEGF was upregulated in MM1.S upon adhesion to stroma, whereas IL-6 and IL-8 levels remained low and were comparable to that secreted by HS-5 cells alone. This is in clear contrast to that seen in the primaries and it highlights the difficulty of extrapolating results from cells lines studies alone, to the *in vivo* situation.

6.4.3 Melphalan, but not bortezomib, modulates secretion of IL6, IL8 and VEGF in MM/HS-5 cocultures

Results of the drug treatments shown for bortezomib in figure 6.12 indicated that it was ineffective at modulating cytokine secretion in HS-5 monocultures. This may be related to its lack of cytotoxicity in HS-5 cells that we demonstrated in chapter 5 (figure 5.11). In MM1.S cells, bortezomib inhibited the secretion of VEGF, IL-6, IL-8 and IL-6R, both in monocultures and in cocultures. In contrast, this effect was completely abrogated in primary MM cocultures, in which cytokine levels remained high (especially in samples P2 and P5, figure 6.12).

In contrast, data shown in figure 6.13 suggests that melphalan (100μM) effectively reduced IL-6 and IL-8 secretion to within 20% of values in HS-5 controls (from

123pg/ml to 27pg/ml and 244pg/ml to 53pg/ml, respectively) and completely abolished VEGF secretion (298pg/ml to <1pg/ml). As we noted with the effect of bortezomib on HS-5 cells, this result may be related to the cytotoxic effect of melphalan on HS-5 observed at 100µM in the adhesion-TW-CM models. Melphalan was similarly effective at suppressing secretion of these cytokines in both MM1.S monocultures and in MM1.S/HS-5 cocultures.

The effect of melphalan in primary cocultures was more variable: P3 responded in a dose-dependent manner and 100µM lowered levels to at least control values in P4 and P5; however the drug had no effect on P1 and P2 (figure 6.13). We hypothesised that this difference may be associated with sensitivity to melphalan and our investigation of this is shown in the following section. Importantly, our results suggest that melphalan is more effective than bortezomib in modulating cytokines levels in the BMM and this may involve its cytotoxicity to HS-5 cells (at 100µM).

Results showed no significant scheduling effect in primary MM cocultures, although there was a slight tendency towards lower cytokine levels with the melphalan pre-treatment schedule (more apparent in MM1.S cell than in primary cells (figure 6.14)). Notably, the combination of bortezomib with melphalan did not downregulate secretion of IL-6, IL-8 or VEGF in the primary samples studied.

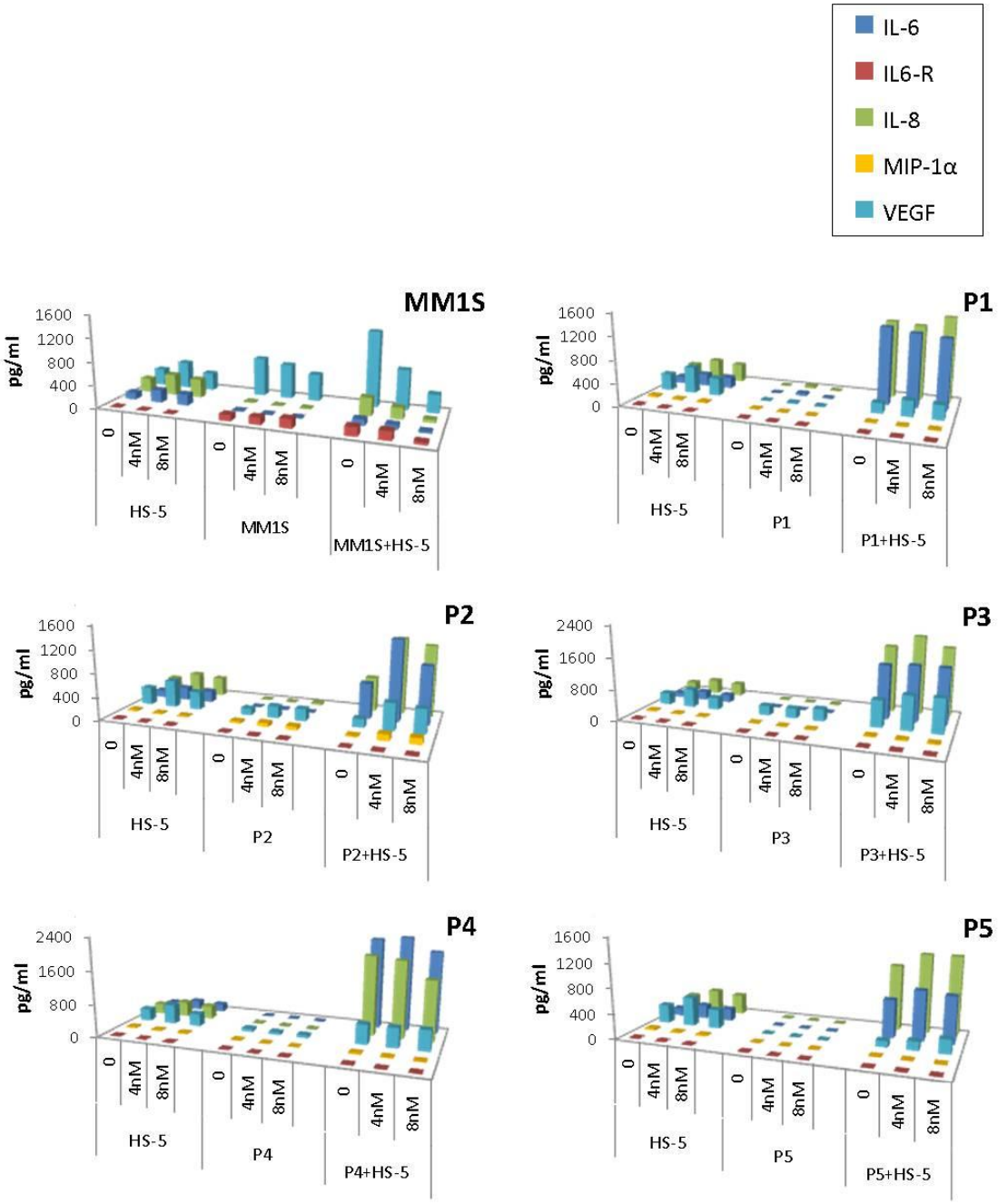

Figure 6.12 Effect of bortezomib on cytokine modulation. Concentrations of cytokines (IL-6, IL-6R, IL-8, MIP-1α and VEGF) detected in supernatants from HS-5/MM1.S or HS-5/MM (P1-P5) cocultures after 48hrs treatment with 2 doses of bortezomib (4ηM and 8ηM). Cytokine levels in HS-5 monocultures and in MM monocultures are also shown.

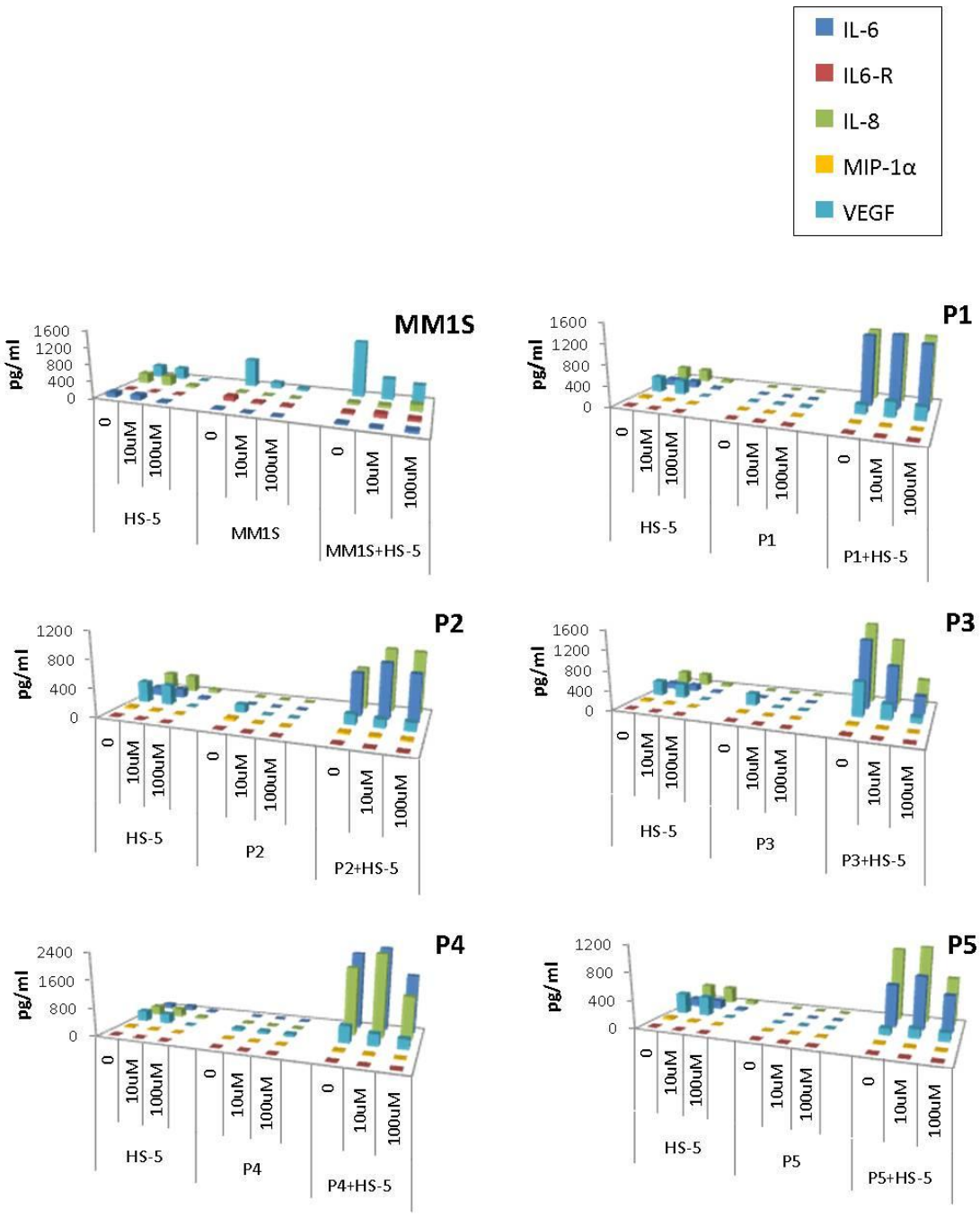

Figure 6.13 Effect of melphalan on cytokine modulation. Concentrations of cytokines (IL-6, IL-6R, IL-8, MIP-1α and VEGF) detected in supernatants from HS-5/MM1.S or HS-5/MM (P1-P5) cocultures after 48hrs treatment with 2 doses melphalan (10µM and 100µM). Cytokine levels in HS-5 monocultures and in MM monocultures are also shown.

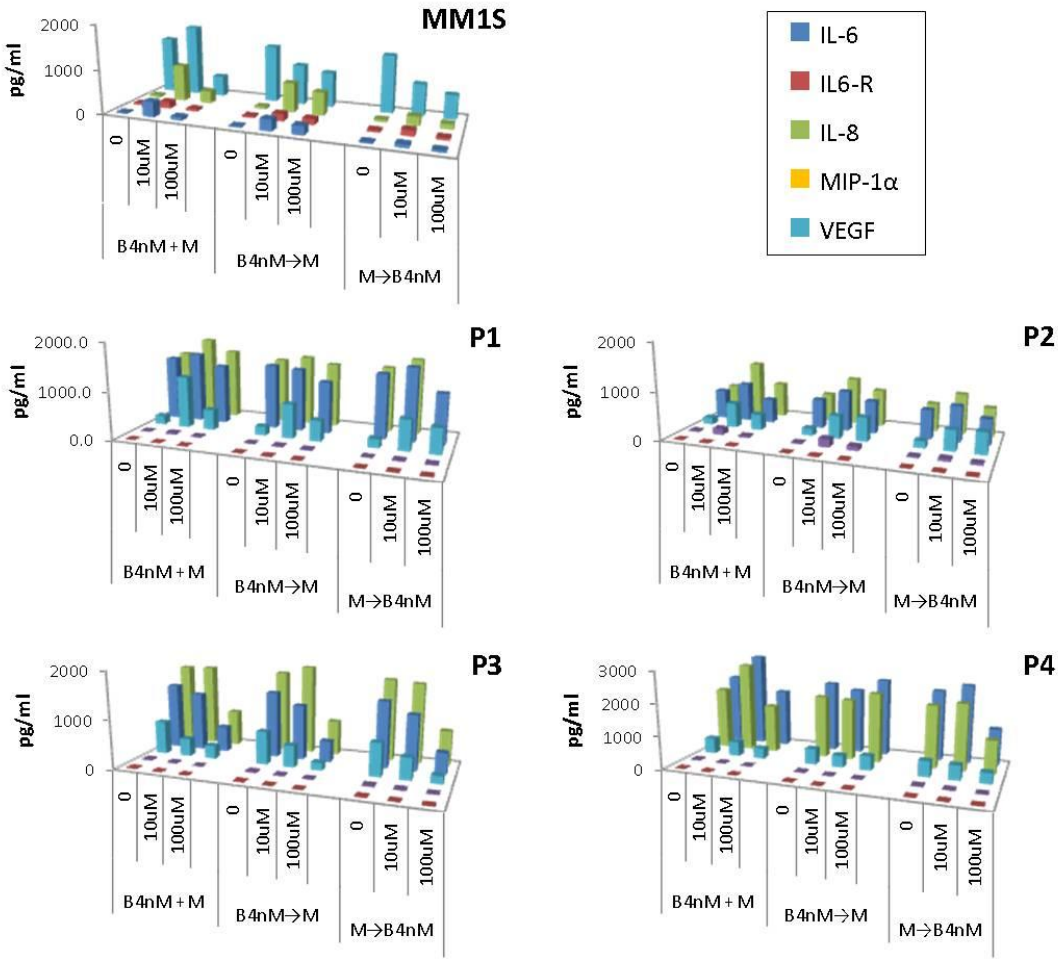

Figure 6.14 Effect of the combination of bortezomib and melphalan on cytokine modulation. IL-6, IL-6R, IL-8, MIP-1α and VEGF detected in supernatants from HS-5/MM1.S or HS-5/MM (P1-P4) cocultures after 48hrs treatment with bortezomib (4ηM) and melphalan (10μM and 100μM): simultaneous exposure, bortezomib pre-treatment and melphalan pre-treatment.

6.4.4 IL-6, IL-8 and VEGF levels correlate with the sensitivity of primary MM samples to bortezomib and melphalan

When concentrations of IL-6, IL-8 and VEGF measured in primary coculture supernatants were related to their sensitivity to bortezomib and melphalan, significant associations were found, shown in figure 6.15: IL-8 levels directly correlated with resistance to bortezomib (at 4ηM p=0.017 Pearson's correlation coefficient), and levels of both IL-8 and VEGF correlated with resistance to melphalan (at 100μM) (p=0.037 and 0.032 for IL-8 and VEGF, respectively). Levels of IL-6 were associated with resistance to both drugs and their combination, although this did not reach significance.

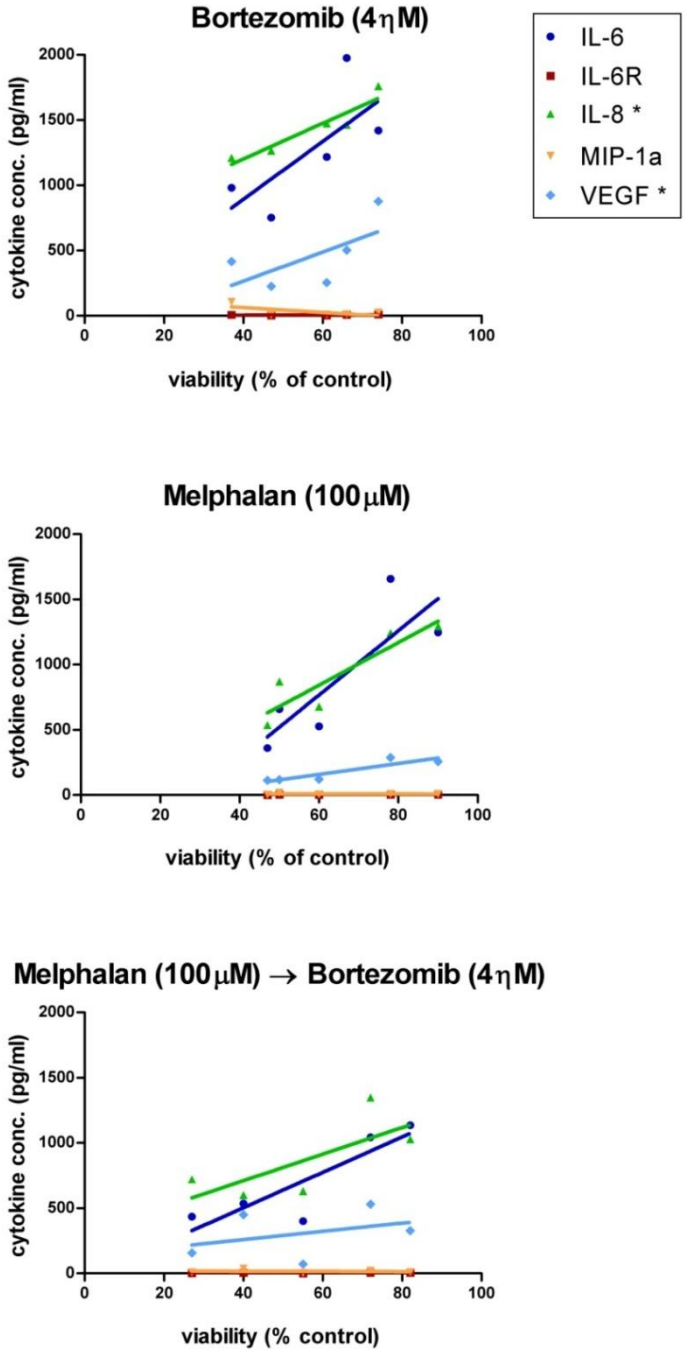

Figure 6.15 IL-8 and VEGF levels correlate with drug sensitivity. Concentration of IL-8 correlates with sensitivity to bortezomib (4ηM, *p=0.017, Pearson's correlation coefficient) and concentrations of IL-8 and VEGF correlates with sensitivity to melphalan (100μM, *p=0.037 and *p=0.032 respectively), but to the combination of melphalan and bortezomib (melphalan pre-exposure schedule) in primary MM samples (n=5).

6.4.5 UCL67022 inhibits secretion of stromal-derived cytokines in two stromal/MM coculture models

In addition, we investigated the role of soluble factors in UCL67022-mediated cytotoxicity in 2 different stromal cell models, 1) using the HS-5 cell line as before or 2) using patient bone marrow-derived stromal cells (hBMSCs). As described in chapter 2.2.3, use of hBMSCs was highly dependent on the availability of patient samples and required 4-6 weeks of culture to generate sufficient volumes to use in experiments. Two new primary MM samples were used in these experiments, labelled MM3 and MM4. Bortezomib effects at 4ηM and 8ηM and UCL67022 at 10μM and 100μM were examined.

As we demonstrated in our previous experiments, negligible levels of IL-6R or MIP-1α were detected in these assays (figures 6.16 and 6.17); however, we observed 30-fold higher levels of IL-6 and IL-8 and a 2-fold higher level of VEGF in supernatants from hBMSCs monocultures compared with HS-5 monocultures (303-768 pg/ml HS-5 vs. 1796-14002pg/ml hBMSC). In contrast, negligible levels of these cytokines were detected in supernatants from primary MM monocultures (mean concentration 3±0.7, 4±0.0, 29±20.5 pg/ml for IL-6, IL-8 and VEGF, respectively, n=2), indicating that they were predominantly stroma-derived. These results therefore support our previous findings.

When primary MM cells were cocultured with HS-5 or with hBMSCs, IL-6 levels increased by 60% of stroma-alone values (from 303pg/ml in HS-5 to 487pg/ml in HS-5+MM) or by 20%, respectively (from 10,369pg/ml in hBMSC to 12,554pg/ml in hBMSC+MM). IL-8 levels were similarly upregulated in HS-5/MM cocultures, and in hBMSC/MM cocultures, a 10% increase in VEGF levels was additionally observed (from 1,796pg/ml in hBMSC to 1,965pgml in hBMSC+MM). These data confirm findings from the experiments presented so far in this chapter, suggesting predominantly paracrine signaling in the BMM, initiated by MM cell adhesion to BMSCs and triggering their secretion of IL-6 (and to a lesser degree, VEGF and IL8). This may in turn lead to an autocrine effect in MM cells resulting in a growth factor-rich BMSC/MM cell milieu which promotes MM cell survival and chemoresistance via activation of anti-apoptotic

signaling pathways. The ability of bortezomib (figure 6.16) and UCL67022 (figure 6.17) to modulate levels of IL-6, IL-8 and VEGF was examined in both the HS-5/MM and the hBMSC/MM models. In keeping with previous results, bortezomib was ineffective at inhibiting cytokine secretion in HS-5 and hBMSC monocultures. Bortezomib had some effect on decreasing cytokine secretion in the MM/HS-5 cocultures although this was not maintained in MM/hBMSC cocultures. In contrast, UCL67022 inhibited cytokine secretion in hBMSC monocultures in a dose-dependent manner (figure 6.17). This effect was clear in HS-5/MM cocultures ($p<0.05$) and was appeared to be maintained in hBMSC/MM cocultures; however this did not reach significance.

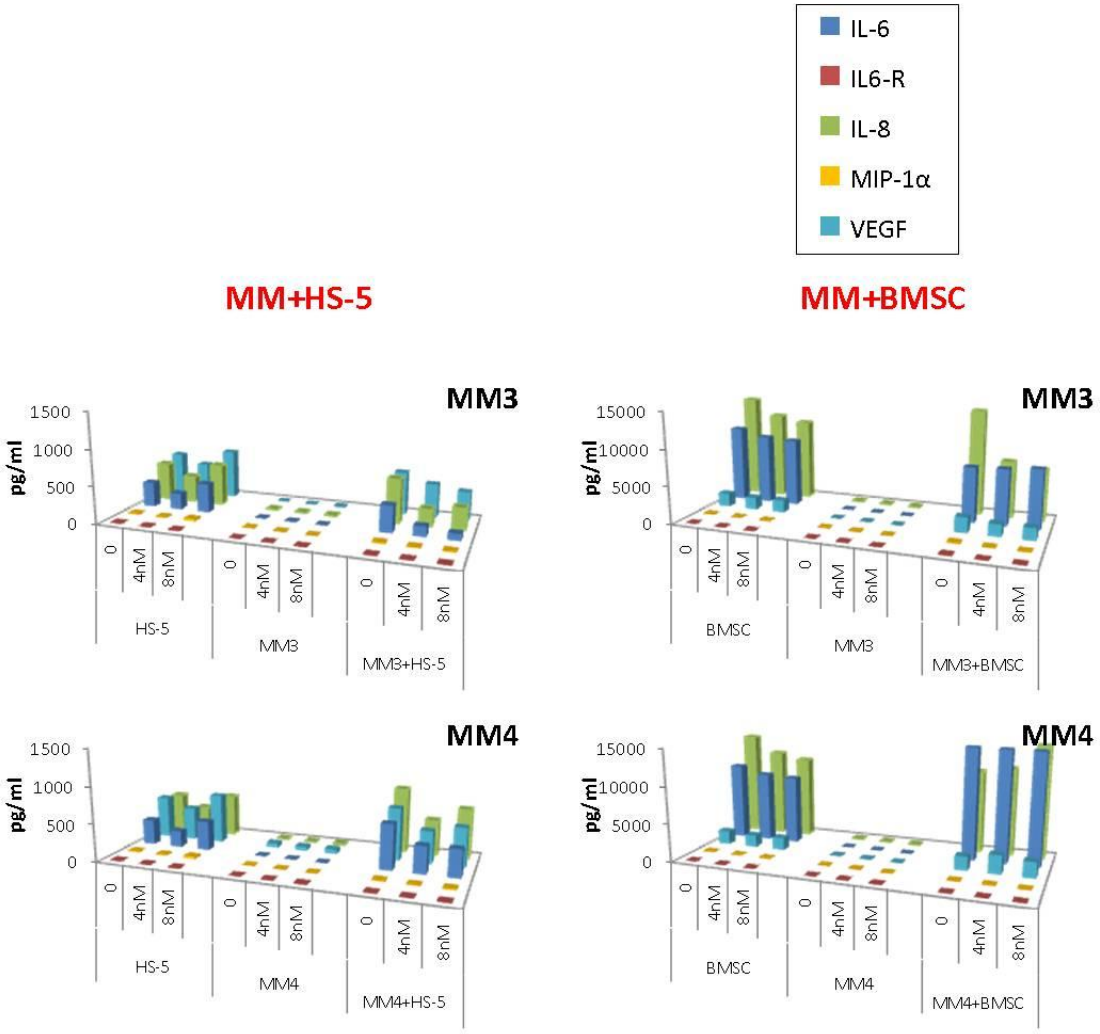

Figure 6.16 Bortezomib cytokine modulation in MM/hBMSC cocultures. Concentration of cytokines (IL-6, IL-6R, IL-8, MIP-1α and VEGF) in supernatants from HS-5/MM or hBMSC/MM (MM3 and MM4) cocultures after 48hrs treatment with bortezomib (4ηM and 8ηM). Cytokine levels in HS-5 or hBMSC monocultures and in MM monocultures are also shown.

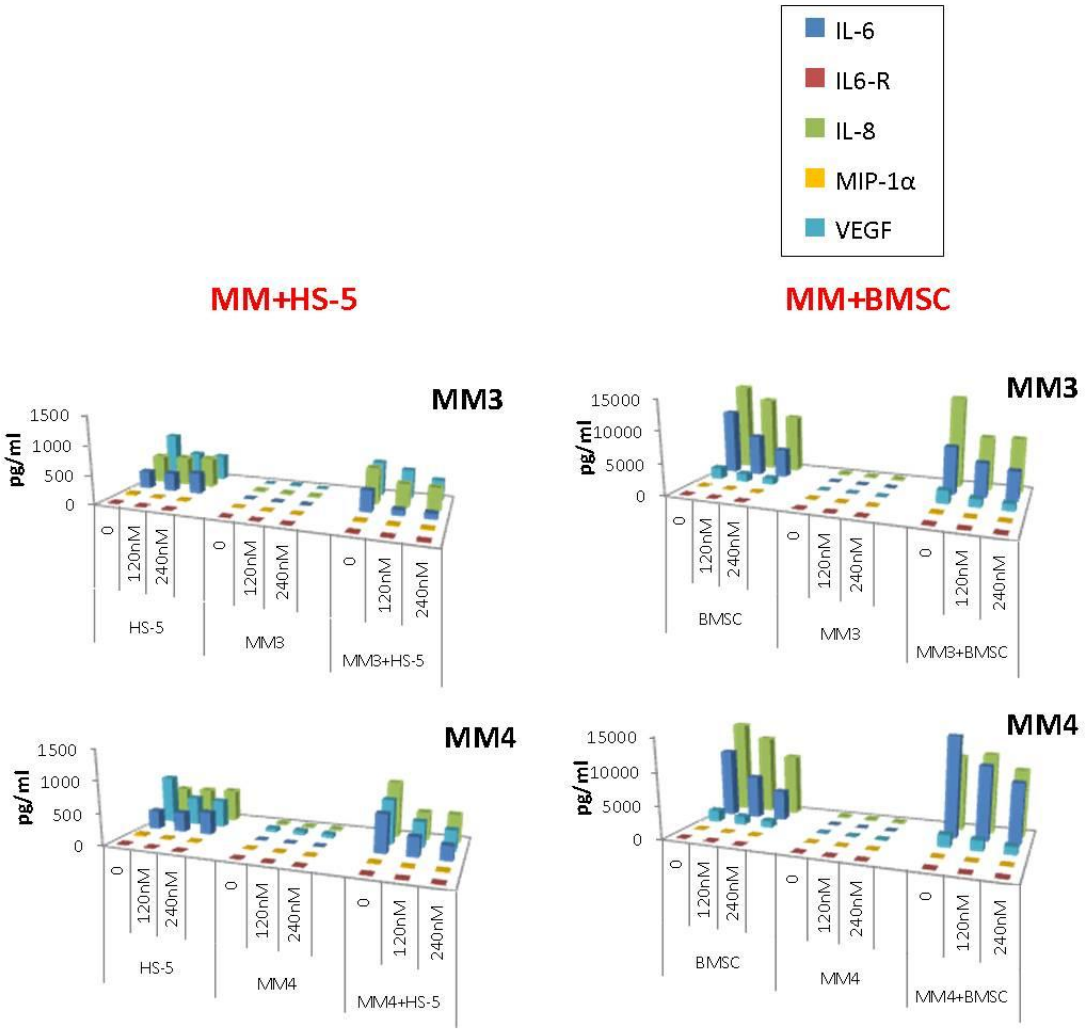

Figure 6.17 UCL67022 cytokine modulation in MM/hBMSC cocultures. Concentration of cytokines (IL-6, IL-6R, IL-8, MIP-1α and VEGF) in supernatants from HS-5/MM or BMSC/MM (MM3 and MM4) cocultures after 48hrs treatment with UCL67022 (10μM and 100μM). Cytokine levels in HS-5 monocultures and in MM monocultures are shown for comparison.

6.5 Neutralisation of IL-6, IL-8 and VEGF restores primary MM chemosensitivity in the MM/HS-5 model

To confirm whether elevated levels of cytokines detected in supernatants from coculture assays were indeed stroma-derived, and to confirm that a paracrine mechanism protects MM cells from the effects of chemotherapy, we performed a final set of experiments. Given that elevated IL-6, IL-8 and VEGF in supernatants from coculture assays correlated with drug resistance, HS-5 monolayers were treated for 4hrs with monoclonal antibodies against IL-6, IL-8 or VEGF, used singly or in 4 different combinations shown in figure 6.18: 1) IL-6+IL-8, 2) IL-6+VEGF, 3) IL-8+VEGF or 4) IL-6+IL-8+VEGF. MM1.S cells or primary MM samples (3 out of the 5 used previously in which cells were available) were exposed to bortezomib (4ηM) or melphalan (10μM) for 48hrs and cultured with HS-5 monolayers pre-treated with each of the 9 treatments, in the transwell model.

Results indicated that pre-treatment of stroma with IL-6, IL-8 or VEGF antibodies singly or in combination had little effect on the viability of MM1.S cells. This was not surprising as our previous results using the transwell model suggested that soluble factors were less important in mediating MM1.S survival/drug resistance than direct cell-to-cell contact (section 6.2.2). This would perhaps explain the lack of any further cell kill produced with cytokine neutralisation.

In contrast, IL-6, IL-8 or VEGF antibodies diminished the protective effect conferred to MM cells via HS-5 coculture, thus restoring sensitivity to bortezomib and melphalan-induced apoptosis (figure 6.18). Pre-treatment of stroma with a combination of 2 antibodies resulted in a mostly additive effect, and the highest neutralising effect was observed when all 3 antibodies were used simultaneously. Whilst IL-6 neutralising antibodies are being currently evaluated in the clinic, these preliminary data provides compelling evidence towards the further evaluation of IL-8 and VEGF antibodies both alone and in combination.

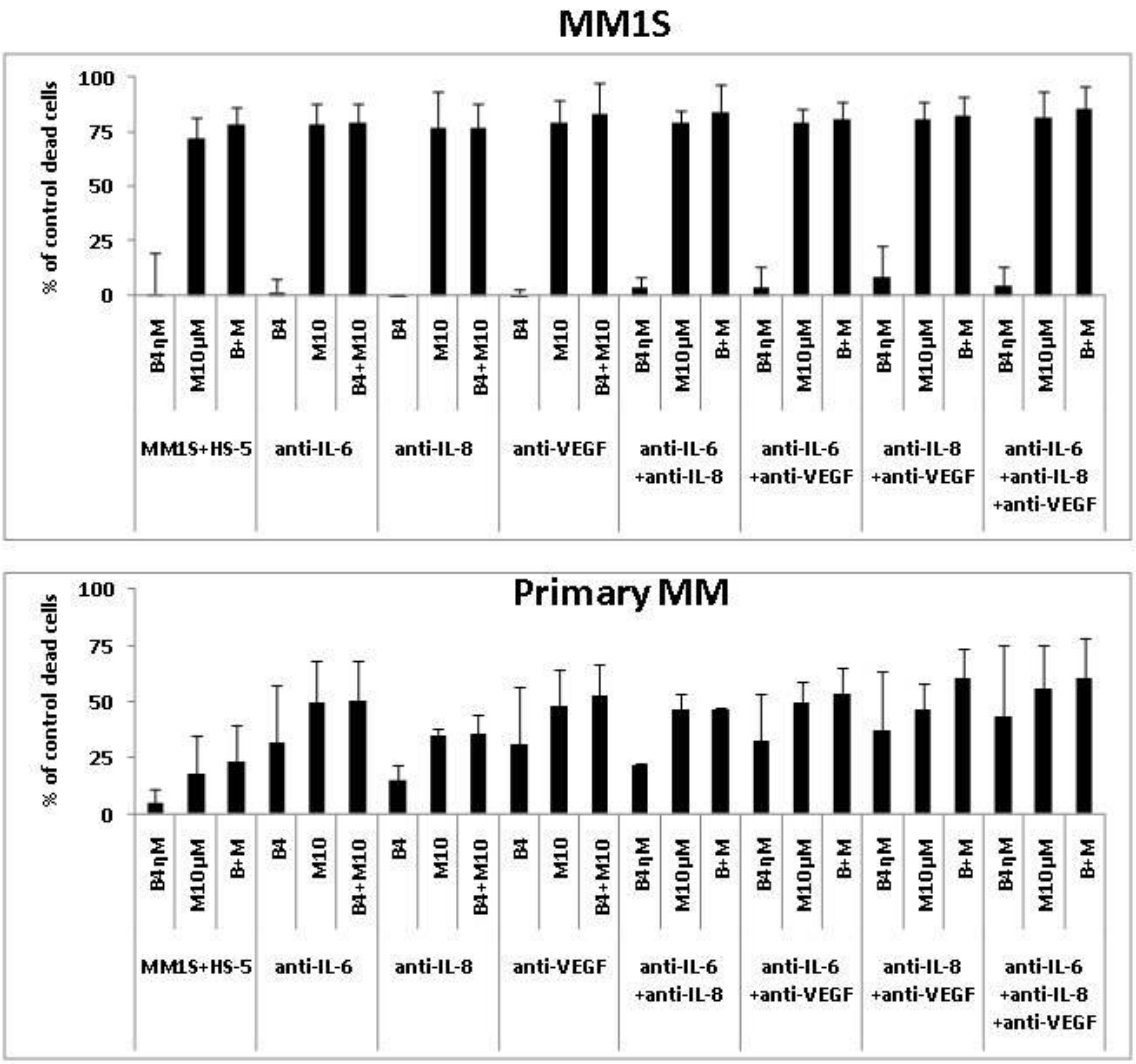

Figure 6.18 Antibody-mediated neutralisation of IL-6, IL-8 and VEGF restores bortezomib and melphalan-induced apoptosis in primary MM/HS-5 cocultures.HS-5 cells were plated and cultured for 24hrs and stromal monolayers were pre-treated with either 1μg/ml normal goat serum as a control, or with goat anti-IL-6, anti-IL-8 or anti-VEGF or combinations of 2 or all 3 together (0.3μg/ml) for 4hrs. MM cells (1x105 cells) were then added in the presence or absence of bortezomib (4ηM) and/or melphalan (10μM). After 48hrs, MM cells were collected and % dead cells were determined by CD38/PI double staining. Data shows the mean ± S.D. of 3 independent experiments for MM1.S and for 3 different patient samples.

6.6 Discussion

The aims of this final part of the project were 3-fold. Firstly, we aimed to use the HS-5/MM coculture method that we validated in chapter 5, to 1) investigate the role of direct adhesion to stroma and of exposure to soluble factors in mediating MM cell survival and drug resistance; 2) to investigate altered signal transduction in the stromal microenvironment and how it relates to drug resistance in MM cells and finally, 3) to investigate the ability of chemotherapy to modulate cytokines secreted in the BMM and to relate this to chemosensitivity.

Prior to addressing these aims, we assessed the use of another technique to measure viability of MM cells in the MM/HS-5 cocultures. Previous studies using the guava assay (presented in chapter 5) demonstrated that it was a useful tool in measuring cell growth in suspension cells; however, a potential limitation of this method may be its difficulty in detecting myeloma cells that are firmly adhered to HS-5 cells in the cocultures. We therefore removed this potential source of inaccuracy by harvesting and using both cell populations present in the cocultures (HS-5 and MM cells) in a flow cytometry assay. Our results confirmed that CD38 labelling coupled with PI labelling (double staining technique) allowed us to efficiently distinguish MM cells (always positive for CD38) from HS-5 cells (which always stained negative for CD38), thus enabling more accurate measurement of MM cell viability than the guava assay. This technique was thus used in all subsequent experiments presented in this chapter.

Our first set of experiments using the adhesion-transwell-conditioned media models demonstrated that MM1.S cells were more reliant on direct stromal cell adhesion than on soluble factors for resistance to spontaneous and drug-induced apoptosis. This may be partly attributable to the IL-6-independence of MM1.S cells. This is confirmed by their lack of expression of IL-6 mRNA (Teoh and Anderson 1997) and by our finding that they express the IL-6 receptor at lower levels than the IL-6-dependent HMCLs RPMI8226 and U266, which was first documented by Catlett-Falcone (Catlett-Falcone, Landowski et al. 1999). Therefore, MM1.S cells may be less responsive to autocrine IL-6-signaling; however our signal transduction studies demonstrated that MM1.S

adhesion to HS-5 cells induced STAT-3 activation. Thus, STAT-3 activation in IL-6 independent cells may require triggering by BMSCs via a paracrine mechanism, and MM1.S cell proliferation in response to exogenous IL-6 (as other groups, including ours have previously shown) confirms this conclusion.

Importantly, the transwell assays provided confirmation of our previous findings demonstrating the increased efficacy of the melphalan pre-exposure combination schedule compared to bortezomib pre-exposure or the simultaneous combination of melphalan and bortezomib. Furthermore, and in contrast, to the MM1.S results, it demonstrated that soluble factors played a more important role in mediating survival and resistance to bortezomib and melphalan in the primary MM samples studied.

In support of this, STAT-3, P38 MAPK, Akt and NFκB were all constitutively activated in primary MM cells. This is supported by data from several studies showing that between 48%-63% of all primary MM cells show constitutive STAT-3 activation, indicative of an autocrine mechanism for the production of IL-6 (Catlett-Falcone, Landowski et al. 1999; Quintanilla-Martinez, Kremer et al. 2003; Bharti, Shishodia et al. 2004; Chatterjee, Stuhmer et al. 2004; Voorhees, Chen et al. 2007). These pathways were further up-regulated upon MM cell adhesion to stroma and this is in accordance with previous studies (Chatterjee, Stuhmer et al. 2004).

Therefore, we have so far demonstrated that stimulation with IL-6 or other soluble factors occurs via predominantly paracrine (via adhesion to BMS) and in some cases autocrine mechanisms in primary MM cells leading to increased activation of a signal transduction cascade via the JAK/STAT-3 and MAPK pathways. This may lead to Akt- and NFκB-mediated growth, survival and drug resistance via transcription of pro-survival/anti-apoptotic mediators. In further support of this, the MAPK pathway has been implicated in conferring resistance to both bortezomib and dexamethasone (Yasui, Hideshima et al. 2007) which again is in agreement with our findings and with those of Perez et al who used comparable concentrations of bortezomib (Perez, Parquet et al. 2009). On the other hand, Hideshima et al used doses 3-4-fold higher than the EC_{50} concentration of bortezomib in MM1.S cells and at these high doses,

showed that bortezomib did inhibit signaling via STAT-3 and the MAPK pathways (Hideshima, Chauhan et al. 2003; Mitsiades, Mitsiades et al. 2003). We did not examine the effects of higher doses of bortezomib in this study but it is possible that this may have led to more effective pathway inhibition. Our studies have however demonstrated that the activity of bortezomib in primary MM cells most likely occurs via mechanisms unrelated to an effect on soluble factors produced in the BMM; and this may instead represent a mechanism of resistance to bortezomib, and also to melphalan. As mentioned above, the BMM is known to protect MM cells from dexamethasone-induced cytotoxicity; and our studies suggest this occurs via the upregulation of MAPK signaling. Interestingly, UCL67022 was the only agent that downregulated phosphorylation of all proteins studied except ERK1/2. This prompted us to investigate this agent further in experiments in which we more closely examined the presence and role of soluble factors on MM chemosensitivity in the HS-5/MM model.

Results from the cytokine profiling studies demonstrated that bone marrow stroma (HS-5 and hBMSCs) secreted high levels of the humoral growth factors: IL-6, IL-8 and VEGF. To confirm that the decrease in IL-6 protein detected was not due to masking of IL-6 by the sIL-6R, we evaluated if BMSCs expressed the sIL-6R. The sIL-6R was not detected in untreated cells or in drug-treated cells, suggesting the sIL-6R is not interfering with our detection of IL-6 protein in cell culture supernatants. More importantly, the adherence of BMS to MM cells triggered upregulation in the secretion of these factors into the BM milieu, which is consistent with our findings demonstrating upregulation of cytokine-induced signaling pathway activation upon MM-stromal interaction. This occurs via binding of IL-6, IL-8 and VEGF to their respective receptors CXCR1, CXCR2, VEGFR-1 and VEGFR-2 on MM cells (Cross and Claesson-Welsh 2001; Waugh and Wilson 2008) thereby activating signalling via the JAK/STAT, MAPK and PI3K/Akt pathways.

Furthermore, MM1.S or primary MM cells did not contribute to cytokine secretion unless they were cocultured with BMSCs, in keeping with paracrine loops. The only factor released by MM1.S cells was VEGF as demonstrated by earlier studies (Dankbar,

Padro et al. 2000; Gupta, Treon et al. 2001; Vacca, Ria et al. 2003). Others have shown that MM cell interaction with BMSC increases the secretion of IL-6 from stromal cells (Uchiyama, Barut et al. 1993; Thalmeier, Meissner et al. 1996; Gupta, Treon et al. 2001), and Gupta et al have also confirmed that this occurs with VEGF; however to our knowledge similar findings have not been demonstrated for IL-8 (currently thought to be secreted solely by endothelial cells and mast cells (Ria, Reale et al. 2011)) and this represents a novel finding.

Importantly, 10 to 30-fold higher concentrations of cytokines were released by hBMSCs than by HS-5 stroma and this was associated with a complete abrogation in the ability of bortezomib to reduce cytokine secretion in primary MM cocultures. This indicates that the efficacy of bortezomib in MM does not involve an effect on humoral factors secreted in the BMM and highlights the importance of studying the disease process in a more clinically relevant model using human-derived samples.

In contrast, melphalan (100μM) modulated secretion of IL-6, IL-8 and VEGF from HS-5 cells, and this was largely maintained in MM/BMSC cocultures. The only other study showing a similar effect was recently reported and found that 50μM melphalan reduced IL-6 secretion from BMSCs, which was associated with decreased expression of IL-6 mRNA (Rellick, Piktel et al. 2012). The mechanism for this did not involve IL-6-regulating transcription factors such as NFκB, nor was it fully explained by accumulation of DNA damage, however, this effect was maintained in a MM/BMSC microenvironment model similar to that used in this study. This study however did not investigate effects on IL-8 or VEGF secretion. Therefore our study is the first to demonstrate the additional connection between melphalan and IL-8 and VEGF, which potentially has important therapeutic implications (discussed below).

We did not find any beneficial effects of combining bortezomib with melphalan in the context of cytokine modulation; however we did find direct correlations between levels of secreted IL-8 and resistance to bortezomib ($p= 0.017$) and levels of IL-8 and VEGF with resistance to melphalan ($p=0.037$ and 0.032, respectively). Furthermore, levels of IL-6 were associated with resistance to both these drugs and to their

combination in primary cocultures. Such findings have not previously been described and thus represent a novel finding suggesting that IL-6, IL-8 and VEGF generated in the BMM synergise to promote MM cell growth and resistance to bortezomib and melphalan. In addition, we demonstrated that the novel HDACi, UCL67022 was even more effective at modulating cytokine secretion in HS-5 and hBMSC stroma and this was maintained in MM/HS-5 cocultures and in MM/hBMSC cocultures. The latter result did not reach significance and this is most likely due to the small sample size used, which was due to very limited availability of patient bone marrow samples. This is therefore the first time that such effects of UCL67022 have been described, and these findings have been recently submitted for publication in a peer reviewed journal.

Of particular therapeutic significance, Gupta et al demonstrated that anti-human neutralising antibodies against both VEGF and IL-6 reduced their secretion from BMSCs and from MM/BMSC cocultures, an effect that was similarly observed with a thalidomide analogue (Gupta, Treon et al. 2001). Due to the potential therapeutic application of this in MM where serum and plasma levels of IL-6, IL-8 and VEGF are increased in patients and reflect disease severity (Klein, Wijdenes et al. 1991; Nachbaur, Herold et al. 1991; Emile, Fermand et al. 1994; Alexandrakis, Passam et al. 2003; Kuku, Bayraktar et al. 2005), we next investigated the effect of neutralising antibodies to IL-6, IL-8 and VEGF in our coculture model. Specifically, we hypothesised that its use may reverse the protection conferred by BMSCs to the effects of bortezomib and melphalan.

We found that pre-treatment of stroma with IL-6, IL-8 or VEGF antibodies singly or in combination had little effect on survival of MM1.S cells indirectly cocultured with HS-5 stroma (in the transwell model) and treated with bortezomib, melphalan or their combination. This was not surprising as both agents were able to reduce cytokine secretion in MM1.S cocultures thus invalidating cytokine neutralisation as a method of restoring drug sensitivity in this cell line. In contrast and more importantly, the simultaneous neutralisation of 2 antibodies resulted in an additive effect in primary MM cells especially when anti-IL-8 and anti-VEGF were combined; and the highest neutralising effect was observed when all 3 antibodies were used simultaneously.

The therapeutic implications of these findings may apply to other haematological malignancies in which pre-treatment plasma levels of IL-6, IL-8 and VEGF were found to be the highest out of eight angiogenesis-related parameters (Negaard, Iversen et al. 2009). Use of anti-IL-6 monoclonal antibodies has been explored, and studies are on-going with agents such as the fully human mAb 1339. This has shown antimyeloma activity in a preclinical model and inhibition of bone marrow turnover *in vitro* and *in vivo* (Fulciniti, Hideshima et al. 2009). Siltuximab (CNTO328) is a chimeric mAb with high affinity for IL-6. It has showed little efficacy as monotherapy in a phase II study in patients with relapsed/refractory MM; however more encouraging results were observed with the addition of dexamethasone (Voorhees, Chen et al. 2007) and its clinical evaluation is currently on-going.

Studies suggest that elevated pre-treatment levels of VEGF do not necessarily imply that anti-VEGF drugs are effective, as this did not correlate with response to the anti-VEGF monoclonal antibody bevacizumab (Avastin) in metastatic colorectal cancer or in advanced pancreatic cancer (Jubb, Oates et al. 2006). On the other hand, the IMiDs thalidomide and lenalidomide have been shown to reduce secretion of VEGF and IL-6 in MM/stromal cocultures resulting in reduced MM growth and angiogenesis (Gupta, Treon et al. 2001; Hideshima, Chauhan et al. 2001; Ribatti and Vacca 2005). Furthermore, bortezomib has also been found to display antiangiogenic effects including inhibition of caveolin-1 activation which is required for VEGF-mediated MM cell migration (Podar and Anderson 2006). To this end, on-going studies are evaluating the efficacy of bevacizumab in patients with relapsed or refractory MM, with or without thalidomide (Podar, Chauhan et al. 2009) and other studies are exploring the combination of bortezomib with bevacizumab or with sorafenib (which targets VEGF1, and VEGF2 amongst other kinases).

In terms of IL-8, humanised monoclonal antibodies such as ABX-IL-8 have been shown to attenuate the growth of bladder cancer xenograft models (Mian, Dinney et al. 2003), to decrease the tumorigenenic and metastatic potential of A375SM and TXM-13 melanoma xenograft models and to enhance the cytotoxicity of chemotherapy in melanoma (Huang, Mills et al. 2002). In ovarian tumour xenografts use of liposome-

encapsulated small interfering RNA (siRNA) suppressed IL-8 expression which resulted in growth inhibition, reduced microvessel density and importantly, increased response to docetaxel (Merritt, Lin et al. 2008). Therefore, targeting IL-8 through use of antibodies or siRNA has proven effective in some solid tumours; however these strategies have not yet been evaluated in MM. Data presented here provides compelling evidence towards the further evaluation of IL-8 and VEGF antibodies both alone and in combination with IL-6 antibodies in MM. This study also supports further investigations into UCL67022-induced immunomodulation in MM.

CHAPTER 7 Final Discussion and Conclusions

7.1 Discussion

Although treatments for haematological malignancies have improved over recent years, there remains a clear need for better therapies: less than 50% of patients with DLBCL are cured with conventional therapeutic approaches and although FL is associated with a median survival of 8-10 years, treatment is characterised by recurrent relapses and the majority of patients will either die as a result of the disease or as a complication of therapy (Gribben 2007). MCL is a rarer more aggressive subtype with a very poor prognosis as responses to chemotherapy and survival are short. CLL is the commonest form of leukaemia in western countries and despite the success of first line therapy in advanced disease the vast majority of patients relapse and require additional lines of established therapies, transplantation or novel therapies. These approaches are less effective than first line treatments and over 1000 CLL patients in the UK go on to die of their disease each year (CRUK 2010). MM remains an incurable disease with conventional therapies and is associated with the sixth worst 5 year survival rates out of the 18 most common cancers in the UK (CRUK 2010) with median overall survival of just 3 to 4 years (Smith, Wisloff et al. 2006). Whilst an improvement in overall survival has been reported in the last decade, the chemotherapy used is toxic and because these malignancies affect mainly older patients, are often not well tolerated. Thus relapses and subsequent resistance to therapy is common to all haematological malignancies and their prognosis remains poor. This underpins the need for new treatment strategies and novel drug therapies.

Thalidomide and subsequently bortezomib were among the first of these novel therapies tried for MM and bortezomib was licensed for EU clinical use in patients with MM in 2004. At the time this course of study was undertaken, little data was available on the effects of bortezomib in lymphoma and a multicentre phase II clinical trial of the drug in patients with relapsed/refractory NHL was underway, in which St. Bartholomew's Hospital was participating. This provided us with samples collected

from patients receiving bortezomib in the trial to use in *in vitro* investigations of the drug. Access to additional non-trial NHL, CLL and MM samples allowed us to also investigate the use of bortezomib in combination with standard chemotherapies, and with novel targeted approaches. The aim of these combination studies was to identify was to increase the efficacy of already approved agents, thereby improving treatment outcomes for patients with haematological malignancies.

Central to fulfilling these aims was the development and validation of *in vitro* primary coculture models that would promote the short-term growth of patient-derived cells, thus enabling the study of these diseases in more clinically relevant models than cell lines. Even though numerous human leukaemia/lymphoma and multiple myeloma cell lines are available for use in pre-clinical studies, and these are a valuable resource for initial drug activity investigations, their weaknesses preclude the extrapolation of data generated in them to the *in vivo*/clinical situation. Such weaknesses include their continual evolution over time during which they acquire mutations not present within a patient; and that they do not fully reflect all the heterogeneity observed in patients or the requirement for stromal interactions. Therefore, cell line studies should be followed by more relevant pre-clinical models (using patient-derived tumour cells) and *in vivo* animal models.

Patient-derived tumour samples are useful for examining characteristics of a patient's own tumour and for individualising their therapy; however unlike cell lines which can proliferate exponentially without basic support, patient-derived tumour cells cannot survive long-term in culture without support from closely associated non-malignant stromal and immune cells present in the tumour microenvironment. Based on this requirement, we refined and validated two different primary coculture models (NHL and MM) which we hoped would to some extent mimic the growth of tumour cells within their *in vivo* microenvironment. We then used these models to investigate the translational potential of our *in vitro* drug activity studies.

The NHL coculture model utilised the growth stimulatory action of CD40 ligation on B-cells as the basis of the culture system. Our version of the 'CD40 system' involved using

an adherent feeder monolayer of fibroblastic CHO cells transfected to express the CD40L to an overlying layer of primary B-cells in suspension. Validation studies established that irradiated CHO-CD40L cells did not proliferate in this model, efficiently presented CD40L to MCL and FL cells and enhanced their growth and survival over 72hrs of culture whilst preserving their immunophenotype.

We were able to apply this model to samples obtained from patients with relapsed or refractory NHL receiving bortezomib in the first European multicentre phase II trial of the drug. This allowed the generation of *in vitro* and *in vivo* sensitivity data in the same patient. Although the number of trial patients in whom this was possible was small, the results demonstrated that *in vitro* sensitivity predicted the clinical response to bortezomib in all patients, findings not previously described (Strauss, Maharaj et al. 2006). This assay has now been reported in other drug development studies, although not alongside clinical data with the same drug (Oltersdorf, Elmore et al. 2005; Tromp, Tonino et al. 2010; McCaig, Cosimo et al. 2011).

Additionally, a difference in *in vitro* sensitivity was demonstrated between MCL and FL samples, in line with that observed in the clinical trial; and this was not a function of the culture system as sensitivity to doxorubicin was comparable between both NHL subtypes. Because the time to response in the trial also differed (median of 5 weeks of treatment in MCL compared with a median of 11 weeks of treatment in FL), it is likely that bortezomib induces cell death by different mechanisms in these lymphomas (Holford and Sheiner 1982). Finally, *in vitro* sensitivity of MCL samples correlated with their CD40 expression, suggesting that CD40 could potentially act as a surrogate biomarker for response to bortezomib in this subset of patients.

Having established the value of using this *in vitro* model to study drug activity in NHL; we then used it to investigate the therapeutic benefit of combination therapy involving bortezomib. Since proteasome inhibitors have distinct mechanisms of action and do not share mechanisms of chemoresistance with conventional chemotherapies, they are a rational addition to standard agents. As such, there are currently a high number of clinical studies exploring its integration into standard regimens used in the

treatment of NHL including cyclophosphamide-doxorubicin-vincristine, and prednisone (CHOP), (plus rituximab (R-CHOP)) and R-EPOCH, rituximab-cyclophosphamide-predinisone and fludarabine (Dreyling 2010; Tilly and Dreyling 2010). We investigated the simultaneous combination of bortezomib with doxorubicin in the coculture model; however we did not observe any synergism in the primary samples studied. This may be partly explained by the fact that the majority of patients had been previously exposed to anthracycline therapy and may have developed a resistance to them. Furthermore, the effect of scheduling may be an important factor, which was not explored in this study.

In recent years, a number of preclinical studies have demonstrated synergistic apoptosis with the combination of bortezomib with HDACis, including vorinostat, romidepsin and panobinostat, amongst others (Heider, von Metzler et al. 2008; Paoluzzi, Scotto et al. 2009; Dasmahapatra, Lembersky et al. 2010; Paoluzzi, Scotto et al. 2010; Rao, Nalluri et al. 2010). We have now provided convincing evidence demonstrating the potent antitumour effects of UCL67022 (representing a new class of hydroxamate-based HDAC inhibitor), not only in NHL cells lines but also in different NHL subtypes: DLBCL, MCL, FL and CLL all cocultured in our CD40 model.

Importantly, UCL67022 demonstrated superior potency compared with vorinostat and this increased potency correlated with increased inhibition of HDAC6 activity as demonstrated by changes in acetylated histone H3 and α-tubulin. Furthermore, in contrast to the doxorubicin combinations, the combination of UCL67022 with bortezomib was highly synergistic in primary samples and was enhanced in comparison with the vorinostat combinations, in line with its increased potency. This is the first preclinical study demonstrating synergy with this novel HDACi and bortezomib in NHL primary samples cultured in this model, and this data is currently being peer-reviewed for publication.

We did not investigate the mechanism for the observed synergy, however, our subsequent studies in multiple myeloma (not shown here) have shown effects on caspase activation and increased ER stress, which is in agreement with reported

findings using other novel HDACis such as the broad spectrum hydroxamic acid PCI-2478; and with vorinostat in combination with next generation proteasome inhibitors such as carfilzomib (Heider, von Metzler et al. 2008; Bhalla, Balasubramanian et al. 2009; Rao, Nalluri et al. 2010). In addition, we demonstrated abrogation of bortezomib-induced aggresome formation with UCL67022 (Maharaj, L; Popat, R et al. manuscript submitted; Maharaj L, Popat R, Maharaj L. EHA 2008) and this has recently been associated with marked reduction in proteasome and NFκB activity, expression of NOXA and CHOP, increased ROS and induction of lethal unfolded protein response (UPR) (Dasmahapatra, Lembersky et al. 2010; Rao, Nalluri et al. 2010). Based on these findings, combined with its more favourable toxicity profile (including its minimal toxicity to normal PBMCs), this agent merits evaluation further in *in vivo* studies.

An important aspect to this project was the validation and standardisation of the *in vitro* coculture models. This was reflected in improvements made to the NHL primary culture model. We originally used a 2-dimensional coculture platform employing an irradiated murine fibroblastic feeder layer as a constant source of CD40 ligand. As work progressed, we observed that use of a recombinant human soluble form of CD40 ligand (sCD40L) completely obviated the need for the fibroblast layer thus simplifying and increasing reproducibility of the model. Furthermore, it allowed us to circumvent problems associated with distinguishing the B-cells from the fibroblast monolayer, which is vital for downstream mechanistic studies.

Another advantage was that it supported the growth of primary CLL cells and our subsequent work using this new version, enabled identification of several novel PI3Kδ inhibitors with potent activity in CLL, some of which have since been selected for further development in human clinical trials (data not presented in this thesis). Its use has also enabled demonstration of the greater efficacy of the dual PI3Kα/δ inhibitor, GDC-0941, compared with the most clinically progressed PI3Kδ inhibitor, GS-1101 in MCL patients (Iyengar, Clear et al. 2013). Since MM cells express CD40 on their surface, (van Kooten and Banchereau 2000; Eliopoulos and Young 2004), we investigated the use of the sCD40L model in validation studies for development of the *in vitro* multiple myeloma model.

Somewhat surprisingly, CD40 stimulation did not result in significant induction in cell growth of primary CD138 positive MM cells, even though this has been previously shown to occur (Urashima, Chauhan et al. 1995; Tai, Podar et al. 2003). We speculated that these results did not reach statistical significance due to the limited number of samples used. We were unable to address this issue in more primary MM cells as obtaining sufficient MM cells from bone marrow samples was a huge limiting factor in these studies. In contrast, results indicated that the use of an EBV transformed BMSC cell line HS-5, caused a significant improvement in primary MM cell viability and induced their proliferation over a 72hr culture period. It is now believed that BMSCs are the main source of soluble growth factors (although some MM cells are capable of autonomous secretion) which support the growth and survival of MM cells in the BMM. Therefore, the growth stimulatory effects of HS-5 cells observed in these experiments provided important validation of our MM/BMSC coculture model incorporating this vital aspect of the tumour microenvironment. Ideally, we would have used BMSCs derived from bone marrow aspirates from patients with MM; however, as stated above, the availability of such samples was the limiting factor.

Another limitation of this model is that MM cells are known to proliferate slowly *in vivo* and stop dividing *in vitro* with a resulting fall in viability over time. We observed variability in MM cell growth in our model and subsequently the cells that do proliferate may have a more aggressive phenotype. Furthermore, in samples in which there were sufficient quantities of bone marrow aspirate, we found variation in their ability to generate adequate numbers of stromal cells suggesting that their ability to produce cytokines may differ between patients. This implies that the hBMSCs used in these experiments would tend to be those that grow well and can support MM cell growth. In light of this, the HS-5 cell line has the added advantage of maintaining the reproducibility of results thus allowing standardisation of the model.

In keeping with published studies, bortezomib retained potent activity in the MM coculture model, whilst dexamethasone did not. Encouragingly, UCL67022 also displayed the ability to overcome the growth-promoting effects of HS-5 stroma; and the activity of melphalan was partially abrogated. The most striking finding however

was a highly synergistic, schedule-dependent cytotoxic effect when primary MM cells were pre-treated with melphalan followed by bortezomib. Synergy was also observed for the simultaneous and bortezomib pre-treatment schedules, although combination index values generated by Calcusyn analysis suggested an enhanced effect of melphalan pre-treatment. Synergistic effects of this combination have been previously observed however; a scheduling effect was not noted. Furthermore, until now, this combination had not been examined in the context of the BMM (Ma, Yang et al. 2003; Mitsiades, Mitsiades et al. 2003).

Data produced subsequently in our group by Dr. Rakesh Popat suggested a mechanism for this schedule dependency involving the rise in anti-apoptotic molecules such as Mcl-1, Akt and heat shock proteins as a result of proteasome inhibition which may render cells more resistant to cell death and subsequently decrease the effect of melphalan administered 24hrs later (Popat, Maharaj et al. 2012). On the other hand, melphalan induces double stranded DNA breaks following formation of inter-strand cross-links (ICLs) (Spanswick, Craddock et al. 2002). Bortezomib prevents ICL repair by inhibition of DNA protein kinases (Mitsiades, Mitsiades et al. 2003) and the Fanconi anaemia complex (Yarde, Oliveira et al. 2009). Consequently, when bortezomib administration follows melphalan, cells sustain irreversible damage leading to apoptosis.

These findings could have larger implications due to the high number of clinical trials currently investigating bortezomib in combination with a variety of cytotoxics. For example, the combination of bortezomib, melphalan and prednisolone has recently been demonstrated to improve progression free survival of elderly patients with MM when compared to melphalan and prednisolone (San Miguel, Schlag et al. 2008). Results presented here therefore warrant the further clinical evaluation of the melphalan pre-treatment schedule which may allow lower drug doses to be used thus reducing treatment-related toxicities.

Use of transwell assays to examine the interactions occurring between the MM cells and the stromal and soluble components in our coculture model demonstrated an

important role for soluble factors in protecting MM cells from the cytotoxic effects of bortezomib and melphalan. This was confirmed by intracellular signal transduction studies which indicated that resistance to these agents was associated with upregulation of cytokine-induced JAK/STAT-3 and MAPK signalling. To further investigate this we performed cytokine profiling experiments on drug-treated coculture supernatants. In keeping with published findings, a largely paracrine mechanism for IL-8 as well as IL-6 production in MM cells was observed. The most interesting finding however, was high levels of IL-6, IL-8 and VEGF originating mainly from BMSCs, which directly correlated with resistance to bortezomib and melphalan and to the combination of both drugs. Importantly, hBMSCs secreted higher levels of these cytokines than HS-5 cells, proving that this also occurs *in vivo*, thus further validating our *in vitro* model. Overall, these data suggest that adhesion of MM cells to BMSCs triggers paracrine secretion of IL-6, IL-8 and VEGF which synergistically activates key intracellular anti-apoptotic, pro-survival signalling pathways such as JAK/STAT, MAPK and PI3K/Akt pathways. This leads to the promotion of MM cell growth, proliferation, angiogenesis and ultimately resistance to commonly used chemotherapeutics.

As serum and plasma levels of IL-6, IL-8 and VEGF are increased in patients with MM and reflect disease severity, and as levels of all three cytokines correlated with resistance to bortezomib and melphalan, our final investigations focused on the effect of cytokine neutralization in the BMM. Results demonstrated that the simultaneous neutralization of two antibodies resulted in an additive effect in primary MM cells especially when anti-IL-8 and anti-VEGF were combined, and the highest neutralising effect was observed when all three antibodies were used simultaneously, resulting in restored drug sensitivity. The therapeutic implications of these findings are of importance and may apply to other haematological malignancies where it has been found that pre-treatment plasma levels of IL-6, IL-8 and VEGF were the highest out of eight angiogenesis-related parameters (Negaard, Iversen et al. 2009).Furthermore, whilst IL-6 neutralising antibodies are being evaluated in the clinic, this data provides compelling evidence towards the further evaluation of IL-8 and VEGF antibodies both alone and in combination.

With regard to the effects of UCL67022 in this system, we demonstrated its effective inhibition of secretion of IL-6, IL-8 and VEGF from BMSCs and in MM/BMSC cocultures (both MM/HS-5 and MM/hBMSCs). Furthermore, it effectively downregulated STAT-3 and NFκB phosphorylation in MM/HS-5 cocultures. This suggests that the activity of UCL67022 in MM may partly be explained by its ability to overcome the protective effects of BMSCs by directly modulating cytokine secretion in the BMM. As high *in vivo* levels of phosphorylated STAT-3 have been shown to predict for poor responses to vorinostat (Fantin, Loboda et al. 2008), these data suggests better responses may be achieved using UCL67022. We demonstrated the synergistic effects of combining UC67022 with bortezomib in our primary NHL coculture model, and Dr. Rakesh Popat recently demonstrated the efficacy of targeting both proteasome-dependent pathways with bortezomib and the aggresome pathway with UCL67022 in MM. These data therefore provide further evidence to support the *in vivo* investigation of UCL67022 in combination with bortezomib in MM.

It is noteworthy that the MM/hBMSC milieu was found to be far more cytokine-rich compared to the MM/HS-5 milieu and this may have important consequences on drug resistance in the *in vivo* BMM. Under these circumstances, it would be preferable to use patient-derived stromal cells in *in vitro* investigations and although we did not attempt signalling experiments using primary stroma, this may also be the case for such studies. This again highlights the significance of using the most relevant *in vitro* model when results are to be extrapolated to the clinical setting.

Our final investigations into novel drug therapy in MM involved studying the effects of a novel Hsp90 inhibitor; KW-2478, in collaboration with Kyowa Hakko Kirin Ltd. Excessive production of immunoglobulin by MM cells may render them particularly sensitive to the effects of Hsp90 inhibition; which leads to an accumulation of mis/un-folded cellular proteins (Davenport, Moore et al. 2007). Furthermore, as Hsp90 is involved in the stabilisation of multiple client proteins involved in apoptosis and tumour angiogenesis, its inhibition leads to combinatorial inhibition of multiple proliferative signal transduction pathways (Mitsiades, Mitsiades et al. 2006). KW-2478 demonstrated potent activity in primary MM cells, when cultured in the presence or

absence of a stromal microenvironment. Importantly, there was evidence of a therapeutic window as normal PBMCs from healthy donors were not sensitive to the cytotoxic effects of the drug, and this suggests that KW-2478 is likely to maintain its effect *in vivo*.

Our combination investigations revealed a sensitising effect of KW-2478 to the effects of bortezomib in primary MM cells, suggesting that resistance to bortezomib can be overcome using KW-2478. Results from an on-going phase I/II multicentre trial in patients with relapsed and/or refractory MM are awaited in order to confirm this hypothesis (NCT01063907). Subsequent studies in our group suggest that the synergy observed with this combination may be due to an overloading of the protein degradation machinery, leading to accumulation of unfolded protein and consequent stress response (UPR). Further data not shown here suggests that this may be mediated by the induction of Noxa (Ishii, Seike et al. 2012). Another interesting finding was a KW-2478-induced increase in the expression of Hsp70 in primary MM samples. This occurs as a compensatory response to Hsp90 inhibition and was also found in the combination studies, in particular in a homologue of Hsp70, Hsp70B. This suggested the potential use of Hsp70B as a surrogate biomarker to monitor the combinatorial effect of Hsp90 inhibition via KW2478 and bortezomib in future clinical trials.

These findings led to evaluation of the combination of bortezomib with KW-2478 in a NCI-H929 s.c. inoculated model and in an OPM-2/GFP orthotopic model (performed by Kyowa Hakko Kirin Ltd.), using a twice-weekly administration schedule similar to the clinical administration schedule of bortezomib. In both *in vivo* models, the combination showed beneficial activities, supporting and confirming our *in vitro* results. The enhanced anti-tumour activity observed in the OPM-2/GFP orthotopic model may be particularly informative, as this model is considered to be more relevant to the pathological condition in MM. Overall, these data provide evidence for further investigation of the KW-2478/bortezomib combination in the clinic, specifically suggesting the potential benefit of a twice-weekly administration schedule (Ishii, Seike et al. 2012). Furthermore, Since KW-2478 has superior physicochemical and toxicological properties to 17-AAG (the most clinically progressed Hsp90 inhibitor) the

combination of KW-2478 and bortezomib is expected to be more promising. As mentioned, the phase I/II study of KW-2478 in combination with bortezomib is currently on-going, results of which are eagerly anticipated.

Synergistic effects were also observed with the combination of low dose melphalan with KW-2478, in the primary coculture model. Additional work not presented here, indicated that KW-2478 treatment resulted in decreases in key client proteins such as Grp78, p-Akt including total Akt, c-Raf and also one of the major receptors for growth factors in MM, IGF-1R. Furthermore, a huge induction of Hsp70 with the melphalan/KW-2478 combination was observed; thus strengthening our previous findings. Results from a subsequent *in vivo* study (Kyowa Hakko Kirin Ltd.) demonstrated that this combination remained effective in an animal model as it resulted in an additive reduction of tumour growth compared to the animal groups that received single agents only. As a quantitative method of monitoring the progression of MM in this study, levels of paraprotein M in the serum of each individual was measured at the end of the experiment (Blade, Samson et al. 1998). This method was used as an indication of the ability of KW-2478 to cause a partial remission (PR) by reducing serum M protein levels. Only the combination treatment caused a <50% reduction in the serum M protein indicating its superiority over administration of the single agents over 28 days in SCID mice (data currently in preparation for publication). Therefore, the *in vitro* and *in vivo* data collectively provide strong evidence for the further clinical evaluation of the combination of KW-2478 and melphalan in MM.

7.2 Future directions and conclusions

To aid our understanding of the action of bortezomib *in vivo,* we would recommend further investigations into the role of CD40 signalling in MCL cells in the coculture model with immunohistochemical analysis of biopsy samples from all patients that were enlisted on the phase II trial of bortezomib. With regard to UCL67022, studies into activation of the ER stress response are warranted as well as acetylation of Hsp90

and its client proteins, when UCL67022 is used singly as well as in combination with bortezomib. It is likely that these processes will be disrupted, as suggested by previous studies with 17-AAG. The subsequent evaluation of UCL67022 in an animal model would also be desirable.

Further investigations on the proposed mechanism for the synergistic interaction between bortezomib and melphalan could be performed. To confirm that increases in anti-apoptotic molecules following bortezomib exposure transiently decrease the subsequent sensitivity of MM cells to other agents, a selective reduction of each molecule is required. Therefore, siRNA to Mcl-1 could be used to assess its individual contribution. The next step would be to confirm the schedule effect in an *in vivo* model. As the safety profiles of both bortezomib and melphalan are already established, it would be ethical to run a randomised clinical trial between the different schedules, based on the MTD defined by biological effect such as an induction in apoptosis.

During the time that this work was undertaken, there was no experience with the use of culture systems of primary MM in the laboratory. There is therefore much room for further development of this model in the future. Such studies could include osteoblast/osteoclast/MM cell triple cultures. This is an important avenue of investigation in MM as more than 80% of myeloma is associated with induction of osteolytic bone disease (Bataille, Chappard et al. 1991). This model could potentially be useful in identifying novel agents that target and inhibit osteoclastogenesis in myeloma. However, drawbacks include its complexity and the time and labour intensive protocols. Substantial cost is associated with using large amounts of cytokines to stimulate differentiation of the generated mesenchymal stem cells (MSCs) into either osteoblasts or osteoclasts, and finally the large starting MSC cell numbers required (~$2.5x10^6$ cells) (Yaccoby, Wezeman et al. 2006) is difficult to acquire from a typical marrow sample.

Furthermore, this assay focuses more on the effect of osteoclasts and osteoblasts and does not include other vital stromal components. Perhaps the way forward is to

generate a system that allows assessment of drug effect on both stromal-induced and osteoclast-induced MM cell survival. Currently, 3-dimensional (3D) tissue culture models for *in vitro* drug testing are being investigated, as they may be a more accurate representation of cell shape, tissue architecture and microenvironmental interactions than 2D BMSC assays. 3D fibroblast spheroids cocultured with suspensions of haematopoietic cells is now enabling investigations of tumour cell invasion or migration and mobility in haematopoietic malignancies (Bug, Rossmanith et al. 2002). In MM, 3D myeloma culture is being investigated where the MM clone expands within a reconstructed bone marrow endosteum; a microenvironmental niche where MM cancer stem cells (CSCs) concentrate and which are thought to give rise to a drug-resistant tumour cell population responsible for patient relapse (Kirshner, Thulien et al. 2008). Similarly, 3D collagen sponge scaffolds (resembling the organic component of bones) have been used to study cytokine production by BMSCs in patients with myeloma (Zdzisinska, Rolinski et al. 2009).

A commonality amongst these 3D models seems to be the complexity and their associated time and cost components compared to 2D cultures. As development of these systems is still in their infancy, a simple, controlled technique and protocol for a rapid, standardized assay, does not yet exist and thus 3D spheroids have not yet been adopted in pre-clinical drug screening tests. Furthermore, they do not provide information on pharmacokinetic factors in drug testing such as absorption, distribution, metabolism and elimination (ADME) and thus can never fully replace animal models. As current technology improves and the associated cost of using such systems decreases, these assays may represent the future in pre-clinical drug-sensitivity testing.

In conclusion, the further development, and standardisation of *in vitro* models of haematological malignancies which utilise patient-derived samples grown in a more biologically relevant format is vital. We have demonstrated that such models have the ability to inform the choice of chemotherapy in the clinical setting. Furthermore, they can be useful in delineating complex *in vivo* tumour microenvironmental interactions responsible for tumour drug resistance, and thereby suggest more effective usage of

current therapies and help identify novel targeted agents. A complimentary two-pronged approach to future management of haematological malignancies may be envisaged involving pre-clinical use of primary culture models followed by quantitative approaches such as gene expression profiling in the same patients enrolled on clinical trials. This would provide new targets for therapy and enable tumour responses to be related to defined tumour phenotypes, whilst increasing the efficiency and cost-effectiveness of the drug development process. It is hoped that this thesis contributes to the body of research to improve this process; and that it contributes to fostering the acceptance of such approaches in cancer research. Ultimately, it is hoped that work presented here, contributes in some small way to improving the survival and quality of life in patients suffering from haematological malignancies.

Publications and abstracts arising from this thesis

Publications:

1. The histone deacetylase inhibitor UCL67022 has potent activity in multiple myeloma and non-Hodgkin lymphoma pre-clinical models. Br J Haematol. 2013 Jul; Epub ahead of print. Maharaj L, Marson CM, Middleton BJ, Rioja AS, Perry J, Oakervee H, Cavenagh J, Joel SP, Popat R.

2. Schedule dependent cytotoxicity of bortezomib and melphalan in multiple myeloma. Br J Haematol. 2013 Jan; 160(1):111-4. Popat R, Maharaj L, Oakervee H, Cavenagh J, Joel SP.

3. P110α mediated constitutive PI3K signaling limits the efficacy of p110δ-selective inhibition in mantle cell lymphoma, particularly with multiple relapse.Blood. 2013 Mar 21;121(12):2274-84. Iyengar S, Clear A, Bödör C, Maharaj L, Lee A, Calaminici M, Matthews J, Iqbal S, Auer R, Gribben J, Joel SP.

4. Anti-tumor activity against multiple myeloma by combination of KW-2478, an Hsp90 inhibitor, with bortezomib. Blood Cancer J. 2012 Apr; 2(4):e68. Ishii T, Seike T, Nakashima T, Juliger S, Maharaj L, Soga S, Akinaga S, Cavenagh J, Joel SP, Shiotsu Y.

5. The proteasome inhibitor bortezomib acts independently of p53 and induces cell death via apoptosis and mitotic catastrophe in B-cell lymphoma cell lines. Cancer Res. 2007 Mar 15;67(6):2783-90.Strauss SJ, Higginbottom K, Jüliger S, Maharaj L, Allen P, Schenkein D, Lister TA, Joel SP.

6. Bortezomib therapy in patients with relapsed or refractory lymphoma: potential correlation of in vitro sensitivity and tumor necrosis factor alpha response with clinical activity. J ClinOncol. 2006 May 1; 24(13):2105-12. Strauss SJ, Maharaj L, Hoare S, Johnson PW, Radford JA, Vinnecombe S, Millard L, Rohatiner A, Boral A, Trehu E, Schenkein D, Balkwill F, Joel SP, Lister TA.

Abstracts:

American Society for Haematology Annual Meetings

1. IL-6, IL-8 and VEGF Neutralisation Restores Drug Sensitivity to Conventional and Novel Treatment Combinations in a Multiple Myeloma Bone Marrow Micro-Environment Model. Lenushka Maharaj, Rakesh Popat, John G Gribben, and Simon Joel (2012 poster presentation).

2. Increased Tonic PI3K Signaling Through p110α Can Limit the Efficacy of P110δ-Selective Inhibition in Mantle Cell Lymphoma, Particularly with Multiple Relapse. Sunil Iyengar, Andrew James Clear, Csaba Bödör, Lenushka Maharaj, Janet Matthews, Rebecca Auer, Sameena Iqbal, John G Gribben, and Simon Joel (2012 poster presentation).

3. PI3K Inhibition with GDC-0941 Has Greater Efficacy Compared to p110δ-Selective Inhibition with CAL-101 in Mantle Cell Lymphoma and May Be Particularly Advantageous in Multiply Relapsed Patients. Sunil Iyengar, Andrew J. Clear, Andrew Owen, Lenushka Maharaj, Janet Matthews, Maria Calaminici, Rebecca Auer, Essam Ghazaly, Sameena Iqbal, John G. Gribben, and Simon Joel (2012 poster presentation).

4. A Novel Heat Shock Protein (HSP) 90 Inhibitor KW-2478 shows Activity in B-Cell Malignancies in Vitro and in Vivo. Simone Juliger, Takayuki Nakashima, Lenushka Maharaj, Toshihiko Ishii, Hiroshi Nakagawa, Yutaka Kanda, Heather Oakervee, James Cavenagh, Shiro Akinaga, Yukimasa Shiotsu, and Simon P Joel (2009 poster presentation).

5. The Novel HDAC Inhibitor UCL67022 Is Highly Potent in Multiple Myeloma and Non-Hodgkin's Lymphoma and Is Enhanced by Bortezomib. Lenushka Maharaj, Rakesh Popat, Angela Chahwan, Andrew T. Lister, James D. Cavenagh, Brian

Middleton, Alf Rioja, Charles Marson, and Simon P. Joel (2007 poster presentation).

6. Mantle Cell and Follicular Lymphoma Samples Demonstrate Differing Sensitivity to Bortezomib in a Primary Culture System. Lenushka Maharaj, Sandra J. Strauss, Jim Stec, Thomas A. Lister, and Simon P. Joel (2005 poster presentation).

7. Phase II Clinical Study of Bortezomib (VELCADE®) in Patients (pts) with Relapsed/Refractory Non-Hodgkin's Lymphoma (NHL) and Hodgkin's Disease (HD).Sandra J. Strauss, Lenushka Maharaj, Jim Stec, Anthony Boral, Elizabeth Trehu, David Schenkein, Simon P. Joel, and T. Andrew Lister (2005 oral presentation).

References

Abe, M., K. Hiura, et al. (2002). "Role for macrophage inflammatory protein (MIP)-1alpha and MIP-1beta in the development of osteolytic lesions in multiple myeloma." Blood**100**(6): 2195-202.

Adams, J. (2003). "The proteasome: structure, function, and role in the cell." Cancer Treat Rev**29** Suppl 1: 3-9.

Adams, J. and M. Kauffman (2004). "Development of the proteasome inhibitor Velcade (Bortezomib)." Cancer Invest**22**(2): 304-11.

Alexandrakis, M. G., F. H. Passam, et al. (2003). "Relationship between circulating serum soluble interleukin-6 receptor and the angiogenic cytokines basic fibroblast growth factor and vascular endothelial growth factor in multiple myeloma." Ann Hematol**82**(1): 19-23.

Allegra, A., E. Sant'antonio, et al. (2011). "Novel therapeutic strategies in multiple myeloma: role of the heat shock protein inhibitors." Eur J Haematol**86**(2): 93-110.

Altman, S. A., L. Randers, et al. (1993). "Comparison of trypan blue dye exclusion and fluorometric assays for mammalian cell viability determinations." Biotechnol Prog**9**(6): 671-4.

Andersen, N. S., J. K. Larsen, et al. (2000). "Soluble CD40 ligand induces selective proliferation of lymphoma cells in primary mantle cell lymphoma cell cultures." Blood**96**(6): 2219-25.

Anderson, K. C. (2007). "Targeted therapy of multiple myeloma based upon tumor-microenvironmental interactions." Exp Hematol**35**(4 Suppl 1): 155-62.

Andreotti, P. E., I. A. Cree, et al. (1995). "Chemosensitivity testing of human tumors using a microplate adenosine triphosphate luminescence assay: clinical correlation for cisplatin resistance of ovarian carcinoma." Cancer Res**55**(22): 5276-82.

Armitage, R. J., B. M. Macduff, et al. (1993). "Human B cell proliferation and Ig secretion induced by recombinant CD40 ligand are modulated by soluble cytokines." J Immunol**150**(9): 3671-80.

Asosingh, K., U. Gunthert, et al. (2001). "A unique pathway in the homing of murine multiple myeloma cells: CD44v10 mediates binding to bone marrow endothelium." Cancer Res**61**(7): 2862-5.

Auer, R. L., J. Gribben, et al. (2007). "Emerging therapy for chronic lymphocytic leukaemia." Br J Haematol**139**(5): 635-44.

Baker, M. P., A. G. Eliopoulos, et al. (1998). "Prolonged phenotypic, functional, and molecular change in group I Burkitt lymphoma cells on short-term exposure to CD40 ligand." Blood**92**(8): 2830-43.

Banchereau, J., F. Briere, et al. (1994). "Molecular control of B lymphocyte growth and differentiation." Stem Cells**12**(3): 278-88.

Banchereau, J., P. de Paoli, et al. (1991). "Long-term human B cell lines dependent on interleukin-4 and antibody to CD40." Science**251**(4989): 70-2.

Banchereau, J. and F. Rousset (1991). "Growing human B lymphocytes in the CD40 system." Nature**353**(6345): 678-9.

Banerji, U. (2009). "Heat shock protein 90 as a drug target: some like it hot." Clin Cancer Res**15**(1): 9-14.

Banfi, A., G. Bianchi, et al. (2002). "Replicative aging and gene expression in long-term cultures of human bone marrow stromal cells." Tissue Eng**8**(6): 901-10.

Barille, S., M. Collette, et al. (1995). "Myeloma cells upregulate interleukin-6 secretion in osteoblastic cells through cell-to-cell contact but downregulate osteocalcin." Blood**86**(8): 3151-9.

Barton, B. E. (2005). "Interleukin-6 and new strategies for the treatment of cancer, hyperproliferative diseases and paraneoplastic syndromes." Expert Opin Ther Targets**9**(4): 737-52.

Bataille, R., D. Chappard, et al. (1991). "Recruitment of new osteoblasts and osteoclasts is the earliest critical event in the pathogenesis of human multiple myeloma." J Clin Invest**88**(1): 62-6.

Bataille, R., M. Jourdan, et al. (1989). "Serum levels of interleukin 6, a potent myeloma cell growth factor, as a reflect of disease severity in plasma cell dyscrasias." J Clin Invest**84**(6): 2008-11.

Baumann, M., S. M. Bentzen, et al. (2001). "The translational research chain: is it delivering the goods?" Int J Radiat Oncol Biol Phys**49**(2): 345-51.

Baumann, P., S. Mandl-Weber, et al. (2009). "The novel orally bioavailable inhibitor of phosphoinositol-3-kinase and mammalian target of rapamycin, NVP-BEZ235, inhibits growth and proliferation in multiple myeloma." Exp Cell Res**315**(3): 485-97.

Baumann, P., S. Mandl-Weber, et al. (2009). "Dihydroorotate dehydrogenase inhibitor A771726 (leflunomide) induces apoptosis and diminishes proliferation of multiple myeloma cells." Mol Cancer Ther**8**(2): 366-75.

Beckwith, M., W. J. Urba, et al. (1991). "Anti-IgM-mediated growth inhibition of a human B lymphoma cell line is independent of phosphatidylinositol turnover and protein kinase C activation and involves tyrosine phosphorylation." J Immunol**147**(7): 2411-8.

Beere, H. M. (2004). ""The stress of dying": the role of heat shock proteins in the regulation of apoptosis." J Cell Sci**117**(Pt 13): 2641-51.

Bellamy, W. T. (1992). "Prediction of response to drug therapy of cancer. A review of in vitro assays." Drugs**44**(5): 690-708.

Bellamy, W. T., L. Richter, et al. (1999). "Expression of vascular endothelial growth factor and its receptors in hematopoietic malignancies." Cancer Res**59**(3): 728-33.

Bendall, L. J., A. Daniel, et al. (1994). "Bone marrow adherent layers inhibit apoptosis of acute myeloid leukemia cells." Exp Hematol**22**(13): 1252-60.

Berenson, J. R., O. Yellin, et al. "A modified regimen of pegylated liposomal doxorubicin, bortezomib and dexamethasone (DVD) is effective and well tolerated for previously untreated multiple myeloma patients." Br J Haematol**155**(5): 580-7.

Bergamo, A., R. Bataille, et al. (1997). "CD40 and CD95 induce programmed cell death in the human myeloma cell line XG2." Br J Haematol**97**(3): 652-5.

Bergsagel, P. L. and W. M. Kuehl (2001). "Chromosome translocations in multiple myeloma." Oncogene**20**(40): 5611-22.

Bertrand, F. E., C. E. Eckfeldt, et al. (2000). "Microenvironmental influences on human B-cell development." Immunol Rev**175**: 175-86.

Bhalla, S., S. Balasubramanian, et al. (2009). "PCI-24781 induces caspase and reactive oxygen species-dependent apoptosis through NF-kappaB mechanisms and is synergistic with bortezomib in lymphoma cells." Clin Cancer Res**15**(10): 3354-65.

Bharti, A. C., S. Shishodia, et al. (2004). "Nuclear factor-kappaB and STAT3 are constitutively active in CD138+ cells derived from multiple myeloma patients, and suppression of these transcription factors leads to apoptosis." Blood**103**(8): 3175-84.

Bi, G. and G. Jiang (2006). "The molecular mechanism of HDAC inhibitors in anticancer effects." Cell Mol Immunol**3**(4): 285-90.

Bisping, G., R. Leo, et al. (2003). "Paracrine interactions of basic fibroblast growth factor and interleukin-6 in multiple myeloma." Blood**101**(7): 2775-83.

Blade, J., D. Samson, et al. (1998). "Criteria for evaluating disease response and progression in patients with multiple myeloma treated by high-dose therapy and haemopoietic stem

cell transplantation. Myeloma Subcommittee of the EBMT. European Group for Blood and Marrow Transplant." Br J Haematol**102**(5): 1115-23.

Bloem, A. C., T. Lamme, et al. (1998). "Long-term bone marrow cultured stromal cells regulate myeloma tumour growth in vitro: studies with primary tumour cells and LTBMC-dependent cell lines." Br J Haematol**100**(1): 166-75.

Blumenthal, R. D. (2005). "An overview of chemosensitivity testing." Methods Mol Med**110**: 3-18.

Bolden, J. E., M. J. Peart, et al. (2006). "Anticancer activities of histone deacetylase inhibitors." Nat Rev Drug Discov**5**(9): 769-84.

Borrello, I. (2012). "Can we change the disease biology of multiple myeloma?" Leuk Res**36 Suppl 1**: S3-12.

Bosanquet, A. G. (1991). "Correlations between therapeutic response of leukaemias and in-vitro drug-sensitivity assay." Lancet**337**(8743): 711-4.

Bug, G., T. Rossmanith, et al. (2002). "Rho family small GTPases control migration of hematopoietic progenitor cells into multicellular spheroids of bone marrow stroma cells." J Leukoc Biol**72**(4): 837-45.

Cabrera, C. M., F. Cobo, et al. (2006). "Identity tests: determination of cell line cross-contamination." Cytotechnology**51**(2): 45-50.

Caldas-Lopes, E., L. Cerchietti, et al. (2009). "Hsp90 inhibitor PU-H71, a multimodal inhibitor of malignancy, induces complete responses in triple-negative breast cancer models." Proc Natl Acad Sci U S A**106**(20): 8368-73.

Capes-Davis, A., G. Theodosopoulos, et al. "Check your cultures! A list of cross-contaminated or misidentified cell lines." Int J Cancer**127**(1): 1-8.

Cardoso, A. A., J. L. Schultze, et al. (1996). "Pre-B acute lymphoblastic leukemia cells may induce T-cell anergy to alloantigen." Blood**88**(1): 41-8.

Carew, J. S., F. J. Giles, et al. (2008). "Histone deacetylase inhibitors: mechanisms of cell death and promise in combination cancer therapy." Cancer Lett**269**(1): 7-17.

Castillo, R., J. Mascarenhas, et al. (2000). "Proliferative response of mantle cell lymphoma cells stimulated by CD40 ligation and IL-4." Leukemia**14**(2): 292-8.

Catlett-Falcone, R., T. H. Landowski, et al. (1999). "Constitutive activation of Stat3 signaling confers resistance to apoptosis in human U266 myeloma cells." Immunity**10**(1): 105-15.

Chan, H. M., M. Krstic-Demonacos, et al. (2001). "Acetylation control of the retinoblastoma tumour-suppressor protein." Nat Cell Biol**3**(7): 667-74.

Chanan-Khan, A. A., I. Borrello, et al. (2010). "Development of target-specific treatments in multiple myeloma." Br J Haematol**151**(1): 3-15.

Chatterjee, M., D. Honemann, et al. (2002). "In the presence of bone marrow stromal cells human multiple myeloma cells become independent of the IL-6/gp130/STAT3 pathway." Blood**100**(9): 3311-8.

Chatterjee, M., T. Stuhmer, et al. (2004). "Combined disruption of both the MEK/ERK and the IL-6R/STAT3 pathways is required to induce apoptosis of multiple myeloma cells in the presence of bone marrow stromal cells." Blood**104**(12): 3712-21.

Chatterjee, R. (2007). "Cell biology. A lonely crusade." Science**315**(5814): 930.

Chauhan, D., D. Auclair, et al. (2002). "Identification of genes regulated by dexamethasone in multiple myeloma cells using oligonucleotide arrays." Oncogene**21**(9): 1346-58.

Chauhan, D., P. Pandey, et al. (1997). "Dexamethasone induces apoptosis of multiple myeloma cells in a JNK/SAP kinase independent mechanism." Oncogene**15**(7): 837-43.

Chauhan, D., H. Uchiyama, et al. (1996). "Multiple myeloma cell adhesion-induced interleukin-6 expression in bone marrow stromal cells involves activation of NF-kappa B." Blood**87**(3): 1104-12.

Chen, L., W. Fischle, et al. (2001). "Duration of nuclear NF-kappaB action regulated by reversible acetylation." Science**293**(5535): 1653-7.

Cheung, W. C. and B. Van Ness (2001). "The bone marrow stromal microenvironment influences myeloma therapeutic response in vitro." Leukemia**15**(2): 264-71.

Chiarle, R., L. M. Budel, et al. (2000). "Increased proteasome degradation of cyclin-dependent kinase inhibitor p27 is associated with a decreased overall survival in mantle cell lymphoma." Blood**95**(2): 619-26.

Choi, S. J., J. C. Cruz, et al. (2000). "Macrophage inflammatory protein 1-alpha is a potential osteoclast stimulatory factor in multiple myeloma." Blood**96**(2): 671-5.

Choi, S. J., Y. Oba, et al. (2001). "Antisense inhibition of macrophage inflammatory protein 1-alpha blocks bone destruction in a model of myeloma bone disease." J Clin Invest**108**(12): 1833-41.

Chou, T. C. and P. Talalay (1984). "Quantitative analysis of dose-effect relationships: the combined effects of multiple drugs or enzyme inhibitors." Adv Enzyme Regul**22**: 27-55.

Clark, E. A. and J. A. Ledbetter (1994). "How B and T cells talk to each other." Nature**367**(6462): 425-8.

Connell, P., C. A. Ballinger, et al. (2001). "The co-chaperone CHIP regulates protein triage decisions mediated by heat-shock proteins." Nat Cell Biol**3**(1): 93-6.

Cress, W. D. and E. Seto (2000). "Histone deacetylases, transcriptional control, and cancer." J Cell Physiol**184**(1): 1-16.

Cross, M. J. and L. Claesson-Welsh (2001). "FGF and VEGF function in angiogenesis: signalling pathways, biological responses and therapeutic inhibition." Trends Pharmacol Sci**22**(4): 201-7.

Crouch, S. P., R. Kozlowski, et al. (1993). "The use of ATP bioluminescence as a measure of cell proliferation and cytotoxicity." J Immunol Methods**160**(1): 81-8.

CRUK. (2010). "Cancer Stats." from http://www.cancerresearchuk.org/cancer-info/cancerstats/types/nhl/incidence/#country.

Cullinan, S. B. and L. Whitesell (2006). "Heat shock protein 90: a unique chemotherapeutic target." Semin Oncol**33**(4): 457-65.

Cusack, J. C., Jr., R. Liu, et al. (2001). "Enhanced chemosensitivity to CPT-11 with proteasome inhibitor PS-341: implications for systemic nuclear factor-kappaB inhibition." Cancer Res**61**(9): 3535-40.

Dalton, W. S. (2002). "Drug resistance and drug development in multiple myeloma." Semin Oncol**29**(6 Suppl 17): 21-5.

Dalton, W. S. (2003). "The tumor microenvironment: focus on myeloma." Cancer Treat Rev**29 Suppl 1**: 11-9.

Damiano, J. S., A. E. Cress, et al. (1999). "Cell adhesion mediated drug resistance (CAM-DR): role of integrins and resistance to apoptosis in human myeloma cell lines." Blood**93**(5): 1658-67.

Dankbar, B., T. Padro, et al. (2000). "Vascular endothelial growth factor and interleukin-6 in paracrine tumor-stromal cell interactions in multiple myeloma." Blood**95**(8): 2630-6.

Darzynkiewicz, Z., X. Li, et al. (1994). "Assays of cell viability: discrimination of cells dying by apoptosis." Methods Cell Biol**41**: 15-38.

Dasmahapatra, G., D. Lembersky, et al. (2010). "The pan-HDAC inhibitor vorinostat potentiates the activity of the proteasome inhibitor carfilzomib in human DLBCL cells in vitro and in vivo." Blood**115**(22): 4478-87.

Dave, S. S., G. Wright, et al. (2004). "Prediction of survival in follicular lymphoma based on molecular features of tumor-infiltrating immune cells." N Engl J Med**351**(21): 2159-69.

Davenport, E. L., H. E. Moore, et al. (2007). "Heat shock protein inhibition is associated with activation of the unfolded protein response pathway in myeloma plasma cells." Blood**110**(7): 2641-9.

Davies, C. C., J. Mason, et al. (2004). "Inhibition of phosphatidylinositol 3-kinase- and ERK MAPK-regulated protein synthesis reveals the pro-apoptotic properties of CD40 ligation in carcinoma cells." J Biol Chem**279**(2): 1010-9.

Decker, S., M. Hollingshead, et al. (2004). "The hollow fibre model in cancer drug screening: the NCI experience." Eur J Cancer**40**(6): 821-6.

Defrance, T., J. P. Aubry, et al. (1986). "Human interferon-gamma acts as a B cell growth factor in the anti-IgM antibody co-stimulatory assay but has no direct B cell differentiation activity." J Immunol**137**(12): 3861-7.

Defrance, T., B. Vanbervliet, et al. (1987). "B cell growth-promoting activity of recombinant human interleukin 4." J Immunol**139**(4): 1135-41.

Defrance, T., B. Vanbervliet, et al. (1992). "Interleukin 10 and transforming growth factor beta cooperate to induce anti-CD40-activated naive human B cells to secrete immunoglobulin A." J Exp Med**175**(3): 671-82.

Deininger, M., E. Buchdunger, et al. (2005). "The development of imatinib as a therapeutic agent for chronic myeloid leukemia." Blood**105**(7): 2640-53.

Dexter, T. M., T. D. Allen, et al. (1977). "Conditions controlling the proliferation of haemopoietic stem cells in vitro." J Cell Physiol**91**(3): 335-44.

Dierks, C., J. Grbic, et al. (2007). "Essential role of stromally induced hedgehog signaling in B-cell malignancies." Nat Med**13**(8): 944-51.

Digirolamo, C. M., D. Stokes, et al. (1999). "Propagation and senescence of human marrow stromal cells in culture: a simple colony-forming assay identifies samples with the greatest potential to propagate and differentiate." Br J Haematol**107**(2): 275-81.

DiSanto, J. P., J. Y. Bonnefoy, et al. (1993). "CD40 ligand mutations in x-linked immunodeficiency with hyper-IgM." Nature**361**(6412): 541-3.

Dong, X., Z. C. Han, et al. (2007). "Angiogenesis and antiangiogenic therapy in hematologic malignancies." Crit Rev Oncol Hematol**62**(2): 105-18.

Drexler, H. G., R. A. MacLeod, et al. (2001). "Cross-contamination: HS-Sultan is not a myeloma but a Burkitt lymphoma cell line." Blood**98**(12): 3495-6.

Drexler, H. G., A. Y. Matsuo, et al. (2000). "Continuous hematopoietic cell lines as model systems for leukemia-lymphoma research." Leuk Res**24**(11): 881-911.

Drexler, H. G. and Y. Matsuo (2000). "Malignant hematopoietic cell lines: in vitro models for the study of multiple myeloma and plasma cell leukemia." Leuk Res**24**(8): 681-703.

Dreyling, M. (2010). "Newly diagnosed and relapsed follicular lymphoma: ESMO Clinical Practice Guidelines for diagnosis, treatment and follow-up." Ann Oncol**21 Suppl 5**: v181-3.

Duus, J., H. I. Bahar, et al. (2006). "Analysis of expression of heat shock protein-90 (HSP90) and the effects of HSP90 inhibitor (17-AAG) in multiple myeloma." Leuk Lymphoma**47**(7): 1369-78.

Duvic, M. and J. Vu (2007). "Vorinostat: a new oral histone deacetylase inhibitor approved for cutaneous T-cell lymphoma." Expert Opin Investig Drugs**16**(7): 1111-20.

Eccles, S. A., A. Massey, et al. (2008). "NVP-AUY922: a novel heat shock protein 90 inhibitor active against xenograft tumor growth, angiogenesis, and metastasis." Cancer Res**68**(8): 2850-60.

Elaut, G., V. Rogiers, et al. (2007). "The pharmaceutical potential of histone deacetylase inhibitors." Curr Pharm Des**13**(25): 2584-620.

Eliopoulos, A. G. and L. S. Young (2004). "The role of the CD40 pathway in the pathogenesis and treatment of cancer." Curr Opin Pharmacol**4**(4): 360-7.

Emile, C., J. P. Fermand, et al. (1994). "Interleukin-6 serum levels in patients with multiple myeloma." Br J Haematol**86**(2): 439-40.

Emmons, M. F., A. W. Gebhard, et al. (2011). "Acquisition of resistance toward HYD1 correlates with a reduction in cleaved alpha4 integrin expression and a compromised CAM-DR phenotype." Mol Cancer Ther**10**(12): 2257-66.

Epstein, A. L., R. Levy, et al. (1978). "Biology of the human malignant lymphomas. IV. Functional characterization of ten diffuse histiocytic lymphoma cell lines." Cancer**42**(5): 2379-91.

Fadden, P., K. H. Huang, et al. (2010). "Application of chemoproteomics to drug discovery: identification of a clinical candidate targeting hsp90." Chem Biol**17**(7): 686-94.

Fahy, B. N., M. G. Schlieman, et al. (2003). "Schedule-dependent molecular effects of the proteasome inhibitor bortezomib and gemcitabine in pancreatic cancer." J Surg Res**113**(1): 88-95.

Fang, J. Y. (2005). "Histone deacetylase inhibitors, anticancerous mechanism and therapy for gastrointestinal cancers." J Gastroenterol Hepatol**20**(7): 988-94.

Fantin, V. R., A. Loboda, et al. (2008). "Constitutive activation of signal transducers and activators of transcription predicts vorinostat resistance in cutaneous T-cell lymphoma." Cancer Res**68**(10): 3785-94.

Farrant, J., S. C. Knight, et al. (1974). "Optimal recovery of lymphocytes and tissue culture cells following rapid cooling." Nature**249**(456): 452-3.

Fiumara, P. and A. Younes (2001). "CD40 ligand (CD154) and tumour necrosis factor-related apoptosis inducing ligand (Apo-2L) in haematological malignancies." Br J Haematol**113**(2): 265-74.

Frassanito, M. A., A. Cusmai, et al. (2001). "Autocrine interleukin-6 production and highly malignant multiple myeloma: relation with resistance to drug-induced apoptosis." Blood**97**(2): 483-9.

Freshney, R. I. (2006). Culture of Cells for Tissue Engineering, John Wiley & Sons, Inc.

Fribley, A., Q. Zeng, et al. (2004). "Proteasome inhibitor PS-341 induces apoptosis through induction of endoplasmic reticulum stress-reactive oxygen species in head and neck squamous cell carcinoma cells." Mol Cell Biol**24**(22): 9695-704.

Friedman, H. M. and D. L. Glaubiger (1982). "Assessment of in vitro drug sensitivity of human tumor cells using [3H]thymidine incorporation in a modified human tumor stem cell assay." Cancer Res**42**(11): 4683-9.

Fulciniti, M., T. Hideshima, et al. (2009). "A high-affinity fully human anti-IL-6 mAb, 1339, for the treatment of multiple myeloma." Clin Cancer Res**15**(23): 7144-52.

Funakoshi, S., D. L. Longo, et al. (1994). "Inhibition of human B-cell lymphoma growth by CD40 stimulation." Blood**83**(10): 2787-94.

Gaillard, J. P., R. Bataille, et al. (1993). "Increased and highly stable levels of functional soluble interleukin-6 receptor in sera of patients with monoclonal gammopathy." Eur J Immunol**23**(4): 820-4.

Garcia-Mata, R., Y. S. Gao, et al. (2002). "Hassles with taking out the garbage: aggravating aggresomes." Traffic**3**(6): 388-96.

Garrido, S. M., F. R. Appelbaum, et al. (2001). "Acute myeloid leukemia cells are protected from spontaneous and drug-induced apoptosis by direct contact with a human bone marrow stromal cell line (HS-5)." Exp Hematol**29**(4): 448-57.

Ghia, P., V. A. Boussiotis, et al. (1998). "Unbalanced expression of bcl-2 family proteins in follicular lymphoma: contribution of CD40 signaling in promoting survival." Blood**91**(1): 244-51.

Gilmore, T. D. (2006). "Introduction to NF-kappaB: players, pathways, perspectives." Oncogene**25**(51): 6680-4.

Glaser, K. B. (2007). "HDAC inhibitors: clinical update and mechanism-based potential." Biochem Pharmacol**74**(5): 659-71.

Glaze, E. R., A. L. Lambert, et al. (2005). "Preclinical toxicity of a geldanamycin analog, 17-(dimethylaminoethylamino)-17-demethoxygeldanamycin (17-DMAG), in rats and dogs: potential clinical relevance." Cancer Chemother Pharmacol**56**(6): 637-47.

Glozak, M. A. and E. Seto (2007). "Histone deacetylases and cancer." Oncogene**26**(37): 5420-32.

Goldberg, A. L., T. N. Akopian, et al. (1997). "New insights into the mechanisms and importance of the proteasome in intracellular protein degradation." Biol Chem**378**(3-4): 131-40.

Goldman-Leikin, R. E., H. R. Salwen, et al. (1989). "Characterization of a novel myeloma cell line, MM.1." J Lab Clin Med**113**(3): 335-45.

Gomez-Bougie, P., S. Wuilleme-Toumi, et al. (2007). "Noxa up-regulation and Mcl-1 cleavage are associated to apoptosis induction by bortezomib in multiple myeloma." Cancer Res**67**(11): 5418-24.

Goy, A. and F. Gilles (2004). "Update on the proteasome inhibitor bortezomib in hematologic malignancies." Clin Lymphoma**4**(4): 230-7.

Grever, M. R., S. A. Schepartz, et al. (1992). "The National Cancer Institute: cancer drug discovery and development program." Semin Oncol**19**(6): 622-38.

Gribben, J. G. (2007). "How I treat indolent lymphoma." Blood**109**(11): 4617-26.

Griffon, G., J. L. Merlin, et al. (1995). "Comparison of sulforhodamine B, tetrazolium and clonogenic assays for in vitro radiosensitivity testing in human ovarian cell lines." Anticancer Drugs**6**(1): 115-23.

Grisham, M. B., V. J. Palombella, et al. (1999). "Inhibition of NF-kappa B activation in vitro and in vivo: role of 26S proteasome." Methods Enzymol**300**: 345-63.

Gschwind, A., O. M. Fischer, et al. (2004). "The discovery of receptor tyrosine kinases: targets for cancer therapy." Nat Rev Cancer**4**(5): 361-70.

Guikema, J. E., E. Vellenga, et al. (2002). "Myeloma clonotypic B cells are hampered in their ability to undergo B-cell differentiation in vitro." Br J Haematol**119**(1): 54-61.

Gupta, D., S. P. Treon, et al. (2001). "Adherence of multiple myeloma cells to bone marrow stromal cells upregulates vascular endothelial growth factor secretion: therapeutic applications." Leukemia**15**(12): 1950-61.

Guzman, M. L., C. F. Swiderski, et al. (2002). "Preferential induction of apoptosis for primary human leukemic stem cells." Proc Natl Acad Sci U S A**99**(25): 16220-5.

Haggarty, S. J., K. M. Koeller, et al. (2003). "Domain-selective small-molecule inhibitor of histone deacetylase 6 (HDAC6)-mediated tubulin deacetylation." Proc Natl Acad Sci U S A**100**(8): 4389-94.

Hayashi, T., T. Hideshima, et al. (2004). "Transforming growth factor beta receptor I kinase inhibitor down-regulates cytokine secretion and multiple myeloma cell growth in the bone marrow microenvironment." Clin Cancer Res**10**(22): 7540-6.

Hazlehurst, L. A., T. H. Landowski, et al. (2003). "Role of the tumor microenvironment in mediating de novo resistance to drugs and physiological mediators of cell death." Oncogene**22**(47): 7396-402.

Heckman, C. A., J. W. Mehew, et al. (2002). "NF-kappaB activates Bcl-2 expression in t(14;18) lymphoma cells." Oncogene**21**(24): 3898-908.

Heider, U., I. von Metzler, et al. (2008). "Synergistic interaction of the histone deacetylase inhibitor SAHA with the proteasome inhibitor bortezomib in mantle cell lymphoma." Eur J Haematol**80**(2): 133-42.

Heinrich, P. C., I. Behrmann, et al. (1998). "Interleukin-6-type cytokine signalling through the gp130/Jak/STAT pathway." Biochem J**334 (Pt 2)**: 297-314.

Hicklin, D. J. and L. M. Ellis (2005). "Role of the vascular endothelial growth factor pathway in tumor growth and angiogenesis." J Clin Oncol**23**(5): 1011-27.

Hideshima, T., J. E. Bradner, et al. (2005). "Small-molecule inhibition of proteasome and aggresome function induces synergistic antitumor activity in multiple myeloma." Proc Natl Acad Sci U S A**102**(24): 8567-72.

Hideshima, T., D. Chauhan, et al. (2003). "Proteasome inhibitor PS-341 abrogates IL-6 triggered signaling cascades via caspase-dependent downregulation of gp130 in multiple myeloma." Oncogene**22**(52): 8386-93.

Hideshima, T., D. Chauhan, et al. (2001). "Novel therapies targeting the myeloma cell and its bone marrow microenvironment." Semin Oncol**28**(6): 607-12.

Hideshima, T., D. Chauhan, et al. (2002). "NF-kappa B as a therapeutic target in multiple myeloma." J Biol Chem**277**(19): 16639-47.

Hideshima, T., C. Mitsiades, et al. (2003). "Molecular mechanisms mediating antimyeloma activity of proteasome inhibitor PS-341." Blood**101**(4): 1530-4.
Hideshima, T., C. Mitsiades, et al. (2007). "Understanding multiple myeloma pathogenesis in the bone marrow to identify new therapeutic targets." Nat Rev Cancer**7**(8): 585-98.
Hideshima, T., N. Nakamura, et al. (2001). "Biologic sequelae of interleukin-6 induced PI3-K/Akt signaling in multiple myeloma." Oncogene**20**(42): 5991-6000.
Hideshima, T., K. Podar, et al. (2004). "p38 MAPK inhibition enhances PS-341 (bortezomib)-induced cytotoxicity against multiple myeloma cells." Oncogene**23**(54): 8766-76.
Hideshima, T., P. Richardson, et al. (2001). "The proteasome inhibitor PS-341 inhibits growth, induces apoptosis, and overcomes drug resistance in human multiple myeloma cells." Cancer Res**61**(7): 3071-6.
Hirano, T., K. Ishihara, et al. (2000). "Roles of STAT3 in mediating the cell growth, differentiation and survival signals relayed through the IL-6 family of cytokine receptors." Oncogene**19**(21): 2548-56.
Hitomi, J., T. Katayama, et al. (2004). "Apoptosis induced by endoplasmic reticulum stress depends on activation of caspase-3 via caspase-12." Neurosci Lett**357**(2): 127-30.
Hitzler, J. K., H. Martinez-Valdez, et al. (1991). "Role of interleukin-6 in the proliferation of human multiple myeloma cell lines OCI-My 1 to 7 established from patients with advanced stage of the disease." Blood**78**(8): 1996-2004.
Holder, M. J., H. Wang, et al. (1993). "Suppression of apoptosis in normal and neoplastic human B lymphocytes by CD40 ligand is independent of Bc1-2 induction." Eur J Immunol**23**(9): 2368-71.
Holford, N. H. and L. B. Sheiner (1982). "Kinetics of pharmacologic response." Pharmacol Ther**16**(2): 143-66.
Holler, N., A. Tardivel, et al. (2003). "Two adjacent trimeric Fas ligands are required for Fas signaling and formation of a death-inducing signaling complex." Mol Cell Biol**23**(4): 1428-40.
Houot, R., S. Le Gouill, et al. (2012). "Combination of rituximab, bortezomib, doxorubicin, dexamethasone and chlorambucil (RiPAD+C) as first-line therapy for elderly mantle cell lymphoma patients: results of a phase II trial from the GOELAMS." Ann Oncol**23**(6): 1555-61.
Hsu, J. H., Y. Shi, et al. (2004). "Interleukin-6 activates phosphoinositol-3' kinase in multiple myeloma tumor cells by signaling through RAS-dependent and, separately, through p85-dependent pathways." Oncogene**23**(19): 3368-75.
Hsu, S. H., B. Z. Schacter, et al. (1976). "Genetic characteristics of the HeLa cell." Science**191**(4225): 392-4.
Huang, S., L. Mills, et al. (2002). "Fully humanized neutralizing antibodies to interleukin-8 (ABX-IL8) inhibit angiogenesis, tumor growth, and metastasis of human melanoma." Am J Pathol**161**(1): 125-34.
Isaacs, J. S., W. Xu, et al. (2003). "Heat shock protein 90 as a molecular target for cancer therapeutics." Cancer Cell**3**(3): 213-7.
Ishii, T., T. Seike, et al. (2012). "Anti-tumor activity against multiple myeloma by combination of KW-2478, an Hsp90 inhibitor, with bortezomib." Blood Cancer J**2**(4): e68.
Iyengar, S., A. Clear, et al. (2013). "P110alpha mediated constitutive PI3K signaling limits the efficacy of p110delta-selective inhibition in mantle cell lymphoma, particularly with multiple relapse." Blood.
Jabbar, S. A., P. R. Twentyman, et al. (1989). "The MTT assay underestimates the growth inhibitory effects of interferons." Br J Cancer**60**(4): 523-8.
Jadayel, D. M., J. Lukas, et al. (1997). "Potential role for concurrent abnormalities of the cyclin D1, p16CDKN2 and p15CDKN2B genes in certain B cell non-Hodgkin's lymphomas. Functional studies in a cell line (Granta 519)." Leukemia**11**(1): 64-72.

Jaffe, E. A., R. L. Nachman, et al. (1973). "Culture of human endothelial cells derived from umbilical veins. Identification by morphologic and immunologic criteria." J Clin Invest**52**(11): 2745-56.

Jeon, H. J., C. W. Kim, et al. (1998). "Establishment and characterization of a mantle cell lymphoma cell line." Br J Haematol**102**(5): 1323-6.

Johnson, P. W., S. M. Watt, et al. (1993). "Isolated follicular lymphoma cells are resistant to apoptosis and can be grown in vitro in the CD40/stromal cell system." Blood**82**(6): 1848-57.

Jubb, A. M., A. J. Oates, et al. (2006). "Predicting benefit from anti-angiogenic agents in malignancy." Nat Rev Cancer**6**(8): 626-35.

Kamal, A., L. Thao, et al. (2003). "A high-affinity conformation of Hsp90 confers tumour selectivity on Hsp90 inhibitors." Nature**425**(6956): 407-10.

Kastritis, E., K. Zervas, et al. (2009). "Improved survival of patients with multiple myeloma after the introduction of novel agents and the applicability of the International Staging System (ISS): an analysis of the Greek Myeloma Study Group (GMSG)." Leukemia**23**(6): 1152-7.

Kawaguchi, Y., J. J. Kovacs, et al. (2003). "The deacetylase HDAC6 regulates aggresome formation and cell viability in response to misfolded protein stress." Cell**115**(6): 727-38.

Kawano, M., T. Hirano, et al. (1988). "Autocrine generation and requirement of BSF-2/IL-6 for human multiple myelomas." Nature**332**(6159): 83-5.

Kehry, M. R. (1996). "CD40-mediated signaling in B cells. Balancing cell survival, growth, and death." J Immunol**156**(7): 2345-8.

Khochbin, S., A. Verdel, et al. (2001). "Functional significance of histone deacetylase diversity." Curr Opin Genet Dev**11**(2): 162-6.

Kirshner, J., K. J. Thulien, et al. (2008). "A unique three-dimensional model for evaluating the impact of therapy on multiple myeloma." Blood**112**(7): 2935-45.

Kishimoto, T., S. Akira, et al. (1995). "Interleukin-6 family of cytokines and gp130." Blood**86**(4): 1243-54.

Kisselev, A. F. and A. L. Goldberg (2001). "Proteasome inhibitors: from research tools to drug candidates." Chem Biol**8**(8): 739-58.

Kitada, S., J. M. Zapata, et al. (1999). "Bryostatin and CD40-ligand enhance apoptosis resistance and induce expression of cell survival genes in B-cell chronic lymphocytic leukaemia." Br J Haematol**106**(4): 995-1004.

Klaus, G. G., M. S. Choi, et al. (1997). "CD40: a pivotal receptor in the determination of life/death decisions in B lymphocytes." Int Rev Immunol**15**(1-2): 5-31.

Klein, B., J. Wijdenes, et al. (1991). "Murine anti-interleukin-6 monoclonal antibody therapy for a patient with plasma cell leukemia." Blood**78**(5): 1198-204.

Klein, B., X. G. Zhang, et al. (1995). "Interleukin-6 in human multiple myeloma." Blood**85**(4): 863-72.

Kluin-Nelemans, H. C., J. Limpens, et al. (1991). "A new non-Hodgkin's B-cell line (DoHH2) with a chromosomal translocation t(14;18)(q32;q21)." Leukemia**5**(3): 221-4.

Knall, C., G. S. Worthen, et al. (1997). "Interleukin 8-stimulated phosphatidylinositol-3-kinase activity regulates the migration of human neutrophils independent of extracellular signal-regulated kinase and p38 mitogen-activated protein kinases." Proc Natl Acad Sci U S A**94**(7): 3052-7.

Knall, C., S. Young, et al. (1996). "Interleukin-8 regulation of the Ras/Raf/mitogen-activated protein kinase pathway in human neutrophils." J Biol Chem**271**(5): 2832-8.

Konopleva, M., S. Konoplev, et al. (2002). "Stromal cells prevent apoptosis of AML cells by up-regulation of anti-apoptotic proteins." Leukemia**16**(9): 1713-24.

Kordes, U., D. Krappmann, et al. (2000). "Transcription factor NF-kappaB is constitutively activated in acute lymphoblastic leukemia cells." Leukemia**14**(3): 399-402.

Korthauer, U., D. Graf, et al. (1993). "Defective expression of T-cell CD40 ligand causes X-linked immunodeficiency with hyper-IgM." Nature**361**(6412): 539-41.

Kovacs, J. J., P. J. Murphy, et al. (2005). "HDAC6 regulates Hsp90 acetylation and chaperone-dependent activation of glucocorticoid receptor." Mol Cell**18**(5): 601-7.

Kuku, I., M. R. Bayraktar, et al. (2005). "Serum proinflammatory mediators at different periods of therapy in patients with multiple myeloma." Mediators Inflamm**2005**(3): 171-4.

Kumar, S. K., S. V. Rajkumar, et al. (2008). "Improved survival in multiple myeloma and the impact of novel therapies." Blood**111**(5): 2516-20.

Kurbacher, C. M. and I. A. Cree (2005). "Chemosensitivity testing using microplate adenosine triphosphate-based luminescence measurements." Methods Mol Med**110**: 101-20.

Kurbacher, C. M., I. A. Cree, et al. (1998). "Use of an ex vivo ATP luminescence assay to direct chemotherapy for recurrent ovarian cancer." Anticancer Drugs**9**(1): 51-7.

Kurbacher, C. M., P. Mallmann, et al. (1994). "In vitro activity of titanocenedichloride versus cisplatin and doxorubicin in primary and recurrent epithelial ovarian cancer." Anticancer Res**14**(5A): 1961-5.

Kurebayashi, J., T. Otsuki, et al. (2001). "A radicicol derivative, KF58333, inhibits expression of hypoxia-inducible factor-1alpha and vascular endothelial growth factor, angiogenesis and growth of human breast cancer xenografts." Jpn J Cancer Res**92**(12): 1342-51.

Kyrtsonis, M. C., G. Dedoussis, et al. (1996). "Soluble interleukin-6 receptor (sIL-6R), a new prognostic factor in multiple myeloma." Br J Haematol**93**(2): 398-400.

Lacroix, M. (2008). "Persistent use of "false" cell lines." Int J Cancer**122**(1): 1-4.

Landowski, T. H., N. E. Olashaw, et al. (2003). "Cell adhesion-mediated drug resistance (CAM-DR) is associated with activation of NF-kappa B (RelB/p50) in myeloma cells." Oncogene**22**(16): 2417-21.

LeBlanc, R., L. P. Catley, et al. (2002). "Proteasome inhibitor PS-341 inhibits human myeloma cell growth in vivo and prolongs survival in a murine model." Cancer Res**62**(17): 4996-5000.

Lee, C. and T. Waldman (2003). "Human somatic cell knockouts reveal determinants of sensitivity and resistance to proteasome inhibitor PS-341." Cancer Biol Ther**2**(6): 700-1.

Lee, J. H., D. Y. Kim, et al. (2012). "Two cycles of the PS-341/bortezomib, adriamycin, and dexamethasone combination followed by autologous hematopoietic cell transplantation in newly diagnosed multiple myeloma patients." Eur J Haematol**88**(6): 478-84.

Lefterova, P., A. Marten, et al. (2000). "Induction of apoptosis in B lymphoma cells by activation with CD40L." Acta Haematol**103**(3): 168-71.

Lentzsch, S., M. Gries, et al. (2003). "Macrophage inflammatory protein 1-alpha (MIP-1 alpha) triggers migration and signaling cascades mediating survival and proliferation in multiple myeloma (MM) cells." Blood**101**(9): 3568-73.

Lenz, G., G. Wright, et al. (2008). "Stromal gene signatures in large-B-cell lymphomas." N Engl J Med**359**(22): 2313-23.

Leonard, J. P., R. R. Furman, et al. (2006). "Proteasome inhibition with bortezomib: a new therapeutic strategy for non-Hodgkin's lymphoma." Int J Cancer**119**(5): 971-9.

Lerescu, L., C. Tucureanu, et al. (2008). "Primary cell culture of human adenocarcinomas--practical considerations." Roum Arch Microbiol Immunol**67**(3-4): 55-66.

Li, L. P., P. M. Schlag, et al. (1997). "Transient expression of SV 40 large T antigen by Cre/LoxP-mediated site-specific deletion in primary human tumor cells." Hum Gene Ther**8**(14): 1695-700.

Linderoth, J., M. Jerkeman, et al. (2003). "Immunohistochemical expression of CD23 and CD40 may identify prognostically favorable subgroups of diffuse large B-cell lymphoma: a Nordic Lymphoma Group Study." Clin Cancer Res**9**(2): 722-8.

Ling, Y. H., L. Liebes, et al. (2003). "Reactive oxygen species generation and mitochondrial dysfunction in the apoptotic response to Bortezomib, a novel proteasome inhibitor, in human H460 non-small cell lung cancer cells." J Biol Chem**278**(36): 33714-23.

Liscovitch, M. and D. Ravid (2007). "A case study in misidentification of cancer cell lines: MCF-7/AdrR cells (re-designated NCI/ADR-RES) are derived from OVCAR-8 human ovarian carcinoma cells." Cancer Lett**245**(1-2): 350-2.

Lisignoli, G., A. Piacentini, et al. (2007). "CCL20 chemokine induces both osteoblast proliferation and osteoclast differentiation: Increased levels of CCL20 are expressed in subchondral bone tissue of rheumatoid arthritis patients." J Cell Physiol**210**(3): 798-806.

Liu, Y. J., D. E. Joshua, et al. (1989). "Mechanism of antigen-driven selection in germinal centres." Nature**342**(6252): 929-31.

Lokhorst, H. M., T. Lamme, et al. (1994). "Primary tumor cells of myeloma patients induce interleukin-6 secretion in long-term bone marrow cultures." Blood**84**(7): 2269-77.

Lomo, J., H. K. Blomhoff, et al. (1997). "Interleukin-13 in combination with CD40 ligand potently inhibits apoptosis in human B lymphocytes: upregulation of Bcl-xL and Mcl-1." Blood**89**(12): 4415-24.

Lonial, S. and J. Cavenagh (2009). "Emerging combination treatment strategies containing novel agents in newly diagnosed multiple myeloma." Br J Haematol**145**(6): 681-708.

Lwin, T., L. A. Hazlehurst, et al. (2007). "Bone marrow stromal cells prevent apoptosis of lymphoma cells by upregulation of anti-apoptotic proteins associated with activation of NF-kappaB (RelB/p52) in non-Hodgkin's lymphoma cells." Leukemia**21**(7): 1521-31.

Ma, M. H., H. H. Yang, et al. (2003). "The proteasome inhibitor PS-341 markedly enhances sensitivity of multiple myeloma tumor cells to chemotherapeutic agents." Clin Cancer Res**9**(3): 1136-44.

MacLeod, R. A., W. G. Dirks, et al. (2008). "One falsehood leads easily to another." Int J Cancer**122**(9): 2165-8.

MacLeod, R. A., W. G. Dirks, et al. (1999). "Widespread intraspecies cross-contamination of human tumor cell lines arising at source." Int J Cancer**83**(4): 555-63.

MacManus, C. F., J. Pettigrew, et al. (2007). "Interleukin-8 signaling promotes translational regulation of cyclin D in androgen-independent prostate cancer cells." Mol Cancer Res**5**(7): 737-48.

Malinowski, K., C. Pullis, et al. (1992). "Modulation of human lymphocyte marker expression by gamma irradiation and mitomycin C." Cell Immunol**143**(2): 368-77.

Maloney, D. G. (2005). "Immunotherapy for non-Hodgkin's lymphoma: monoclonal antibodies and vaccines." J Clin Oncol**23**(26): 6421-8.

Mann, B. S., J. R. Johnson, et al. (2007). "Vorinostat for treatment of cutaneous manifestations of advanced primary cutaneous T-cell lymphoma." Clin Cancer Res**13**(8): 2318-22.

Margulies, L. and P. B. Sehgal (1993). "Modulation of the human interleukin-6 promoter (IL-6) and transcription factor C/EBP beta (NF-IL6) activity by p53 species." J Biol Chem**268**(20): 15096-100.

Marzio, G., C. Wagener, et al. (2000). "E2F family members are differentially regulated by reversible acetylation." J Biol Chem**275**(15): 10887-92.

Mascotti, K., J. McCullough, et al. (2000). "HPC viability measurement: trypan blue versus acridine orange and propidium iodide." Transfusion**40**(6): 693-6.

Masdehors, P., S. Omura, et al. (1999). "Increased sensitivity of CLL-derived lymphocytes to apoptotic death activation by the proteasome-specific inhibitor lactacystin." Br J Haematol**105**(3): 752-7.

Matsuoka, Y., G. E. Moore, et al. (1967). "Production of free light chains of immunoglobulin by a hematopoietic cell line derived from a patient with multiple myeloma." Proc Soc Exp Biol Med**125**(4): 1246-50.

Maxwell, P. J., R. Gallagher, et al. (2007). "HIF-1 and NF-kappaB-mediated upregulation of CXCR1 and CXCR2 expression promotes cell survival in hypoxic prostate cancer cells." Oncogene**26**(52): 7333-45.

McCaig, A. M., E. Cosimo, et al. (2011). "Dasatinib inhibits B cell receptor signalling in chronic lymphocytic leukaemia but novel combination approaches are required to overcome additional pro-survival microenvironmental signals." Br J Haematol**153**(2): 199-211.

Meads, M. B., L. A. Hazlehurst, et al. (2008). "The bone marrow microenvironment as a tumor sanctuary and contributor to drug resistance." Clin Cancer Res**14**(9): 2519-26.

Meister, S., U. Schubert, et al. (2007). "Extensive immunoglobulin production sensitizes myeloma cells for proteasome inhibition." Cancer Res**67**(4): 1783-92.

Merritt, W. M., Y. G. Lin, et al. (2008). "Effect of interleukin-8 gene silencing with liposome-encapsulated small interfering RNA on ovarian cancer cell growth." J Natl Cancer Inst**100**(5): 359-72.

Mian, B. M., C. P. Dinney, et al. (2003). "Fully human anti-interleukin 8 antibody inhibits tumor growth in orthotopic bladder cancer xenografts via down-regulation of matrix metalloproteases and nuclear factor-kappaB." Clin Cancer Res**9**(8): 3167-75.

Mimnaugh, E. G., W. Xu, et al. (2004). "Simultaneous inhibition of hsp 90 and the proteasome promotes protein ubiquitination, causes endoplasmic reticulum-derived cytosolic vacuolization, and enhances antitumor activity." Mol Cancer Ther**3**(5): 551-66.

Minucci, S. and P. G. Pelicci (2006). "Histone deacetylase inhibitors and the promise of epigenetic (and more) treatments for cancer." Nat Rev Cancer**6**(1): 38-51.

Mitsiades, C. S., N. Mitsiades, et al. (2006). "Proteasome inhibition as a new therapeutic principle in hematological malignancies." Curr Drug Targets**7**(10): 1341-7.

Mitsiades, C. S., N. Mitsiades, et al. (2004). "Focus on multiple myeloma." Cancer Cell**6**(5): 439-44.

Mitsiades, C. S., N. Mitsiades, et al. (2002). "Activation of NF-kappaB and upregulation of intracellular anti-apoptotic proteins via the IGF-1/Akt signaling in human multiple myeloma cells: therapeutic implications." Oncogene**21**(37): 5673-83.

Mitsiades, C. S., N. S. Mitsiades, et al. (2006). "Antimyeloma activity of heat shock protein-90 inhibition." Blood**107**(3): 1092-100.

Mitsiades, C. S., N. S. Mitsiades, et al. (2004). "Inhibition of the insulin-like growth factor receptor-1 tyrosine kinase activity as a therapeutic strategy for multiple myeloma, other hematologic malignancies, and solid tumors." Cancer Cell**5**(3): 221-30.

Mitsiades, C. S., N. S. Mitsiades, et al. (2006). "The role of the bone microenvironment in the pathophysiology and therapeutic management of multiple myeloma: interplay of growth factors, their receptors and stromal interactions." Eur J Cancer**42**(11): 1564-73.

Mitsiades, N., C. S. Mitsiades, et al. (2002). "Molecular sequelae of proteasome inhibition in human multiple myeloma cells." Proc Natl Acad Sci U S A**99**(22): 14374-9.

Mitsiades, N., C. S. Mitsiades, et al. (2002). "Biologic sequelae of nuclear factor-kappaB blockade in multiple myeloma: therapeutic applications." Blood**99**(11): 4079-86.

Mitsiades, N., C. S. Mitsiades, et al. (2003). "Molecular sequelae of histone deacetylase inhibition in human malignant B cells." Blood**101**(10): 4055-62.

Mitsiades, N., C. S. Mitsiades, et al. (2003). "The proteasome inhibitor PS-341 potentiates sensitivity of multiple myeloma cells to conventional chemotherapeutic agents: therapeutic applications." Blood**101**(6): 2377-80.

Monks, A., D. Scudiero, et al. (1991). "Feasibility of a high-flux anticancer drug screen using a diverse panel of cultured human tumor cell lines." J Natl Cancer Inst**83**(11): 757-66.

Mosmann, T. (1983). "Rapid colorimetric assay for cellular growth and survival: application to proliferation and cytotoxicity assays." J Immunol Methods**65**(1-2): 55-63.

Mudry, R. E., J. E. Fortney, et al. (2000). "Stromal cells regulate survival of B-lineage leukemic cells during chemotherapy." Blood**96**(5): 1926-32.

Munshi, N. C. (2004). "Recent advances in the management of multiple myeloma." Semin Hematol**41**(2 Suppl 4): 21-6.

Myung, J., K. B. Kim, et al. (2001). "The ubiquitin-proteasome pathway and proteasome inhibitors." Med Res Rev**21**(4): 245-73.

Nabhan, C., D. Villines, et al. (2012). "Bortezomib (Velcade), rituximab, cyclophosphamide, and dexamethasone combination regimen is active as front-line therapy of low-grade non-Hodgkin lymphoma." Clin Lymphoma Myeloma Leuk**12**(1): 26-31.

Nachbaur, D. M., M. Herold, et al. (1991). "Serum levels of interleukin-6 in multiple myeloma and other hematological disorders: correlation with disease activity and other prognostic parameters." Ann Hematol**62**(2-3): 54-8.

Nakashima, T., T. Ishii, et al. (2010). "New molecular and biological mechanism of antitumor activities of KW-2478, a novel nonansamycin heat shock protein 90 inhibitor, in multiple myeloma cells." Clin Cancer Res**16**(10): 2792-802.

Nawrocki, S. T., J. S. Carew, et al. (2005). "Bortezomib inhibits PKR-like endoplasmic reticulum (ER) kinase and induces apoptosis via ER stress in human pancreatic cancer cells." Cancer Res**65**(24): 11510-9.

Nawrocki, S. T., J. S. Carew, et al. (2006). "Aggresome disruption: a novel strategy to enhance bortezomib-induced apoptosis in pancreatic cancer cells." Cancer Res**66**(7): 3773-81.

Nawrocki, S. T., J. S. Carew, et al. (2005). "Bortezomib sensitizes pancreatic cancer cells to endoplasmic reticulum stress-mediated apoptosis." Cancer Res**65**(24): 11658-66.

Neckers, L. (2003). "Development of small molecule Hsp90 inhibitors: utilizing both forward and reverse chemical genomics for drug identification." Curr Med Chem**10**(9): 733-9.

Nefedova, Y., T. H. Landowski, et al. (2003). "Bone marrow stromal-derived soluble factors and direct cell contact contribute to de novo drug resistance of myeloma cells by distinct mechanisms." Leukemia**17**(6): 1175-82.

Negaard, H. F., N. Iversen, et al. (2009). "Increased bone marrow microvascular density in haematological malignancies is associated with differential regulation of angiogenic factors." Leukemia**23**(1): 162-9.

Nencioni, A., F. Grunebach, et al. (2007). "Proteasome inhibitors: antitumor effects and beyond." Leukemia**21**(1): 30-6.

Neri, A., L. Baldini, et al. (1993). "p53 gene mutations in multiple myeloma are associated with advanced forms of malignancy." Blood**81**(1): 128-35.

NHL (1997). "A clinical evaluation of the International Lymphoma Study Group classification of non-Hodgkin's lymphoma. The Non-Hodgkin's Lymphoma Classification Project " Blood**89**(11): 3909-18

Nilsson, K. (1970). "Long term culture of bone-marrow biopsies and peripheral blood leucocytes from patients with multiple myeloma." Acta Pathol Microbiol Scand A**78**(4): 492-3.

Nilsson, K. (1992). "Human B-lymphoid cell lines." Hum Cell**5**(1): 25-41.

Nilsson, K., H. Bennich, et al. (1970). "Established immunoglobulin producing myeloma (IgE) and lymphoblastoid (IgG) cell lines from an IgE myeloma patient." Clin Exp Immunol**7**(4): 477-89.

Nishimoto, N., Y. Shima, et al. (1997). "Myeloma biology and therapy. Present status and future developments." Hematol Oncol Clin North Am**11**(1): 159-72.

Noureen, N., H. Rashid, et al. (1997). "Identification of type-specific anticancer histone deacetylase inhibitors: road to success." Cancer Chemother Pharmacol**66**(4): 625-33.

Nussbaum, A. K., T. P. Dick, et al. (1998). "Cleavage motifs of the yeast 20S proteasome beta subunits deduced from digests of enolase 1." Proc Natl Acad Sci U S A**95**(21): 12504-9.

Okamatsu, Y., D. Kim, et al. (2004). "MIP-1 gamma promotes receptor-activator-of-NF-kappa-B-ligand-induced osteoclast formation and survival." J Immunol**173**(3): 2084-90.

Oltersdorf, T., S. W. Elmore, et al. (2005). "An inhibitor of Bcl-2 family proteins induces regression of solid tumours." Nature**435**(7042): 677-81.

Orlowski, R. Z., J. R. Eswara, et al. (1998). "Tumor growth inhibition induced in a murine model of human Burkitt's lymphoma by a proteasome inhibitor." Cancer Res**58**(19): 4342-8.
Palazzo, A., B. Ackerman, et al. (2003). "Cell biology: Tubulin acetylation and cell motility." Nature**421**(6920): 230.
Panayiotidis, P., D. Jones, et al. (1996). "Human bone marrow stromal cells prevent apoptosis and support the survival of chronic lymphocytic leukaemia cells in vitro." Br J Haematol**92**(1): 97-103.
Pantel, K., A. Dickmanns, et al. (1995). "Establishment of micrometastatic carcinoma cell lines: a novel source of tumor cell vaccines." J Natl Cancer Inst**87**(15): 1162-8.
Paoluzzi, L., L. Scotto, et al. (2009). "The anti-histaminic cyproheptadine synergizes the antineoplastic activity of bortezomib in mantle cell lymphoma through its effects as a histone deacetylase inhibitor." Br J Haematol**146**(6): 656-9.
Paoluzzi, L., L. Scotto, et al. (2010). "Romidepsin and belinostat synergize the antineoplastic effect of bortezomib in mantle cell lymphoma." Clin Cancer Res**16**(2): 554-65.
Park, J. H., Y. Jung, et al. (2004). "Class I histone deacetylase-selective novel synthetic inhibitors potently inhibit human tumor proliferation." Clin Cancer Res**10**(15): 5271-81.
Parker, T. L. and M. P. Strout (2011). "Chronic lymphocytic leukemia: prognostic factors and impact on treatment." Discov Med**11**(57): 115-23.
Pearl, L. H., C. Prodromou, et al. (2008). "The Hsp90 molecular chaperone: an open and shut case for treatment." Biochem J**410**(3): 439-53.
Peart, M. J., G. K. Smyth, et al. (2005). "Identification and functional significance of genes regulated by structurally different histone deacetylase inhibitors." Proc Natl Acad Sci U S A**102**(10): 3697-702.
Pei, X. Y., Y. Dai, et al. (2004). "Synergistic induction of oxidative injury and apoptosis in human multiple myeloma cells by the proteasome inhibitor bortezomib and histone deacetylase inhibitors." Clin Cancer Res**10**(11): 3839-52.
Pellat-Deceunynck, C., M. Amiot, et al. (1996). "CD11a-CD18 and CD102 interactions mediate human myeloma cell growth arrest induced by CD40 stimulation." Cancer Res**56**(8): 1909-16.
Pellat-Deceunynck, C., R. Bataille, et al. (1994). "Expression of CD28 and CD40 in human myeloma cells: a comparative study with normal plasma cells." Blood**84**(8): 2597-603.
Pellegrino, A., R. Ria, et al. (2005). "Bone marrow endothelial cells in multiple myeloma secrete CXC-chemokines that mediate interactions with plasma cells." Br J Haematol**129**(2): 248-56.
Perez, L. E., N. Parquet, et al. (2009). "Bortezomib restores stroma-mediated APO2L/TRAIL apoptosis resistance in multiple myeloma." Eur J Haematol**84**(3): 212-22.
Pham, L. V., A. T. Tamayo, et al. (2003). "Inhibition of constitutive NF-kappaB activation in mantle cell lymphoma B cells leads to induction of cell cycle arrest and apoptosis." J Immunol**171**(1): 88-95.
Piekarz, R. L., R. Frye, et al. (2009). "Phase II multi-institutional trial of the histone deacetylase inhibitor romidepsin as monotherapy for patients with cutaneous T-cell lymphoma." J Clin Oncol**27**(32): 5410-7.
Pike, B. L. and W. A. Robinson (1970). "Human bone marrow colony growth in agar-gel." J Cell Physiol**76**(1): 77-84.
Planken, E. V., N. H. Dijkstra, et al. (1996). "Proliferation of B cell malignancies in all stages of differentiation upon stimulation in the 'CD40 system'." Leukemia**10**(3): 488-93.
Plemper, R. K. and D. H. Wolf (1999). "Endoplasmic reticulum degradation. Reverse protein transport and its end in the proteasome." Mol Biol Rep**26**(1-2): 125-30.
Podar, K. and K. C. Anderson (2005). "The pathophysiologic role of VEGF in hematologic malignancies: therapeutic implications." Blood**105**(4): 1383-95.
Podar, K. and K. C. Anderson (2006). "Caveolin-1 as a potential new therapeutic target in multiple myeloma." Cancer Lett**233**(1): 10-5.

Podar, K., D. Chauhan, et al. (2009). "Bone marrow microenvironment and the identification of new targets for myeloma therapy." Leukemia**23**(1): 10-24.
Podar, K., Y. T. Tai, et al. (2001). "Vascular endothelial growth factor triggers signaling cascades mediating multiple myeloma cell growth and migration." Blood**98**(2): 428-35.
Popat, R., L. Maharaj, et al. (2012). "Schedule dependent cytotoxicity of bortezomib and melphalan in multiple myeloma." Br J Haematol**160**(1): 111-4.
Popat, R., H. Oakervee, et al. (2009). "Bortezomib, low-dose intravenous melphalan, and dexamethasone for patients with relapsed multiple myeloma." Br J Haematol**144**(6): 887-94.
Portier, M., J. P. Moles, et al. (1992). "p53 and RAS gene mutations in multiple myeloma." Oncogene**7**(12): 2539-43.
Pound, J. D. and J. Gordon (1997). "Maintenance of human germinal center B cells in vitro." Blood**89**(3): 919-28.
Price, P. and T. J. McMillan (1990). "Use of the tetrazolium assay in measuring the response of human tumor cells to ionizing radiation." Cancer Res**50**(5): 1392-6.
Puck, T. T. (1957). "The genetics of somatic mammalian cells." Adv Biol Med Phys**5**: 75-101.
Qin, J. Z., J. Ziffra, et al. (2005). "Proteasome inhibitors trigger NOXA-mediated apoptosis in melanoma and myeloma cells." Cancer Res**65**(14): 6282-93.
Qiu, L., M. J. Kelso, et al. (1999). "Anti-tumour activity in vitro and in vivo of selective differentiating agents containing hydroxamate." Br J Cancer**80**(8): 1252-8.
Quintanilla-Martinez, L., M. Kremer, et al. (2003). "Analysis of signal transducer and activator of transcription 3 (Stat 3) pathway in multiple myeloma: Stat 3 activation and cyclin D1 dysregulation are mutually exclusive events." Am J Pathol**162**(5): 1449-61.
Rao, R., S. Nalluri, et al. (2010). "Role of CAAT/enhancer binding protein homologous protein in panobinostat-mediated potentiation of bortezomib-induced lethal endoplasmic reticulum stress in mantle cell lymphoma cells." Clin Cancer Res**16**(19): 4742-54.
Rayanade, R. J., M. I. Ndubuisi, et al. (1998). "Regulation of IL-6 signaling by p53: STAT3- and STAT5-masking in p53-Val135-containing human hepatoma Hep3B cell lines." J Immunol**161**(1): 325-34.
Rees-Unwin, K. S., R. A. Craven, et al. (2007). "Proteomic evaluation of pathways associated with dexamethasone-mediated apoptosis and resistance in multiple myeloma." Br J Haematol**139**(4): 559-67.
Rellick, S. L., D. Piktel, et al. (2012). "Melphalan exposure induces an interleukin-6 deficit in bone marrow stromal cells and osteoblasts." Cytokine**58**(2): 245-52.
Ria, R., A. Reale, et al. (2011). "Bone marrow angiogenesis and progression in multiple myeloma." Am J Blood Res**1**(1): 76-89.
Ribatti, D. and A. Vacca (2005). "Therapeutic renaissance of thalidomide in the treatment of haematological malignancies." Leukemia**19**(9): 1525-31.
Richardson, P. G., A. Z. Badros, et al. (2010). "Tanespimycin with bortezomib: activity in relapsed/refractory patients with multiple myeloma." Br J Haematol**150**(4): 428-37.
Rizzatti, E. G., H. Mora-Jensen, et al. (2008). "Noxa mediates bortezomib induced apoptosis in both sensitive and intrinsically resistant mantle cell lymphoma cells and this effect is independent of constitutive activity of the AKT and NF-kappaB pathways." Leuk Lymphoma**49**(4): 798-808.
Roecklein, B. A. and B. Torok-Storb (1995). "Functionally distinct human marrow stromal cell lines immortalized by transduction with the human papilloma virus E6/E7 genes." Blood**85**(4): 997-1005.
Roue, G., P. Perez-Galan, et al. (2010). "The Hsp90 inhibitor IPI-504 overcomes bortezomib resistance in mantle cell lymphoma in vitro and in vivo by down-regulation of the prosurvival ER chaperone BiP/Grp78." Blood**117**(4): 1270-9.

Rousset, F., E. Garcia, et al. (1991). "Cytokine-induced proliferation and immunoglobulin production of human B lymphocytes triggered through their CD40 antigen." J Exp Med**173**(3): 705-10.

Rousset, F., E. Garcia, et al. (1992). "Interleukin 10 is a potent growth and differentiation factor for activated human B lymphocytes." Proc Natl Acad Sci U S A**89**(5): 1890-3.

Roy, A., E. Krzykwa, et al. (2001). "Increased efficiency of gamma-irradiated versus mitomycin C-treated feeder cells for the expansion of normal human cells in long-term cultures." J Hematother Stem Cell Res**10**(6): 873-80.

Runge, H. M., H. A. Neumann, et al. (1986). "Growth patterns and hormonal sensitivity of primary tumor, abdominal metastasis and ascitic fluid from human epithelial ovarian carcinomas in the tumor colony-forming assay." Eur J Cancer Clin Oncol**22**(6): 691-6.

San Miguel, J. F., R. Schlag, et al. (2008). "Bortezomib plus melphalan and prednisone for initial treatment of multiple myeloma." N Engl J Med**359**(9): 906-17.

Sanderson, S., M. Valenti, et al. (2006). "Benzoquinone ansamycin heat shock protein 90 inhibitors modulate multiple functions required for tumor angiogenesis." Mol Cancer Ther**5**(3): 522-32.

Sawas, A., C. Diefenbach, et al. (2011). "New therapeutic targets and drugs in non-Hodgkin's lymphoma." Curr Opin Hematol**18**(4): 280-7.

Schenkein, D. (2002). "Proteasome inhibitors in the treatment of B-cell malignancies." Clin Lymphoma**3**(1): 49-55.

Schmidmaier, R., P. Baumann, et al. (2004). "The HMG-CoA reductase inhibitor simvastatin overcomes cell adhesion-mediated drug resistance in multiple myeloma by geranylgeranylation of Rho protein and activation of Rho kinase." Blood**104**(6): 1825-32.

Schultze, J. L., A. A. Cardoso, et al. (1995). "Follicular lymphomas can be induced to present alloantigen efficiently: a conceptual model to improve their tumor immunogenicity." Proc Natl Acad Sci U S A**92**(18): 8200-4.

Schweigerer, L., G. Neufeld, et al. (1987). "Basic fibroblast growth factor as a growth inhibitor for cultured human tumor cells." J Clin Invest**80**(5): 1516-20.

Shah, S. A., M. W. Potter, et al. (2001). "26S proteasome inhibition induces apoptosis and limits growth of human pancreatic cancer." J Cell Biochem**82**(1): 110-22.

Shain, K. H., T. H. Landowski, et al. (2002). "Adhesion-mediated intracellular redistribution of c-Fas-associated death domain-like IL-1-converting enzyme-like inhibitory protein-long confers resistance to CD95-induced apoptosis in hematopoietic cancer cell lines." J Immunol**168**(5): 2544-53.

Shao, Y., Z. Gao, et al. (2004). "Apoptotic and autophagic cell death induced by histone deacetylase inhibitors." Proc Natl Acad Sci U S A**101**(52): 18030-5.

Shoemaker, R. H. (2006). "The NCI60 human tumour cell line anticancer drug screen." Nat Rev Cancer**6**(10): 813-23.

Skehan, P., R. Storeng, et al. (1990). "New colorimetric cytotoxicity assay for anticancer-drug screening." J Natl Cancer Inst**82**(13): 1107-12.

Smith, A., F. Wisloff, et al. (2006). "Guidelines on the diagnosis and management of multiple myeloma 2005." Br J Haematol**132**(4): 410-51.

Soliman, M. A., A. A. Fathy, et al. (2009). "Impact of CD40 expression by flowcytometry on outcome of patients with non-Hodgkin's lymphoma." Egypt J Immunol**16**(1): 61-70.

Spanswick, V. J., C. Craddock, et al. (2002). "Repair of DNA interstrand crosslinks as a mechanism of clinical resistance to melphalan in multiple myeloma." Blood**100**(1): 224-9.

Sreedhar, A. S., E. Kalmar, et al. (2004). "Hsp90 isoforms: functions, expression and clinical importance." FEBS Lett**562**(1-3): 11-5.

Stacchini, A., M. Aragno, et al. (1999). "MEC1 and MEC2: two new cell lines derived from B-chronic lymphocytic leukaemia in prolymphocytoid transformation." Leuk Res**23**(2): 127-36.

Stasi, R., M. Brunetti, et al. (1998). "The prognostic value of soluble interleukin-6 receptor in patients with multiple myeloma." Cancer**82**(10): 1860-6.

Stasi, R., M. L. Evangelista, et al. (2008). "Gemtuzumab ozogamicin in the treatment of acute myeloid leukemia." Cancer Treat Rev**34**(1): 49-60.

Strauss, S. J., K. Higginbottom, et al. (2007). "The proteasome inhibitor bortezomib acts independently of p53 and induces cell death via apoptosis and mitotic catastrophe in B-cell lymphoma cell lines." Cancer Res**67**(6): 2783-90.

Strauss, S. J., L. Maharaj, et al. (2006). "Bortezomib therapy in patients with relapsed or refractory lymphoma: potential correlation of in vitro sensitivity and tumor necrosis factor alpha response with clinical activity." J Clin Oncol**24**(13): 2105-12.

Sunwoo, J. B., Z. Chen, et al. (2001). "Novel proteasome inhibitor PS-341 inhibits activation of nuclear factor-kappa B, cell survival, tumor growth, and angiogenesis in squamous cell carcinoma." Clin Cancer Res**7**(5): 1419-28.

Supko, J. G., R. L. Hickman, et al. (1995). "Preclinical pharmacologic evaluation of geldanamycin as an antitumor agent." Cancer Chemother Pharmacol**36**(4): 305-15.

Swerdlow, S. H. (2008). WHO Classification of Tumours of the Haematopoietic and Lymphoid Tissues Lyon, IARC Press.

Sydor, J. R., E. Normant, et al. (2006). "Development of 17-allylamino-17-demethoxygeldanamycin hydroquinone hydrochloride (IPI-504), an anti-cancer agent directed against Hsp90." Proc Natl Acad Sci U S A**103**(46): 17408-13.

Szocinski, J. L., A. R. Khaled, et al. (2002). "Activation-induced cell death of aggressive histology lymphomas by CD40 stimulation: induction of bax." Blood**100**(1): 217-23.

Tai, Y. T., X. Li, et al. (2005). "Human anti-CD40 antagonist antibody triggers significant antitumor activity against human multiple myeloma." Cancer Res**65**(13): 5898-906.

Tai, Y. T., K. Podar, et al. (2003). "CD40 induces human multiple myeloma cell migration via phosphatidylinositol 3-kinase/AKT/NF-kappa B signaling." Blood**101**(7): 2762-9.

Teicher, B. A., G. Ara, et al. (1999). "The proteasome inhibitor PS-341 in cancer therapy." Clin Cancer Res**5**(9): 2638-45.

Teoh, G. and K. C. Anderson (1997). "Interaction of tumor and host cells with adhesion and extracellular matrix molecules in the development of multiple myeloma." Hematol Oncol Clin North Am**11**(1): 27-42.

Teoh, G., Y. T. Tai, et al. (2000). "CD40 activation mediates p53-dependent cell cycle regulation in human multiple myeloma cell lines." Blood**95**(3): 1039-46.

Teoh, G., M. Urashima, et al. (1998). "The 86-kD subunit of Ku autoantigen mediates homotypic and heterotypic adhesion of multiple myeloma cells." J Clin Invest**101**(6): 1379-88.

Teoh, G., M. Urashima, et al. (1997). "MDM2 protein overexpression promotes proliferation and survival of multiple myeloma cells." Blood**90**(5): 1982-92.

Terashita, G. (2003). A Better Alternative to Traditional Methods for Cell Counting and Viability Assessments? I. Guava Technologies**:** 1-2.

Terpos, E., M. Politou, et al. (2003). "Serum levels of macrophage inflammatory protein-1 alpha (MIP-1alpha) correlate with the extent of bone disease and survival in patients with multiple myeloma." Br J Haematol**123**(1): 106-9.

Thalmeier, K., P. Meissner, et al. (1996). "Constitutive and modulated cytokine expression in two permanent human bone marrow stromal cell lines." Exp Hematol**24**(1): 1-10.

Tilly, H. and M. Dreyling (2010). "Diffuse large B-cell non-Hodgkin's lymphoma: ESMO Clinical Practice Guidelines for diagnosis, treatment and follow-up." Ann Oncol**21 Suppl 5**: v172-4.

Tong, A. W. and M. J. Stone (1996). "CD40 and the effect of anti-CD40-binding on human multiple myeloma clonogenicity." Leuk Lymphoma**21**(1-2): 1-8.
Tong, A. W. and M. J. Stone (2003). "Prospects for CD40-directed experimental therapy of human cancer." Cancer Gene Ther**10**(1): 1-13.
Tong, A. W., B. Q. Zhang, et al. (1994). "Anti-CD40 antibody binding modulates human multiple myeloma clonogenicity in vitro." Blood**84**(9): 3026-33.
Torok-Storb, B., M. Iwata, et al. (1999). "Dissecting the marrow microenvironment." Ann N Y Acad Sci**872**: 164-70.
Treon, S. P. and K. C. Anderson (1998). "Interleukin-6 in multiple myeloma and related plasma cell dyscrasias." Curr Opin Hematol**5**(1): 42-8.
Tromp, J. M., S. H. Tonino, et al. (2010). "Dichotomy in NF-kappaB signaling and chemoresistance in immunoglobulin variable heavy-chain-mutated versus unmutated CLL cells upon CD40/TLR9 triggering." Oncogene**29**(36): 5071-82.
Tu, Y., A. Gardner, et al. (2000). "The phosphatidylinositol 3-kinase/AKT kinase pathway in multiple myeloma plasma cells: roles in cytokine-dependent survival and proliferative responses." Cancer Res**60**(23): 6763-70.
Uchiyama, H., B. A. Barut, et al. (1993). "Adhesion of human myeloma-derived cell lines to bone marrow stromal cells stimulates interleukin-6 secretion." Blood**82**(12): 3712-20.
Urashima, M., D. Chauhan, et al. (1995). "CD40 ligand triggered interleukin-6 secretion in multiple myeloma." Blood**85**(7): 1903-12.
Urashima, M., A. Ogata, et al. (1996). "Transforming growth factor-beta1: differential effects on multiple myeloma versus normal B cells." Blood**87**(5): 1928-38.
Urashima, M., G. Teoh, et al. (1997). "Interleukin-6 overcomes p21WAF1 upregulation and G1 growth arrest induced by dexamethasone and interferon-gamma in multiple myeloma cells." Blood**90**(1): 279-89.
Vacca, A., R. Ria, et al. (2003). "A paracrine loop in the vascular endothelial growth factor pathway triggers tumor angiogenesis and growth in multiple myeloma." Haematologica**88**(2): 176-85.
van Kooten, C. and J. Banchereau (1997). "Functions of CD40 on B cells, dendritic cells and other cells." Curr Opin Immunol**9**(3): 330-7.
van Kooten, C. and J. Banchereau (1997). "Immune regulation by CD40-CD40-L interactions." Front Biosci**2**: d1-11.
van Kooten, C. and J. Banchereau (2000). "CD40-CD40 ligand." J Leukoc Biol**67**(1): 2-17.
Viani, R. M., L. Peralta, et al. (2006). "Prevalence of primary HIV-1 drug resistance among recently infected adolescents: a multicenter adolescent medicine trials network for HIV/AIDS interventions study." J Infect Dis**194**(11): 1505-9.
Visser, H. P., M. Tewis, et al. (2000). "Mantle cell lymphoma proliferates upon IL-10 in the CD40 system." Leukemia**14**(8): 1483-9.
Vistica, D. T., P. Skehan, et al. (1991). "Tetrazolium-based assays for cellular viability: a critical examination of selected parameters affecting formazan production." Cancer Res**51**(10): 2515-20.
Voges, D., P. Zwickl, et al. (1999). "The 26S proteasome: a molecular machine designed for controlled proteolysis." Annu Rev Biochem**68**: 1015-68.
Vonderheide, R. H., J. P. Dutcher, et al. (2001). "Phase I study of recombinant human CD40 ligand in cancer patients." J Clin Oncol**19**(13): 3280-7.
Voorhees, P. M., Q. Chen, et al. (2007). "Inhibition of interleukin-6 signaling with CNTO 328 enhances the activity of bortezomib in preclinical models of multiple myeloma." Clin Cancer Res**13**(21): 6469-78.
Walkinshaw, D. R. and X. J. Yang (2008). "Histone deacetylase inhibitors as novel anticancer therapeutics." Curr Oncol**15**(5): 237-43.
Wang, L., R. J. Rayanade, et al. (1995). "Modulation of interleukin-6-induced plasma protein secretion in hepatoma cells by p53 species." J Biol Chem**270**(39): 23159-65.

Wang, Q., H. Mora-Jensen, et al. (2009). "ERAD inhibitors integrate ER stress with an epigenetic mechanism to activate BH3-only protein NOXA in cancer cells." Proc Natl Acad Sci U S A**106**(7): 2200-5.

Wang, Z. Y. and Z. Chen (2008). "Acute promyelocytic leukemia: from highly fatal to highly curable." Blood**111**(5): 2505-15.

Waugh, D. J. and C. Wilson (2008). "The interleukin-8 pathway in cancer." Clin Cancer Res**14**(21): 6735-41.

Weekes, C. D., S. J. Pirruccello, et al. (1998). "Lymphoma cells associated with bone marrow stromal cells in culture exhibit altered growth and survival." Leuk Lymphoma**31**(1-2): 151-65.

Weigert, O., A. Pastore, et al. (2007). "Sequence-dependent synergy of the proteasome inhibitor bortezomib and cytarabine in mantle cell lymphoma." Leukemia**21**(3): 524-8.

Weinstein, I. B. and A. Joe (2008). "Oncogene addiction." Cancer Res**68**(9): 3077-80; discussion 3080.

Westendorf, J. J., G. J. Ahmann, et al. (1994). "CD40 expression in malignant plasma cells. Role in stimulation of autocrine IL-6 secretion by a human myeloma cell line." J Immunol**152**(1): 117-28.

Whitesell, L. and S. L. Lindquist (2005). "HSP90 and the chaperoning of cancer." Nat Rev Cancer**5**(10): 761-72.

Whitlock, C. A. and O. N. Witte (1982). "Long-term culture of B lymphocytes and their precursors from murine bone marrow." Proc Natl Acad Sci U S A**79**(11): 3608-12.

Wilson, A. J., D. S. Byun, et al. (2006). "Histone deacetylase 3 (HDAC3) and other class I HDACs regulate colon cell maturation and p21 expression and are deregulated in human colon cancer." J Biol Chem**281**(19): 13548-58.

Wilson, C., T. Wilson, et al. (2008). "Interleukin-8 signaling attenuates TRAIL- and chemotherapy-induced apoptosis through transcriptional regulation of c-FLIP in prostate cancer cells." Mol Cancer Ther**7**(9): 2649-61.

Woltman, A. M., S. de Haij, et al. (2000). "Interleukin-17 and CD40-ligand synergistically enhance cytokine and chemokine production by renal epithelial cells." J Am Soc Nephrol**11**(11): 2044-55.

Wright, J. J. (2010). "Combination therapy of bortezomib with novel targeted agents: an emerging treatment strategy." Clin Cancer Res**16**(16): 4094-104.

Yaccoby, S., M. J. Wezeman, et al. (2006). "Inhibitory effects of osteoblasts and increased bone formation on myeloma in novel culture systems and a myelomatous mouse model." Haematologica**91**(2): 192-9.

Yarde, D. N., V. Oliveira, et al. (2009). "Targeting the Fanconi anemia/BRCA pathway circumvents drug resistance in multiple myeloma." Cancer Res**69**(24): 9367-75.

Yasui, H., T. Hideshima, et al. (2007). "BIRB 796 enhances cytotoxicity triggered by bortezomib, heat shock protein (Hsp) 90 inhibitor, and dexamethasone via inhibition of p38 mitogen-activated protein kinase/Hsp27 pathway in multiple myeloma cell lines and inhibits paracrine tumour growth." Br J Haematol**136**(3): 414-23.

Yasukawa, K., K. Futatsugi, et al. (1992). "Association of recombinant soluble IL-6-signal transducer, gp130, with a complex of IL 6 and soluble IL-6 receptor, and establishment of an ELISA for soluble gp130." Immunol Lett**31**(2): 123-30.

Yonish-Rouach, E., D. Grunwald, et al. (1993). "p53-mediated cell death: relationship to cell cycle control." Mol Cell Biol**13**(3): 1415-23.

Yonish-Rouach, E., D. Resnitzky, et al. (1991). "Wild-type p53 induces apoptosis of myeloid leukaemic cells that is inhibited by interleukin-6." Nature**352**(6333): 345-7.

Yoshida, M., Y. Hoshikawa, et al. (1990). "Structural specificity for biological activity of trichostatin A, a specific inhibitor of mammalian cell cycle with potent differentiation-inducing activity in Friend leukemia cells." J Antibiot (Tokyo)**43**(9): 1101-6.

Younes, A. and A. Carbone (1999). "CD30/CD30 ligand and CD40/CD40 ligand in malignant lymphoid disorders." Int J Biol Markers**14**(3): 135-43.

Zanella, F., J. B. Lorens, et al. "High content screening: seeing is believing." Trends Biotechnol**28**(5): 237-45.

Zdzisinska, B., J. Rolinski, et al. (2009). "A comparison of cytokine production in 2-dimensional and 3-dimensional cultures of bone marrow stromal cells of multiple myeloma patients in response to RPMI8226 myeloma cells." Folia Histochem Cytobiol**47**(1): 69-74.

Zhang, L., M. A. Freitas, et al. (2004). "Differential expression of histone post-translational modifications in acute myeloid and chronic lymphocytic leukemia determined by high-pressure liquid chromatography and mass spectrometry." J Am Soc Mass Spectrom**15**(1): 77-86.

Zhang, X., L. Li, et al. (2001). "The distinct roles of T cell-derived cytokines and a novel follicular dendritic cell-signaling molecule 8D6 in germinal center-B cell differentiation." J Immunol**167**(1): 49-56.

Zhu, P., E. Huber, et al. (2004). "Specific and redundant functions of histone deacetylases in regulation of cell cycle and apoptosis." Cell Cycle**3**(10): 1240-2.

Zips, D., H. D. Thames, et al. (2005). "New anticancer agents: in vitro and in vivo evaluation." In Vivo**19**(1): 1-7.